Characterization of Puumala Orthohantavirus - Host Interactions: From the Field to the Bench

I n a u g u r a l d i s s e r t a t i o n

zur

Erlangung des akademischen Grades eines

Doktors der Naturwissenschaften
(Dr. rer. nat.)

der

Mathematisch-Naturwissenschaftlichen Fakultät

der

Universität Greifswald

vorgelegt von

Florian Binder

geboren am 27.01.1989

in Nürnberg

Greifswald, 02.07.2020

Dekan: Prof. Dr. Gerald Kerth

1. Gutachter: Prof. Rainer G. Ulrich

2. Gutachter: Prof. Georg Kochs

Tag der Promotion: 06.01.2021

CONTENT

List of abbreviations

ANDV	Andes orthohantavirus
BW	Baden-Wuerttemberg
BUNV	Bunyamwera orthobunyavirus
C	cytosine
CE	central European
cDNA	complementary deoxynucleic acid
ds	double stranded
cRNA	complementary ribonucleic acid
C-terminal	carboxy-terminal
CPXV	Cowpox virus
CTLs	cytotoxic T-lymphocytes
DAF	decay accelerating factor
DCs	dendritic cells
DOBV	Dobrava-Belgrade orthohantavirus
ECs	endothelial cells
ER	endoplasmic reticulum
ERGIC	endoplasmatic reticulum - Golgi apparatus intermediate compartment
G	guanine
Gc	carboxy-terminal glycoprotein
gC1qR	globular head domain of complement C1q
Gn	amino-terminal glycoprotein
GPC	glycoprotein precursor
HCPS	hantavirus cardiopulmonary syndrome
HFRS	hemorrhagic fever with renal syndrome
HTNV	Hantaan orthohantavirus
HOKV	Hokkaido virus
HRTV	Heartland bandavirus
IFN	interferon
IFN-I	type I interferon
IKKε	IκB-kinase ε
IPS2	IFN-β promoter stimulator 2
IRF-3/7	interferon regulatory factor-3 or -7
ISG	interferon stimulated gene
ISRE	interferon sensitive responsive element
JAK	Janus kinase
kDa	kilo Dalton
KHAV	Khabarovsk orthohantavirus
L	large
LACV	La Crosse orthobunyavirus
M	medium
MDA-5	melanoma differentiation associated gene 5
MERS-CoV	Middle east respiratory syndrome coronavirus
mRNA	messenger ribonucleic acid
MxA/2	Myxovirus resistance gene A or 2

N	nucleocapsid
NAP1	Nucleosome assembly protein 1
NCR	non-coding region
NE	*Nephropathia epidemica*
NEMO	NF-kappa-B essential modulator
NFκB	nuclear factor 'kappa-light-chain-enhancer' of activated B-cells
NK-cells	natural killer cells
nm	nanometer
NO	nitric oxide
NSs	non-structural small segment
N-SCA	Northern Scandinavian
N-terminal	amino-terminal
NW	North Rhine-Westphalia
NYV	New York virus
ORF	open reading frame
P-bodies	processing bodies
PAMP	pathogen associated molecular pattern
PCDH1	procadherin-1
pppG	guanine triphosphate
PHV	Prospect Hill orthohantavirus
PKR	protein kinase R
PRR	pattern recognition receptor
PUUV	Puumala orthohantavirus
qRT-PCR	quantitative reverse transcription polymerase chain reaction
RdRP	RNA-dependent RNA polymerase
RIG-I	retinoic acid inducible gene-I
RNA	ribonucleic acid
RT-PCR	reverse transcription-polymerase chain reaction
S	small
ss	single stranded
SARS-CoV-2	Severe acute respiratory syndrome coronavirus 2
SEOV	Seoul orthohantavirus
SIKE	IKKε and its suppressor
SFTSV	Severe fever with thrombocytopenia syndrome virus
SNV	Sin Nombre orthohantavirus
STAT	signal transducers and activators of transcription
TANK1	TRAF family member-associated NF-kappa-B activator 1
TBEV	Tick-borne encephalitis virus
TBK-1	TRAF-family member-associated NFκB activator binding kinase 1
TLR-7	Toll like receptor 7
TNF	tumor necrosis factor
TOSV	Toscana virus
TRAF3	TNF receptor associated factor 3
TULV	Tula orthohantavirus
vRNA	viral ribonucleic acid

1. INTRODUCTION

1.1 VIRION STRUCTURE AND GENOME ORGANIZATION OF HANTAVIRUSES

Orthohantaviruses are members of the family *Hantaviridae* within the order *Bunyavirales* (Table 1). The genome of these single-stranded (ss) RNA viruses has negative polarity (Schmaljohn et al., 1985) and consists of the three segments small (S), medium (M) and large (L) (Figure 1). The viral RNA (vRNA) of each segment includes an open reading frame (ORF) flanked by non-coding regions (NCRs) at the 3' and 5' ends of each segment. The S segment encodes a nucleocapsid (N) protein, the M segment codes for a glycoprotein precursor (GPC), which eventually matures into the glycoproteins Gn and Gc and the L segment codes for the RNA-dependent RNA polymerase (RdRP). The very termini of the NCRs contain nucleotide sequence repeats that form a panhandle-like structure, which functions as the viral promoter and is crucial for transcription and replication (Hussein et al., 2011; Vaheri et al., 2013b).

Table 1: Taxonomic classification of the order Bunyavirales and viruses that have been used for studies on the nonstructural (NSs) protein (Source: ICTV, 2020).

Phylum: *Negarnaviricota*		
Subphylum: *Polyploviricotina*		
Class: *Ellioviricetes*		
Order: *Bunyavirales*		**Representative**
Family:	*Arenaviridae*	
	Cruliviridae	
	Fimoviridae	
	Hantaviridae	Genus *Orthohantavirus*: Andes-, Puumla-, Tula-, Sin Nombre-, Prospect Hill-, Seoul-, Hantaan-, Khabarovsk, Dobrava-Belgrade orthohantavirus
	Leishbuviridae	
	Mypoviridae	
	Nairoviridae	
	Peribunyaviridae	Bunyamwera orthobunyavirus, La Crosse orthobunyavirus
	Phasmaviridae	
	Phenuiviridae	Rift Valley fever phlebovirus, Toscana phlebovirus, Severe fever with thrombocytopenia virus, Heartland bandavirus
	Tospoviridae	
	Wupedeviridae	

In addition to encoding the N protein, the small segment of orthohantaviruses carried by rodents of the family Cricetidae contains an additional ORF that is conserved among these viruses. This +1 overlapping reading frame encodes the non-structural protein NSs, which was suggested as a putative interferon (IFN) inhibitor (Jääskelainen et al., 2007) but is likely to have other functions as well (Virtanen et al., 2010;

Ronnberg et al., 2012). The PUUV and TULV NSs ORF ranges from nucleotide position 83 to position 352 and is expressed as a protein of about 13kDa in size (Jääskelainen et al., 2007). Non-structural proteins encoded by the small segment are common for bunyaviruses and are typically associated with IFN antagonism (Hedil and Kormelink, 2016). The genome segments of hantaviruses are each encapsidated by the N protein and packed within the virus particle (Figure 1). This virion is round or pleomorphic and its size ranges from 120 nm to 160 nm in diameter (Hepojoki et al., 2012). The virion comprises a lipid envelope, which is covered with spikes protruding from the membrane envelope (Huiskonen et al., 2010). Four Gn and four Gc units form each spike, which has a unique four-fold symmetry (Huiskonen et al., 2010; Hepojoki et al., 2012). The overall composition of a virion is >50% protein, 20–30% lipid, 7% carbohydrate and 2% RNA (Schmaljohn et al., 1985). The virion is unexpectedly stable and can survive outside the host for more than 12-15 days at room temperature, more than 18 days at +4 °C, and even weeks at –20 °C (Kallio et al., 2006a). This is a key feature for hantavirus transmission to humans, which - unlike transmission of other bunyaviruses - does not involve an arthropod vector.

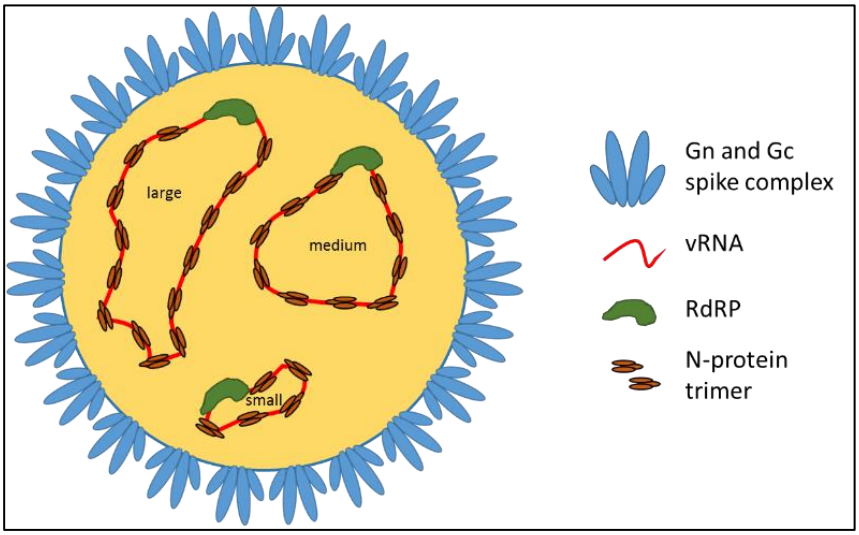

Figure 1: Schematic representation of the hantavirus virion. *The three genome segments are encapsidated by trimeric nucleocapsid (N) proteins and associated with the viral RNA-dependent RNA polymerase (RdRP). The glycoproteins are shown in blue as a spike complex in the lipid membrane envelope.*

1.2 RODENT RESERVOIRS OF HANTAVIRUSES

Hantaviruses are small mammal-borne pathogens that can cause a mild to severe disease in humans but can also stay asymptomatic in many cases. They are usually associated with a single reservoir host and do not cause obvious disease in their reservoirs (Table 2). The most important orthohantaviruses, pathogenic for humans, and their hosts are summarized in Table 2. The main causative agent of hantavirus disease in Europe, Puumala orthohantavirus (PUUV), was discovered in Finland in the 1980ies (Niklasson and Le Duc, 1984). PUUV is transmitted by its reservoir, the bank vole (*Clethrionomys glareolus*) and has a wide distribution in Europe and Asia (Heyman et al., 2011). PUUV disease outbreaks are usually synchronized Germany-wide, driven by beech mast-induced irruptions of its host populations. Phylogenetic analysis separates PUUV into clades, depending on their geographic origin. In Germany, PUUV is only present in the western, central and southern parts and belongs to the Central European (CE) clade of PUUV (Drewes et al., 2017a).

In addition to the described pathogenic viruses there are hantaviruses which are not or have not yet been associated to disease in humans. Such hantaviruses were found amongst others in insectivores like moles, shrews, and in bats, but also in some rodent species (Kang et al., 2009; Schlegel et al., 2012; Gu et al., 2013; Radosa et al., 2013; Holmes and Zhang, 2015; Strakova et al., 2017; Laenen et al., 2018).

The occurrence of PUUV and related disease frequency is mainly dependent on the population density of infected reservoir hosts. This influences the probability to get in touch with an infected reservoir animal. The size of a rodent population obligates annual and seasonal oscillations (Kallio et al., 2009). These oscillations in population sizes are very prominent among wild vole species. In mass reproduction cycles, the bank vole population size can expand by 1-2 orders of magnitude (Reil et al., 2017). As causes of these changes many hypotheses were developed including predators, food supply, landscape, climate, genetics, pathogens or social behavior (Jacob et al., 2014). Beech masts, for example, are critical for mass reproduction of bank voles in central Europe and thereby influence the prevalence of PUUV within bank vole populations (Reil et al., 2015). Similar processes were observed in the deer mouse – Sin Nombre orthohantavirus (SNV) system (Luis et al., 2010; Bagamian et al., 2012).

Table 2: Zoonotic orthohantaviruses and their hosts.

Orthohantavirus species	Distribution	Host	Zoonotic potential	Disease Severity	Reference
Hantaan orthohantavirus (HNTV)	East Asia	Striped field mouse (*Apodemus agrarius*)	yes	++	(Lee et al., 1978; Lee et al., 1983)
Puumala orthohantavirus (PUUV)	Eurasia	Bank vole (*Clethrionomys glareolus*)	yes	+	(Niklasson and Le Duc, 1984; Krautkrämer et al., 2013)
Tula orthohantavirus (TULV)	Eurasia	Common vole (*Microtus arvalis*), Field vole (*Microtus agrestis*)	unknown	(+)	(Plyusnin et al., 1994; Schultze et al., 2002; Schmidt et al., 2016)
Dobrava-Belgrade orthohantavirus (DOBV)	Central, Eastern, Southern Europe	Striped field mouse (*Apodemus agrarius*), Yellow-necked mouse (*Apodemus flavicollis*), Black sea field mouse (*Apodemus ponticus*)	yes	++	(Klempa et al., 2013; Kruger et al., 2015)
Sin Nombre orthohantavirus (SNV)	North America	Deer mouse (*Peromyscus maniculatus*)	yes	+++	(Nichol et al., 1993; Vaheri et al., 2013b)
Andes orthohantavirus (ANDV)	South America	Long-tailed pygmy rice rat (*Oligoryzomys longicaudatus*)	yes	+++	(Padula et al., 1998; Vaheri et al., 2013b)
Seoul orthohantavirus (SEOV)	worldwide	Black rat (*Rattus rattus*), Norway rat (*Rattus norvegicus*)	yes	++	(Lee et al., 1982; Heyman et al., 2004)

(+), rare - single patients; +, mild; ++, moderate; +++, severe

1.3 HANTAVIRUS REPLICATION CYCLE

1.3.1 Virus entry

A variety of host cell surface proteins have been suggested to be involved in the entry of hantaviruses into human cells. These include β3 integrins, decay-accelerating factor (DAF) and the receptor for the globular head domain of complement C1q (gC1qR) (Gavrilovskaya et al., 1999; Choi et al., 2008; Krautkrämer and Zeier, 2008; Albornoz et al., 2016). Recently it was reported, that procadherin-1 (PCDH1) is essential for cell attachment and entry of New World hantaviruses like Andes orthohantavirus (ANDV) and SNV (Jangra et al., 2018). It is not clear whether the Gn or Gc glycoprotein alone, or both consecutively, interact with cell surface molecules (Cifuentes-Munoz et al., 2014). There is evidence indicating that pathogenic and non-pathogenic hantaviruses may use different integrins for entry: αVβ3 as the receptor for pathogenic viruses, and α5β1 for non-pathogenic viruses (Mackow and Gavrilovskaya, 2001). After binding to a cell surface receptor, the invading hantavirus is taken up by the cell (Figure 2), presumably through clathrin-dependent endocytosis (Jin et al., 2002). Increasing evidence suggests that hantaviruses use more than

one pathway for cellular entry including macropinocytosis, clathrin-independent receptor-mediated endocytosis, caveolae or cholesterol-dependent endocytosis, or additional routes (Lozach et al., 2010; Albornoz et al., 2016).

1.3.2 Uncoating

After internalization, the virions are transported to endosomes, where a decrease in pH leads to detaching of the virion from the cellular receptor (Figure 2). This low pH of 5-6.5 in endosomes triggers a change in the conformation of the Gc glycoprotein that allows binding of the Gc fusion loop to the endosomal membrane. Further conformational changes cause fusion of viral and cellular membranes (Cifuentes-Munoz et al., 2014; Albornoz et al., 2016). The vRNA is then released into the cytoplasm and presumably transported to the putative site of viral replication (Ramanathan et al., 2007).

1.3.3 Transcription and replication

Viral RNAs are produced from the hantavirus genome by two processes: transcription (generation of messengerRNAs (mRNAs) coding the viral proteins) and replication (vRNA for generation of new virions). Both of these activities are dependent on the viral RdRP (Spiropoulou, 2011). To date, a detailed characterization of the RNA synthesis mechanisms of hantaviruses has not been possible due to the lack of suitable reverse genetics systems. A common feature in the transcription of negative-sense segmented RNA viruses is a process called cap-snatching. In the case of hantaviruses the viral N protein and the RdRP are involved in this process. They can bind the cap structures of host mRNAs (preferably mRNAs for degradation) and use these for initiation of mRNA transcription (Mir et al., 2008; Reguera et al., 2010).

The site of replication could be either cytoplasmic processing bodies (P-bodies) or the intermediate compartment between endoplasmatic reticulum and the Golgi apparatus (ERGIC) where the N- or RdRP-bound RNA primers are transported. Assembled viral ribonucleoproteins (RNPs) are then transported to the site of viral assembly (Figure 2) mediated by interactions between N protein and host cell actin or microtubules (Ramanathan et al., 2007; Ramanathan and Jonsson, 2008). In case of the replication site residing in the P-bodies, an alternative to the viral RdRP nuclease activity is that cellular endonucleases generate the capped primers (Mir et al., 2008). The resulting capped RNA primer with its single 3’ terminal guanin (G) residue can pair with the complementary cytosin (C) residue at the AUC repeats of the vRNA terminus (Spiropoulou, 2011; Reuter and Krüger, 2017). A prime-and-realign process successively adds missing bases and slips back until the vRNA terminal repeats are newly formed (Garcin et al., 1995).

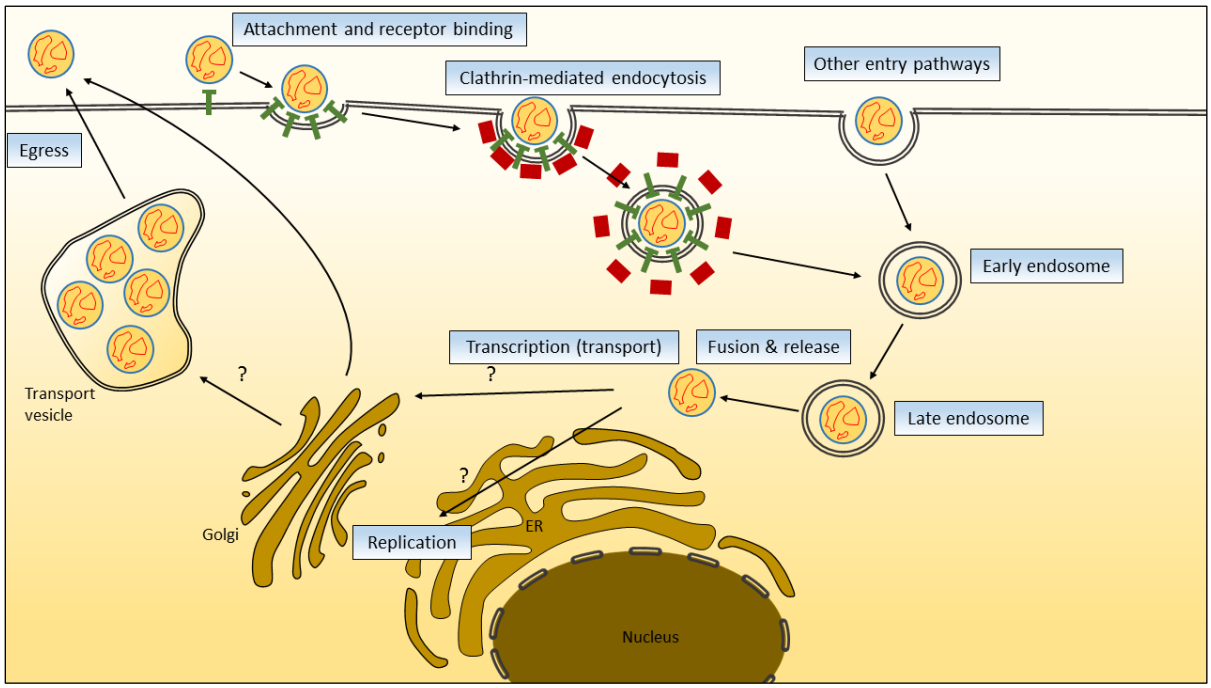

Figure 2: Hantavirus replication cycle. *The virion attaches to a receptor, induces endocytosis and enters the cell in clathrin-coated vesicles. In the endosome, fusion between the viral and endosomal membranes is driven by acid-induced conformation changes in the viral fusion protein. The viral ribonucleoproteins (RNPs) are released and transcription might take place at the site of release; alternatively, the RNPs might be transported to the Endoplasmic Reticulum (ER)–Golgi intermediate compartment for transcription and replication. The nascent viruses are thought to bud into the cis-Golgi. They are transported to the plasma membrane for release.*

For replication of the viral genome, the vRNA first needs to be transfered into complementary RNA (cRNA), which can then be used as a template for the multiplication of vRNA. This cRNA differs from viral mRNA: the synthesis is thought to start *de novo* without the need for capped primers and the cRNA is encapsidated by the N protein, similarly to the vRNA (Spiropoulou, 2011). cRNA synthesis also proceeds via a prime-and-realign mechanism through initial binding of a triphosphorylated G (pppG) to a C residue in the vRNA. The pppG is then cleaved by the RdRP to produce the monophosporylated 5’ terminus of the cRNA (Garcin et al., 1995). The same mechanism is used to multiply vRNA using cRNA as a template. During the course of vRNA synthesis, there might be a switch from transcription to replication.

1.3.4 Assembly and release

After replication of the viral genome it is encapsidated by the N protein (Spiropoulou, 2011; Hepojoki et al., 2012). For encapsidation of hantavirus vRNA, the N protein is thought to form trimers (Kaukinen et al., 2005; Reuter and Krüger, 2017). The complementary NCRs in the vRNA form a panhandle-like structure that is unique for each hantavirus. It has been suggested that the trimeric N protein complex specifically recognizes the panhandle structure to form an RNP complex with a single vRNA segment (Hussein et al., 2011).

The GPC encoded by the M segment is a polypeptide that is co-translationally cleaved by the cellular signal peptidase complex. GPC is coordinated by two signal sequences. The first one at the N-terminus, targeting the GPC to the lumen of the ER. A second cleavage site, is located in the GPC and can be cleaved by a cellular signal peptidase complex giving rise to the mature Gn and Gc glycoproteins (Hepojoki et al., 2012; Cifuentes-Munoz et al., 2014). When the spike complex, consisting of four Gn and four Gc molecules (Hepojoki et al., 2009), is assembled and transported to the Golgi compartment, the cytoplasmic tails of Gn and Gc interact with the newly formed RNPs (Hepojoki et al., 2010; Wang et al., 2010). It is still unclear how the RdRP is packed into mature virions. It is thought to be associated with the RNPs and could be packaged together with this complex. It is also not known how hantaviruses ensure that three different vRNA-containing RNPs are packed inside each virion. It is possible that the Gn cytoplasmic tail, having RNA-binding activity (Strandin et al., 2011), guides the vRNA segments, as shown for other segmented negative-sense RNA viruses (Terasaki et al., 2011; Zheng and Tao, 2013).

Finally, the virion buds inside the Golgi (Figure 2), and the newly formed virion is released to the extracellular milieu from the Golgi, probably via exocytosis (Rowe et al., 2008). Glycoproteins and budding of ANDV, HTNV, and SNV have also been detected at the plasma membrane of the cell (Cifuentes-Munoz et al., 2014). Details of virion egress are still largely unknown.

1.4 HANTAVIRUS INFECTION IN HUMANS

1.4.1 Disease manifestation and epidemiology

Hantaviruses are zoonotic viruses, meaning they can be transmitted from an animal to humans. Pathogenic hantaviruses are mainly transmitted to humans through the inhalation of aerosols from virus-contaminated rodent excreta (Figure 3a). In humans they can cause two diseases: hemorrhagic fever with renal syndrome (HFRS), which is primarily caused by Hantaan orthohantavirus (HTNV) and related viruses in Asia, PUUV and Dobrava-Belgrade orthohantavirus (DOBV) in Europe and Seoul orthohantavirus (SEOV), which is distributed worldwide; or hantavirus cardiopulmonary syndrome (HCPS), which is mainly caused by SNV in North America, and ANDV in Latin America (Figure 3a, Vaheri et al., 2013b; Jiang et al., 2017).

Annually, more than 10,000 individuals are diagnosed with HFRS and numbers are increasing (Vaheri et al., 2013a). Early disease manifestations come with flu-like symptoms, head and abdominal pain, myalgia and gastrointestinal symptoms and in severe cases, hypotension, acute shock, vascular leakage, and kidney failure. Reported case-fatality rates are up to 10% for HFRS and around 35%–40% for HCPS (Figure 3a, Krautkrämer et al., 2013; Manigold and Vial, 2014). Hantavirus disease in Europe, called *Nephropathia epidemica* (NE, caused by PUUV), normally shows only mild to moderate symptoms (Faber et al., 2019).

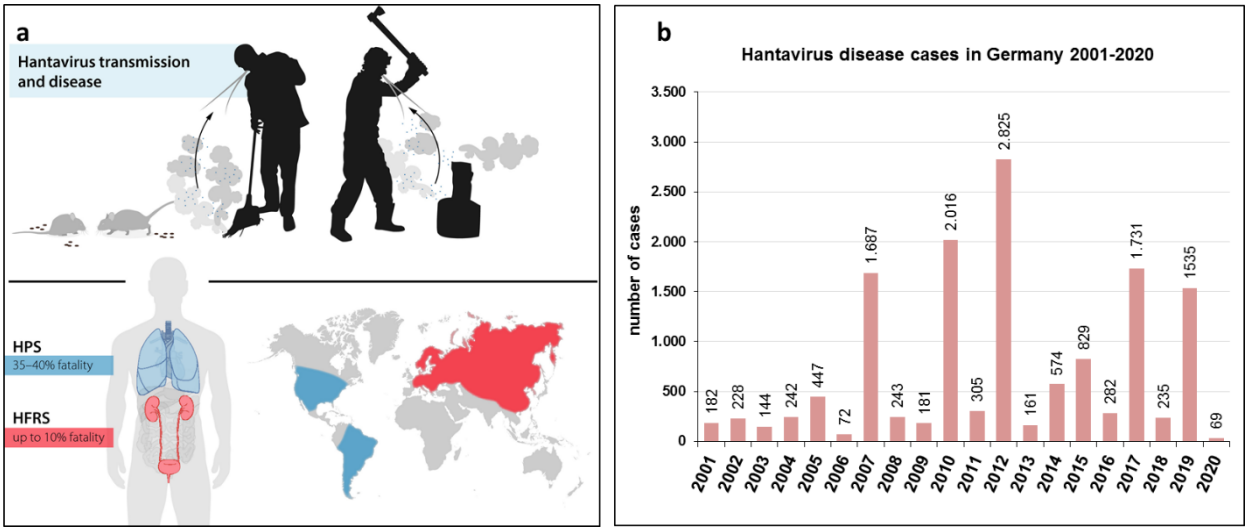

Figure 3: Hantavirus transmission and disease. (a) *Infectious particles are trasmitted by inhalation of rodent excreta. Disease manifestations are Hantavirus pulmonary syndrome (HCPS) or hemorrhagic fever with renal syndrome (HFRS) dependent on the virus involved (Adapted from Klingström et al., 2019).* ***(b)*** *Hantavirus disease cases in Germany since the introduction of the German Protection against Infection Act in 2001 until 29.06.2020 (Source: survstat.rki.de).*

Hemorrhages and hypotension causing severe shock syndrome are rarely observed. Infection with DOBV genotypes Dobrava and Sochi can result in severe disease outcome, whereas genotype Kurkino leads to milde disease, similar to NE. Specific kidney therapy such as dialysis is only necessary in less than 5% and case fatality rates for PUUV are less than 1% (Krautkrämer et al., 2013; Latus et al., 2015; Avšič-Županc et al., 2019).

In Germany, hantavirus infections are notifiable since 2001 and more than 14,000 cases were reported since then. Interestingly, outbreak years (with more than 1,500 cases each) were reported in 2007, 2010, 2012, 2017, and 2019 which might be associated to bank vole mass reproduction in the same year (Figure 3b) (Faber et al., 2019). Currently, there is no treatment or approved preventive vaccine available for this disease. The two syndromes HFRS and HCPS share most aspects of disease, and the pathogenesis is rather similar. However there are some differences in organ manifestations and, importantly, in severity of disease outcome. Hantavirus infection in humans causes an excessive immune activation including massive cytokine responses and activation of cytotoxic lymphocytes (CTLs) (Schönrich et al., 2008; Björkström et al., 2011; Lindgren et al., 2011; García et al., 2017). Patients also show increased infiltration of immune cells into target organs (Linderholm et al., 1993; Klingström et al., 2006b; Scholz et al., 2017; Klingström et al., 2019). Together, these responses contribute to the pathological outcome during infection, highlighting the fact that hantavirus-induced pathogenesis in humans is clearly driven by immunological factors (Schönrich et al., 2008).

1.4.2 Human innate immune response

Interactions of hantaviruses and the host immune system are of outstanding importance for course of infection, susceptibility, transmission, and outcome in host organisms. The host immune response to viral pathogens can be broadly divided into an adaptive and an innate part. The adaptive immune response is characterized by specific pathogen recognition by T- and B-cells. They have to develop before they can act against viral invaders to form a highly diverse repertoire of antigen receptors. This delays the adaptive responses for 5–7 days. In the early phase of infection, pathogens have to be dealt with by the innate immune response, which represents the more universal part of host defense (Murphy et al., 2008).

Viruses invading a host are detected early during infection mainly by pattern recognition receptors (PRRs) on cells at the host-pathogen interface (Takeuchi and Akira, 2007; Kell and Gale, 2015). PRRs interact with conserved structural motifs, called pathogen-associated molecular patterns (PAMPs), displayed by infectious agents. They activate the innate immune response such as type I IFN (IFN-I) and pro-inflammatory cytokines which impair virus replication and induce long-term immune responses for elimination of viral infections (Takeuchi and Akira, 2007). Such PRRs include sensors like retinoic acid inducible gene-I (RIG-I) or melanoma differentiation antigen-5 (MDA-5). RIG-I recognizes uncapped 5'-triphosphate ends of ssRNA and double stranded (ds) RNA with blunt ends or 5'-overhang (Kell and Gale, 2015). Activation of RIG-I initiates a signaling cascade through tumor necrosis factor (TNF) receptor associated factor 3 (TRAF3), TRAF-family member-associated NFκB activator binding kinase 1 (TBK-1) and IκB-Kinase ε (IKKε), leading to phosphorylation of transcription factors such as interferon regulatory factor-3 or -7 (IRF-3/-7). When phosphorylated, IRF-3/-7 dimerizes and translocates to the nucleus, where it initiates IFN-I synthesis (Kell and Gale, 2015). IFN-β is then secreted from the cell and binds to its receptor initiating the IFN signaling pathway and thereby an antiviral state in infected and neighboring cells (Figure 4). Thus, TRAF3, TBK1, IKKε and IRF-3 represent important factors for activation of innate antiviral IFN response (Rang, 2010).

The Janus kinase/signal transducers and activators of transcription (JAK/STAT) pathway, is the principal signaling mechanism for a wide array of cytokines and growth factors in mammals (Figure 4). It is activated by IFN and causes expression of interferon stimulated genes (ISGs), such as Myxovirus resistance (Mx) genes or Protein kinase R (PKR), by translocating ISG-factor 3 into the nucleus. The human MxA protein shows antiviral activity against different members of the order *Bunyavirales* by recognizing and segregating the RNP complex (Frese et al., 1996). It was shown to inhibit hantavirus growth *in vitro* (Kanerva et al., 1996; Oelschlegel et al., 2007).

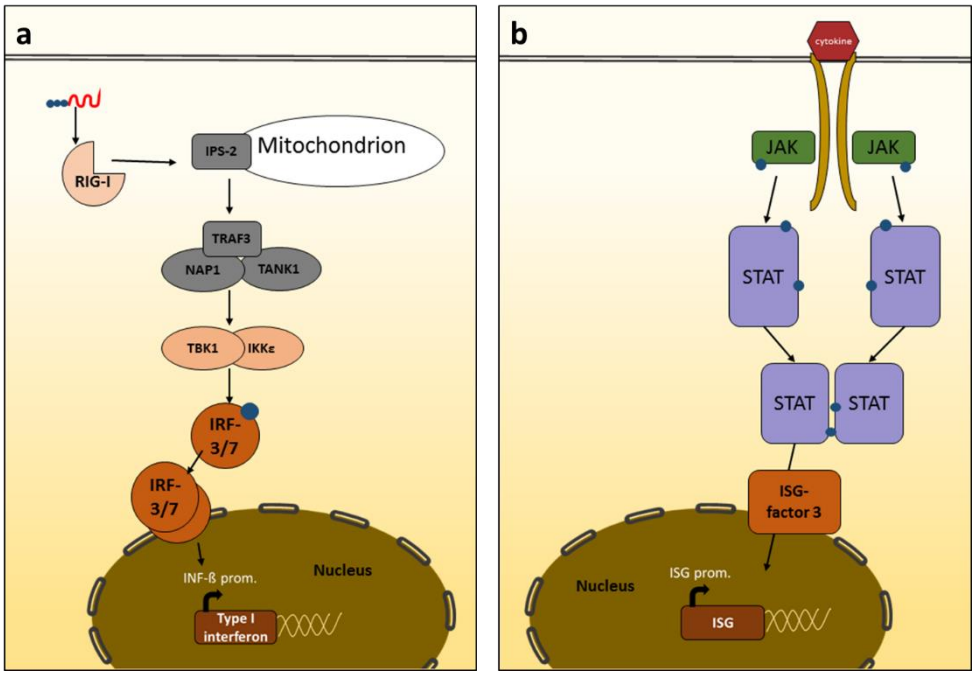

Figure 4: Signaling cascade of interferon (IFN) induction in infected cells (a) and the Janus kinase/signal transducers and activators of transcription (JAK/STAT) pathway (b). (a) *Retinoic acid inducible gene-I (RIG-I) and/or melanoma differentiation antigen-5 (MDA-5) recognize uncapped ssRNA 5'-triphosphates/5'-overhang or blunt dsRNA ends and lead to activation of signaling through TNF receptor associated factor 3 (TRAF3). TRAF-family member-associated NFκB activator binding kinase 1 (TBK1) and IκB-Kinase ε (IKKε) phosphorylate transcription factors interferon regulatory factor-3/-7 (IRF-3/-7) which dimerize and translocate to the nucleus for activation of IFN synthesis (left).* ***(b)*** *The JAK/STAT pathway recognizes cytokines such as interferon sequestered from infected cells in neighboring cells and activates the expression of interferon stimulated genes (ISGs) by translocating ISG-factor 3 into the nucleus (right).*

Even though hantaviruses are relatively poor inducers of IFN-I, induction of ISGs including the MxA protein has been observed after hantavirus (TULV, HTNV) infection (Kraus et al., 2004). The induction of ISGs by hantaviruses requires viral replication and was associated at least in part with activation of IRF-3 (Spiropoulou et al., 2007). Most likely, not a single factor but multiple IFN induced antiviral components are required for efficient clearance of hantavirus infection and prevention of disease manifestations in humans (Rang, 2010). There is also a clear difference between pathogenic and non-pathogenic hantaviruses when it comes to induction of an early IFN response. Non-pathogenic hantaviruses, like Prospect Hill orthohantavirus (PHV), induce a robust IFN response early after onset of infection whereas pathogenic ones (PUUV, SNV) do not (Spiropoulou et al., 2007; Rang, 2010; Spiropoulou, 2011).

1.5 HANTAVIRUS INFECTION IN RODENT RESERVOIRS

1.5.1 Virus-host adaptation

In small mammal reservoirs, virus-host interaction has been evolved during a long lasting co-evolution scenario. In general, hantavirus infection is described as persistent in its reservoir hosts, meaning the virus is present in host cells at low levels, maintaining the capacity for replication at some time point (Villarreal et al., 2000; Voutilainen et al., 2015). However, hantavirus-induced immune responses can have influence on rodent reservoir hosts such as the hantavirus transmission between rodents and the fitness of infected rodents.

Infection experiments of natural reservoirs of HTNV, SEOV, PUUV, and SNV have shown different time points of viremia onset in hosts after infection: approximately a few days for SEOV (Kariwa et al., 1996) or 2–3 weeks for PUUV, HTNV and SNV (Lee et al., 1981; Yanagihara et al., 1985; Botten et al., 2000). Early during infection, infectious virus can be detected and recovered from different organs. The acute phase usually ends after 2–3 weeks but viral shedding by saliva, urine, and feces is then detectable throughout the course of infection and seems to be persistent (Lee et al., 1981; Yanagihara et al., 1985; Kariwa et al., 1996; Bernshtein et al., 1999; Voutilainen et al., 2015). Examination of tissues from infected rodents more than one year after infection showed that only lungs (PUUV, HTNV, SEOV, and SNV), heart (SNV), or liver (PUUV) exhibited signs of infection (Lee et al., 1981; Yanagihara et al., 1985; Kariwa et al., 1996; Netski et al., 1999; Botten et al., 2003; Voutilainen et al., 2015), indicating that virus RNA positive tissues from the acute phase can become negative during the persistent phase. High titers of hantavirus-specific antibodies circulating in the rodents can be detected lifelong and the antibody response to the N protein is broadly used for diagnostics in reservoir rodents. Additionally, the envelope glycoproteins Gn and Gc are main inducers of this protective humoral response (Cifuentes-Munoz et al., 2014). Animal studies have shown that hantaviruses can persist in hosts despite the presence of high titers of neutralizing antibodies. These observations have led to the assumption that hantaviruses can escape immune responses and that infection is asymptomatic and has no impact on survival or fertility in their reservoir hosts (Childs et al., 1989). In contrast, more recent experimental and field data do not support these assumptions, e.g. PUUV infection has a negative influence on the over-winter survival of an island population of bank voles (Kallio et al., 2007). There are also reports of histopathologic lesions in some of the natural hosts of certain HCPS-causing hantaviruses (Lyubsky et al., 1996; Netski et al., 1999).

1.5.2 Innate immunity in rodents

To date only little attention has been given to innate immunity in natural rodent reservoirs. Current knowledge mainly originates from studies on gender dependent expression of genes encoding for proteins associated with innate antiviral defenses in SEOV-infected rats. SEOV-infected female rats showed higher expression of Toll-like receptor-7 (TLR-7), RIG-I, and IRF-7, than SEOV-infected males (Hannah et al., 2008). This results in higher production of IFN-I, which leads to an increased expression of ISGs. In particular, the gene expression of cytoplasmic Mx2 is suppressed in male rats during SEOV infection and may contribute to increased virus shedding and viral RNA levels in lung tissues (Klein et al., 2001). Elevated pro-inflammatory cytokine levels are not systematically detected in hantavirus infected rodents. Considering nitric oxide (NO), laboratory mice that die after DOBV (strain Slovenia) inoculation exhibit high levels of nitrites, whereas no evidence of elevated NO is found in SNV-infected deer mice (Klingström et al., 2006a).

In contrast to the activation of an innate immune response in human endothelial cells, characterized by the upregulation of IFN-β and subsequent activation of ISGs, PUUV did not trigger this response in primary fibroblastoid cells of the reservoir host (Stoltz et al., 2011). This may lead to the assumption that PRRs of reservoir host cells either do not detect the vRNAs or are inhibited by a still unknown mechanism. Additionally, dendritic cells (DCs) encountering viruses respond to different signals received through several PRRs, which then determine the quality of the T-cell response. In their rodent reservoir host, DCs could be primed by hantavirus-associated PRRs to stimulate regulatory T-cells that can suppress virus-specific CTLs (Klingström et al., 2019). This would lead to viral persistence and at the same time preventing virus-induced immunopathology.

1.6 VIRAL COUNTER MEASURES TO HOST IMMUNE DEFENSE

For efficient replication and establishment of an infection, most, if not all, pathogenic viruses have evolved sophisticated mechanisms to escape induction of the antiviral immune response at least in part. The ability to escape or block the innate IFN system is a key feature for the virulence of most pathogenic viruses (Haller et al., 2007; Randall and Goodbourn, 2008). The exact mechanisms regulating replication of hantaviruses are still not well understood. This is particularly true for natural rodent reservoirs. RNA viruses have evolved with multifunctional proteins (Reuter and Krüger, 2017) or overlapping coding strategies within other ORFs (Jayaraman et al., 2016). Capsid proteins, as the hantaviral N protein, or the glycoproteins have multiple functions. Glycoproteins exist in dynamic conformations that can switch between two states, maintaining their respective biological functions. ANDV-N protein was reported to inhibit IFN signaling by the cytoplasmic dsRNA sensors RIG-I and MDA-5. This mechanism was found to be mediated by a single serine residue at position 386 in the N protein (Levine et al., 2010; Simons et al.,

2019). It was also shown that ANDV-N inhibits IFN signaling responses by interfering with TBK-1 activation, upstream of IRF-3 phosphorylation (Cimica et al., 2014). There is also evidence, that in human primary endothelial cells, IFN-I response including MxA expression is delayed in cells that are infected with pathogenic hantaviruses in contrast to non-, or low-pathogenic hantaviruses (Geimonen et al., 2002; Kraus et al., 2004). For PUUV this may be caused by an increased turnover of MxA protein (Handke et al., 2010). Moreover, hantaviruses cannot only downregulate PRR-mediated IFN-I production but also interfere with IFN signaling by yet undefined mechanisms (Spiropoulou et al., 2007; Stoltz and Klingström, 2010).

Another counter mechanism, used by hantaviruses, is to avoid IFN induction by modification of their 5' vRNA ends. This is caused by the viral RdRP activity as it cleaves off the first nucleotide at the 5'-end of the genome, resulting in a monophosphorylated 5'-end (Garcin et al., 1995; Habjan et al., 2008). There is also evidence that the Gn cytoplasmic tail of TULV and New York virus (NYV), a SNV strain, can interfere with RIG-I-mediated signaling (Alff et al., 2006; Matthys et al., 2011). New world hantavirus Gn/Gc was also reported to reduce Sendai virus induced IFN-β promoter-driven reporter gene activity (Levine et al., 2010).

Finally, one possible way of hantaviral immune counteraction is the recently described non-structural protein NSs. It was suggested that NSs proteins of PUUV and TULV function as a weak inhibitor of the IFN response. For PUUV, two variants of the prototype strain Sotkamo were plaque-purified, of which one was found to have a stop codon in the NSs ORF (Rang et al., 2006). However, these viruses have not been analyzed on potential differences in their replication kinetics and their ability to overcome innate immune responses.

1.7 CELL CULTURE SYSTEMS USED FOR HANTAVIRUSES

Hantaviruses replicate primarily in endothelial cells (ECs) of an infected patient and endothelial cell cultures are therefore often used *as in vitro* models for hantavirus infection (Temonen et al., 1993; Hepojoki et al., 2014). Hantaviruses were also found to infect cell lines like Vero (African green monkey) but also Huh7, A549 (human liver or lung carcinoma) and primary human monocytes or DCs *in vitro* (Pensiero et al., 1992; Temonen et al., 1993; Raftery et al., 2002). VeroE6 cells are most commonly used for virus production. Their high productivity is due to the lack of IFN-I production caused by a huge chromosomal deletion. In most of the cell lines infected, no obvious cytopathic effects caused by the infection could be detected. A major drawback for studying pathogenesis and replication of hantaviruses is, that they are difficult to isolate and to propagate. Several groups have tried isolation of HTNV since it was identified in 1952. However, it was not until 1981 that adaptation and propagation of HTNV strain

76–118 isolated from *Apodemus agrarius coreae* was described *in vitro* (French et al., 1981). In the following years several cell culture systems were established based on VeroE6 cells (Yanagihara et al., 1984; Pensiero et al., 1992; Temonen et al., 1993; Raftery et al., 2002). Propagation of hantaviruses is mainly successful with highly cell culture adapted strains. This adaptation can lead to severe restrictions for hantavirus infectivity (Lundkvist et al., 1997; Nemirov et al., 2003).

Rodent-derived cell culture models, which reflect the unique virus-host adaptation, are still rare (Eckerle et al., 2014b). They can be beneficial in virus isolation, functional studies, and strategies counteracting these pathogens (Drewes et al., 2017b). Mainly primary bank vole cells were used for functional analysis of PUUV so far (Temonen et al., 1993; Stoltz et al., 2011). One attempt to establish a bank vole derived permanent cell line for PUUV studies was partly successful: A spontaneously immortalized kidney cell line of a bank vole was susceptible for a variety of different viruses. However, when infected with PUUV strain Vranica/Hällnäs, these cells could be infected but did not replicate and produce infectious virus (Essbauer et al., 2011). A successful attempt to isolate Hokkaido virus (HOKV), a PUUV strain, was recently possible through the establishment of a kidney cell line from its host the grey red-backed vole (*Clethrionomys rufocanus bedfordiae*) that also showed high replication capacities for other PUUV isolates from Europe (Sanada et al., 2012).

1.8 OBJECTIVES

In the recent years many emerging RNA viruses from wildlife reservoirs, such as hantaviruses, have gained more and more attention and are perceived as a major threat for human health. So far, there is little knowledge on hantavirus-host interaction in their natural reservoir and most currently available *in vitro* systems do not reflect characteristics of reservoir specific virus-host interactions. Investigating the immune mechanisms underlying the characteristics of hantavirus infection in their natural reservoirs appears essential in terms of assessing persistence and susceptibility to infection. Therefore, the aims of this work were:

- → to conduct PUUV surveillance studies in bank voles from Germany for the future development of an early warning model
- → to investigate the spatially and temporally driven evolution of PUUV S segment in bank voles
- → to characterize novel vole-derived cell lines for their susceptibility and replication capacity for PUUV, TULV and other viruses
- → to isolate a central European PUUV strain
- → to assess the function of the hantaviral NSs protein in the inhibition of the IFN-I response in the human system

2. PUBLICATIONS

(I) HETEROGENEOUS PUUMALA ORTHOHANTAVIRUS SITUATION IN ENDEMIC REGIONS IN GERMANY IN SUMMER 2019

Binder, F.*, Drewes, S.*, Imholt, C., Saathoff, M., Below, A.D., Bendl, E., Conraths, F.J., Tenhaken, P., Mylius, M., Brockmann, S., Oehme, R., Freise, J., Jacob, J., Ulrich, R.G.

Transboundary and Emerging Diseases

Volume 67, Issue 2

November 2019

DOI:10.1111/tbed.13408.

*authors contributed equally to this publication

Received: 18 July 2019 | Revised: 10 October 2019 | Accepted: 25 October 2019

DOI: 10.1111/tbed.13408

RAPID COMMUNICATION

Transboundary and Emerging Diseases WILEY

Heterogeneous Puumala orthohantavirus situation in endemic regions in Germany in summer 2019

Florian Binder[1] | Stephan Drewes[1] | Christian Imholt[2] | Marion Saathoff[3] | Diana Alexandra Below[2] | Elias Bendl[1] | Franz J. Conraths[4] | Peter Tenhaken[5] | Maren Mylius[6] | Stefan Brockmann[7] | Rainer Oehme[7] | Jona Freise[3] | Jens Jacob[2] | Rainer G. Ulrich[1]

[1]Friedrich-Loeffler-Institut, Federal Research Institute for Animal Health, Institute of Novel and Emerging Infectious Diseases, Greifswald-Insel Riems, Germany

[2]Julius Kühn-Institut, Federal Research Centre for Cultivated Plants, Institute for Plant Protection in Horticulture and Forests, Vertebrate Research, Münster, Germany

[3]Lower Saxony State Office for Consumer Protection and Food Safety, Veterinary Task-Force, Department of Pest Control, Oldenburg, Germany

[4]Friedrich-Loeffler-Institut, Federal Research Institute for Animal Health, Institute of Epidemiology, Greifswald-Insel Riems, Germany

[5]Health Office, Osnabrück, Germany

[6]The Governmental Institute of Public Health of Lower Saxony, Hannover, Germany

[7]State Health Office Baden-Württemberg, Stuttgart, Germany

Correspondence
Jens Jacob, Julius Kühn-Institute, Federal Research Centre for Cultivated Plants, Institute for Plant Protection in Horticulture and Forests, Vertebrate Research, Münster, Germany.
Email: jens.jacob@julius-kuehn.de

Funding information
The work of the RoBoPub consortium was supported by the Federal Ministry of Education and Research (BMBF) within the Research Network Zoonotic Infectious Diseases (FKZ 01KI1721A RGU, 01KI1721H JF, 01KI1721D MM, 01KI1721E JJ). Further funding was provided by the Federal Environment Agency (UBA) within the Environment Research Plan of the German Federal Ministry for the Environment, Nature Conservation, Building and Nuclear Safety (BMUB) (FKZ 3716484310 JJ). The funding organizations had no influence on the data collection, data interpretation and decision to publish.

Abstract

Puumala orthohantavirus (PUUV) causes most human hantavirus disease cases in Europe. PUUV disease outbreaks are usually synchronized Germany-wide driven by beech mast-induced irruptions of its host (bank vole, *Myodes glareolus*). Recent data indicate high vole abundance, high PUUV prevalence and high human incidence in summer 2019 for some regions, but elsewhere values were low to moderate. This significant lack of synchrony among regions in Germany is in contrast to previous studies. Health institutions need to be informed about the heterogeneous distribution of human PUUV infection risk to initiate appropriate actions.

KEYWORDS

bank vole, emerging virus, HFRS, infection risk, outbreak, Puumala orthohantavirus

Binder and Drewes contributed equally to this publication.

1 | INTRODUCTION

Hantaviruses are emerging pathogens that can cause human disease worldwide (Krüger, Figueiredo, Song, & Klempa, 2015). Puumala orthohantavirus (PUUV) is the most relevant hantavirus in Europe: It causes the majority of human hantavirus disease cases in Europe and is distributed in several parts of the continent. The number of human cases in Fennoscandia, Belgium, France and Germany oscillates among outbreak and non-outbreak years (Ettinger et al., 2012; Heyman, Ceianu, Christova, Tordo, & Vaheri, 2011; Olsson, Leirs, & Henttonen, 2010; Reil, Imholt, Eccard, & Jacob, 2015; Reil et al., 2017). Human PUUV infections lead to a mild to moderate course of symptoms called nephropathia epidemica (NE) characterized by an acute onset of high fever, headache, myalgias, gastrointestinal symptoms and thrombocytopenia (Latus et al., 2015). Later, renal insufficiency or an acute renal failure may occur. Severe haemorrhagic fever with renal syndrome (HFRS) rarely appears in patients with PUUV infection (Heyman, Vaheri, Lundkvist, & Avšič-Županc, 2009; Krüger, Ulrich, & Hofmann, 2013; Latus et al., 2015; Vaheri et al., 2013). The reservoir of PUUV is the bank vole (*Myodes glareolus*), which is a forest rodent distributed in most parts of Europe (Mitchell-Jones et al., 1999). PUUV, as all hantaviruses that are pathogenic for humans, is transmitted to humans by aerosols of dried rodent faeces and urine or by biting via infectious saliva (Vaheri et al., 2013). Bank vole population abundance fluctuates more or less regularly across Europe (Jacob & Tkadlec, 2010) but the degree of regularity may vary depending on region and time. In temperate Europe, population peaks are driven by food supply available through tree seed mast in beech (*Fagus* spec.) and other forest trees (Clement et al., 2009). This provides ample food over winter resulting in early reproduction (Eccard & Ylönen, 2001) and population irruption in the following year (Reil et al., 2015).

In Germany, human NE cases are mainly restricted to the southern and western parts of the country (Drewes, Ali, et al., 2017) (Figure 1). This heterogeneous distribution of PUUV has been explained by postglacial recolonization of Central and Western Europe by the Western evolutionary lineage of the bank vole (Drewes, Ali, et al., 2017). There is considerable fluctuation in human hantavirus disease cases in Germany with outbreaks in the years 2007, 2010, 2012 and 2017. Outbreaks are usually spatially synchronized among endemic regions of Germany (Ettinger et al., 2012) (Figure 1). Human PUUV prevalence can be high in any endemic region but more people seem to be affected in the south. The variation in human PUUV prevalence in endemic regions of western Germany may be due to regional differences in forest structure (Magnusson et al., 2015; Voutilainen et al., 2012). This region exhibits the highest degree of landscape fragmentation in Germany (Walz, Krüger, & Schumacher, 2011), a more continuous forest cover in the south can increase human PUUV incidence (Drewes, Turni, et al., 2017).

The objective of this study was to find out putative early predictors of a hantavirus outbreak year in Germany and to prove if these parameters and the human incidence data in 2019 indicate a homogenous outbreak pattern.

2 | MATERIAL AND METHODS

Regular bank vole monitoring was conducted in several German federal states (Figure 2) following a standard snap trapping protocol (Drewes, Schmidt, Jacob, Imholt, & Ulrich, 2016). Trapped bank voles were stored frozen at −20°C until dissection. Data are reported as individuals per 100 trap nights (TN) to adjust for variation in trap success. Sites were selected because they are situated in or close to known endemic regions (see Drewes, Turni, et al., 2017; Ettinger et al., 2012; Faber et al., 2013; Reil et al., 2017; Weber de Melo et al., 2015).

To determine the PUUV infection rate in bank voles, lung tissue was sampled from 249 of the 375 bank voles trapped. A pin head-sized piece was minced, RNA isolated and tested by conventional standard RT-PCR targeting the small (S) segment (Drewes, Ali, et al., 2017). RT-PCR products were sequenced for PUUV detection by dideoxy-chain termination method using BigDye Terminator v1.1 Kit (Applied Biosystems, Darmstadt, Germany).

Beech fructification intensity was estimated between July and August 2018 as the percentage of fruiting beech trees older than 49 years, classified in absent, scarce, common and abundant fructification. Beech fructification is assessed annually by State Forest Authorities and reported as a mean value for each Federal State (Reil et al., 2015).

Human PUUV incidence was retrieved from SurvStat@RKI 2.0, https://survstat.rki.de and is reported as cases per 100,000 inhabitants (data status 30.08.2019). These data are reported to the national register irrespective of the hantavirus species. The vast majority of human hantavirus infections in Germany is caused by PUUV, whereas Dobrava-Belgrade virus (DOBV, genotype Kurkino) infections are largely restricted to the east of Germany where the reservoir species, the striped field mouse (*Apodemus agrarius*) is present (Faber et al., 2019; Hofmann et al., 2014; Krüger et al., 2013). Therefore, we use the reported incidence data as a proxy for human infection with PUUV and use the term 'PUUV infection' throughout, since our analysed data come from the southern and western part of Germany rather than the eastern part where DOBV mostly occur.

To test for differences between human PUUV incidence patterns in 2019 and the mean pattern of previous outbreak years, we conducted a multiple linear regression analysis with incidence as the dependent variable and the respective week and year (2019 vs. mean outbreak) as well as their interaction as explanatory variables.

FIGURE 1 Spatial distribution of cumulative incidence classes of notified human hantavirus disease cases per district per 100,000 inhabitants for the years 2001–2018. The number of districts per class is stated in parentheses. Map and data retrieved on 30th August 2019, Robert Koch-Institute, SurvStat@RKI 2.0, https://survstat.rki.de

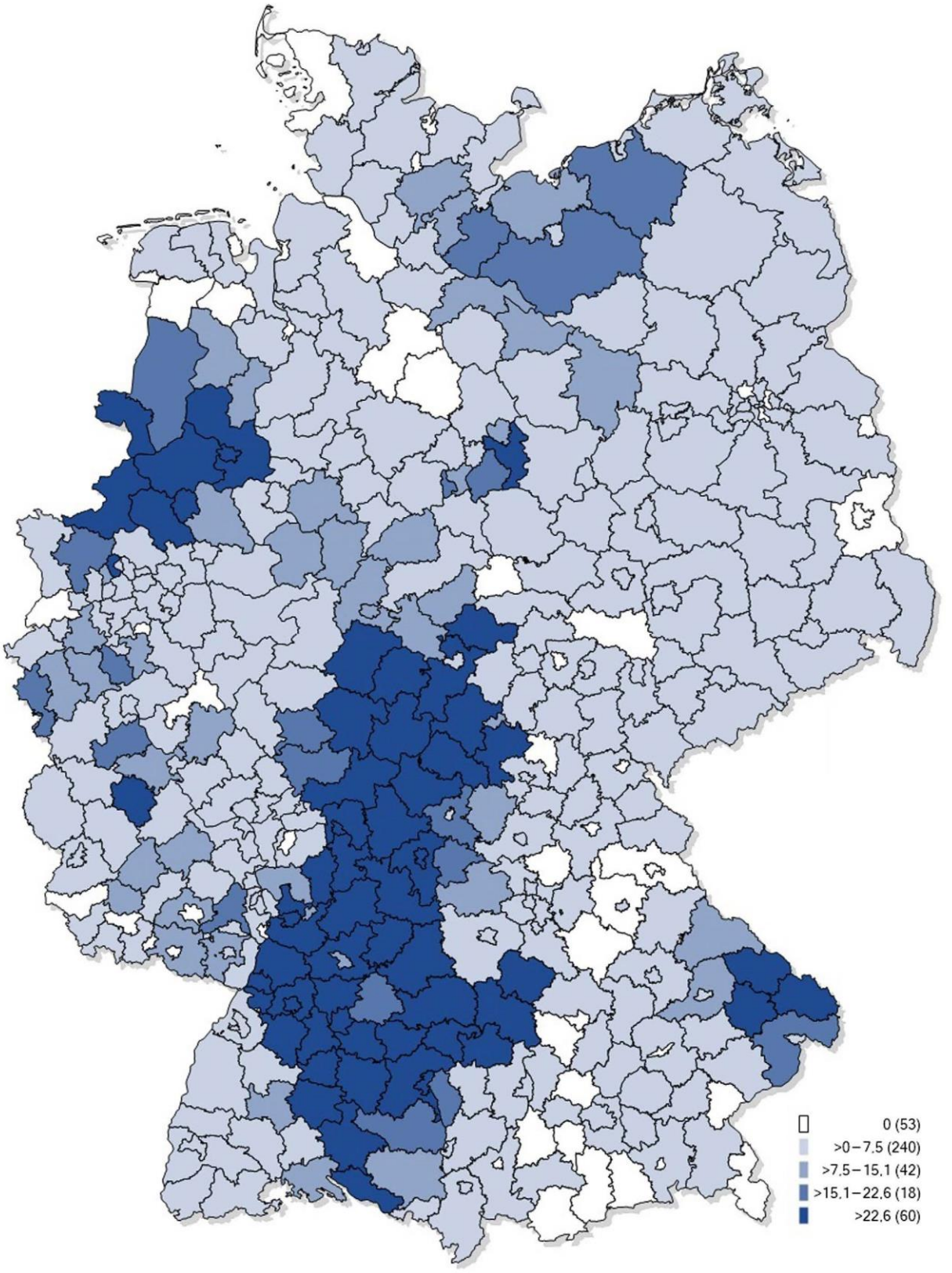
0 (53)
>0–7.5 (240)
>7.5–15.1 (42)
>15.1–22.6 (18)
>22.6 (60)

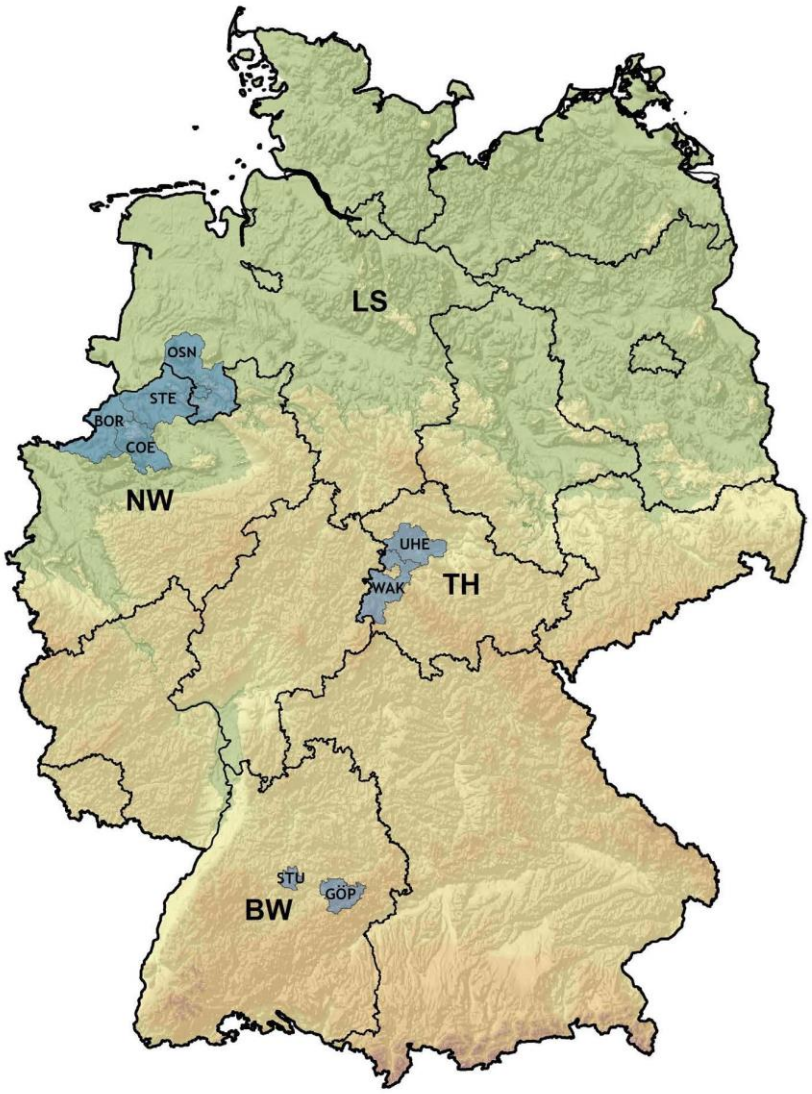

FIGURE 2 Regions in the north-west, centre and south of Germany, where vole abundance was recorded, samples for PUUV RNA detection were collected and matching information for human incidence was available. Map origin: Federal Agency for Cartography and Geodesy. Federal States: LS, Lower Saxony; NW, North Rhine-Westphalia; TH, Thuringia: BW, Baden-Wuerttemberg. Districts: OSN, Osnabrück; STE, Steinfurt; COE, Coesfeld; BOR, Borken; WAK, Wartburgkreis; UHE, Unstrut-Hainich-Kreis; GÖP, Göppingen; STU, Stuttgart

Non-significant interaction terms indicated no difference in the slope between 2019 and outbreak years.

3 | RESULTS AND DISCUSSION

Beech fructification intensity (Table 1) varied in 2018 from 18% to 65% indicating medium to abundantly fruiting trees. Beech mast has been reported to be highly synchronous but may differ regionally in some years (Reil et al., 2015). Bank vole abundance in spring 2019 varied strongly between regions (Table 1). Particularly high abundance was recorded in districts Steinfurt (north-west) and Göppingen (south) but elsewhere abundance was low (central) to moderate (regionally in the north-west) and was highly variable between regions and plots (Table 1).

Puumala orthohantavirus RNA detection rate generally followed beech mast intensity with high values in the south, regionally high-moderate values in the north-west and no evidence for PUUV RNA in bank voles from the central region but data were scarce for the latter. This pattern was roughly mirrored by human PUUV incidence (cumulative incidence of calendar weeks 1–33 in 2019) in these regions (Table 1). For comparison, incidence data for PUUV outbreak years (2007, 2010, 2012 and 2017) and intermittent non-outbreak years (2011, 2013–2016, 2018) are presented in Table 1.

Beech fructification in 2018 in the north-west and south was mainly at levels that can trigger bank vole population irruptions (Reil et al., 2015). This was well reflected in several locations where high bank vole abundance was recorded in spring 2019 but not everywhere. Especially in parts of the north-west, bank vole abundance was not particularly high. The high abundance values were in the range found during PUUV outbreaks in Germany in previous years (Reil et al., 2015). The regional and local differences in abundance might be explained by heterogeneous beech fructification and little beech fructification in the central region but there is no regional

TABLE 1 Beech fructification per region, bank vole trap success (individuals per 100 trap nights) per plot in spring 2019, PUUV RNA detection rate in bank voles in spring 2019 and human PUUV incidence in 2019 and in PUUV outbreak (2007, 2010, 2012, 2017) and non-outbreak years (2011, 2013–16, 2018) (cumulative for calendar weeks 1–33). Incidence values are values per district (2019) or means of districts across outbreak and non-outbreak years. Variance: standard deviation

Region	District	Beech fructification 2018	Bank vole trap success (plots)	PUUV RNA Detection rate (plots, total number of voles)	Human PUUV incidence		
					2019 (districts)	Outbreak (years, districts)	Non-outbreak (years, districts)
North-west	OSN	48%	5.3 ± 3.1 (8)	63 ± 13% (5, 75)	14.2 (1)	12.2 ± 1.3 (4, 1)	1.2 ± 1.0 (6, 1)
	STE	ca. 45%	15.4 ± 14.8 (3)	18 ± 19% (3, 24)	4.7 (1)	3.0 ± 2.2 (4, 1)	1.7 ± 1.4 (6, 1)
	COE/BOR	ca. 45%	7.6 ± 4.57 (9)	18 ± 23% (9, 80)	2.8–4.9 (2)	4.2 ± 0.9 (4, 2)	1.9 ± 1.2 (6, 2)
Central	WAK/UHE	18%	2.5 ± 4.0 (15)	0.0 (1, 11)	0–4.1 (2)	8.9 ± 5.2 (4, 2)	1.4 ± 1.9 (6, 2)
South	GÖP	ca. 65%	70 (1)*	57% (1, 7)	17.9 (1)	31.2 ± 14.2 (4, 1)	3.2 ± 4.8 (6, 1)
	STU	ca. 65%	2.9 (1)*	63% (1, 52)	15.2 (1)	15.6 ± 10.9 (4, 1)	2.1 ± 2.7 (6, 1)

Districts: OSN, Osnabrück; STE, Steinfurt; COE, Coesfeld; BOR, Borken; WAK, Wartburgkreis; UHE, Unstrut-Hainich-Kreis; GÖP, Göppingen; STU, Stuttgart.
*Trapping in GÖP and STU did not follow the protocol of Drewes et al. (2016).

information available for beech mast intensity (Table 1; Lower Saxony Ministry of Food, Agriculture, & Consumer Protection, 2018; Thuringian Ministry for Infrastructure & Agriculture, 2018). Despite the overwhelming effect of beech mast on bank vole population dynamics, it is possible that other factors such as local interaction in the food web or diseases have caused heterogeneous abundance of bank voles.

Puumala orthohantavirus RNA detection rate in the bank vole varied considerably with a peak at about 60% in the south and parts of the north-west, almost reaching values observed during previous PUUV outbreaks. For instance, PUUV RNA detection rate in district Osnabrück in spring of previous outbreak years was 86% (2010) and 75% (2012) (Weber de Melo et al., 2015). However, in other regions in the north-west and in central Germany PUUV RNA detection rate was low and did not reach prevalence values reported for previous outbreaks of PUUV in Germany (Reil et al., 2017). Although the relationship between abundance and RNA detection rate/seroprevalence varies seasonally and demographically (Reil et al., 2017), it is highly likely that some combination of bank vole abundance and RNA detection rate is an important risk factor for human PUUV infection. The snap-shot data from a limited selection of districts makes it difficult to draw firm conclusions in this regard, but earlier reports support this assumption (Drewes, Turni, et al., 2017).

A pattern similar to PUUV RNA detection rate in voles was found for the cumulative human PUUV incidence up to calendar week 33 (mid-August 2019). For some districts in the north-west and in the south, it reached or even exceeded values known from former outbreaks. However, PUUV incidence until mid-August 2019 in other districts in the north-west and in the central region was lower than the mean in outbreak years. In fact, only the curves for human PUUV incidence in Stuttgart ($p = .937$) and Osnabrück ($p = .201$) were similar to the mean outbreak curves (Figure 3), while this was not the case in all other districts ($p < .001$) indicating a typical outbreak situation in 2019 in two districts only. In Borken and Steinfurt, the curves for 2019 were different from the mean outbreak curve because the values in 2019 in these districts were higher than in the mean outbreak scenario. In all other districts, weekly cumulative PUUV incidence values until the mid-August 2019 were in between PUUV incidences of outbreak and non-outbreak years. These observations indicate a heterogeneous situation in 2019 in Germany and possibly the neighbouring countries in the west and south where PUUV occurs.

Temporal trends of cumulative human PUUV incidence appeared mostly consistent. In comparison to outbreak years, the temporal trends until mid-August 2019 show similar patterns of a steady increase with an initial flat rise and a steeper rise from spring on (Figure 3). This seems to be a promising feature for the development of district scale prediction of human risk based on PUUV incidence early in the year.

The lack of synchrony within and among regions contrasts earlier findings (Ettinger et al., 2012) and may be a new pattern. However, a similar phenomenon can occur at larger spatial scale: in 2005, a small outbreak was reported that seemingly affected only the western part of Germany and neighbouring countries (Mailles et al., 2005). Physicians and public health institutions should be aware of the

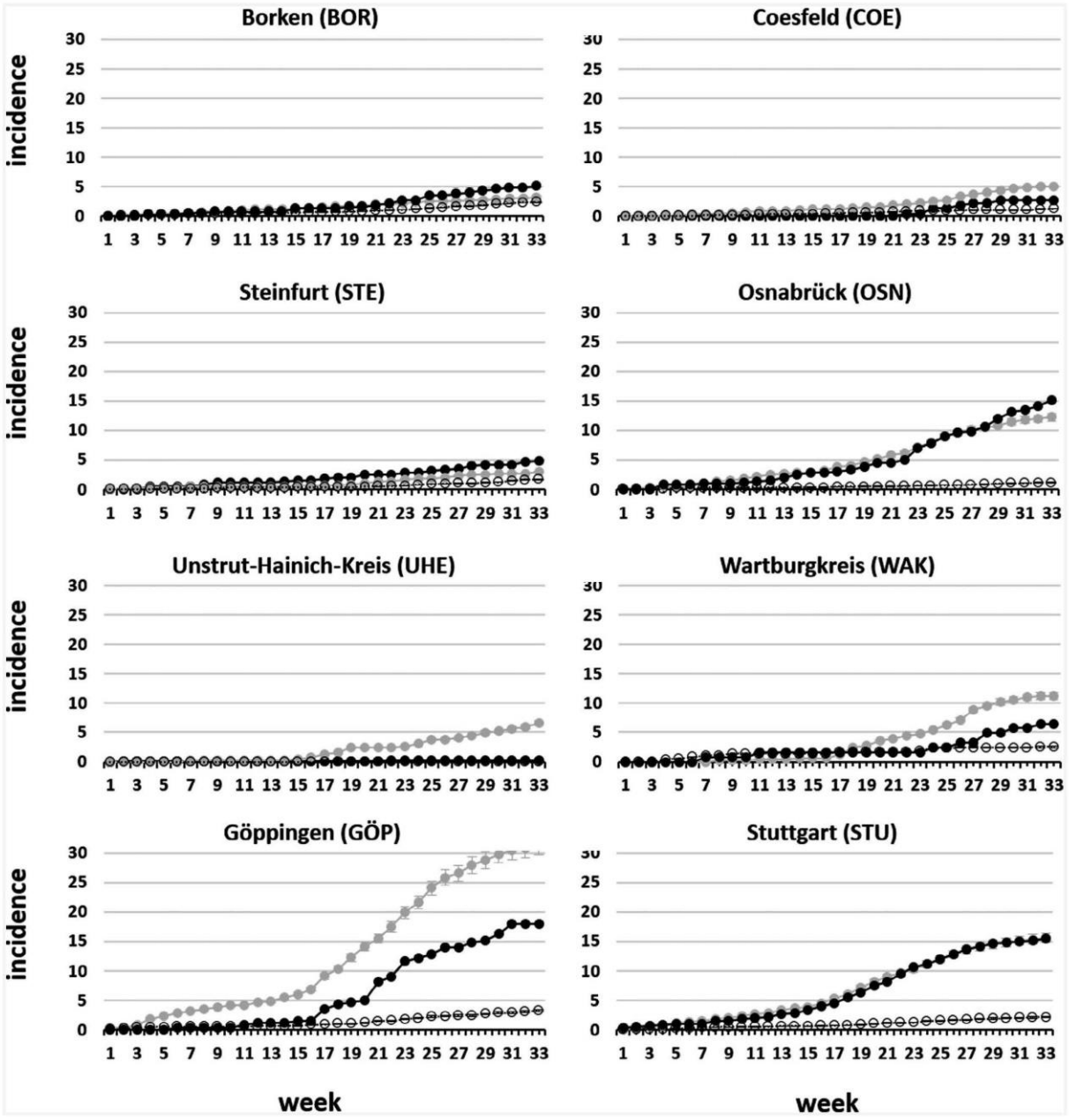

FIGURE 3 Weekly cumulative hantavirus incidence from 1st January until 18th August per district for 2019 (black line/dots), mean values for outbreak years (2007, 2010, 2012, 2017 – medium grey line/dots) and non-outbreak years (2011, 2013–2016, 2018 – dotted black line/dots). Data retrieved on 30th August 2019, Robert Koch-Institute, SurvStat@RKI 2.0, https://survstat.rki.de. 95% confidence intervals for the cumulative incidence of human infections in outbreak and non-outbreak years are given as error bars in the corresponding line colour

potential scenario of more localized outbreaks. The abundance of PUUV-infected bank voles is a major risk factor for human infection (Reil et al., 2015; Vanwambeke et al., 2019). It therefore seems reasonable to use information about vole abundance and PUUV prevalence in addition to data of human infections to assess human risk. Robust predictive models can aid such an approach but so far are only available at country (Tersago et al., 2009) or district scale (Reil et al., 2018), and the pathogen transmission system is still complex (Vanwambeke et al., 2019).

Physicians should consider hantavirus disease as differential diagnosis in patients to avoid false diagnoses, especially in risk groups that are prone to contract diseases with similar symptoms such as leptospirosis. Public health institutions can provide information on prevention of rodent infestations and other actions to minimize

hantavirus infections focusing on regions with higher risk for infections. Future investigations should evaluate the reasons for the lack of synchrony of outbreaks. This could include modelling population abundance of bank voles based on interactions with food, predators and landscape factors. Future studies might explore the effect of the ongoing drought in Central Europe on tree mast synchrony as well as the subsequent effects on spatial and temporal bank vole dynamics.

ACKNOWLEDGEMENTS

We thank Maya Braun, Hendrik Ennen, Philipp Harpering, Kyra Jacoblinnert, Engelbert Kampling, Jennifer Krieg, Philipp Koch and Sönke Röhrs for assistance in rodent trapping, Dörte Kaufmann, René Ryll, Elisa Heuser and Kim Usko for organ sampling and Gerhard Bojara for continuous support. We thank Nicole Reimer for creating Figure 2.

CONFLICT OF INTEREST

The authors declare that they have no conflict of interest.

ETHICAL APPROVAL

The authors confirm that the ethical policies of the journal, as noted on the journal's author guidelines page, have been adhered to. All relevant guidelines for the use of animals in scientific studies were followed.

ORCID

Christian Imholt https://orcid.org/0000-0002-7504-9509
Franz J. Conraths https://orcid.org/0000-0002-7400-9409
Jens Jacob https://orcid.org/0000-0002-5136-6606
Rainer G. Ulrich https://orcid.org/0000-0002-5620-1528

REFERENCES

Clement, J., Vercauteren, J., Verstraeten, W. W., Ducoffre, G., Barrios, J. M., Vandamme, A. M., … Van Ranst, M. (2009). Relating increasing hantavirus incidences to the changing climate: The mast connection. *International Journal of Health Geographics*, *8*, 1. https://doi.org/10.1186/1476-072X-8-1

Drewes, S., Ali, H. S., Saxenhofer, M., Rosenfeld, U. M., Binder, F., Cuypers, F., … Ulrich, R. G. (2017). Host-associated absence of human Puumala Virus infections in northern and eastern Germany. *Emerging Infectious Diseases*, *23*(1), 83–86. https://doi.org/10.3201/eid2301.160224

Drewes, S., Schmidt, S., Jacob, J., Imholt, C., & Ulrich, R. G. (2016). *APHAEA/EWDA Species card: Voles and Mouses*. Retrieved from http://www.aphaea.org/cards/species.

Drewes, S., Turni, H., Rosenfeld, U. M., Obiegala, A., Straková, P., Imholt, C., … Ulrich, R. G. (2017). Reservoir-driven heterogeneous distribution of recorded human Puumala virus cases in South-West Germany. *Zoonoses and Public Health*, *64*(5), 381–390. https://doi.org/10.1111/zph.12319

Eccard, J. A., & Ylönen, H. (2001). Initiation of breeding after winter in bank voles: Effects of food and population density. *Canadian Journal of Zoology*, *79*, 1743–1753. https://doi.org/10.1139/z01-133

Ettinger, J., Hofmann, J., Enders, M., Tewald, F., Oehme, R. M., Rosenfeld, U. M., … Krüger, D. H. (2012). Multiple synchronous outbreaks of Puumala virus, Germany, 2010. *Emerging Infectious Diseases*, *18*(9), 1461–1464. https://doi.org/10.3201/eid1809.111447

Faber, M., Krüger, D. H., Auste, B., Stark, K., Hofmann, J., & Weiss, S. (2019). Molecular and epidemiological characteristics of human Puumala and Dobrava-Belgrade hantavirus infections, Germany, 2001 to 2017. *Eurosurveillance*, *24*(32), 1–11. https://doi.org/10.2807/1560-7917.ES.2019.24.32.1800675

Faber, M., Wollny, T., Schlegel, M., Wanka, K. M., Thiel, J., Frank, C., … Stark, K. (2013). Puumala virus outbreak in Western Thuringia, Germany, 2010: Epidemiology and strain identification. *Zoonoses and Public Health*, *60*(8), 549–554. https://doi.org/10.1111/zph.12037

Heyman, P., Ceianu, C. S., Christova, I., Tordo, N., Beersma, M., João Alves, M., … Vaheri, A. (2011). A five-year perspective on the situation of haemorrhagic fever with renal syndrome and status of the hantavirus reservoirs in Europe, 2005–2010. *Euro Surveillance*, *16*(36), pii=19961. https://doi.org/10.2807/ese.16.36.19961-en

Heyman, P., Vaheri, A., Lundkvist, Å., & Avšič-Županc, T. (2009). Hantavirus infections in Europe: From virus carriers to a major public-health problem. *Expert Review of Anti-infective Therapy*, *7*(2), 205–217. https://doi.org/10.1586/14787210.7.2.205

Hofmann, J., Meier, M., Enders, M., Führer, A., Ettinger, J., Klempa, B., … Krüger, D. H. (2014). Hantavirus disease in Germany due to infection with Dobrava-Belgrade virus genotype Kurkino. *Clinical Microbiology and Infection*, *20*(10), O648–O655. https://doi.org/10.1111/1469-0691.12543

Jacob, J., & Tkadlec, E. (2010). Rodent outbreaks in Europe: Dynamics and damage. In G. R. Singleton, S. R. Belmain, P. R. Brown, & B. Hardy (Eds.), *Rodent outbreaks: Ecology and impacts* (pp. 207–223). Los Baños (Philippines): International Rice Research Institute.

Krüger, D. H., Figueiredo, L. T., Song, J. W., & Klempa, B. (2015). Hantaviruses–globally emerging pathogens. *Journal of Clinical Virology*, *64*, 128–136. https://doi.org/10.1016/j.jcv.2014.08.033

Krüger, D. H., Ulrich, R. G., & Hofmann, J. (2013). Hantaviruses as zoonotic pathogens in Germany. *Deutsches Ärzteblatt International*, *110*(27–28), 461–467. https://doi.org/10.3238/arztebl.2013.0461

Latus, J., Schwab, M., Tacconelli, E., Pieper, F. M., Wegener, D., Dippon, J., … Braun, N. (2015). Clinical course and long-term outcome of hantavirus-associated nephropathia epidemica, Germany. *Emerging Infectious Diseases*, *21*(1), 76–83. https://doi.org/10.3201/eid2101.140861

Lower Saxony Ministry of Food, Agriculture and Consumer Protection (2018). *Forest condition report 2018*. Retrieved from https://www.ml.niedersachsen.de/startseite/themen/wald_holz_jagd/wald_und_forstwirtschaft/zustand-des-niedersaechsischen-waldes-waldschaeden-und-risiken-5181.html.

Magnusson, M., Ecke, F., Khalil, H., Olsson, G., Evander, M., Niklasson, B., & Hornfeldt, B. (2015). Spatial and temporal variation of hantavirus bank vole infection in managed forest landscapes. *Ecosphere*, *6*(9), art163. https://doi.org/10.1890/Es15-00039.1

Mailles, A., Sin, M. A., Ducoffre, G., Heyman, P., Koch, J., & Zeller, H. (2005). Larger than usual increase in cases of hantavirus infections in Belgium, France and Germany, June 2005. *Eurosurveillance*, *10*(7), E050721.050724. https://doi.org/10.2807/esw.10.29.02754-en

Mitchell-Jones, A., Amori, G., Bogdanowicz, W., Kryštufek, B., Reijnders, P., Spitzenberger, F., … Zima, J. (1999). *The atlas of European mammals*. London: Academic Press T & AD Poyser Ltd.

Olsson, G. E., Leirs, H., & Henttonen, H. (2010). Hantaviruses and their hosts in Europe: Reservoirs here and there, but not everywhere? *Vector Borne Zoonotic Diseases*, *10*(6), 549–561. https://doi.org/10.1089/vbz.2009.0138

Reil, D., Binder, F., Freise, J., Imholt, C., Beyrer, K., Jacob, J., Ulrich, R. G. (2018). *Hantaviren in Deutschland: Aktuelle Erkenntnisse zu Erreger, Reservoir, Verbreitung und Prognosemodellen*. Berliner und Münchener Tierärztliche Wochenschrift, [online first - open access: https://vetline.de/index.cfm?cxml:id=2806&q=hantaviren+in+deutschland]. https://doi.org/10.2376/0005-9366-18003

Reil, D., Imholt, C., Eccard, J. A., & Jacob, J. (2015). Beech fructification and bank vole population dynamics-combined analyses of promoters of human Puumala virus infections in Germany. *PLoS ONE*, *10*(7), e0134124. https://doi.org/10.1371/journal.pone.0134124

Reil, D., Rosenfeld, U. M., Imholt, C., Schmidt, S., Ulrich, R. G., Eccard, J. A., & Jacob, J. (2017). Puumala hantavirus infections in bank vole populations: Host and virus dynamics in Central Europe. *BioMed Central Ecology*, *17*(1), 9. https://doi.org/10.1186/s12898-017-0118-z

Tersago, K., Verhagen, R., Servais, A., Heyman, P., Ducoffre, G., & Leirs, H. (2009). Hantavirus disease (nephropathia epidemica) in Belgium: Effects of tree seed production and climate. *Epidemiology and Infection*, *137*(2), 250–256. https://doi.org/10.1017/S0950268808000940

Thuringian Ministry for Infrastructure and Agriculture (2018). *Forest condition report 2018*. Retrieved from https://www.thueringen.de/de/publikationen/pic/pubdownload1791.pdf.

Vaheri, A., Strandin, T., Hepojoki, J., Sironen, T., Henttonen, H., Mäkelä, S., & Mustonen, J. (2013). Uncovering the mysteries of hantavirus infections. *Nature Reviews Microbiology*, *11*(8), 539–550. https://doi.org/10.1038/nrmicro3066

Vanwambeke, S. O., Zeimes, C. B., Drewes, S., Ulrich, R. G., Reil, D., & Jacob, J. (2019). Spatial dynamics of a zoonotic orthohantavirus disease through heterogenous data on rodents, rodent infections, and human disease. *Scientific Reports*, *9*(1), 2329. https://doi.org/10.1038/s41598-019-38802-5

Voutilainen, L., Savola, S., Kallio, E. R., Laakkonen, J., Vaheri, A., Vapalahti, O., & Henttonen, H. (2012). Environmental change and disease dynamics: Effects of intensive forest management on Puumala hantavirus infection in boreal bank vole populations. *PLoS ONE*, *7*(6), e39452. https://doi.org/10.1371/journal.pone.0039452

Walz, U., Krüger, T., & Schumacher, U. (2011). Landschaftszerschneidung und Waldfragmentierung-Neue Indikatoren des IÖR-Monitors. In G. Meinel, & U. Schumacher (Eds.), *Flächennutzungsmonitoring III, Erhebung – Analyse – Bewertung, IÖR Schriften*, Vol. *58* (pp. 163–170). Berlin: Rhombos.

Weber de Melo, V., Sheikh Ali, H., Freise, J., Kühnert, D., Essbauer, S., Mertens, M., … Heckel, G. (2015). Spatiotemporal dynamics of Puumala hantavirus associated with its rodent host, *Myodes glareolus*. *Evolutionary Applications*, *8*(6), 545–559. https://doi.org/10.1111/eva.12263

How to cite this article: Binder F, Drewes S, Imholt C, et al. Heterogeneous Puumala orthohantavirus situation in endemic regions in Germany in summer 2019. *Transbound Emerg Dis*. 2019;00:1–8. https://doi.org/10.1111/tbed.13408

(II) SPATIAL AND TEMPORAL EVOLUTIONARY PATTERNS IN PUUMALA ORTHOHANTAVIRUS (PUUV) S SEGMENT

Binder, F., Ryll, R., Drewes, S., Jagdmann, S., Reil,D., Hiltbrunner, M., Rosenfeld, U.M., Imholt, C., Jacob, J., Heckel, G., Ulrich, R.G.

Pathogens - Hantavirus Special Issue

Volume 9, 548

July 2020

DOI: 10.3390/pathogens9070548

pathogens

MDPI

Research Article

Spatial and Temporal Evolutionary Patterns in Puumala Orthohantavirus (PUUV) S segment

Florian Binder[1], René Ryll[1,4], Stephan Drewes[1], Sandra Jagdmann[1,5], Daniela Reil[2,6], Melanie Hiltbrunner[3], Ulrike M. Rosenfeld[1], Christian Imholt[2], Jens Jacob[2], Gerald Heckel[3] and Rainer G. Ulrich[1,*]

[1] Friedrich-Loeffler-Institut, Federal Research Institute for Animal Health, Institute of Novel and Emerging Infectious Diseases, 17493 Greifswald - Insel Riems, Germany
[2] Julius Kühn-Institut, Federal Research Centre for Cultivated Plants, Institute for Plant Protection in Horticulture and Forest, Vertebrate Research, 48161 Münster, Germany
[3] University of Bern, Institute of Ecology and Evolution, 3012 Bern, Switzerland
[4] Current address: Cheplapharm Arzneimittel-GmbH, 17489 Greifswald, Germany
[5] Current address: Institute for Medical Immunology, Charité-Universitätsmedizin Berlin, Corporate member of Freie Universität Berlin, Humboldt-Universität zu Berlin, Berlin Institute of Health, 13353 Berlin, Germany
[6] Current address: Institute of Biochemistry and Biology, Animal Ecology, University of Potsdam, 14469 Potsdam, Germany
*Correspondence: rainer.ulrich@fli.de; Tel.: +49 38351 7-1159

Received: date; Accepted: date; Published: date

Abstract: The S segment of bank vole (*Clethrionomys glareolus*) associated Puumala orthohantavirus (PUUV) contains two overlapping open reading frames coding for the nucleocapsid (N) and a non-structural (NSs) protein. To identify the influence of bank vole population dynamics on PUUV S segment sequence evolution and test for spillover infections in sympatric rodent species, during 2010-2014 883 bank voles, 357 yellow-necked mice (*Apodemus flavicollis*), 62 wood mice (*A. sylvaticus*), 149 common voles (*Microtus arvalis*) and eight field voles (*M. agrestis*) were collected in Baden-Wuerttemberg and North Rhine-Westphalia, Germany. In total 27.9% and 22.3% of bank voles were positive for PUUV-reactive antibodies and PUUV-specific RNA, respectively. One of eight field voles was PUUV RNA-positive indicating a spillover infection, but none of the other species showed evidence of PUUV infection. Phylogenetic and isolation by distance analyses demonstrated a spatial clustering of PUUV S segment sequences. In the hantavirus outbreak years 2010 and 2012, PUUV RNA prevalence was higher in our study regions compared to non-outbreak years 2011, 2013 and 2014. NSs amino acid and nucleotide sequence types showed temporal and/or local variation, whereas the N protein was highly conserved in the NSs overlapping region and, to a lower rate, in the N alone coding part.

Keywords: hantavirus; bank vole; evolution; N protein; NSs protein; S segment

1. Introduction

The family *Hantaviridae*, order *Bunyavirales*, comprises rodent, insectivore and bat-borne viruses. The enveloped virion of about 80-120 nm in diameter contains three genome segments of single-stranded RNA with negative polarity [1]. The large (L) segment encodes the RNA dependent RNA polymerase (RdRP). The medium (M) segment encodes the glycoprotein precursor that is co-translationally processed and cleaved into the two glycoproteins Gn and Gc. The small (S) segment encodes the nucleocapsid (N) protein, which is the most abundant hantaviral protein. The N protein is involved in multiple processes during the replication cycle and is highly immunogenic and therefore used as an antigen in serodiagnostics [2]. In addition, the S segment of Puumala orthohantavirus (PUUV) and other vole-associated hantaviruses encodes in a second, overlapping open reading frame (ORF) a non-structural (NSs) protein. This NSs protein was shown to be functional and involved in suppression of interferon production and related mechanisms for antiviral

activity [3]. Recent studies in Lower Saxony, Germany confirmed the conservation of a putative NSs-ORF in PUUV strains concerning its position within the S segment and length of 270 nucleotides [4,5].

PUUV is the geographically most widely distributed human pathogenic hantavirus in Europe. It is the main causative agent of hemorrhagic fever with renal syndrome (HFRS) and its milder form nephropathia epidemica (NE). The natural host of PUUV is the bank vole (*Clethrionomys glareolus* syn. *Myodes glareolus*) that is commonly believed to be persistently infected without signs of disease [6]. However, one investigation of bank vole populations on Finnish islands indicated a slightly decreased overwinter survival rate of PUUV infected bank voles compared to non-infected animals [7]. Bank voles are distributed across large areas of Eurasia and infections with PUUV are recorded in almost all parts of the continent [8,9]. Transmission to humans occurs by inhaling aerosols comprised of dried saliva, feces and urine of virus-infected rodents. Furthermore, a rare transmission route for the virus can be rodent bites [10]. Bank vole abundance in Central Europe was shown to fluctuate depending on beech mast intensity in the previous year [11]. The proportion of PUUV infections within host populations is influenced by the population density of bank voles, habitat properties and the presence of maternal antibodies in juvenile voles [12–14].

In Europe PUUV disease outbreak years are characterized by a high incidence of human PUUV cases and occur roughly every 2–3 years depending on host dynamics. In Germany, increased numbers of notified cases were observed in the outbreak years 2007 (1,678 cases), 2010 (2,016), 2012 (2,852), 2017 (1,697), and 2019 (1,530) [9,15]. The occurrence of PUUV in Germany is tied to the occurrence of the Western evolutionary lineage of the bank vole [16,17], which is present in Southern and Western Germany and absent in the eastern part of Germany. Phylogenetic analysis typically shows geographical clustering of PUUV S segment sequences independent of the year of collection [18,19]. Analysis of the temporal variation of PUUV sequences in the bank vole population demonstrated the continuous presence of certain sequence types over multiple years, whereas other minor sequence types seemed to emerge and disappear again [20].

A previous study in Baden-Wuerttemberg and North Rhine-Westphalia revealed, based on live trapping, that fluctuation of PUUV seroprevalence is dependent on multi-annual dynamics of rodent host abundance [13]. The aim of this parallel snap trapping study in these two endemic regions was to evaluate the influence of rodent population fluctuation on PUUV prevalence, molecular evolution and genetic diversity of two coding regions of the PUUV S segment in its natural host and the frequency of potential PUUV spillover infections into non-reservoir species.

2. Results

2.1. Temporal Fluctuation of PUUV Prevalence in Bank Voles from Baden-Wuerttemberg and North Rhine-Westphalia

Results of snap trapping displayed multiannual dynamics similar to parallel live-trapping, presented in Reil et al., 2017 [13]. Reverse transcription-polymerase chain reaction (RT-PCR) screening of all 851 bank vole lung samples and subsequent sequencing of the amplification products resulted in 193 PUUV RNA-positive samples (22.7%, 95% confidence interval, CI, 20.0%–25.6%). In none of the bank voles, Tula orthohantavirus (TULV) RNA was detected. PUUV-reactive antibodies were detected in 242/851 (28.4%, CI, 25.5%–31.6%) of the bank voles (Figure 2). At the plots in BW 18.1% (CI, 15%–21.6%) and at the plots in NW 14.3% (CI, 11.0%–18.4%) of the tested bank voles were positive in both assays, indicating a persistent infection. A total of 5.6% (CI, 4.0%–8.0%) in BW and 6.0% (CI, 3.9%–9.0%) in NW showed PUUV RNA but not an anti-PUUV antibody response, indicating an acute infection (Figure 2a). In 39 of 515 (7.6%; CI, 5.6%–10.2%) of the bank voles in BW PUUV-reactive antibodies were detected, but no PUUV RNA (Figure 2a). Four of these seropositive animals were juvenile (≤15 g), what might indicate a presence of maternal antibodies. The other 35 seropositive voles were adults, therefore the lack of RNA detection might suggest a clearance of the virus from the voles. The investigations of the bank voles from NW indicated a similar picture, although an even larger part, 57 of 336 (17.0%; CI, 13.3%-21.4%) of the bank voles, were anti-PUUV antibody positive, but RT-PCR negative (Figure 2b). Here, 12 of the 57 seroreactive animals were

juveniles. Overall PUUV RNA detection rates were higher in bank voles during the outbreak years 2010 and 2012 and lower in non-outbreak years 2011, 2013 and 2014 (Figure 2c and d)

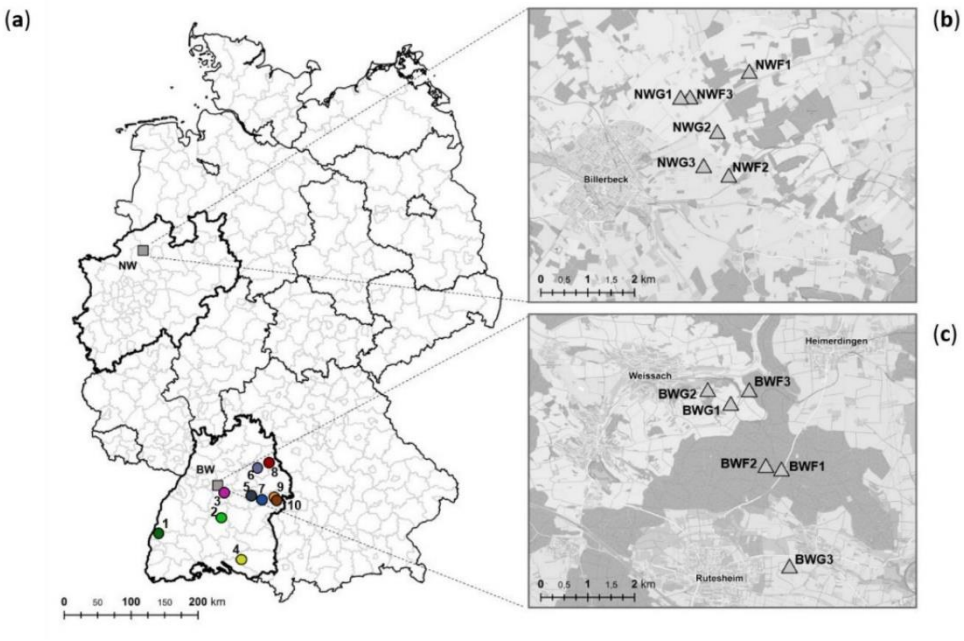

Figure 1. Location of study sites for Puumala orthohantavirus (PUUV) analysis in Germany (**a**) with trapping plots in North Rhine-Westphalia (NW-mo) (**b**) and Baden-Wuerttemberg (BW-mo) (**c**). Study sites consisted of six trapping plots, three in forest (F) and three in grassland (G) habitats. Single plots of trapping regions in BW and NW are shown as triangles. (b) NW-Billerbeck: NWF1 (51.998752 North (N) latitude, 7.335144 East (E) longitude), NWF2 (51.978863 N, 7.329545 E), NWF3 (51.993606 N, 7.316983 E), NWG1 (51.993511 N, 7.314114 E), NWG2 (51.987140 N, 7.325719 E), NWG3 (51.980575 N, 7.321710 E). (c) BW-Weissach: BWF1 (48.829307 N, 8.966542 E), BWF2 (48.829981 N, 8.962033 E), BWF3 (48.844419 N, 8.957213 E), BWG1 (48.841850 N, 8.951865 E), BWG2 (48.844470 N, 8.945196 E), BWG3 (48.810801 N, 8.968887 E). Additional trapping plots in BW from 2007 and 2012 are shown in (a) as circles. 1: Kenzingen (year 2012, 48.11369, 7.50524); 2: Mössingen-Belsen (2012, 48.23227 N, 9.03068 E); 3: Stuttgart-Büsnau (2012, 48.44273 N, 9.03288 E); 4: Zußdorf-Wilhelmsdorf (2007, 47.54104 N, 9.23288 E); 5: Goeppingen (2012, 48.724673 N, 9.710510 E); 6: Michelbach (2007, 49.04597 N, 9.46563 E); 7: Geislingen-Stötten (2012, 48.38513 N, 9.52201 E); 8: Crailsheim-Roßfeld (2012, 49.07519 N, 9.59161 E); 9: Steinheim (2012, 48.40546 N, 10.02022 E); 10: Steinheim (2007, 48.6982 N, 10.06625 E). The colour code was also used in the phylogenetic tree in Figure 3a.

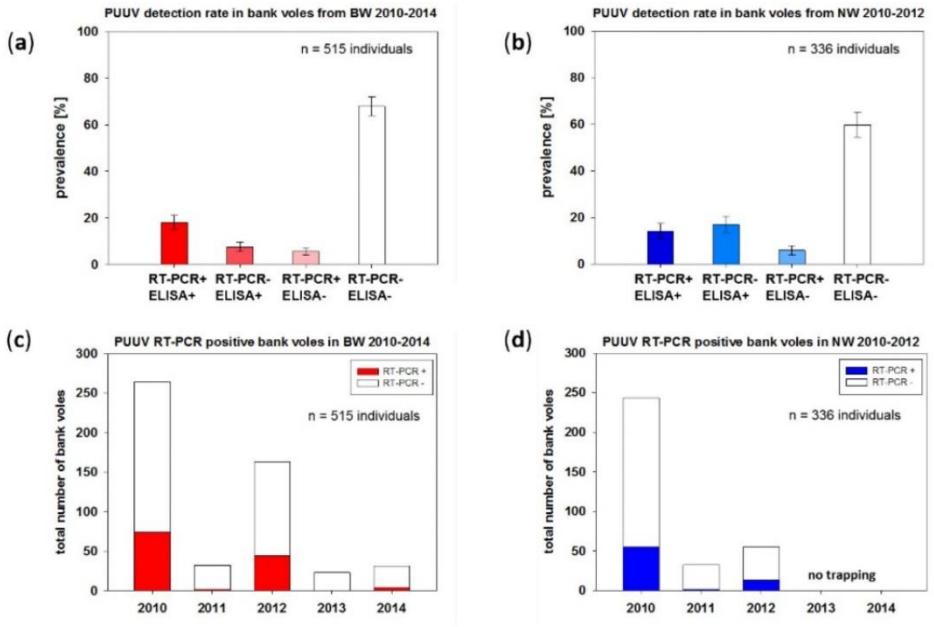

Figure 2. Serology and reverse transcription-polymerase chain reaction (RT-PCR) screening of voles from Baden-Wuerttemberg (**a**) and North Rhine-Westphalia (**b**) and distribution of RT-PCR positive bank voles over time in Baden-Wuerttemberg (**c**) and North Rhine-Westphalia (**d**). In a and b, results are given in percentage of all voles investigated from the respective trapping region. Animals for which no lung or chest cavity lavage sample could be obtained are left out. RT-PCR and ELISA positive animals are shown as dark columns, RT-PCR and ELISA negative animals are shown as white columns. Only PUUV RNA or anti-PUUV positive animals are shown in blue/red scale. In c and d, the total number of bank voles is shown in columns on the y-axis. Chest cavity lavage samples were used for serological testing by IgG ELISA. For detection of PUUV RNA, a small piece of lung tissue was used for RNA extraction with Qiazol lysis reagent and RT-PCR screening with subsequent sequencing of amplification products.

2.2. Phylogenetic and Isolation-by-Distance Analysis of Non-NSs-overlapping S Segment Sequences

For all PUUV RNA-positive bank voles, partial S segment sequences of 1,007 nucleotides were generated covering a major part of the coding sequence of the N protein including the NSs-overlapping region. Phylogenetic analysis of a 465 nucleotide long, non-NSs overlapping part of the S segment sequences showed two distinct clades for BW and NW within the Central European (CE) PUUV clade. The sequences from NW clustered together with a previously determined bank vole sequence from the same region from 2007 and sequences from human patients, in sister relationship to the subclade Osnabrück hills, north-west Germany (Figure 3a). The sequences from the BW region clustered in another clade with further bank vole- and human patient-derived sequences from BW, with close relationship to clades from Rhoen mountains and Bavarian forest (Figure 3a). PUUV sequences from 31 additional animals from nine plots in BW (sites 2–10 in Figure 1a) from the outbreak years 2007 and 2012 (Supplementary Table S1) also clustered in the Swabian Jura clade as the continuously found BWF2/BWF3 sequences. One bank vole-derived sequence from Kenzingen (site 1 in Figure 1a) clustered with sequences from France (Figure 3a).

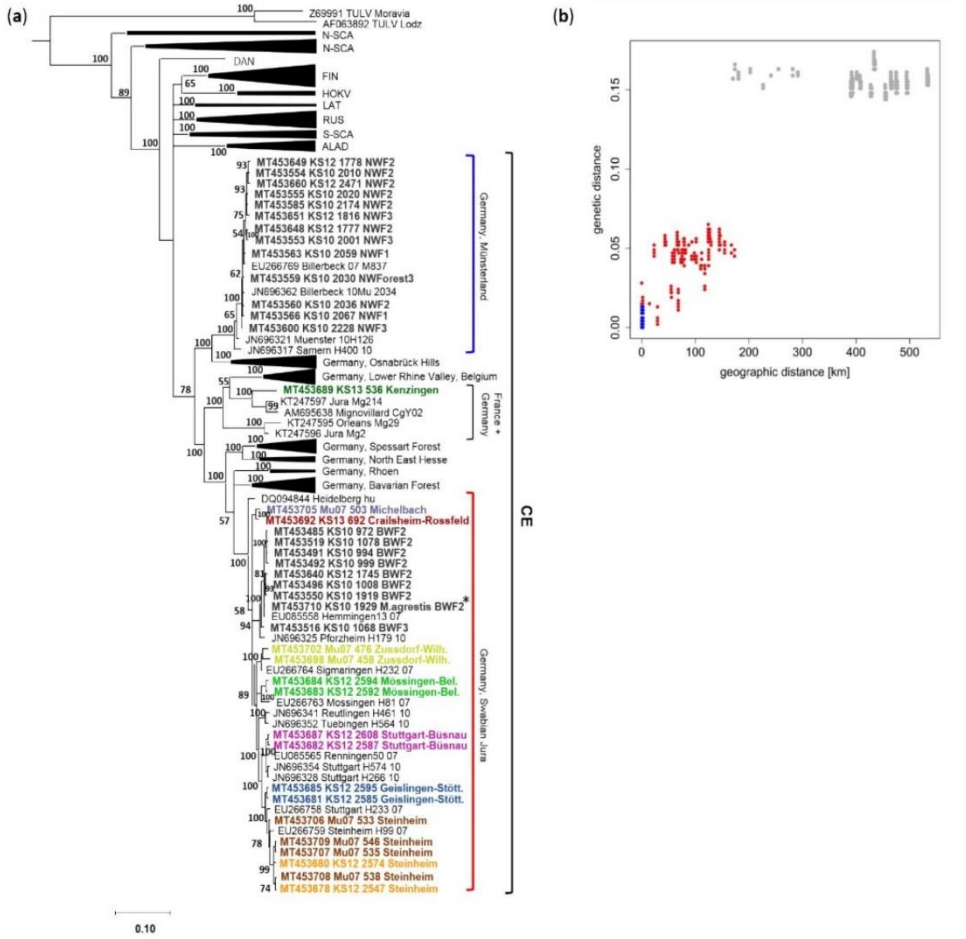

Figure 3. Phylogenetic tree of PUUV strains (**a**) and isolation-by-distance analysis (**b**). The phylogenetic tree (a) was constructed on the basis of 213 unique partial sequences of the N protein-encoding but not NSs overlapping S segment region (465 nucleotides, nucleotides 436-900 of the S-segment, numbering according to PUUV strain Sotkamo, accession number HE801633.1). In total, 226 new individual PUUV S segment sequences were generated (see Tables S1 and S2) and 39 unique sequences were used for phylogenetic analysis. Analysis was performed using the CIPRES gateway and MrBayes v.3.2.7 [47]. A mixed nucleotide substitution matrix was specified in 4 independent runs of 10^7 generations. Phylogenetic relations are shown as a maximum clade credibility phylogenetic tree with posterior probabilities for major nodes. Tula orthohantavirus (TULV) sequences Lodz and Moravia were used as outgroup. Sample numbers for identification consisted of the indicated dissection year, section number and trapping site. Novel sequences from this study are indicated by bold font. * = sequence from the spillover infected field vole. For clarity, previously characterized PUUV clades are shown in simplified form [17,18]. NW, North Rhine-Westphalia; BW, Baden-Wuerttemberg; HOKV, Hokkaido; LAT, Latvian; ALAD, Alpe-Adrian; S-SCA, South Scandinavian; N-SCA, North Scandinavian; RUS, Russian; FIN, Finnish; DAN, Danish. The extent of local transmission and evolution of PUUV was investigated by isolation-by-distance patterns in BW and NW (b). Pairwise genetic distances were estimated based on the same 465 nucleotide-long S segment region, assuming uniform mutation rates among sites. Statistical significance of the association between the half-matrices of both distance types was estimated with a Mantel test. Coordinates given in Figure 1 were used for isolation-by-distance analysis. Blue dots indicate comparisons between sequences from NW, red dots comparisons between sequences from BW. Grey dots indicate

comparisons between the populations in BW and NW that do not show isolation-by-distance patterns due to mutational saturation of sequences [19]. Genetic distance is given as percentage (%), geographic distance in kilometers (km).

Genetic differences between PUUV sequences showed a strong positive relationship with geographical distance between sampling locations resulting in an isolation-by-distance pattern (R^2 = 0.91; $p<0.001$; Figure 3b). PUUV S segment sequences from the same phylogenetic clade were up to 7% different within the same sampling region but differed by 14% to 17% between clades or sampling regions. The low number of sampling locations (N = 3) in NW (blue dots) prevented statistical testing for isolation-by-distance in this region but PUUV sequences from BW (red dots) showed a significant increase of genetic distance between sampling locations less than 120km apart (R^2 = 0.596; $p<0.001$;Figure 3b).

2.3. Frequency of Spillover Infections

To evaluate if bank vole population dynamics influence the frequency of PUUV spillover infection, 397 yellow-necked mice (*Apodemus flavicollis*) and 68 wood mice (*A. sylvaticus*) were screened for the presence of PUUV-reactive antibodies and lung tissue samples of 176 common voles (*Microtus arvalis*) and eight field voles (*M. agrestis*) were investigated by S segment RT-PCR (Supplementary Table S1). Common and field voles were not screened for antibodies as they represent reservoirs of TULV, which cannot be distinguished by immunoglobulin G (IgG) enzyme-linked immunosorbent assay (ELISA) from PUUV. Yellow-necked mice and wood mice were tested for antibodies only, as they were not expected to allow PUUV RNA replication. RT-PCR and subsequent sequencing detected PUUV RNA in one field vole from the outbreak year 2010, but in none of the common voles (Supplementary Table S2). There was high similarity of the field vole-derived sequence to sequences from the same forest plot within the BW clade (BWF2*, Figure 3a). None of the yellow-necked mice and wood mice were found to have PUUV-reactive antibodies (Supplementary Table S2).

2.4. Sequence Variability in the N/NSs Overlapping and N Encoding Regions

For all PUUV RNA-positive bank voles the NSs ORF of 270 nucleotides (90 amino acid residues) was detected in a +1 reading frame relative to the N-encoding ORF. The positions of the start codon and the stop codon as well as the presence and location of multiple translation initiation sites are conserved (Supplementary Figure S1). The stop codon UAA was found for all NSs sequences from NW and site 1 (Kenzingen) in BW, whereas the NSs sequences from all other BW sites have a UGA stop codon.

Comparison of the NSs and N segment sequences (nt 58–1065) was done group wise by SimPlot analysis on nucleotide (Figure 4a) and amino acid level (Figure 4b and c). The NSs sequences of the monitoring trapping regions in BW (BW-mo) and NW (NW-mo) show only little sequence diversity among each other (Figure 4a). To gain insights into the NSs sequence variation in Germany, NSs nucleotide and amino acid sequences from BW-mo and NW-mo trapping sites were compared to additional NSs sequences from other trapping sites in BW and the CE clade (Figure 4, CE). All these sequences from Germany had a low nucleotide sequence divergence in the NSs protein-coding sequence (CDS, Figure 4a, green line). When we compared sequences from all over Europe and Asia including clades CE, FIN, LAT, RUS, DEN, N-SCA, S-SCA, ALAD, and HOKV (black line) the NSs CDS showed a sequence divergence of 35% at the 5′ end and almost homogeneously distributed peaks of around 20% divergence. This indicates that the NSs CDS is variable among European and Asian PUUV strains, but regional sequences are less divergent. On amino acid level the overall pattern was the same, however, variability was particularly high (70%) at NSs amino acid positions 5–15, 40–50, and the C-terminal part of residues 70-90 among all PUUV sequences (Figure 4b).

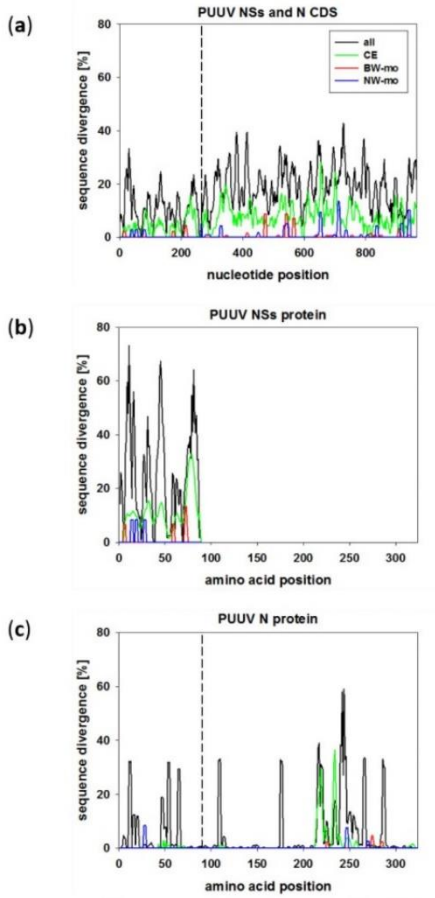

Figure 4. PUUV S segment sequence divergence investigated by SimPlot analysis of the PUUV NSs and N segment nucleotide sequence (**a**), PUUV NSs amino acid sequence (**b**), and PUUV N amino acid sequence (**c**). Sequences from BW (5 unique sequences) are shown in red, sequences from NW (4) in blue, combined sequences from CE clade (35) are shown in green, and an overall PUUV N or NSs SimPlot of 94 sequences from this study and published sequences from all clades (see 4.4) from Europe and Asia is shown as a black line. The N/NSs overlapping region is indicated by a dotted line in (a) and (c). Divegence is given as percentage between the compared sequences. Identical sequences are shown in Supplementary Tables S3 and S4. CDS = coding sequence.

235

236

237 The N protein coding ORF was analyzed the same way (Figure 4a and c) and showed largely
238 homogeneously distributed nucleotide sequence divergence. BW-mo and NW-mo sequences each
239 were highly similar, but the CE clade sequences showed peaks of up to 30% nucleotide sequence
240 divergence (Figure 4a) and 40% amino acid sequence divergence (Figure 4c). The NSs overlapping
241 region was more conserved than the N alone coding part of the S segment (Figure 4a and c, compare
242 the left side of dotted line to the right side). The overall average nucleotide divergence for the N/NSs
243 overlapping CDS was 3.9% for the CE clade and 11% for all sequences, whereas the N alone coding
244 part was less conserved with 6.9% and 19% sequence divergence, respectively (Figure 4a). When
245 translated, PUUV N protein showed only at a few regions high amino acid sequence divergence
246 independent of the NSs overlapping region (Figure 4c). PUUV N protein sequences had a highly
247 variable region at amino acid positions 220-240. However, the main part of the N protein was highly
248 conserved on amino acid sequence level.

249 *2.5. Spatial and Temporal Evolution of Different Regions of the PUUV S segment*

250 In addition to the phylogenetic analysis of partial sequences (nucleotides 436-900), larger S
251 segment sequences spanning nucleotides 58-1065 from lung samples of all 193 PUUV RNA-positive
252 bank voles were analyzed. For this purpose nucleotide and amino acid sequence types were defined
253 for the NSs +1 ORF (nucleotides 83-356/complete NSs amino acid residues 1-90, reference PUUV
254 Sotkamo HE801633.1), the overlapping N/NSs coding region (nucleotides 82-355/N protein amino
255 acid residues 13-103), and the N ORF alone (nucleotides 359-1065/N amino acid residues 104-340).
256 Each sequence type was defined as a unique sequence found in a bank vole (or the single field vole)
257 with at least one nucleotide/amino acid residue difference to any other sequence (for details see
258 Supplementary Tables S3 and S4 and Supplementary Figures S1 and S2).

In total, the sequences of the NSs coding region and the N/NSs overlapping part from BW represented five types (Figure 5a, NSs-nt-BW1-5; N/NSs-nt-BW1-5), which differed only by one single nucleotide exchange each. Interestingly, when translated, all four single nucleotide exchanges were synonymous for the N/NSs overlap but remained non-synonymous for the NSs-ORF (Figure 5a, N/NSs-aa-BW1, NSs-aa-BW1-5). Similar observations were made for PUUV sequences from the NW region, where the NSs showed three non-synonymous single nucleotide exchanges resulting in four amino acid sequence types. The N/NSs overlapping nucleotide sequence types (N/NSs-nt-NW1-4) represented a major amino acid sequence type (N/NSs-aa-NW1) and one animal with a single amino acid exchange (Figure 5b, N/NSs-aa-NW4).

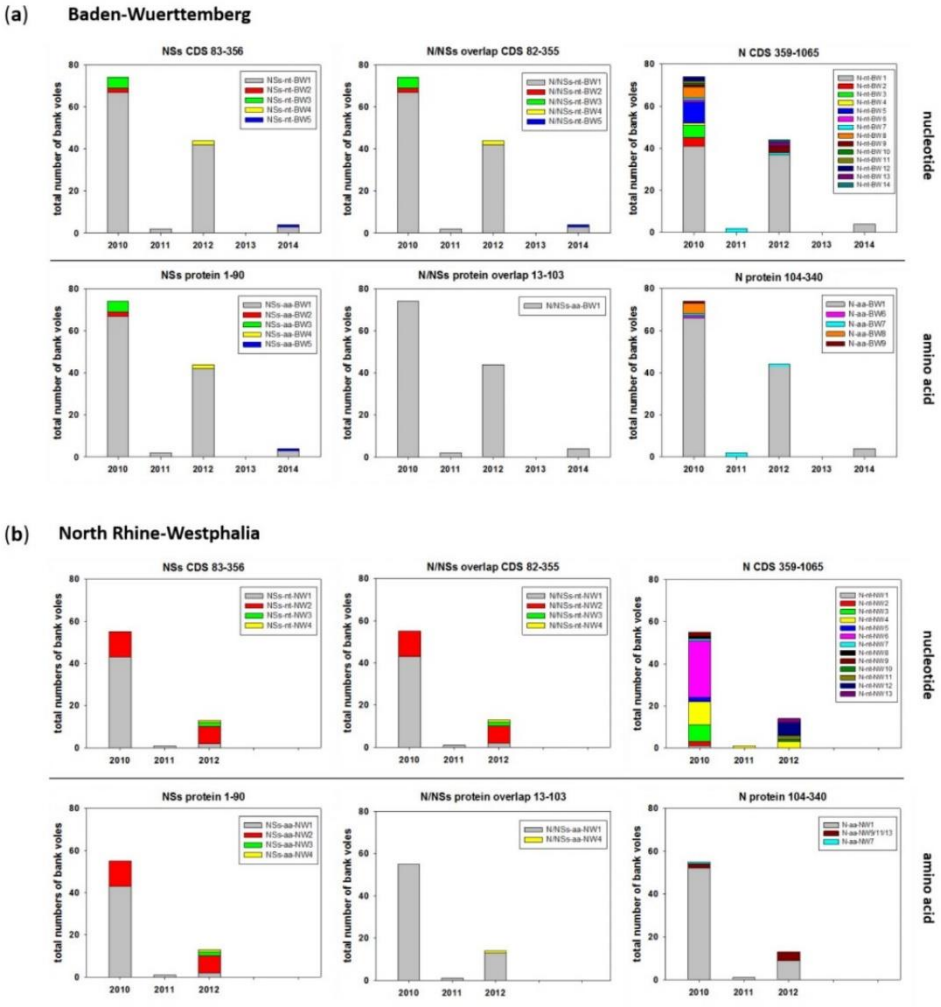

Figure 5. Temporal distribution of PUUV N and NSs sequence types from bank voles collected during 2010-2014 in Baden-Wuerttemberg (**a**) and North Rhine-Westphalia (**b**). The distribution over the trapping period is shown as numbers of bank voles carrying the respective sequence type. A sequence type is defined as a unique sequence found in a bank vole (or field vole) with at least one nucleotide/amino acid difference to any other sequence. Numbers in titles indicate the nucleotide/amino acid positions for the respective ORF analyzed in each panel. Assignment of single sequences to a sequence type is given in Supplementary Tables S3 and S4 and is illustrated for amino acid sequence types in Supplementary Figures S1 and S2. CDS = coding sequence.

276 The partial N protein-encoding nucleotide sequence, downstream of the overlapping region
277 (nucleotides 359 to 1065), showed a high number of nucleotide exchanges that resulted in 14 different
278 nucleotide sequence types in BW (Figure 5a) and 13 in NW (Figure 5b). However, nucleotide
279 exchanges were mainly synonymous, resulting in one major amino acid sequence type (N-aa-BW1,
280 N-aa-NW1) and 4 (BW) or 2 (NW) minor types (Figure 5a and b).
281 The major sequence type (nucleotide and amino acid) for the NSs alone and N/NSs overlapping
282 coding regions in BW was present over the whole trapping period from 2010-2014 (Figure 5a, NSs-
283 nt/aa-BW1, N/NSs-nt/aa-BW1). Minor sequence types occurred only sporadically in a single year. The
284 N alone coding part (359-1065) also showed a major nucleotide sequence type. However, it was not
285 continuously observed, as 2011 only two PUUV-infected voles were found representing the minor
286 type (Figure 5a, N-nt-BW7). The same minor type was also present in 2010 and 2012, whereas all
287 other minor types were single occurrences in the outbreak years 2010 and 2012. These nucleotide
288 exchanges were mostly synonymous. However, four minor types were present in outbreak years,
289 including N-aa-BW7 that was found consistently three years in a row (Figure 5a).
290 Similar to BW, the major NSs and N/NSs sequence types were observed over the whole period
291 in NW (Figure 5b, N-nt/aa-NW1, N/NSs-nt/aa-NW1). Here, the second, more prominent minor type
292 (NSs-nt-NW2) was observed in the outbreak years 2010 and 2012 but disappeared in 2011 (Figure 5b).
293 Concerning the N part, a more diverse picture was observed in NW. On nucleotide level, one
294 sequence type was observed in all three years (N-nt-NW4, 2010–2012), but this sequence type did not
295 represent a major type, and strains were more equally distributed to several nucleotide sequence
296 types than in BW. Most of these sequence variations were synonymous, except for three minor
297 nucleotide sequence types that had the same amino acid sequence, present in the outbreak years 2010
298 and 2012 (Figure 5b, N-aa-NW9/11/13). One animal in 2010 showed a single amino acid exchange
299 compared to all others (Figure 5b, N-aa-NW7).
300 The spatial analysis of NSs sequence types indicated also the occurrence of major nucleotide and
301 amino acid sequence types at all forest plots in BW (Figure 6a). The two PUUV RNA-positive bank
302 voles trapped in grassland habitats carried the main NSs sequence type and a second minor one. At
303 each of the three plots in NW, multiple, mostly unique nucleotide sequence types were observed for
304 the non-NSs overlapping region (N 359–1065), indicating less exchange of bank vole populations
305 between the plots in NW; in the N/NSs overlapping region two main N/NSs nucleotide sequence
306 types were present at all three forest plots (Figure 6b). Again, the N protein amino acid sequence
307 types were represented by a major type at all forest plots in BW and NW. In contrast, for the NW
308 plots two main NSs amino acid sequence types were observed, whereas at the forest plots in BW
309 there was only one major type.

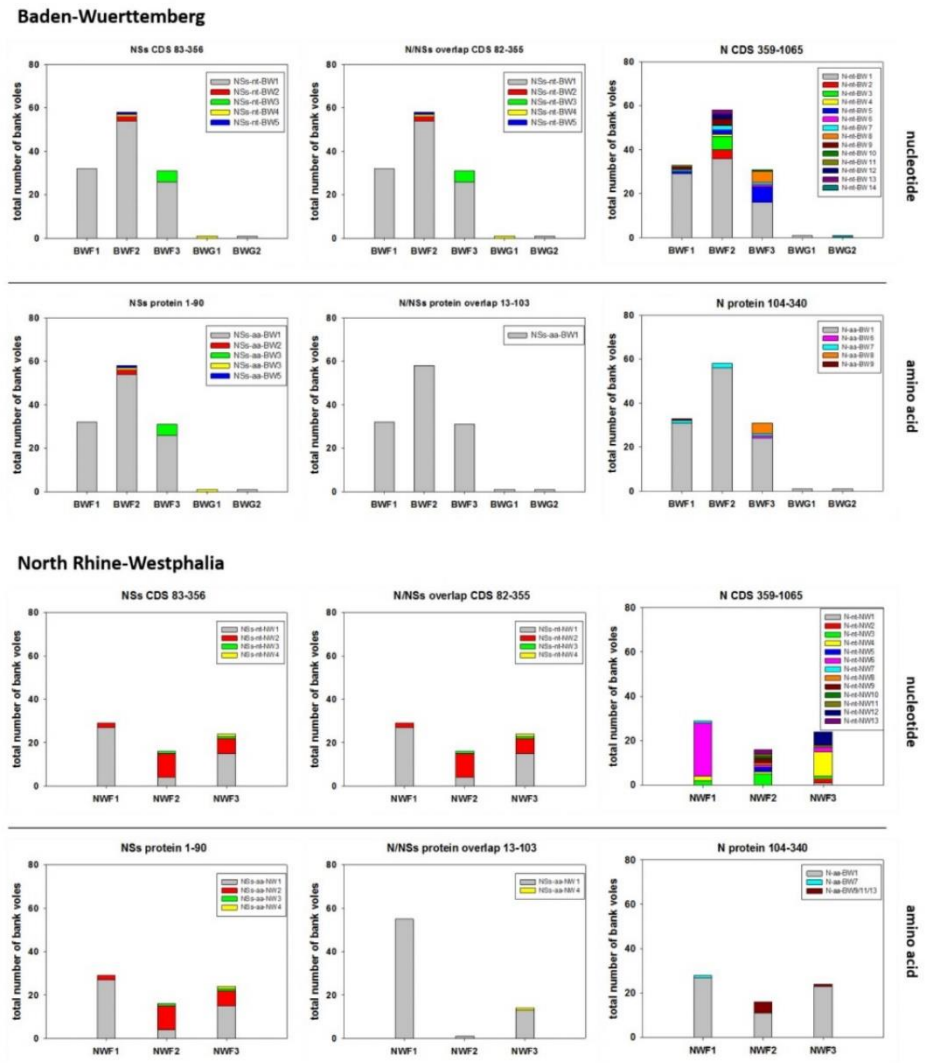

Figure 6. Spatial distribution of PUUV N and NSs sequence types from bank voles collected during 2010-2014 in Baden-Wuerttemberg (**a**) and North Rhine-Westphalia (**b**). The distribution over the trapping plots is shown as numbers of bank voles carrying the respective sequence type. A sequence type is defined as a unique sequence found in a bank vole with at least one nucleotide/amino acid difference to any other sequence. Numbers in titles indicate the nucleotide/amino acid positions for the respective ORF/protein analyzed in each panel. Assignment of single sequences to a sequence type is given in Supplementary Tables S3 and S4 and is illustrated for amino acid sequence types in Supplementary Figures S1 and S2. CDS = coding sequence.

3. Discussion

Here we investigated the influence of fluctuations in bank vole populations on PUUV prevalence, the sequence evolution of different regions of the S segment of PUUV and the frequency of spillover infections in sympatric rodents of other species.

The trapping regime reflected the multiannual fluctuations with abundance peaks in 2010 and 2012 and low abundance in 2011, 2013, 2014, similar to the results presented by Reil et al., 2017.

The PUUV-RNA detection rate at the site in BW reached 28%, 6.2%, 27%, 0% and 12.9% during 2010 – 2014, and at the site in NW 22.6%, 3.1% and 23.6% during 2010-2012. The detection rates during outbreak years 2010 and 2012 are similar to results of a study in the Bavarian forest during 2004 (RNA detection rate of 24%, [21]), but much lower than those observed during outbreak years at a site in Western Thuringia (77.3 %; [22]) and two sites in district Osnabrück, Lower Saxony. Here the RNA detection rate varied during 2010–2012 between 85%, 13.7% and 86.2% at one site and 100%, 40% and 86.7% at a second site [20]. A preliminary analysis of the seasonality suggests that the ratio of PUUV RNA positive bank voles was the highest in spring, which mimics the results of the PUUV seroprevalence in live trapping shown by Reil et al. (2017). In our study, the average seroprevalence of 25.8% (BW) and 32.4% (NW) was higher than the average RNA detection rate (24.1% and 20.5%, respectively). This discrepancy between seroprevalence and PUUV RNA detection can only partially be explained by the presence of maternal antibodies in juvenile individuals, as there were adult animals with anti-PUUV antibodies but without PUUV RNA. Therefore, we speculate that clearance of the PUUV infection had occurred in adult animals. Alternatively, an oscillation of viral RNA load might influence the RNA detection as discussed earlier [23].

Phylogenetic and isolation-by-distance analysis of the novel PUUV S segment sequences confirmed strict spatial clustering. This phylogenetic clustering was already described in studies before [18-20,24,25]. In our study, the novel sequences from NW clustered with other sequences from NW in a single clade and the sequences from BW clustered in two clades: the major one with additional sequences from BW and a single sequence from the geographically distant western region of BW with sequences from France. Sequence type analysis indicated the temporal persistence of a single major sequence type over time, but the occurrence of additional minor types during outbreak years. These spatial and temporal patterns are in line with patterns of PUUV sequence variation in another endemic region close to Osnabrück [20].

Interestingly, sequence divergence varied within the S segment and the encoded N and NSs proteins. As expected, the overlapping NSs/N coding region seemed to result in a higher sequence conservation of the N protein when compared to the more downstream N alone coding region [26]. Nevertheless, the position and length of the NSs ORF and the occurrence of multiple translation initiation codons was conserved despite a high level of nucleotide sequence divergence observed for PUUV strains of different European clades. Obviously, local evolution of PUUV strains was not only indicated in the non-overlapping region of the S segment, but also in the NSs/N overlapping region as evidenced by SimPlot analysis. The spatial distribution of nucleotide sequence types may indicate also an "exchange" of the local PUUV strains between individuals at different plots. This was not only seen at forest plots, but also by the rare detection of PUUV-positive bank voles at grassland plots in BW. Here, bank voles from the same plot in NW showed different NSs nucleotide and amino acid sequence types, whereas in BW voles from one plot carried mainly one NSs sequence type indicating higher exchange or contact of territories in BW. This can be explained by the location of trapping plots in this study, as they were only a few hundred meters apart in BW. In NW, forest sites were not connected among each other and more separated than in BW. However, we cannot exclude the influence of different population sizes or their fluctuations and of migration processes on these observations. Thus, larger populations of bank voles may contribute to a higher sequence variability, that is driven by the high mutation rate of RNA viruses, or re-populating of areas after bottleneck events can also increase variability [20]. Spontaneously occurring sequence types of NSs and N, only present in years with high vole abundance, were probably detected due to larger sample size in outbreak years and were not necessarily absent in non-outbreak years. In a previous study, land cover type influenced dispersal dynamics of PUUV, with forests facilitating and croplands impeding virus spread [27].

Usually, a hantavirus is found in a single reservoir species, although there is increasing evidence that some vole associated orthohantaviruses might be capable of replication in several closely related rodent species. TULV initially was found in the common vole and its sibling species the East European vole (*M. levis*) [28,29] but was later also detected in the field vole, the European pine vole (*M. subterraneus*), and even the European water vole (*Arvicola amphibius*) [30-32]. Molecular evidence

for PUUV spillover infection was obtained in our study for a single field vole collected during the outbreak year 2010 at a forest plot in BW. None of the common voles were PUUV RNA positive, and none of the bank voles were positive for TULV RNA, although in another study, TULV RNA was detected in several common and field voles (Schmidt, Reil et al., in preparation). These results confirm the host specificity of hantaviruses in general (for review see [10]), and of PUUV for the bank vole and TULV for common vole and related *Microtus* species in particular, which is consistent with results of a recent *in vitro* study [33]. The very low proportion of PUUV spillover infection observed in our study (1 of 649) is in line with an experimental rodent infection study [34]. Furthermore, PUUV-reactive antibodies were not found here in yellow-necked mice and wood mice, although previous studies have detected anti-PUUV antibody positive yellow-necked mice occurring sympatrically with PUUV-infected bank voles in PUUV endemic regions in NW (city of Cologne) and Bavarian forest [21,35].

Viruses co-evolve with their hosts and the principle of overlapping genes has resulted in a highly efficient viral gene expression strategy and genome size minimization. Mechanisms such as leaky scanning (in the case of NSs) or usage of different reading frames have led to highly economical coding strategies [36]. The NSs protein is highly dependent on the N protein in terms of transcription as it uses the same mRNA by leaky scanning [37]. Our data show that the N protein of local PUUV strains is highly conserved. In particular, the residues 175–215 of the N protein are highly conserved, most likely due to their function in RNA binding [38,39]. The N-terminal part of N has interaction domains for RdRP [40] and Gc [41] but is also highly immunogenic. Therefore the sequence evolution of the encoding region, that overlaps that of the NSs protein, needs to be well balanced for overall N and NSs functions. The high variability at amino acid residues 220-240 has been observed also in previous studies on N protein of TULV [2,42,43].

4. Materials and Methods

4.1. Study Animals

Rodents were captured using snap traps in spring, summer and autumn 2010-2014 in Baden-Wuerttemberg (BW, Germany), except spring 2014, and in spring, summer and autumn 2010 to 2012 in North Rhine-Westphalia (NW, Germany), except autumn 2012 (Figure 1a). In the two regions three forest (F) and three grassland (G) plots were established (Figure 1b and c). A total of 851 bank voles, 397 yellow-necked mice, 68 wood mice, 176 common voles and eight field voles were trapped in these two regions (Supplementary Table S2). From these animals, 36 bank voles were found dead during live trapping in BW nearby snap trapping plots (BWF2, BWF3) and were included in the study. Additionally, 32 bank voles were obtained during the outbreak years 2007 and 2012 from 10 plots in BW [16,17] (Figure 1a, Supplementary Table S1). All animals were dissected and tissue and chest cavity lavage samples collected according to standard protocols. Animals of ≤15 g were considered juvenile [14].

4.2. Serology

Investigation of chest cavity lavage samples from bank voles, yellow-necked mice and wood mice was done by IgG ELISA using recombinant N protein of PUUV strain BaWa, as described earlier [44]. The monoclonal antibody 5E11 was used as a positive control [45]. Sera of PUUV RT-PCR and IgG ELISA-negative bank vole and yellow-necked mouse were used as negative controls for serological investigation of bank voles and *Apodemus* mice, respectively. The definition of positive, negative and equivocal followed a previously introduced workflow [44].

4.3. Detection of Hantavirus RNA

For detection of PUUV nucleic acids, RNA was extracted from homogenized lung tissue using QIAzol Lysis Reagent (QIAGEN, Hilden, Germany) followed by S segment-specific RT-PCR that allows detection of RNA of PUUV, TULV and related viruses. Primers 342F (5′-TATGGTAATGTCCTTGATGT-3′) and 1102R (5′-GCCATDATDGTRTTYCTCAT-3′) were applied to

amplify the main part of the N protein-coding region [17]. The amplification with Superscript TM III RT/Platinum Taq Mix (Invitrogen, Karlsruhe, Germany) followed the instructions of the manufacturer. Following reverse transcription at 50 °C for 30 min and denaturation at 94 °C for 2 min, cDNA was amplified in 40 cycles for 30 s at 94 °C, 30 s at 46 °C, 1 min at 68 °C with a final extension for 10 min at 68 °C. For identification of PUUV, sequences were generated from each RT-PCR positive animal (see 4.4.). Few partial sequences of 504 nucleotides from BW and NW have been reported before ([18], accession numbers JN696363, JN696359, JN696362, JN696360, JN696370). For PUUV RNA-positive animals, the NSs-overlapping region was additionally amplified using the primers 40F (5′-CTGGAATGAGTGACTTAAC-3′) and 393R (5′-CTCCAATTGTATACCAATCT-3′) with the same cycler protocol.

4.4. Sequence, Phylogenetic and Statistical Analysis

Amplified PUUV cDNA was sequenced with the primers used for RT-PCR in four independent runs using the BigDye™ Terminator v1.1 Cycle Sequencing Kit (Thermo Fisher, Waltham, MA, USA) and the following reaction profile: 96 °C for 1 min, followed by 30 cycles of 96 °C for 15 s, 50 °C for 15 s and 60 °C for 90 s. Sequences (n=226, accession numbers: MT453485-MT453710) were assembled and aligned using MEGA 10 [46]. Published sequences of other hantaviruses were obtained from GenBank. Phylogenetic trees were reconstructed with 213 non-identical partial S segment sequences of 465 nucleotides length (nucleotides 436-900 of the S segment, numbering according PUUV strain Sotkamo, accession number HE801633.1). A total of 39 unique sequences from the newly generated 226 individual sequences were used for phylogenetic reconstruction. Analysis was performed by Bayesian algorithms via MrBayes v.3.2.7 on the CIPRES online portal [47]. A mixed nucleotide substitution matrix was specified in four independent runs of 10^7 generations. Phylogenetic relationships are shown as a maximum clade credibility phylogenetic tree with posterior probabilities for major nodes.

We investigated the extent of local transmission and evolution of PUUV by testing for isolation-by-distance patterns [19] within and among the sampling regions in BW and NW. Pairwise genetic distances were estimated based on the same above mentioned 465 nucleotides-long S segment sequence in MEGA 7 [48] including transitions and transversions and assuming uniform mutation rates among sites. Geographic distances between sampling locations were calculated using the Geographic Distance Matrix Generator v. 1.2.3 [49]. We tested for statistical significance of the association between the half-matrices of both distance types with a Mantel test using R software [50]. The same software was used to plot the genetic distances against the geographic distances for each sequence pair.

For SimPlot analysis, NSs and N nucleotide and amino acid sequences from our study were compared among each other and with NSs and N sequences of 78 sequences from all PUUV clades obtained from GenBank NCBI (accession numbers: AB010730, AB010731, AB297665, AB433843, AB433845, AB675453, AB675463, AF063892, AF294652, AF367071, AF442613, AJ223369, AJ223371, AJ223374, AJ223375, AJ223380, AJ238790, AJ238791, AJ277030, AJ277031, AJ277033, AJ314598, AJ314599, AJ888751, AM695638, AY526219, AY954722, DQ016432, EU439968, FN377821, GQ339474, GQ339476, GQ339477, GQ339478, GQ339479, GQ339480, GQ339481, GQ339482, GQ339483, GQ339484, GQ339485, GQ339486, GQ339487, GU808824, GU808825, JN657228, JN657229, JN657230, JN657231, JN696358, JN696372, JN696373, JN696374, JN696375, JN831943, JQ319162, JQ319163, JQ319168, JQ319170, JQ319171, KJ994776, KT247592, KT247593, KT247595, KT247596, KT247597, L08804, M32750, U14137, U22423, Z21497, Z30702, Z30704, Z30705, Z46942, Z48586, Z69991, Z84204). For SimPlot analysis, a window size of 9 and a step size of 3 for nucleotide sequence analysis as well as window size of 3 and step size of 1 for amino acid sequence analysis were used; scripts for SimPlot analysis were written in R software [50].

Comparison of N and NSs sequences was done by grouping all PUUV sequences into sequence types. A sequence type is defined as a unique sequence found in a bank vole (or field vole) with at least one nucleotide/amino acid difference to any other sequence (Supplementary Tables S3 and S4).

For statistical analysis of PUUV RNA detection and serological investigations, CI based on a binomial distribution were calculated.

5. Conclusions

Our study added novel knowledge on the fluctuation of PUUV prevalence in local bank vole populations during outbreak and non-outbreak years and the differences of sequence conservation and variability in the S segment regions encoding NSs and N or N protein alone. The persistence of sequence types over time and the emergence of novel sequence types might be explained by bottleneck event-driven genetic drift or selection processes in the bank vole population that shape the genetic diversity of PUUV. These evolutionary processes need to be evaluated in future studies. The general conservation of the NSs ORF is in contrast to the high amino acid sequence variability that raises questions about its functional consequences. The low frequency of spillover infections in general, but the PUUV spillover to one of eight field voles observed here indicated the necessity of further studies on the virus-host interaction on cellular and organismic level. Finally, our study increases our sequence knowledge for future identification of the geographical origin of human infections in high endemic regions of NW and BW [18,24].

Supplementary Materials: The following are available online at www.mdpi.com/xxx/s1. Table S1: Trapping site and season information for PUUV positive bank voles from Baden-Wuerttemberg from outbreak years 2007 and 2012. Table S2: Rodents trapped for PUUV investigations over a five year period and results of serological tests (ELISA) and RNA detection (RT-PCR). Table S3: Assignment of nucleotide sequences to sequence types for PUUV strains from Baden-Wuerttemberg. Table S4: Assignment of nucleotide sequences to sequence types for PUUV strains from North Rhine-Westphalia. Figure S1: Amino acid sequence alignment of unique putative NSs proteins of Puumala orthohantavirus (PUUV) strains from Baden-Wuerttemberg (BW) and North Rhine-Westphalia (NW) and previously described PUUV isolates from Osnabrück region, Lower Saxony. Figure S2: Amino acid sequence alignment of unique partial N protein segments encoded by overlapping (a) or non-overlapping NSs ORF (b) parts of Puumala orthohantavirus (PUUV) strains from Baden-Wuerttemberg (BW) and North Rhine-Westphalia (NW) and previously described PUUV isolates from Osnabrück region, Lower Saxony.

Author Contributions: Conceptualization, Christian Imholt, Jens Jacob and Rainer G. Ulrich; Data curation, Florian Binder, Christian Imholt, Jens Jacob, Gerald Heckel and Rainer G. Ulrich; Formal analysis, Florian Binder, René Ryll and Gerald Heckel; Funding acquisition, Jens Jacob, Gerald Heckel and Rainer G. Ulrich; Investigation, Florian Binder, René Ryll, Stephan Drewes, Sandra Jagdmann and Melanie Hiltbrunner; Methodology, Florian Binder, René Ryll, Stephan Drewes, Sandra Jagdmann, Daniela Reil, Melanie Hiltbrunner, Ulrike M. Rosenfeld and Christian Imholt; Project administration, Jens Jacob and Rainer G. Ulrich; Resources, Daniela Reil, Christian Imholt and Jens Jacob; Supervision, Jens Jacob, Gerald Heckel and Rainer G. Ulrich; Validation, Florian Binder, René Ryll, Stephan Drewes, Gerald Heckel and Rainer G. Ulrich; Visualization, Florian Binder, Melanie Hiltbrunner and Gerald Heckel; Writing – original draft, Florian Binder and Rainer G. Ulrich; Writing – review & editing, Florian Binder, René Ryll, Stephan Drewes, Daniela Reil, Melanie Hiltbrunner, Christian Imholt, Jens Jacob, Gerald Heckel and Rainer G. Ulrich. All authors have read and agreed to the published version of the manuscript.

Ethical statement: Collection of samples was done according to relevant legislation and by permission of the federal authorities (permits: Regierungspräsidium Stuttgart 35-9185.82/0261; Landesamt für Natur, Umwelt und Verbraucherschutz Nordrhein-Westfalen 8.87- 51.05.20.09.210).

Funding: The investigations were funded in part by the Deutsche Forschungsgemeinschaft (SPP 1596, UL 405/1-1) and Bundesminsterium für Bildung und Forschung through the Research Network Zoonotic Infections (RoBoPub consortium, FKZ 01KI1721A) awarded to R.G.U., and partly commissioned and funded by the Federal Environment Agency (UBA) within the Environment Research Plan of the German Federal Ministry for the Environment, Nature Conservation and Nuclear Safety (BMU) (grant number 3709 41 401 and grant number 3713 48 401) awarded to J.J. Gerald Heckel was supported by the Swiss National Science Foundation (grant 31003A-176209). Florian Binder acknowledges intramural funding by the Friedrich-Loeffler-Institut.

Acknowledgments: We thank Sabrina Schmidt, Dörte Kaufmann, Elisa Heuser, Stefan Fischer, Marie Luisa Schmidt, Julia Schneider, Hanan Sheikh Ali, Mathias Schlegel, Paul Dremsek, Christin Trapp, Konrad Wanka, Ute Wessels, Kathrin Baumann, Franziska Thomas, Christian Kretzschmar, Anke Mandelkow, Grit Möwert,

Nadja Lorenz, Henrike Gregersen, Theres Wollny, Sylvia Ferguson, Katja Plifke and Annemarie Steiner for their support with the small mammal dissections.

Conflicts of Interest: The authors declare that they have no conflict of interest.

References

1. Vaheri, A.; Strandin, T.; Hepojoki, J.; Sironen, T.; Henttonen, H.; Mäkelä, S.; Mustonen, J. Uncovering the mysteries of hantavirus infections. *Nature Reviews Microbiology* **2013**, *11*, 539-550, doi:10.1038/nrmicro3066.
2. Reuter, M.; Krüger, D.H. The nucleocapsid protein of hantaviruses: much more than a genome-wrapping protein. *Virus genes* **2017**, *54*, 5-16, doi:10.1007/s11262-017-1522-3.
3. Jääskelainen, K.M.; Kaukinen, P.; Minskaya, E.S.; Plyusnina, A.; Vapalahti, O.; Elliott, R.M.; Weber, F.; Vaheri, A.; Plyusnin, A. Tula and Puumala hantavirus NSs ORFs are functional and the products inhibit activation of the interferon-beta promoter. *Journal of medical virology* **2007**, *79*, 1527-1536, doi:10.1002/jmv.20948.
4. Ali, H.S.; Drewes, S.; Weber de Melo, V.; Schlegel, M.; Freise, J.; Groschup, M.H.; Heckel, G.; Ulrich, R.G. Complete genome of a Puumala virus strain from Central Europe. *Virus genes* **2015**, *50*, 292-298, doi:10.1007/s11262-014-1157-6.
5. Binder, F.; Reiche, S.; Roman-Sosa, G.; Saathoff, M.; Ryll, R.; Trimpert, J.; Kunec, D.; Hoper, D.; Ulrich, R.G. Isolation and characterization of new Puumala orthohantavirus strains from Germany. *Virus genes* **2020**, 10.1007/s11262-020-01755-3, doi:10.1007/s11262-020-01755-3.
6. Meyer, B.J.; Schmaljohn, C.S. Persistent hantavirus infections: characteristics and mechanisms. *Trends in microbiology* **2000**, *8*, 61-67.
7. Kallio, E.R.; Voutilainen, L.; Vapalahti, O.; Vaheri, A.; Henttonen, H.; Koskela, E.; Mappes, T. Endemic hantavirus infection impairs the winter survival of its rodent host. *Ecology* **2007**, *88*, 1911-1916.
8. Vapalahti, O.; Mustonen, J.; Lundkvist, Å.; Henttonen, H.; Plyusnin, A.; Vaheri, A. Hantavirus Infections in Europe. *The Lancet Infectious Diseases* **2003**, *3*, 653-661, doi:10.1016/s1473-3099(03)00774-6.
9. Faber, M.; Krüger, D.H.; Auste, B.; Stark, K.; Hofmann, J.; Weiss, S. Molecular and epidemiological characteristics of human Puumala and Dobrava-Belgrade hantavirus infections, Germany, 2001 to 2017. *Euro surveillance* **2019**, *24*, doi:10.2807/1560-7917.Es.2019.24.32.1800675.
10. Schlegel, M.; Jacob, J.; Krüger, D.H.; Rang, A.; Ulrich, R.G. Hantavirus Emergence in Rodents, Insectivores and Bats: What Comes Next? *In: Johnson N, ed. The Role of Animals in Emerging Viral Diseases* **2014**, 235-292.
11. Reil, D.; Imholt, C.; Eccard, J.A.; Jacob, J. Beech Fructification and Bank Vole Population Dynamics - Combined Analyses of Promoters of Human Puumala Virus Infections in Germany. *PloS one* **2015**, *10*, e0134124, doi:10.1371/journal.pone.0134124.
12. Vanwambeke, S.O.; Zeimes, C.B.; Drewes, S.; Ulrich, R.G.; Reil, D.; Jacob, J. Spatial dynamics of a zoonotic orthohantavirus disease through heterogenous data on rodents, rodent infections, and human disease. *Scientific reports* **2019**, *9*, 2329, doi:10.1038/s41598-019-38802-5.
13. Reil, D.; Rosenfeld, U.M.; Imholt, C.; Schmidt, S.; Ulrich, R.G.; Eccard, J.A.; Jacob, J. Puumala hantavirus infections in bank vole populations: host and virus dynamics in Central Europe. *BMC ecology* **2017**, *17*, 9, doi:10.1186/s12898-017-0118-z.
14. Kallio, E.R.; Begon, M.; Henttonen, H.; Koskela, E.; Mappes, T.; Vaheri, A.; Vapalahti, O. Hantavirus infections in fluctuating host populations: the role of maternal antibodies. *Proceedings of the Royal Society B: Biological sciences* **2010**, *277*, 3783-3791, doi:10.1098/rspb.2010.1022.
15. Robert-Koch-Institut. Hantavirus Infektionen. Availabe online: https://www.rki.de/DE/Content/InfAZ/H/Hantavirus/Hantavirus.html (accessed on 04-15-2020).
16. Drewes, S.; Turni, H.; Rosenfeld, U.M.; Obiegala, A.; Strakova, P.; Imholt, C.; Glatthaar, E.; Dressel, K.; Pfeffer, M.; Jacob, J., et al. Reservoir-Driven Heterogeneous Distribution of Recorded Human Puumala virus Cases in South-West Germany. *Zoonoses and public health* **2017**, 64, 5, 381-390 10.1111/zph.12319, doi:10.1111/zph.12319.
17. Drewes, S.; Ali, H.S.; Saxenhofer, M.; Rosenfeld, U.M.; Binder, F.; Cuypers, F.; Schlegel, M.; Rohrs, S.; Heckel, G.; Ulrich, R.G. Host-Associated Absence of Human Puumala Virus Infections in Northern and Eastern Germany. *Emerging infectious diseases* **2017**, *23*, 83-86, doi:10.3201/eid2301.160224.

18. Ettinger, J.; Hofmann, J.; Enders, M.; Tewald, F.; Oehme, R.M.; Rosenfeld, U.M.; Ali, H.S.; Schlegel, M.; Essbauer, S.; Osterberg, A., et al. Multiple synchronous outbreaks of Puumala virus, Germany, 2010. *Emerging infectious diseases* **2012**, *18*, 1461-1464, doi:10.3201/eid1809.111447.
19. Saxenhofer, M.; Weber de Melo, V.; Ulrich, R.G.; Heckel, G. Revised time scales of RNA virus evolution based on spatial information. *Proceedings of the Royal Society B: Biological sciences* **2017**, *284*, doi:10.1098/rspb.2017.0857.
20. Weber de Melo, V.; Sheikh Ali, H.; Freise, J.; Kuhnert, D.; Essbauer, S.; Mertens, M.; Wanka, K.M.; Drewes, S.; Ulrich, R.G.; Heckel, G. Spatiotemporal dynamics of Puumala hantavirus associated with its rodent host, *Myodes glareolus*. *Evolutionary applications* **2015**, *8*, 545-559, doi:10.1111/eva.12263.
21. Essbauer, S.; Schmidt, J.; Conraths, F.J.; Friedrich, R.; Koch, J.; Hautmann, W.; Pfeffer, M.; Wolfel, R.; Finke, J.; Dobler, G., et al. A new Puumala hantavirus subtype in rodents associated with an outbreak of Nephropathia epidemica in South-East Germany in 2004. *Epidemiology and infection* **2006**, *134*, 1333-1344, doi:10.1017/S0950268806006170.
22. Faber, M.; Wollny, T.; Schlegel, M.; Wanka, K.M.; Thiel, J.; Frank, C.; Rimek, D.; Ulrich, R.G.; Stark, K. Puumala virus outbreak in Western Thuringia, Germany, 2010: epidemiology and strain identification. *Zoonoses and public health* **2013**, *60*, 549-554, doi:10.1111/zph.12037.
23. Voutilainen, L.; Sironen, T.; Tonteri, E.; Back, A.T.; Razzauti, M.; Karlsson, M.; Wahlstrom, M.; Niemimaa, J.; Henttonen, H.; Lundkvist, A. Life-long shedding of Puumala hantavirus in wild bank voles (*Myodes glareolus*). *The Journal of general virology* **2015**, *96*, 1238-1247, doi:10.1099/vir.0.000076.
24. Weiss, S.; Klempa, B.; Tenner, B.; Kruger, D.H.; Hofmann, J. Prediction of the Spatial Origin of Puumala Virus Infections Using L Segment Sequences Derived from a Generic Screening PCR. *Viruses* **2019**, *11*, doi:10.3390/v11080694.
25. Heyman, P.; Ceianu, S.; Christova, I.; Tordo, N.; Vaheri, A. A five-year perspective on the situation of haemorrhagic fever with renal syndrome and status of the hantavirus reservoirs in Europe, 2005–2010. *Euro surveillance* **2011**, *16*.
26. Krakauer, D.C. Stability and evolution of overlapping genes. *Evolution; international journal of organic evolution* **2000**, *54*, 731-739, doi:10.1111/j.0014-3820.2000.tb00075.x.
27. Laenen, L.; Vergote, V.; Vanmechelen, B.; Tersago, K.; Baele, G.; Lemey, P.; Leirs, H.; Dellicour, S.; Vrancken, B.; Maes, P. Identifying the patterns and drivers of Puumala hantavirus enzootic dynamics using reservoir sampling. *Virus evolution* **2019**, *5*, vez009, doi:10.1093/ve/vez009.
28. Plyusnin, A.; Vapalahti, O.; Lankinen, H.; Lehväslaiho, H.; Apekina, N.; Myasnikov, Y.; Kallio-Kokko, H.; Henttonen, H.; Lundkvist, A.; Brummer-Korvenkontio, M., et al. Tula Virus: a Newly Detected Hantavirus Carried by European Common Voles. *Journal of virology* **1994**, *68*, p. 7833-7839.
29. Sibold, C.; Sparr, S.; Schulz, A.; Labuda, M.; Kozuch, O.; Lysy, J.; Kruger, D.H.; Meisel, H. Genetic characterization of a new hantavirus detected in *Microtus arvalis* from Slovakia. *Virus genes* **1995**, *10*, 277-281.
30. Schmidt-Chanasit, J.; Essbauer, S.; Petraityte, R.; Yoshimatsu, K.; Tackmann, K.; Conraths, F.J.; Sasnauskas, K.; Arikawa, J.; Thomas, A.; Pfeffer, M., et al. Extensive host sharing of central European Tula virus. *Journal of virology* **2010**, *84*, 459-474, doi:10.1128/JVI.01226-09.
31. Scharninghausen, J.J.; Pfeffer, M.; Meyer, H.; Davis, D.S.; Honeycutt, R.L.; Faulde, M. Genetic evidence for Tula virus in *Microtus arvalis* and *Microtus agrestis* populations in Croatia. *Vector borne and zoonotic diseases (Larchmont, N.Y.)* **2002**, *2*, 19-27, doi:10.1089/153036602760260742.
32. Schlegel, M.; Kindler, E.; Essbauer, S.S.; Wolf, R.; Thiel, J.; Groschup, M.H.; Heckel, G.; Oehme, R.M.; Ulrich, R.G. Tula virus infections in the Eurasian water vole in Central Europe. *Vector borne and zoonotic diseases (Larchmont, N.Y.)* **2012**, *12*, 503-513, doi:10.1089/vbz.2011.0784.
33. Binder, F.; Lenk, M.; Weber, S.; Stoek, F.; Dill, V.; Reiche, S.; Riebe, R.; Wernike, K.; Hoffmann, D.; Ziegler, U., et al. Common vole (*Microtus arvalis*) and bank vole (*Myodes glareolus*) derived permanent cell lines differ in their susceptibility and replication kinetics of animal and zoonotic viruses. *Journal of virological methods* **2019**, 10.1016/j.jviromet.2019.113729, 113729.
34. Klingström, J.; Heyman, P.; Escutenaire, S.; Sjolander, K.B.; De Jaegere, F.; Henttonen, H.; Lundkvist, A. Rodent host specificity of European hantaviruses: evidence of Puumala virus interspecific spillover. *Journal of medical virology* **2002**, *68*, 581-588, doi:10.1002/jmv.10232.
35. Essbauer, S.S.; Schmidt-Chanasit, J.; Madeja, E.L.; Wegener, W.; Friedrich, R.; Petraityte, R.; Sasnauskas, K.; Jacob, J.; Koch, J.; Dobler, G., et al. Nephropathia epidemica in metropolitan area, Germany. *Emerging infectious diseases* **2007**, *13*, 1271-1273, doi:10.3201/eid1308.061425.
36. Holmes, E.C.; Zhang, Y.Z. The evolution and emergence of hantaviruses. *Current opinion in virology* **2015**, *10*, 27-33, doi:10.1016/j.coviro.2014.12.007.

636 37. Vera-Otarola, J.; Solis, L.; Soto-Rifo, R.; Ricci, E.P.; Pino, K.; Tischler, N.D.; Ohlmann, T.; Darlix, J.L.; Lopez-
637 Lastra, M. The Andes hantavirus NSs protein is expressed from the viral small mRNA by a leaky scanning
638 mechanism. *Journal of virology* **2012**, *86*, 2176-2187, doi:10.1128/JVI.06223-11.
639 38. Severson, W.; Xu, X.; Kuhn, M.; Senutovitch, N.; Thokala, M.; Ferron, F.; Longhi, S.; Canard, B.; Jonsson,
640 C.B. Essential amino acids of the Hantaan virus N protein in its interaction with RNA. *Journal of virology*
641 **2005**, *79*, 10032-10039, doi:10.1128/jvi.79.15.10032-10039.2005.
642 39. Xu, X.; Severson, W.; Villegas, N.; Schmaljohn, C.S.; Jonsson, C.B. The RNA binding domain of the Hantaan
643 virus N protein maps to a central, conserved region. *Journal of virology* **2002**, *76*, 3301-3308,
644 doi:10.1128/jvi.76.7.3301-3308.2002.
645 40. Cheng, E.; Wang, Z.; Mir, M.A. Interaction between hantavirus nucleocapsid protein (N) and RNA-
646 dependent RNA polymerase (RdRp) mutants reveals the requirement of an N-RdRp interaction for viral
647 RNA synthesis. *Journal of virology* **2014**, *88*, 8706-8712, doi:10.1128/JVI.00405-14.
648 41. Shimizu, K.; Yoshimatsu, K.; Koma, T.; Yasuda, S.P.; Arikawa, J. Role of nucleocapsid protein of
649 hantaviruses in intracellular traffic of viral glycoproteins. *Virus research* **2013**, *178*, 349-356,
650 doi:10.1016/j.virusres.2013.09.022.
651 42. Plyusnin, A. Genetics of hantaviruses: implications to taxonomy. *Archives of virology* **2002**, *147*, 665-682.
652 43. Plyusnin, A.; Cheng, Y.; Lehvaslaiho, H.; Vaheri, A. Quasispecies in wild-type Tula hantavirus populations.
653 *Journal of virology* **1996**, *70*, 9060-9063.
654 44. Mertens, M.; Kindler, E.; Emmerich, P.; Esser, J.; Wagner-Wiening, C.; Wolfel, R.; Petraityte-Burneikiene,
655 R.; Schmidt-Chanasit, J.; Zvirbliene, A.; Groschup, M.H., et al. Phylogenetic analysis of Puumala virus
656 subtype Bavaria, characterization and diagnostic use of its recombinant nucleocapsid protein. *Virus genes*
657 **2011**, *43*, 177-191, doi:10.1007/s11262-011-0620-x.
658 45. Kucinskaite-Kodze, I.; Petraityte-Burneikiene, R.; Zvirbliene, A.; Hjelle, B.; Medina, R.A.; Gedvilaite, A.;
659 Razanskiene, A.; Schmidt-Chanasit, J.; Mertens, M.; Padula, P., et al. Characterization of monoclonal
660 antibodies against hantavirus nucleocapsid protein and their use for immunohistochemistry on rodent and
661 human samples. *Archives of virology* **2011**, *156*, 443-456, doi:10.1007/s00705-010-0879-6.
662 46. Kumar, S.; Stecher, G.; Li, M.; Knyaz, C.; Tamura, K. MEGA X: Molecular Evolutionary Genetics Analysis
663 across Computing Platforms. *Molecular biology and evolution* **2018**, *35*, 1547-1549,
664 doi:10.1093/molbev/msy096.
665 47. Miller, M.A.; Schwartz, T.; Pickett, B.E.; He, S.; Klem, E.B.; Scheuermann, R.H.; Passarotti, M.; Kaufman, S.;
666 O'Leary, M.A. A RESTful API for Access to Phylogenetic Tools via the CIPRES Science Gateway.
667 *Evolutionary Bioinformatics Online* **2015**, *11*, 43-48, doi:10.4137/EBO.S21501.
668 48. Kumar, S.; Stecher, G.; Tamura, K. MEGA7: Molecular Evolutionary Genetics Analysis Version 7.0 for
669 Bigger Datasets. *Molecular biology and evolution* **2016**, *33*, 1870-1874, doi:10.1093/molbev/msw054.
670 49. Ersts, P.J. Geographic Distance Matrix Generator (version 1.2.3). Availabe online:
671 http://biodiversityinformatics.amnh.org/open_source/gdmg (accessed on 03-26-2020).
672 50. R Core team *R: A Language and Environment for Statistical Computing*, R Foundation for Statistical
673 Computing: 2015.

674

Supplementary Table S1: Trapping site and season information for PUUV positive bank voles from Baden-Wuerttemberg from outbreak years 2007 and 2012.

Animal number	Trapping Site (see Fig. 1a)	Trapping season	Published in
Mu07/458	4 Zußdorf-Wilhelmsdorf	2007 summer	[1]
Mu07/459	4 Zußdorf-Wilhelmsdorf	2007 summer	[1]
Mu07/460	4 Zußdorf-Wilhelmsdorf	2007 summer	[1]
Mu07/473	4 Zußdorf-Wilhelmsdorf	2007 summer	[1]
Mu07/476	4 Zußdorf-Wilhelmsdorf	2007 summer	[1]
Mu07/477	4 Zußdorf-Wilhelmsdorf	2007 summer	[1]
Mu07/492	4 Zußdorf-Wilhelmsdorf	2007 summer	[1]
Mu07/503	6 Michelbach	2007 summer	[1]
Mu07/533	10 Steinheim B	2007 summer	[1]
Mu07/535	10 Steinheim B	2007 summer	[1]
Mu07/538	10 Steinheim B	2007 summer	[1]
Mu07/546	10 Steinheim B	2007 summer	[1]
KS12/2547	9 Steinheim A	2012 summer	[2]
KS12/2573	9 Steinheim A	2012 summer	[2]
KS12/2574	9 Steinheim A	2012 summer	[2]
KS12/2585	7 Geislingen-Stoetten	2012 summer	[2]
KS12/2587	3 Stuttgart-Buesnau	2012 summer	[2]
KS12/2592	2 Moessingen-Belsen	2012 summer	[2]
KS12/2594	2 Moessingen-Belsen	2012 summer	[2]
KS12/2595	7 Geislingen-Stoetten	2012 summer	[2]
KS12/2606	3 Stuttgart-Buesnau	2012 summer	[2]
KS12/2608	3 Stuttgart-Buesnau	2012 summer	[2]
KS12/2709	2 Moessingen-Belsen	2012 summer	[2]
KS13/536	1 Kenzingen	2012 summer	[2]
KS13/651	1 Kenzingen	2012 summer	[2]
KS13/656	1 Kenzingen	2012 summer	[2]
KS13/692	8 Crailsheim-Rossfeld	2012 summer	[2]
KS13/695	8 Crailsheim-Rossfeld	2012 summer	[2]
KS13/700	8 Crailsheim-Rossfeld	2012 summer	[2]
KS13/703	5 Goeppingen	2012 autumn	[2]
KS13/704	5 Goeppingen	2012 autumn	[2]
KS13/711	5 Goeppingen	2012 autumn	[2]

PUUV S segment sequences were generated for all 32 animals.

Supplementary Table S2: Rodents trapped for PUUV investigations over a five year period and results of serological tests (ELISA) and RNA detection (RT-PCR).

			PUUV-IgG ELISA		RT-PCR	
Trapping region	**Species**	**Year**	**Number of positive/total number investigated animals**	**Seroprevalence (%) and (95% CI)**	**Number of positive/total number investigated animals**	**RNA prevalence (%) and (95% CI)**
Baden-Wuerttemberg (BW)	Bank vole (*Clethrionomys glareolus*)	2010	77/266	29.0 (23.8-34.7)	74/266	27.8 (22.8-33.5)
		2011	2/32	5.4 (1.7-20.2)	2/32	6.3 (1.7-20.2)
		2012	45/163	27.6 (21.3-34.9)	44/163	27.0 (20.8-34.3)
		2013	0/23	0 (0-14.3)	0/23	0 (0-14.3)
		2014	9/31	29.0 (16.1-46.6)	4/31	12.9 (5.13-28.9)
		total	133/515	25.8 (22.2-29.8)	124/515	24.1 (20.6-28.0)
	Yellow-necked mouse (*Apodemus flavicollis*)	2010	0/88	0 (0-4.2)	n.d.	
		2011	0/24	0 (0-13.9)	n.d.	
		2012	0/103	0 (0-3.6)	n.d.	
		2013	0/20	0 (0-16.1)	n.d.	
		2014	0/20	0 (0-16.1)	n.d.	
		total	0/255	0 (0-1.5)		
	Wood mouse (*Apodemus sylvaticus*)	2010	0/4	0 (0-49.0)	n.d.	
		2011	0/10	0 (0-27.8)	n.d.	
		2012	0/3	0 (0-56.2)	n.d.	
		2013	0/5	0 (0-43.5)	n.d.	
		2014	0/1	0 (0-79.4)	n.d.	
		total	0/23	0 (0-14.3)		
	Common vole (*Microtus arvalis*)	2010	n.d.		0/45	0 (0-7.9)
		2011	n.d.		0/78	0 (0-4.7)
		2012	n.d.		0/8	0 (0-32.4)
		2013	not trapped		not trapped	
		2014	n.d.		0/27	0 (0-12.5)
		total			0/158	0 (0-2.4)
	Field vole (*Microtus agrestis*)	2010	n.d.		1/6	16.67 (3.0-56.4)
		2011	n.d.		0/1	0 (0-79.4)
		2012	not trapped		not trapped	
		2013	not trapped		not trapped	
		2014	not trapped		not trapped	
		total			1/7	14.3 (2.6-51.3)
North Rhine-Westphalia (NW)	Bank vole (*Clethrionomys glareolus*)	2010	86/249	34.5 (28.9-40.6)	55/249	22.1 (17.4-27.6)
		2011	2/32	6.3 (1.7-20.2)	1/32	3.1 (0.6-15.7)
		2012	21/55	38.2 (26.5-51.4)	13/55	23.6 (14.4-36.4)
		total	109/336	32.4 (27.7-37.6)	69/336	20.5 (16.6-25.2)
	Yellow-necked mouse (*Apodemus flavicollis*)	2010	0/96	0 (0-3.9)	0/96	0 (0-3.9)
		2011	0/9	0 (0-29.9)	0/9	0 (0-29.9)
		2012	0/37	0 (0-9.4)	0/37	0 (0-9.4)
		total	0/142	0 (0-2.6)	0/142	0 (0-2.6)
	Wood mouse (*Apodemus sylvaticus*)	2010	0/24	0 (0-13.8)	0/24	0 (0-13.8)
		2011	0/11	0 (0-25.9)	0/11	0 (0-25.9)
		2012	0/10	0 (0-27.8)	0/10	0 (0-27.8)
		total	0/45	0 (0-7.9)	0/45	0 (0-7.9)
	Common vole (*Microtus arvalis*)	2010	n.d.		0/9	0 (0-29.9)
		2011	n.d.		0/6	0 (0-39.0)
		2012	n.d.		0/3	0 (0-56.2)
		total			0/18	0 (0-17.6)
	Field vole (*Microtus agrestis*)	2010	n.d.		not trapped	
		2011	n.d.		0/1	0 (0-79.4)
		2012	n.d.		not trapped	
		total			0/1	0 (0-79.4)

n.d., not done; CI, confidence interval; ELISA, enzyme-linked immunosorbent assay; RT-PCR, reverse transcription-polymerase chain reaction. In common voles and field voles, TULV was found by sequencing and results will be included in a separate publication (Schmidt, Reil et al., in prep.). PUUV S segment sequences were generated for all 194 RNA positive animals, including 193 bank voles and a field vole.

Supplementary Table S3: Assignment of nucleotide sequences to sequence types for PUUV strains from Baden-Wuerttemberg

Animal number	Sequence types NSs	Sequence types N/NSs	Sequence types N
	NSs-nt-BW1: KS10/972, KS10/978, KS10/979, KS10/983, KS10/984, KS10/987, KS10/999, KS10/1001, KS10/1002, KS10/1006, KS10/1008, KS10/1011, KS10/1015, KS10/1017, KS10/1025, KS10/1026, KS10/1027, KS10/1029, KS10/1035, KS10/1039, KS10/1048, KS10/1049, KS10/1053, KS10/1054, KS10/1056, KS10/1060, KS10/1064, KS10/1065, KS10/1066, KS10/1076, KS10/1077, KS10/1078, KS10/1081, KS10/1082, KS10/1084, KS10/1086, KS10/1089, KS10/1093, KS10/1098, KS10/1099, KS10/1103, KS10/1109, KS10/1114, KS10/1115, KS10/1118, KS10/1121, KS10/1124, KS10/1127, KS10/1128, KS10/1135, KS10/1850, KS10/1854, KS10/1865, KS10/1869, KS10/1871, KS10/1876, KS10/1886, KS10/1887, KS10/1919, KS10/1928, KS10/1935, KS10/3423, KS10/3440, KS10/3556, KS10/3562, KS10/3571, KS11/2037, KS12/1679, KS12/1680, KS12/1681, KS12/1682, KS12/1683, KS12/1685, KS12/1686, KS12/1687, KS12/1688, KS12/1689, KS12/1696, KS12/1700, KS12/1702, KS12/1703, KS12/1705, KS12/1706, KS12/1709, KS12/1713, KS12/1716, KS12/1737, KS12/1740, KS12/1741, KS12/1742, KS12/1745, KS12/1749, KS12/1753, KS12/1756, KS12/1757, KS12/1768, KS12/1769, KS12/1774, KS12/2326, KS12/2327, KS12/2331, KS12/2414, KS12/2427, KS12/2429, KS12/2443, KS13/258, KS13/267, KS13/281, KS13/289, KS15/207, KS15/315, KS15/317, KS10/1083, KS11/2364	**N/NSs-nt-BW1:** KS10/972, KS10/978, KS10/979, KS10/983, KS10/984, KS10/987, KS10/999, KS10/1001, KS10/1002, KS10/1006, KS10/1008, KS10/1011, KS10/1015, KS10/1017, KS10/1025, KS10/1026, KS10/1027, KS10/1029, KS10/1035, KS10/1039, KS10/1048, KS10/1049, KS10/1053, KS10/1054, KS10/1056, KS10/1060, KS10/1064, KS10/1065, KS10/1066, KS10/1076, KS10/1077, KS10/1078, KS10/1081, KS10/1082, KS10/1084, KS10/1086, KS10/1089, KS10/1093, KS10/1098, KS10/1099, KS10/1103, KS10/1109, KS10/1114, KS10/1115, KS10/1118, KS10/1121, KS10/1124, KS10/1127, KS10/1128, KS10/1135, KS10/1850, KS10/1854, KS10/1865, KS10/1869, KS10/1871, KS10/1876, KS10/1886, KS10/1887, KS10/1919, KS10/1928, KS10/1935, KS10/3423, KS10/3440, KS10/3556, KS10/3562, KS10/3571, KS11/2037, KS12/1679, KS12/1680, KS12/1681, KS12/1682, KS12/1683, KS12/1685, KS12/1686, KS12/1687, KS12/1688, KS12/1689, KS12/1696, KS12/1700, KS12/1702, KS12/1703, KS12/1705, KS12/1706, KS12/1709, KS12/1713, KS12/1716, KS12/1737, KS12/1740, KS12/1741, KS12/1742, KS12/1745, KS12/1749, KS12/1753, KS12/1756, KS12/1757, KS12/1768, KS12/1769, KS12/1774, KS12/2326, KS12/2327, KS12/2331, KS12/2414, KS12/2427, KS12/2429, KS12/2443, KS13/258, KS13/267, KS13/281, KS13/289, KS15/207, KS15/315, KS15/317, KS10/1083, KS11/2364	**N-nt-BW1:** KS10/978, KS10/979, KS10/984, KS10/987, KS10/1001, KS10/1002, KS10/1006, KS10/1015, KS10/1017, KS10/1026, KS10/1029, KS10/1035, KS10/1048, KS10/1049, KS10/1053, KS10/1054, KS10/1056, KS10/1076, KS10/1077, KS10/1081, KS10/1082, KS10/1084, KS10/1093, KS10/1098, KS10/1099, KS10/1103, KS10/1109, KS10/1114, KS10/1115, KS10/1124, KS10/1127, KS10/1128, KS10/1135, KS10/1854, KS10/1865, KS10/1871, KS10/1886, KS10/3440, KS10/3556, KS10/3562, KS10/3571, KS12/1679, KS12/1680, KS12/1681, KS12/1682, KS12/1683, KS12/1685, KS12/1686, KS12/1687, KS12/1688, KS12/1689, KS12/1696, KS12/1702, KS12/1703, KS12/1705, KS12/1706, KS12/1709, KS12/1713, KS12/1716, KS12/1737, KS12/1740, KS12/1741, KS12/1742, KS12/1749, KS12/1753, KS12/1768, KS12/1769, KS12/2326, KS12/2327, KS12/2331, KS12/2383, KS12/2414, KS12/2427, KS12/2429, KS12/2443, KS13/233, KS13/267, KS13/281, KS15/207, KS15/307, KS15/315, KS15/317
	NSs-nt-BW2-T20G: KS10/994, KS10/1019	**N/NSs-nt-BW2-T20G:** KS10/994, KS10/1019	**N-nt-BW2:** KS10/972, KS10/994, KS10/1019, KS10/1935
	NSs-nt-BW3-T218A: KS10/1068, KS10/1100, KS10/1848, KS10/1851, KS10/3428	**N/NSs-nt-BW3-T218A:** KS10/1068, KS10/1100, KS10/1848, KS10/1851, KS10/3428	**N-nt-BW3:** KS10/983, KS10/1011, KS10/1025, KS10/1027, KS10/1039, KS10/1118
	NSs-nt-BW4-C221T: KS12/2383, KS13/233	**N/NSs-nt-BW4-C221T:** KS12/2383, KS13/233	**N-nt-BW4:** KS10/999
	NSs-nt-BW5-G179A: KS15/307	**N/NSs-nt-BW5-G179A:** KS15/307	**N-nt-BW5:** KS10/1008, KS10/1060, KS10/1065, KS10/1086, KS10/1089, KS10/1121, KS10/1850, KS10/1876, KS10/1887, KS10/3423
			N-nt-BW6: KS10/1064
			N-nt-BW7: KS10/1066, KS11/2037, KS11/2364, KS13/258
			N-nt-BW8: KS10/1068, KS10/1100, KS10/1848, KS10/1851, KS10/3428
			N-nt-BW9: KS10/1869
			N-nt-BW10: KS10/1083
			N-nt-BW11: KS10/1078, KS12/1700, KS12/1757, KS12/1774
			N-nt-BW12: KS10/1919, KS10/1928
			N-nt-BW13: KS12/1745, KS12/1756
			N-nt-BW14: VKS13/289

Animal numbers of identical partial S segment nucleotide sequences are grouped together as one sequence type. Colors of text shade indicate the sequence type shown in Figure 5a. Light gray background indicates the cumulative amino acid sequence type N/NSs-aa-BW1 or N-aa-BW1. The amino acid sequences of the NSs-aa sequence types are given in Supplementary Figure S1, the amino acid sequences of the N-aa sequence types (overlapping and non-overlapping NSs) are shown in Supplementary Figure S2a and b. Nucleotide exchanges in the N/NSs overlapping region in comparison to sequence type BW1 are given next to sequence type names (residue in sequence type BW1/position/residue in the other sequence type).

Supplementary Table S4: Assignment of nucleotide sequences to sequence types for PUUV strains from North Rhine-Westphalia

Animal number	Sequence types NSs	Sequence type N/NSs	Sequence type N
	NSs-nt-NW1: KS10/2030, KS10/2036, KS10/2038, KS10/2040, KS10/2059, KS10/2060, KS10/2061, KS10/2067, KS10/2073, KS10/2083, KS10/2092, KS10/2094, KS10/2095, KS10/2098, KS10/2099, KS10/2100, KS10/2103, KS10/2104, KS10/2159, KS10 2167, KS10/2169, KS10/2171, KS10/2173, KS10/2175, KS10/2178, KS10/2179, KS10/2186, KS10/2188, KS10/2195, KS10/2199, KS10/2200, KS10/2203, KS10/2204, KS10/2219, KS10/2222, KS10/2228, KS10/2234, KS10/2235, KS10/2243, KS10/2668, KS10/2705, KS10/2990, KS11/2251, KS12/1808, KS12/2478, KS10/2170	**N/NSs-nt-NW1:** KS10/2030, KS10/2036, KS10/2038, KS10/2040, KS10/2059, KS10/2060, KS10/2061, KS10/2067, KS10/2073, KS10/2083, KS10/2092, KS10/2094, KS10/2095, KS10/2098, KS10/2099, KS10/2100, KS10/2103, KS10/2104, KS10/2159, KS10 2167, KS10/2169, KS10/2171, KS10/2173, KS10/2175, KS10/2178, KS10/2179, KS10/2186, KS10/2188, KS10/2195, KS10/2199, KS10/2200, KS10/2203, KS10/2204, KS10/2219, KS10/2222, KS10/2228, KS10/2234, KS10/2235, KS10/2243, KS10/2668, KS10/2705, KS10/2990, KS11/2251, KS12/1808, KS12/2478, KS10/2170	**N-nt-NW1:** KS10/2001
	NSs-nt-NW2-A44G: KS10/2001, KS10/2010, KS10/2020, KS10/2022, KS10/2025, KS10/2028, KS10/2090, KS10/2102, KS10/2174, KS10/2190, KS10/2192, KS10/2592, KS12/1777, KS12/1816, KS12/2471, KS12/2476, KS12/2515, KS12/2517, KS12/2520, KS12/2522	**N/NSs-nt-NW2-A44G:** KS10/2001, KS10/2010, KS10/2020, KS10/2022, KS10/2025, KS10/2028, KS10/2090, KS10/2102, KS10/2174, KS10/2190, KS10/2192, KS10/2592, KS12/1777, KS12/1816, KS12/2471, KS12/2476, KS12/2515, KS12/2517, KS12/2520, KS12/2522	**N-nt-NW2:** KS10/2228, KS10/2235
	NSs-nt-NW3-G59A: KS12/1778, KS12/2510	**N/NSs-nt-NW3-G59A:** KS12/1778, KS12/2510	**N-nt-NW3:** KS10/2020, KS10/2022, KS10/2025, KS10/2028, KS10/2090, KS10/2102, KS10/2190, KS10/2192
	NSs-nt-NW4-A85G: KS12/2519	**N/NSs-nt-NW4-A85G:** KS12/2519	**N-nt-NW4:** KS10/2030, KS10/2038, KS10/2159, KS10/2175, KS10/2186, KS10/2188, KS10/2199, KS10/2203, KS10/2204, KS10/2243, KS10/2705, KS11/2251, KS12/1808, KS12/2478
			N-nt-NW5: KS10/2036, KS10/2040
			N-nt-NW6: KS10/2059, KS10/2060, KS10/2061, KS10/2073, KS10/2083, KS10/2092, KS10/2094, KS10/2095, KS10/2098, KS10/2099, KS10/2100, KS10/2103, KS10/2104, KS10/2167, KS10/2169, KS10/2170, KS10/2171, KS10/2173, KS10/2178, KS10/2179, KS10/2195, KS10/2200, KS10/2219, KS10/2222, KS10/2234, KS10/2668, KS10/2990
			N-nt-NW7: KS10/2067
			N-nt-NW8: KS10/2174
			N-nt-NW9: KS10/2010, KS10/2592
			N-nt-NW10: KS12/1777
			N-nt-NW11: KS12/1778, KS12/2510
			N-nt-NW12: KS12/1816, KS12/2515, KS12/2517, KS12/2519, KS12/2520, KS12/2522
			N-nt-NW13KS12/2471, KS12/2476

Animal numbers of identical partial S segment nucleotide sequences are grouped together as one sequence type. Colors of text shade indicate the sequence type shown in Figure 5b. Light gray background indicates the cumulative major amino acid sequence types N/NSs-aa-NW1 and N-aa-NW1. Dark grey background shows the cumulative minor amino acid sequence type N-aa-NW9/11/13. The amino acid sequences of the NSs-aa sequence types are given in Supplementary Figure S1, the amino acid sequences of the N-aa sequence types (overlapping and non-overlapping NSs) are shown in Supplementary Figure S2a and b. Nucleotide exchanges in the N/NSs overlapping region in comparison to sequence type NW1 are given next to sequence type names (residue in sequence type NW1/position/residue in the other sequence type).

Supplementary Figure S1: Amino acid sequence alignment of unique putative NSs proteins of Puumala orthohantavirus (PUUV) strains from Baden-Wuerttemberg (BW) and North Rhine-Westphalia (NW) and previously described PUUV isolates from Osnabrück region, Lower Saxony.

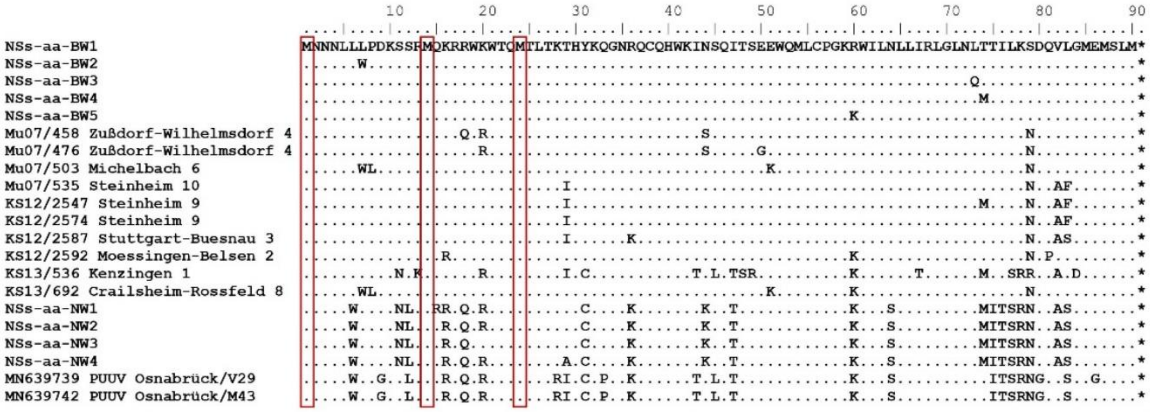

The main amino acid sequence type of NSs served as a reference (NSs-aa-BW1). Identical amino acid residues are shown as dots. NSs sequences from Goeppingen, Geislingen and additional samples from other trapping sites were identical to the shown sequences from BW. *, stop codon; putative methionine start codons are framed in red.

Supplementary Figure S2: Amino acid sequence alignment of unique partial N protein segments encoded by overlapping (a) or non-overlapping NSs ORF (b) parts of Puumala orthohantavirus (PUUV) strains from Baden-Wuerttemberg (BW) and North Rhine-Westphalia (NW) and previously described PUUV isolates from Osnabrück region, Lower Saxony.

a

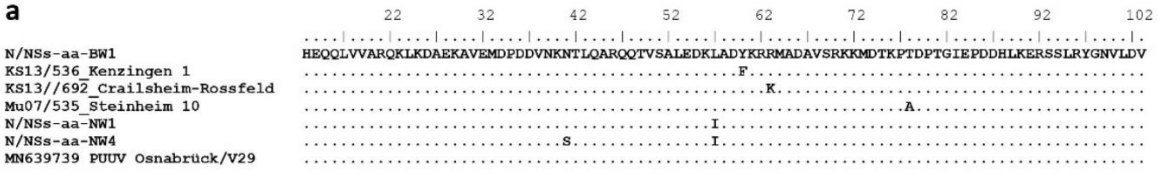

b

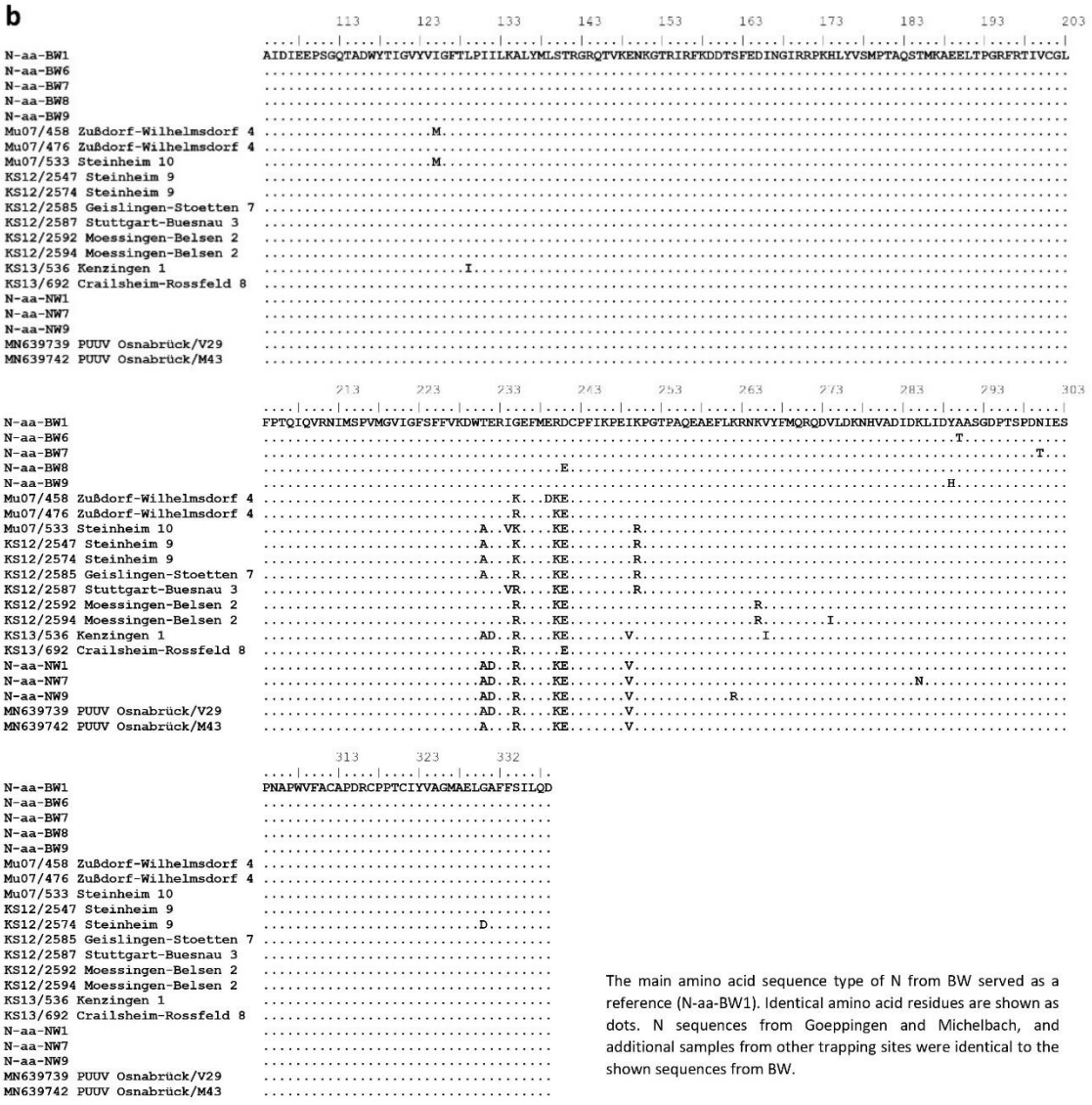

The main amino acid sequence type of N from BW served as a reference (N-aa-BW1). Identical amino acid residues are shown as dots. N sequences from Goeppingen and Michelbach, and additional samples from other trapping sites were identical to the shown sequences from BW.

References

1. Drewes, S.; Ali, H.S.; Saxenhofer, M.; Rosenfeld, U.M.; Binder, F.; Cuypers, F.; Schlegel, M.; Rohrs, S.; Heckel, G.; Ulrich, R.G. Host-Associated Absence of Human Puumala Virus Infections in Northern and Eastern Germany. *Emerging infectious diseases* **2017**, *23*, 83-86, doi:10.3201/eid2301.160224.
2. Drewes, S.; Turni, H.; Rosenfeld, U.M.; Obiegala, A.; Strakova, P.; Imholt, C.; Glatthaar, E.; Dressel, K.; Pfeffer, M.; Jacob, J., et al. Reservoir-Driven Heterogeneous Distribution of Recorded Human Puumala virus Cases in South-West Germany. *Zoonoses and public health* **2017**, 10.1111/zph.12319, doi:10.1111/zph.12319.

(III) COMMON VOLE (*MICROTUS ARVALIS*) AND BANK VOLE (*MYODES GLAREOLUS*) DERIVED PERMANENT CELL LINES DIFFER IN THEIR SUSCEPTIBILITY AND REPLICATION KINETICS OF ANIMAL AND ZOONOTIC VIRUSES

Binder, F., Lenk, M., Weber, S., Stoek, F., Dill, V., Reiche, S., Riebe, R., Wernike, K., Hoffmann, D., Ziegler, U., Adler, H., Essbauer, S., Ulrich, R.G.

Journal of Virological Methods

Volume 274, 113729

December 2019

DOI:10.1016/j.jviromet.2019.113729.

Journal of Virological Methods 274 (2019) 113729

Contents lists available at ScienceDirect

Journal of Virological Methods

journal homepage: www.elsevier.com/locate/jviromet

Common vole (*Microtus arvalis*) and bank vole (*Myodes glareolus*) derived permanent cell lines differ in their susceptibility and replication kinetics of animal and zoonotic viruses

Florian Binder[a], Matthias Lenk[b], Saskia Weber[c], Franziska Stoek[a], Veronika Dill[c], Sven Reiche[b], Roland Riebe[b], Kerstin Wernike[c], Donata Hoffmann[c], Ute Ziegler[a,g], Heiko Adler[d,e], Sandra Essbauer[f], Rainer G. Ulrich[a,g,*]

[a] Friedrich-Loeffler-Institut, Federal Research Institute for Animal Health, Institute of Novel and Emerging Infectious Diseases, Südufer 10, 17493 Greifswald - Insel Riems, Germany
[b] Friedrich-Loeffler-Institut, Federal Research Institute for Animal Health, Department of Experimental Animal Facilities and Biorisk Management, Bio-Bank, Collection of Cell Lines in Veterinary Virology (CCLV), Südufer 10, 17493, Greifswald - Insel Riems, Germany
[c] Friedrich-Loeffler-Institut, Federal Research Institute for Animal Health, Institute of Diagnostic Virology, Südufer 10, 17493 Greifswald - Insel Riems, Germany
[d] Comprehensive Pneumology Center, Research Unit Lung Repair and Regeneration, Helmholtz Zentrum München - German Research Center for Environmental Health (GmbH), Marchioninistrasse 25, 81377 Munich, Germany
[e] University Hospital Grosshadern, Ludwig-Maximilians-University, 81377 Munich, Germany
[f] Bundeswehr Institute of Microbiology, Department Virology and Rickettsiology, Neuherbergstr. 11, 80937 Munich, Germany
[g] German Center for Infection Research (DZIF), Partner site Hamburg-Lübeck-Borstel-Insel Riems, Germany

ARTICLE INFO

Keywords:
Cell line
Cytopathic effect
Host
Vole

ABSTRACT

Pathogenesis and reservoir host adaptation of animal and zoonotic viruses are poorly understood due to missing adequate cell culture and animal models. The bank vole (*Myodes glareolus*) and common vole (*Microtus arvalis*) serve as hosts for a variety of zoonotic pathogens. For a better understanding of virus association to a putative animal host, we generated two novel cell lines from bank voles of different evolutionary lineages and two common vole cell lines and assayed their susceptibility, replication and cytopathogenic effect (CPE) formation for rodent-borne, suspected to be rodent-associated or viruses with no obvious rodent association. Already established bank vole cell line BVK168, used as control, was susceptible to almost all viruses tested and efficiently produced infectious virus for almost all of them. The Puumala orthohantavirus strain Vranica/Hällnäs showed efficient replication in a new bank vole kidney cell line, but not in the other four bank and common vole cell lines. Tula orthohantavirus replicated in the kidney cell line of common voles, but was hampered in its replication in the other cell lines. Several zoonotic viruses, such as Cowpox virus, Vaccinia virus, Rift Valley fever virus, and Encephalomyocarditis virus 1 replicated in all cell lines with CPE formation. West Nile virus, Usutu virus, Sindbis virus and Tick-borne encephalitis virus replicated only in a part of the cell lines, perhaps indicating cell line specific factors involved in replication. Rodent specific viruses differed in their replication potential: Murine gammaherpesvirus-68 replicated in the four tested vole cell lines, whereas murine norovirus failed to infect almost all cell lines. Schmallenberg virus and Foot-and-mouth disease virus replicated in some of the cell lines, although these viruses have never been associated to rodents. In conclusion, these newly developed cell lines may represent useful tools to study virus-cell interactions and to identify and characterize host cell factors involved in replication of rodent associated viruses.

1. Introduction

Emerging viruses play an important role in animal and human health and zoonotic agents cause a variety of human infections in the world (Jones et al., 2008). New high-throughput methods allowed the rapid identification of novel animal or zoonotic pathogens (Drewes et al., 2017a). Small mammals and rodents in particular represent a substantial part of the worldwide mammal diversity and have an

* Corresponding author at: Friedrich-Loeffler-Institut, Federal Research Institute for Animal Health, Institute of Novel and Emerging Infectious Diseases, Südufer 10, 17493 Greifswald - Insel Riems, Germany.
E-mail address: Rainer.Ulrich@fli.de (R.G. Ulrich).

https://doi.org/10.1016/j.jviromet.2019.113729
Received 9 May 2019; Received in revised form 15 August 2019; Accepted 7 September 2019
Available online 09 September 2019
0166-0934/

Table 1
Viruses wild rodent cell lines.

Family	Genus	Group/Virus	Strain	Reference cell line	Zoonotic potential	Host/origin	Detection in rodents
Picornaviridae	*Cardiovirus*	Encephalomyocarditis virus 1 (EMCV 1)	Hungary IV29	BHK-21	+	Rodents (Carocci and Bakkali-Kassimi, 2012)	yes
Picornaviridae	*Cardiovirus*	Encephalomyocarditis virus 2 (EMCV 2)	RD 1338 (D28/05)	BHK-21	+	Rodents (Carocci and Bakkali-Kassimi, 2012)	yes
Picornaviridae	*Aphthovirus*	Foot-and-mouth disease virus (FMDV)	A24 Cruzeiro	BHK-21	–	Cattle (Mowat et al., 1962)	no
Caliciviridae	*Norovirus*	Murine norovirus (MNV)	S99	RAW 264.7	–	Rodents (Wobus et al., 2004)	yes
Togaviridae	*Alphavirus*	Sindbis virus (SINV)	Hooded Crow (JX570540)	Vero 76	+	Birds (Eiden et al., 2014)	yes
Flaviviridae	*Flavivirus*	Usutu virus (USUV)	USUV Europe 3 (BH65/11-02-03)	Vero 76	+	Birds (Becker et al., 2012)	yes
Flaviviridae	*Flavivirus*	Tick-borne encephalitis virus (TBEV)	TBEV Neudoerfl	Vero B4	+	Rodents (Mandl et al., 1989)	yes
Flaviviridae	*Flavivirus*	West Nile virus (WNV)	WNV Austria (lineage 2)	Vero B4	+	Birds (Wodak et al., 2011)	yes
Phenuiviridae	*Phlebovirus*	Rift Valley fever virus (RVFV)	MP-12	Vero 76	+	Ruminants (McMillen and Hartman, 2018)	yes
Hantaviridae	*Orthohantavirus*	Puumala orthohantavirus (PUUV)	Vranica/Hällnäs	Vero E6	+	Rodents (Essbauer et al., 2011)	yes
Hantaviridae	*Orthohantavirus*	Tula orthohantavirus (TULV)	Moravia	Vero E6	(+)	Rodents (Vapalahti et al., 1996)	yes
Peribunyaviridae	*Orthobunyavirus*	Schmallenberg virus (SBV)	BH80/11	BHK-21	–	Cattle (Varela et al., 2013)	no
Poxviridae	*Orthopox virus*	Vaccinia virus (VACV)	Ankara 091	Vero E6	+	Rodents (Antoine et al., 1998)	yes
Poxviridae	*Orthopox virus*	Cowpox virus (CPXV)	2	Vero 76	+	Cattle (Liebermann et al., 1967)	yes
Herpesviridae	*Rhadinovirus*	Murid herpesvirus 4	Murine gammaherpesvirus 68	BHK-21	–	Mice (Virgin et al., 1997)	yes

important impact on human civilization (Lloyd-Smith et al., 2009). In addition to their role as pests in agriculture and forestry they are frequently competing with human and domestic animal food resources. Most importantly, they are associated with numerous zoonotic agents, such as orthohanta-, arena- and orthopoxviruses, *Leptospira* spp. or a variety of endoparasites (Meerburg et al., 2009). Due to their wide distribution, high abundance and close proximity to humans or farm, companion and pet animals, human infections with rodent-borne pathogens are frequently observed.

Bank vole (*Myodes glareolus*) and common vole (*Microtus arvalis*) harbor a variety of zoonotic agents, *e.g.* orthohantaviruses (Vaheri et al., 2013; see Table 1). Tula orthohantavirus (TULV) is frequently detected in the common vole, but also in related *Microtus* and other vole species (Schmidt et al., 2016; Schmidt-Chanasit et al., 2010). Large-scale sequence analyses of TULV strains indicated well-separated genetic clades with defined geographical distribution, *e.g.* Moravia strain belongs to the Eastern South (EST.S) clade in the Eastern evolutionary lineage of the common vole (Plyusnin and Vaheri, 1994; Saxenhofer et al., 2017). The zoonotic potential of TULV is controversially discussed (Vapalahti et al., 2003). Puumala orthohantavirus (PUUV) in contrast is the main causative agent of hemorrhagic fever with renal syndrome (HFRS) in Europe (Vapalahti et al., 2003). It is excreted by the bank vole in feces, urine, and saliva and is transmitted *via* inhalation of aerosols or by biting. PUUV in Germany and its neighboring countries in the west is associated with the Western evolutionary lineage of the bank vole (Drewes et al., 2017b). Sympatrically occurring bank voles of the Eastern lineage or the Carpathian lineage seem to be susceptible for PUUV carried by the Western lineage in Germany (Drewes et al., 2017b). PUUV and TULV are difficult to grow in cell culture as they need long incubation times and replicate only to low titers (Meyer and Schmaljohn, 2000).

Cowpox virus (CPXV), family *Poxviridae*, is another zoonotic virus associated with rodents, and common and bank vole in particular, as reservoirs (Essbauer et al., 2010; Hoffmann et al., 2015). Vaccinia virus (VACV) is a further zoonotic orthopox virus that is detected in rodents in South America (Oliveira et al., 2017; Peres et al., 2018, Table 1). The encephalomyocarditis virus (EMCV) has a worldwide distribution and can infect a broad spectrum of mammal species, but its natural reservoir host is believed to be a rodent. It was described to be a zoonotic agent, but an association between human infection and disease has still not been clearly established (Carocci and Bakkali-Kassimi, 2012).

Rodents also play a pivotal role in the infection cycle of many important arthropod-borne viruses, such as tick-borne encephalitis virus (TBEV). This virus was detected in wild and experimentally infected common and bank voles (Achazi et al., 2011). Voles are discussed to serve as a reservoir on which ticks and their larvae and nymphs get TBEV infected during blood-feeding or co-feeding (Jaenson et al., 2012). Usutu virus (USUV) and Sindbis virus (SINV) affect birds, but were also detected in rodents and discussed to have zoonotic potential (Becker et al., 2012; Eiden et al., 2014). Rift Valley fever virus (RVFV) is another vector-borne zoonotic pathogen that was detected in rodents (Table 1). West nile virus (WNV) is transmitted by *Culex* mosquitoes and was repeatedly introduced into Europe, especially Italy, Greece, Romania (Johnson et al., 2018), and recently Germany (Ziegler et al., 2018). The WNV replication cycle involves mosquito species as vector and wild birds acting as the reservoir, but with spillover to humans, rodents and other mammals (Suthar et al., 2013). Currently, there are not many studies exploring the WNV host range. In contrast, Schmallenberg virus (SBV) is a vector borne, non-zoonotic pathogen that has not been detected in rodents before (Mouchantat et al., 2015; see Table 1).

Murine norovirus (MNV) and Murine gammaherpesvirus 68 (MHV-68) are rodent-specific model viruses used for studies on noro- and herpesviruses (Blaškovič et al., 1980). MHV-68 was isolated from rodents and showed a high prevalence in yellow necked mouse (*Apodemus flavicollis)* and bank vole (Vrbová et al., 2016). Foot-and-mouth disease

virus (FMDV) is a picornavirus that affects livestock worldwide. It can infect a variety of hosts with cloven-hoofed animals playing a central role in its cycle, however it was never detected in rodents (Brito et al., 2017; Alexandersen and Mowat, 2005; see Table 1).

Currently, many viruses, including those associated to rodents, are isolated and propagated in standard cell lines from African green monkeys (Vero cells), baby hamster kidney cells (BHK-21) or mosquito cells (clone C6/36) (Eckerle et al., 2014). The Vero cell subclone E6 provides an excellent environment for viruses to replicate as it cannot provide a functional type-I interferon response (Emeny and Morgan, 1978). Vero E6 cells have enabled the isolation of a variety of hantaviruses, however most novel rodent-borne viruses remain uncultured (Kitamura et al., 1983; Elliott et al., 1994; Jameson et al., 2013; Vapalahti et al., 1996; Papa et al., 2001; Yanagihara et al., 1984). Rodent-derived cell culture models, which reflect the unique virus-host adaptation, are still rare. They can be beneficial for virus isolation and characterization of host specificity and identification of cellular receptors or host cell factors that are essential for development of strategies counteracting these pathogens (Drewes et al., 2017a). Previously the characterization of a permanent bank vole-derived kidney cell line (BVK168) for propagation of different viruses was described (Essbauer et al., 2011). However, mainly primary bank vole cells were used for propagation of hantaviruses so far (Stoltz et al., 2011; Temonen et al., 1993). Primary cell cultures are tissue derived cells that were freshly isolated and have a limited live span *in vitro*. They mostly keep their *in vivo* properties and therefore are often used for studying cellular processes and gene expression. However, as they derive from blood or organ tissue, the operator faces challenges like fragile handling processes or higher risk due to unknown infectious status. Additionally, experiments depend on the availability of fresh organ material for cell extraction. Permanent cell culture systems on the other hand are immortalized cells or tumor cells, which are available on request as their lifespan is not limited. The drawback of these cells is that they lose many of their natural properties as they undergo mutations in the genome or accumulate chromosome multiplications. These are valuable for research as storage by cryo-conservation is possible, which allows standardized long-term experiments. This also leads to less dependency on certain growth factors associated with easier handling (Schmitz, 2011).

Herein we describe the establishment of four novel cell lines: the common vole kidney cell line FMN-R (FMN), the common vole brain cell line FMG-R (FMG), the Eastern lineage bank vole lung cell line MGLU-2-R (MGLU) and the Carpathian lineage bank vole kidney cell line MGN-2-R (MGN). We have chosen 14 laboratory adapted viruses out of nine virus families that are either rodent-borne and zoonotic, suspected to be rodent-associated or have no obvious association to rodents (Table 1). The replication and cytopathic effect (CPE) formation in FMN, FMG and MGLU cell lines and the previously described Western lineage bank vole-derived BVK168 kidney cell line (Essbauer et al., 2011) were compared. The MGN cell line was used here exclusively for infection studies of PUUV as the previously described BVK168 cell line was not able to efficiently replicate PUUV.

2. Materials and methods

2.1. Cell lines

The generation and characterization of the cell line BVK168 (Collection of Cell Lines in Veterinary Medicine – Riems (CCLV-RIE) 1313) was described previously to be of epitheloid morphology and male origin (Essbauer et al., 2011).

To generate the MGN cell line (CCLV-RIE 1494), an adult bank vole was obtained from the holding of the Friedrich-Loeffler-Institut, Greifswald - Insel Riems, Germany. The animal was anaesthetized with isofluran and euthanized by using CO_2. The kidney of the bank vole was extracted and minced. Cultures were generated by explant culture method in an equal mixture of Ham's F12 and Iscove's modified Dulbecco's medium (IMDM) containing 10% fetal calf serum (FCS). Resulting cells were subcultured to passage 12 and determined to be of epithelial-like morphology. PCR-typing revealed a male sex of the cell line.

To generate the MGLU cell line (CCLV-RIE 1304), an adult female bank vole was live trapped on the island of Riems, Greifswald, Germany (permission of the trapping: Landesamt für Landwirtschaft, Lebensmittelsicherheit und Fischerei Mecklenburg-Vorpommern 7221. 3-030/09). The animal was anaesthetized with isofluran and euthanized by using CO_2. During dissection the whole right lung (*pulmo dexter*) was taken, fractionated and trypsinized three times for 30 min at room temperature. The resulting cells were seeded in a mixture of equal volumes of minimal essential medium (MEM) with Earle's balanced salt solution (BSS) and MEM (Hanks' BSS), containing 10% fetal calf serum. The cells were propagated continuously in a closed system to subculture no. 54 showing an increase in proliferation around subculture no. 25 (altered splitting ratio from 1:2 to 1:6 to 1:10), where we suppose that spontaneous immortalization occurred. Cells were determined as fibroblast-like and of female sex by PCR typing.

For generation of novel common vole cell lines FMN (CCLV-RIE 1102) and FMG (CCLV-RIE 1129), common voles were obtained from the holding of the Julius Kühn-Institute, Münster, Germany. To generate FMN, kidneys of six newborn common voles (4–6 days old) were minced together. After fractionated trypsination three times for 30 min at room temperature, the cells were seeded in MEM including Hanks' BSS and 10% FCS. After changing the medium to a mixture of equal volumes of Ham's F12 and Iscove's modified Dulbecco's medium containing 20% FCS, the cells were subcultured in a closed system without any sign of crisis to subculture no. 70. Spontaneous immortalization seemed to occur around subculture no. 20, when the splitting ratio could be increased from 1:2 to 1:4. Cells at this passage demonstrated a fibroblastoid morphology.

To generate FMG, brains of six newborn common voles were pooled, minced with scissors and a syringe with a needle. The cells were seeded in MEM (Hanks' BSS) containing 10% FCS. After changing the medium to a mixture of equal volumes of Hams' F12 and IMDM with 20% FCS, the cells showed better proliferation. The fibroblastoid cells were subcultured in a closed system continuously without any crisis until subculture no. 100. Spontaneous immortalization seemed to happen around passage no. 40.

All viruses and cell lines were tested free of bacterial contamination by mycoplasma PCR screening and standard in-house bacterial isolation approaches. Analysis of potential contaminations for all cell lines was further investigated by the Multiplex cell Contamination Test (McCT) Service, Heidelberg, Germany (http://www.multiplexion.de). This test includes multiplex PCR assays for 14 *Mycoplasma* species, Squirrel monkey retrovirus, and Epstein-Barr virus. In addition, potential contamination with human, *Macaca cynomolgus*, mouse, rat, Chinese hamster, Syrian hamster, feline, canine, rabbit, pig, Guinea pig and *Drosophila* cells was excluded.

Cells were regularly grown in MEM containing non-essential amino acids and 10% FCS. MGN cell line was grown in Ham's F12/IMDM + 10% FCS. Passaging was done twice a week by trypsinating cells and seeding in a ratio of 1:4 for BVK168, 1:10 for MGLU, 1:6 for MGN, 1:3 for FMN, and 1:20 for FMG.

2.2. Determination of the species, evolutionary lineage origin and sex of the cell lines

The species and evolutionary lineage origin of the cell lines were determined by PCR-based determination of a partial sequence of the mitochondrial cytochrome *b* gene as described previously (Drewes et al., 2017b; Schlegel et al., 2012a). Cell culture samples were directly used for DNA extraction with a GeneMATRIX Tissue DNA Purification Kit (Roboklon, Potsdam, Germany). Sequences of the cytochrome *b*

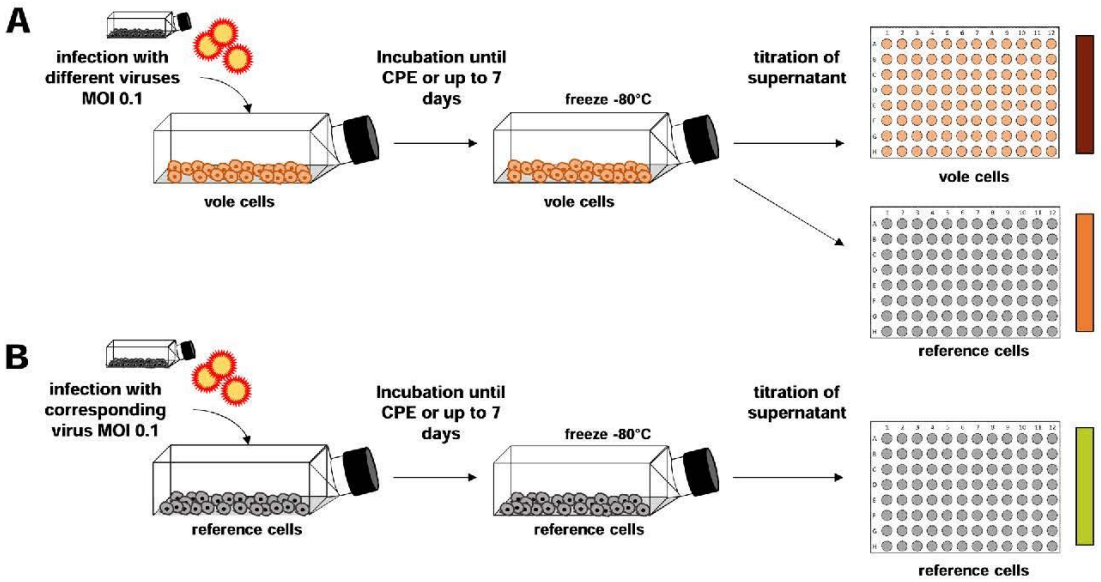

Fig. 1. Schematic representation of the workflow. Infection experiments of vole cell lines and back-titration on vole and reference cell lines (A) and positive control setup on the reference cell line for each virus (B). Pattern bars indicate identification code for titer diagrams in Fig. 3. For reference cell lines see Table 1. Infection protocol for non-cytolytic hantaviruses differs from the protocol shown here and is described separately.

gene were deposited in GenBank with accession numbers FJ528598 (BVK168), MK559348 (MGLU), MK559347 (MGN), MK559346 (FMN) and MK559345 (FMG) (Supplementary Fig. 1). Molecular sex determination was done as described previously using a PCR targeting the Sry and ZFX genes (Bryja and Konečný, 2003).

2.3. Virus inoculation and CPE detection

For analysis of the susceptibility and virus replication in the newly established cell lines and the BVK168 cell line we used 14 laboratory adapted viruses of different taxa and host association (Table 1). To evaluate virus propagation in the vole cell lines, a positive control infection was done in parallel on the specific reference cell line for each virus (see Fig. 1B, Table 1). Viruses were inoculated with a multiplicity of infection (MOI) of 0.1 in 1 ml serum free Leibovitz (L)-EM medium to 24 h old cell-monolayers in 12.5cm² flasks. After adsorption for 1 h at 37 °C, 4 ml L-EM containing 2% FCS was added and cells were observed daily until a prominent CPE formation was observed. CPE formation was documented by imaging with a Nikon Eclipse TS100 microscope coupled to a Nikon Digital Sight DS-L3 imaging system. Flasks of infected cells were frozen after prominent CPE (60–80%) was obtained or ultimately 7 days post inoculation (p.i.). For CPXV total cell sediments were collected in Tris-HCl pH 8 buffer and lysates were used for further investigations.

The protocol was modified for TULV and PUUV infection, as these viruses do not induce a visible CPE (Sola-Riera et al., 2019). FMN, FMG, MGLU and BVK168 cell lines were inoculated with TULV strain Moravia (Vapalahti et al., 1996) or PUUV strain Vranica/Hällnäs with a MOI of 0.1 for 2 h in 0.5 ml MEM containing 5% FCS in a 6-well plate. After adsorption, 1.5 ml MEM with 5% FCS were added and cells were incubated at 37 °C for up to 10 days. PUUV infection was tested at day 10 by immunofluorescence staining with nucleocapsid (*N*)-protein specific monoclonal antibody 5E11 (Kucinskaite-Kodze et al., 2011) and an Alexa fluor 488 labelled secondary anti-mouse antibody (Abcam, Cambridge, UK). Nuclei were stained with 4′,6-diamidino-2-phenylindole (DAPI, Thermo Fisher Scientific, Waltham, MA, USA). For TULV, infected cells were harvested at several time points, lysed in 2x SDS-PAGE sample buffer (0.5 M Tris pH 6.8, 25% glycerin, 10% SDS and 0.5% bromphenolblue) and subjected to Western blot analysis with N-protein specific monoclonal antibody TULV1 diluted 1:10 in PBS-Tween 0.05% (Spakova, Koellner, Ulrich et al., unpubl. data) and a horse radish peroxidase (HRP) labelled secondary goat anti-mouse IgG antibody diluted 1:3000 in PBS-Tween 0.05% (Bio-Rad, Hercules, CA, USA). Alternatively, FMN and BVK168 cells were incubated with TULV strain Moravia for 2 h, washed 3 times and kept at 37 °C for 18 days until supernatant was collected and frozen at −80 °C. Subsequently, Vero E6 reference cells and FMN or BVK168 cells were incubated with supernatants of infected cells. Infection was evaluated after 10 days by immunostaining of hantaviral N protein using antibody TULV1 and an Alexa-Fluor 488 labelled secondary anti-mouse antibody (Abcam). Nuclei were stained with DAPI.

2×10^5 cells of the MGN cell line were seeded in 6-well plates one day before inoculated with PUUV strain Vranica/Hällnäs at MOI of 0.1 or 0.001 for 2 h in 0.5 ml Ham's F12/IMDM containing 5% FCS. After inoculation, cells were washed 3 times with Ham's F12/IMDM containing 5% FCS and incubated at 37 °C for up to 14 days. Every two days one well of cells was fixed and stained with N-protein specific monoclonal antibody 5E11 (Kucinskaite-Kodze et al., 2011) and an Alexa fluor 488 labelled secondary anti-mouse antibody (Abcam). Nuclei were stained with DAPI as described above. For investigation of infectious particles released from MGN cells, supernatant was taken at day 10 from MOI 0.1 infected cells. As an infection control Vero E6 reference cells were infected in parallel. Fresh naive 24 h old monolayers of MGN cells and Vero E6 cells were incubated with the supernatant from MGN cells. Virus propagation was monitored at day 10 by immunostaining of hantaviral N protein as described above.

2.4. Virus titration

Virus titration of cell supernatants/lysates was done in parallel on the original reference cell line for each virus (Table 1, Fig. 1B) and the vole cell line used (Fig. 1A). After one freeze-thaw cycle, the virus supernatants were serially diluted from 10^{-1} to 10^{-11} in L-EM containing 2% FCS in a 96-well plate with four replicates each. For CPXV two independent experiments with 8 replicates each were performed. Cell monolayers of vole cells or the corresponding reference cell line (see

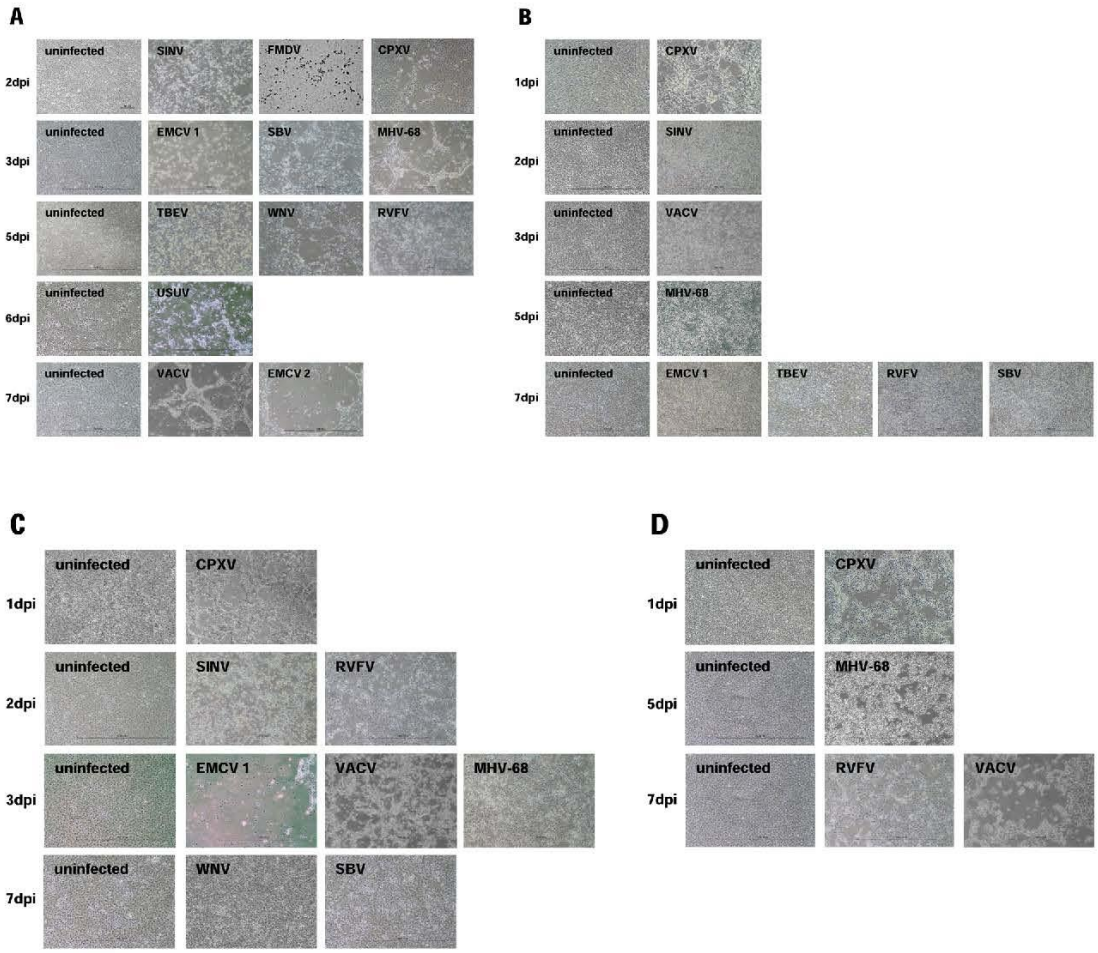

Fig. 2. Cytopathic effect (CPE) on virus inoculated vole-derived cell lines BVK168 (A), MGLU (B), FMN (C), FMG (D). Phase contrast images are shown for time points with most prominent CPE in comparison to uninfected cells until day 7 post inoculation (p.i.). Abbreviations: viruses as they appear in Table 1: CPXV, Cowpox virus; EMCV, Encephalomyocarditis virus; FMDV, Foot-and-mouth disease virus; MHV-68, Murine gammaherpesvirus 68; MNV, Murine norovirus; RVFV, Rift Valley fever virus; SBV, Schmallenberg virus; SINV, Sindbis virus; TBEV, Tick-borne encephalitis virus; USUV, Usutu virus; VACV, Vaccinia virus; WNV, West Nile virus.

Table 1) were seeded in a 96-well plate one day before. A volume of 100 µl of each virus dilution was added to the confluent cells. After incubation for three (FMDV, CPXV, MNV), six (USUV, SINV, RVFV, VACV, SBV, EMCV) or seven (WNV, TBEV, MHV-68) days the 50% tissue culture infectious dose ($TCID_{50}$) was calculated using the Spearman/Kärber method based on the CPE detection on the cells (Kärber, 1931). Virus titers are shown as means with standard deviations. For PUUV and TULV titration of day 10 supernatants, infection of the dilutions was evaluated after 10 days using the immunofluorescence test protocol described above.

For titration of PUUV, MGN and Vero E6 reference cells were infected with MOI 0.1 and 0.001 as described in detail in chapter 2.3. Supernatants of both cell lines were collected every two days and frozen at −80 °C. Subsequently, supernatants were serially diluted from 10^{-1} to 10^{-7} in MEM containing 5% FCS in a 96-well plate with three replicates each. Vero E6 cells were seeded in 96-well plates one day before, and a volume of 100 µl of each virus dilution was added to these cell monolayers for virus titration. After incubation for 10 days, the $TCID_{50}$ was calculated using indirect immunofluorescence for PUUV N protein detection as described. Titers were calculated by the Spearman/Kärber method and mean titers of three experiments are given with standard deviation (SD).

3. Results

3.1. BVK168 cell line is highly susceptible and promotes replication of almost all viruses investigated

The BVK168 cell line was determined to originate from a bank vole of the Western evolutionary lineage (Supplementary Fig. 1). All viruses chosen for the infection resulted in visible CPE and viral propagation, as documented in reference and BVK168 cell lines, except for MNV (Figs. 2A and 3A , Tables 2 and 3A). Hantaviruses as non-cytolytic viruses were evaluated separately and are described below.

Endpoint titration showed that CPXV and VACV amplified to similar quite high titers of about 10^5 $TCID_{50}$/ml, independently if back-titrated to reference or BVK168 cells (Fig. 3A). However, the titer in the reference control cell line was about 0.5 logs higher for both orthopox viruses. The kinetics of CPE formation differed between both viruses (Table 3A).

Additional testing of this cell line indicated a high susceptibility for the tick-borne zoonotic TBEV (Table 3A, Figs. 2A and 3A). The obtained titer in the back-titration was higher in the bank vole cell line compared to the reference cell line. However, when the original virus was grown on the reference cell line Vero B4 titers were still highest (Fig. 3A).

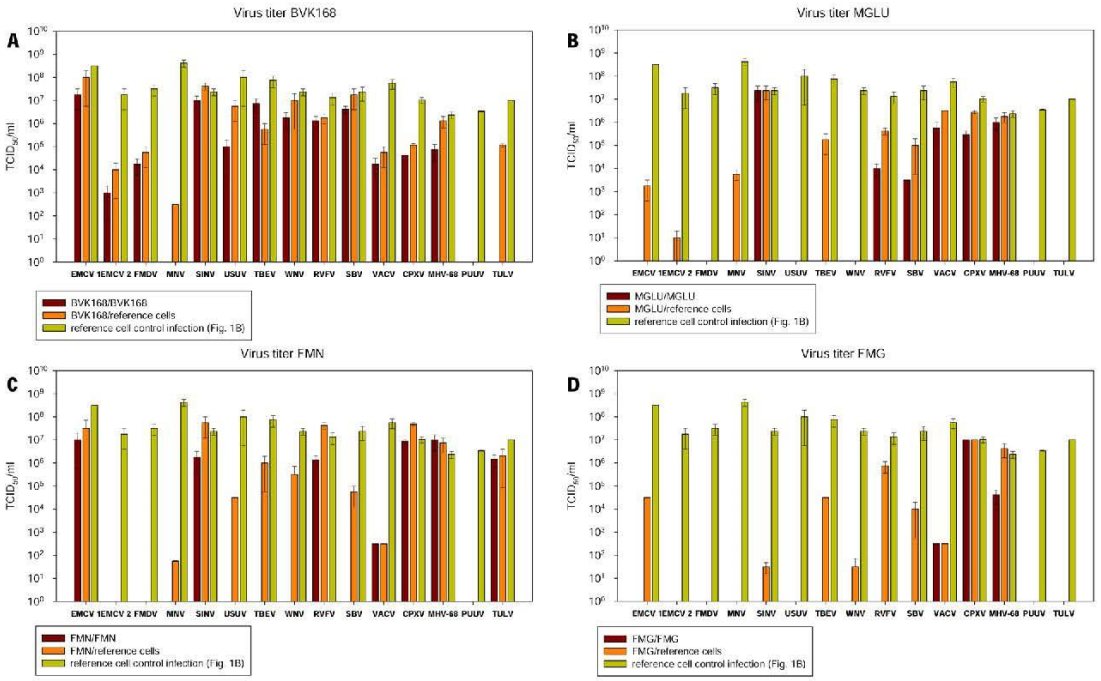

Fig. 3. Results of virus titrations on vole cells in comparison to back-titration on reference cells. Vole cells were infected and titers observed from titration on vole cells are shown in brown bars. Titers from vole cell infection, titrated on reference cells are shown in orange. Positive control infection was done on the reference cell line (Table 1) for each virus and titration is indicated by green bars. Titrations are shown as means with standard deviations of 4 replicates each. CPXV was titrated in two independent titrations and 8 replicates. Abbreviations: TCID, tissue culture infectious dose; CPXV, Cowpox virus; EMCV, Encephalomyocarditis virus; FMDV, Foot-and-mouth disease virus; MHV-68, Murine gammaherpesvirus 68; MNV, Murine norovirus; PUUV, Puumala orthohantavirus; RVFV, Rift Valley fever virus; SBV, Schmallenberg virus; SINV, Sindbis virus; TBEV, Tick-borne encephalitis virus; TULV, Tula orthohantavirus; USUV, Usutu virus; VACV, Vaccinia virus; WNV, West Nile virus (For interpretation of the references to colour in this figure legend, the reader is referred to the web version of this article).

Mosquito-borne viruses like SINV, WNV and RVFV replicated in BVK168 cells to titers that differed only slightly in the back-titration between reference cell line and BVK168 cell line. For another mosquito-borne virus, USUV, titers after inoculation of BVK168 cells were about two logs lower when back titrated on BVK168 cells in comparison to the Vero E6 reference cells (Fig. 3A). Even higher was the observed titer, when original USUV was grown on the reference Vero E6 cells (Fig. 3A). CPE was observed at 2 (SINV) up to 6 (USUV) days p.i. (Table 3A, Figs. 2A and 3A).

Inoculation of the BVK168 cell line with non-zoonotic viruses (MNV, FMDV) and with EMCV 2 indicated delayed or no replication and CPE formation if compared to their corresponding reference cell lines (Tables 2 and 3A, Figs. 2A and 3A). MHV-68 was demonstrated to behave similar in terms of CPE formation kinetics in BVK168 and reference cells. Virus titers on BVK168 differ only by about one log when back titrated on both cell lines (Fig. 3A, Tables 2 and 3A). Interestingly, SBV replicated in the BVK168 cell line similar as on BHK21 reference cells. BVK168 and BHK21 cell lines were frozen 3 days p.i. due to prominent disruption of the cell monolayer and similar titers of 10^7 $TCID_{50}$/ml were observed on both cells.

3.2. MGLU cell line differs in its susceptibility and support of replication of several animal and zoonotic viruses

As expected due to the trapping site of the bank vole, the novel cell line MGLU originated from a bank vole of the Eastern evolutionary lineage (see Supplementary Fig. 1). The MGLU cell line supported the replication of SINV, RVFV, SBV, VACV, CPXV and MHV-68 as evidenced by titration of the supernatants in the vole and the corresponding reference cell lines (Fig. 3B, Tables 2 and 3A). For SINV and MHV-68 the titer in the MGLU and the reference cell lines was the same, whereas for RVFV, CPXV, SBV and VACV the titer in the vole cell line was approximately 3 - 1.5 logs reduced compared to the reference cell line. CPXV very rapidly induced a CPE manifested as prominent plaques in MGLU cells (Table 3B and Fig. 2B). Similar results were observed for SINV and VACV with only slight variation of the induction of CPE formation (Table 3, Fig. 2B).

FMDV, USUV and WNV showed no or for EMCV 2 very little (residual virus) replication in the MGLU cell line when back-titrated to the same cell line or the virus-specific reference cell lines (Fig. 3B). The detection of the CPE formation confirmed this obvious difference: None of these four viruses showed a CPE (Table 3B and Fig. 2B). The cell line was also susceptible for TBEV infection, but showed only weak CPE at late time points (Table 3B). Virus replication was detected only by back-titration in the reference cell line (Fig. 3B) indicating low or inefficient replication without induction of visible CPE. Similar results were observed for EMCV 1.

MNV showed no CPE and very limited replication when back-titrated to the vole cell line (Fig. 3B and Table 3). In contrast, RVFV and SBV were able to induce a CPE in the MGLU cell line after longer incubation times. Titers of 10^3 to 10^6 could be determined on both, reference and MGLU cells with prominent CPE (Figs. 2B and 3B).

3.3. FMN and FMG cell lines are highly susceptible for CPXV, RVFV and MHV-68, but differ in their susceptibility to EMCV 1 and SINV

The susceptibility of FMN and FMG cell lines for CPXV and MHV-68 did not differ significantly when evaluating CPE and titer (Table 4C and D, Figs. 2C and D, 3C and D). Similarly, both cell lines were also susceptible for VACV, but differed slightly in the kinetics of CPE formation.

Table 2
Cytopathic effect (CPE) of viruses on reference cell lines.

days p.i.	EMCV 1 BHK-21	EMCV 2 BHK-21	FMDV BHK-21	MNV RAW 264.7	SINV Vero 76	USUV Vero 76	TBEV Vero B4	WNV Vero B4	RVFV Vero 76	SBV BHK-21	VACV Vero E6	CPXV Vero 76	MHV-68 BHK-21
1	+ + + +, f	–	+ + + +, f	+	+	–	–	–	–	+	+	+ + + +, f	–
2		(+)		+ + + +, f	+ + + +, f	+	(+)	–	+	+ +	+ +		+ +
3		+ +				+ +	+	(+)	+ + +, f	+ + + +, f	+ + + +, f		+ + + +, f
4		+ + + +, f				+ + + +, f	+	+					
5							+ +	+ +					
6							+ + +, f	+ + +, f					
7													

Abbreviations: p.i., post inoculation; EMCV, Encephalomyocarditis virus; FMDV, Foot-and-mouth disease virus; MNV, Murine norovirus; SINV, Sindbis virus; USUV, Usutu virus; TBEV, Tick-borne encephalitis virus; WNV, West Nile virus; RVFV, Rift Valley fever virus; SBV, Schmallenberg virus; VACV, Vaccinia virus; CPXV, Cowpox virus; MHV-68, Murine gammaherpesvirus 68; –, no CPE; (+), < 20% visible CPE; +, 20–40% visible CPE; + +, 40–60% visible CPE; + + +, 60–80% visible CPE; + + + +, > 80% visible CPE; f, culture frozen until further use. Viral cytopathic effect in cell lines was evaluated semi-quantitative.

For both cell lines the titration in the vole and reference cell lines revealed similar titers that are 5 logs lower than the original ones in the positive controls indicating limitations in replication (Fig. 3C and D).

Analyses of SINV and EMCV 1 showed most obvious differences between both cell lines: In the FMN cell line, a rapid CPE was induced and high titers were observed in both titrations, similar to the titers observed in the control experiments. In the FMG cell line no CPE and a low titer was measured only in the back-titration to the reference cell line (Figs. 2C and D, 3C and D, and Table 4).

RVFV caused CPE in both cell lines, but with different kinetics (Table 4). Back titration of the vole cell-derived supernatants in the reference cell line resulted in titers almost identical to those observed in the positive control experiment, but reduced titers for FMN or no titer at all in the back-titration to the FMG cell line (Fig. 3C and D).

WNV caused CPE on the FMN cell line, but only titers in the back-titration on Vero cells were observed (Table 4A, Fig. 3C). Both cell lines did not show any signs of virus infection for EMCV 2, FMDV, USUV and TBEV. However, the back-titration of TBEV and USUV supernatants from infected FMN cells on Vero cells indicated moderate titers, suggesting replication without signs of CPE formation (Fig. 3C and D).

3.4. FMN cells productively replicate TULV, whereas TULV loses infectivity in BVK168 cells

TULV inoculation of FMN cells resulted in antigen expression as evidenced by Western blot analysis (Fig. 4B). Re-inoculation of Vero E6 and FMN cells with supernatant from day 18 of initially infected and washed FMN cells showed infection of both cell monolayers after 10 days (Fig. 4D, Table 5). About 70% of FMN cells were infected but showed altered morphology (Fig. 4D and E). Titers observed on FMN cells after 10 days were comparable to the reference infection and reached titers of 10^6 $TCID_{50}$/ml (Fig. 3C). TULV inoculation of BVK168 cells resulted in an increasing N protein detection in cells from day 4 to day 10 p.i. (Fig. 4A). Re-inoculation of the supernatant from initially infected and washed BVK168 cells to fresh Vero E6 reference cells resulted in detection of hantaviral N-protein after 10 days and virus titers of approximately 10^5 $TCID_{50}$/ml (Figs. 4C and 3 A). In contrast, BVK168 cells inoculated with the same supernatant did not show any signs of infection (Fig. 4C and E) suggesting a common vole specific phenotype. In neither the BVK168 nor the reference cells a CPE was observed at any timepoint (Fig. 4C and D). FMG and MGLU cells could not be infected with TULV (Fig. 3B and D, Table 5).

3.5. PUUV replicates efficiently in the bank vole MGN cell line, but not in any other cell line

Analysis of the partial mitochondrial cytochrome *b* gene assigned MGN cells to the Carpathian bank vole lineage (Supplementary Fig. 1). When inoculated with PUUV, the cells showed accumulation of hantaviral N protein over time. After inoculation with MOI 0.001, infection of the cells could be observed at day 6 p.i. When using a higher dose (MOI 0.1), infection could already be detected by immunofluorescence staining of N protein after 2 days indicating virus entry and replication (Fig. 5A, Table 5). Confluent infection of around 60% of the cell layer was observed 12 days (MOI 0.001) or 8 days (MOI 0.1) after inoculation (Fig. 5B). To test whether infectious virus was released from the MGN cells, the supernatant of infected MGN cells was taken after 10 days (Fig. 5C, left panel) and inoculated to fresh MGN and Vero E6 reference cells (Fig. 5C, right panel). The supernatant was able to again infect these cells indicating that MGN cells allow productive PUUV replication and formation of infectious virions (Fig. 5C). To compare the replicative capacity of MGN cells with Vero E6, the standard cell line for hantaviruses, both cell lines were infected at two different MOI (0.1 and 0.001) and supernatant was harvested every two days. The resulting titrations showed a slightly delayed increase of the viral titer on MGN cells until day 8 when infected at MOI 0.1 if compared to the Vero E6

Table 3
Cytopathic effect (CPE) of viruses in bank vole derived kidney cell line BVK168 (A) and lung cell line MGLU (B).

A

bank vole kidney BVK168													
days p.i.	EMCV 1	EMCV 2	FMDV	MNV	SINV	USUV	TBEV	WNV	RVFV	SBV	VACV	CPXV	MHV-68
1	(+)	–	–	–	–	–	–	–	–	–	(+)	+	+
2	+	–	–	–	+ + + + , f	–	(+)	–	+	+	+	+ + + , f	+ +
3	+ + + + , f	–	+ + + , f	–		–	+	(+)	+ +	+ + + , f	+		+ + + + , f
4		–		–		+	+ +	+ +	+ +		+		
5		–		–		+ +	+ + + , f	+ +	+ + + , f		+		
6		+		–		+ + + , f					+ +		
7		+ + , f		– , f							+ + + , f		

B

bank vole lung MGLU													
days p.i.	EMCV 1	EMCV 2	FMDV	MNV	SINV	USUV	TBEV	WNV	RVFV	SBV	VACV	CPXV	MHV-68
1	–	–	–	–	+ +	–	–	–	–	–	–	+ + + + , f	–
2	–	–	–	–	+ + + + , f	–	–	–	–	–	+		–
3	(+)	–	–	–		–	–	–	–	–	+ + + , f		+ +
4	(+)	–	–	–		–	–	–	+	–			+ +
5	+	–	–	–		–	–	–	+	–			+ +
6	+ +	–	–	–		–	(+)	–	+	+			+ + + + , f
7	+ + , f	– , f	– , f	– , f		– , f	(+) , f	– , f	+ + , f	+ , f			

Abbreviations: p.i., post inoculation; EMCV, Encephalomyocarditis virus; FMDV, Foot-and-mouth disease virus; MNV, Murine norovirus; SINV, Sindbis virus; USUV, Usutu virus; TBEV, Tick-borne encephalitis virus; WNV, West Nile virus; RVFV, Rift Valley fever virus; SBV, Schmallenberg virus; VACV, Vaccinia virus; CPXV, Cowpox virus; MHV-68, Murine gammaherpesvirus 68; – , no CPE; (+), < 20% visible CPE; +, 20–40% visible CPE; + +, 40–60% visible CPE; + + +, 60–80% visible CPE; + + + +, > 80% visible CPE; f, culture frozen until further use. Viral cytopathic effect was evaluated semi-quantitative.

Table 4
Cytopathic effect (CPE) of viruses in common vole derived kidney cell line FMN (A) and brain cell line FMG (B).

A

common vole kidney FMN days p.i.	EMCV 1	EMCV 2	FMDV	MNV	SINV	USUV	TBEV	WNV	RVFV	SBV	VACV	CPXV	MHV-68
1	(+)	–	–	–	+	–	–	–	+ +	–	(+)	+ + + + , f	–
2	+ +	–	–	–	+ + + + , f	–	–	–	+ + + , f	–	+		+
3	+ + + + , f	–	–	–		–	–	–		–	+ + + , f		+ + + + , f
4		–	–	–		–	–	(+)		–			
5		–	–	–		–	–	+		–			
6		–	–	–		–	–	+ +		–			
7		– , f	– , f	– , f		– , f	– , f	+ + , f		(+), f			

B

common vole brain FMG days p.i.	EMGV 1	EMCV 2	FMDV	MNV	SINV	USUV	TBEV	WNV	RVFV	SBV	VACV	CPXV	MHV-68
1	–	–	–	–	–	–	–	–	–	–	–	+ + + + , f	–
2	–	–	–	–	–	–	–	–	–	–	(+)		–
3	–	–	–	–	–	–	–	–	+	–	+		(+)
4	–	–	–	–	–	–	–	–	+ +	–	+		+ +
5	–	–	–	–	–	–	–	–	+ +	–	+ +		+ + + , f
6	–	–	–	–	–	–	–	–	+ +	–	+ +		
7	– , f	– , f	– , f	– , f	– , f	– , f	– , f	– , f	+ + + , f	– , f	+ + + , f		

Abbreviations: p.i., post inoculation; EMCV, Encephalomyocarditis virus; FMDV, Foot-and-mouth disease virus; MNV, Murine norovirus; SINV, Sindbis virus; USUV, Usutu virus; TBEV, Tick-borne encephalitis virus; WNV, West Nile virus; RVFV, Rift Valley fever virus; SBV, Schmallenberg virus; VACV, Vaccinia virus; CPXV, Cowpox virus; MHV-68, Murine gammaherpesvirus 68; –, no CPE; (+), < 20% visible CPE; +, 20–40% visible CPE; + +, 40–60% visible CPE; + + +, 60–80% visible CPE; + + + +, > 80% visible CPE; f, culture frozen until further use. Viral cytopathic effect was evaluated semi-quantitative.

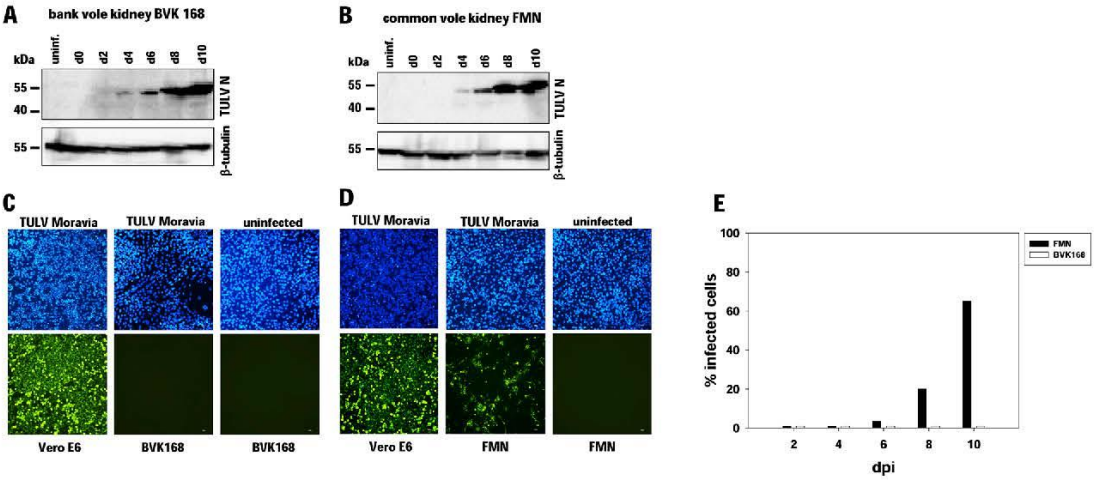

Fig. 4. Reinfection of Vero E6 and bank vole and common vole-derived kidney cell lines with supernatants of vole cells inoculated with Tula orthohantavirus (TULV). Infection of TULV on vole cell lines was monitored over 10 days by Western blot staining for TULV N protein (A and B) and β-Tubulin as loading control. Vero E6 and BVK168 or FMN cells were incubated with supernatant taken from TULV-infected BVK168 (C) or FMN (D) cells. Percentage of infected cells from C and D over time is shown in (E). Uninfected cells served as a control. Infected cells were detected by Western blot and immunofluorescence staining of hantaviral N protein.

cells (Fig. 5D). After day 8 titers reached the same level on both cell types. When using a lower infectious dose, the PUUV titer on MGN cells was about 2 log lower each day than on Vero E6 cells until day 14 when titers reached a plateau on the same level (Fig. 5D). All other bank vole and common vole cell lines failed to replicate PUUV strain Vranica/Hällnäs and did not show any CPE at any time point (Fig. 3A–D, Table 5).

4. Discussion

This study revealed differences in the susceptibility of the tested bank vole and common vole cell lines that may reflect species-, evolutionary lineage- and tissue-specific differences in the susceptibility, replication capacity and CPE formation for various viruses (Table 5). The initial analysis of BVK168 cells confirmed results of a previous study for CPXV, VACV, SINV and USUV in terms of viral titers and CPE induction (Essbauer et al., 2011). Thus, neither the passage number of this cell line nor differences in the strain origin and passage history of the viruses used, influenced their interaction drastically.

Here, we developed novel cell lines that support productive replication of TULV and PUUV. We failed to detect any CPE of TULV in FMN cells and of PUUV in MGN cells, therefore these cell lines may reflect a natural infection in the reservoir that is believed to be non-cytolytic (Meyer and Schmaljohn, 2000). Inoculation of TULV to kidney cell lines of both vole species resulted in TULV N-protein expression after incubation of up to 10 days p.i. When testing cells for production of infectious particles in the supernatant, incubation after extensive washing had to be prolonged to 18 days for sufficient virus growth. Inoculation of the resulting supernatants from both cell lines was leading to complete infection of Vero E6 cells after 10 days, but only the FMN derived supernatant was able to re-infect this common vole cell line. This observation supports a host specificity of TULV for the common vole. In line, studies in wildlife small mammal populations detected TULV mainly in common vole, but only rarely in field vole and water vole, but not in the bank vole (Schmidt-Chanasit et al., 2010; Schlegel et al., 2012b). Experimental inoculation of bank voles with TULV could be shown, but only few animals seroconverted and antibody titers remained low (Klingström et al., 2002). Therefore, FMN cell line might be suitable as a cell culture model system for TULV investigations. Future investigations should prove if the infection of FMN cells of the Central evolutionary lineage of the common vole with an EST.S TULV strain reflects the situation in natural populations at a hybrid zone of the Central and Eastern evolutionary lineages of the common vole as described recently (Saxenhofer et al., 2019). Alternatively, the reference cell adaption of the TULV strain (Plyusnin et al., 1996) might have influenced the host factor-dependence of the virus.

PUUV is another hantavirus that is commonly grown on Vero E6 cells. Here our novel bank vole cell line MGN of the Carpathian lineage was reliably infected and replicated PUUV strain Vranica/Hällnäs of the Northern Scandinavian (N-SCA) clade (Castel et al., 2019), but not the bank vole cell lines of the Western lineage (BVK168) and Eastern lineage (MGLU). The lacking replication of PUUV in the common vole cell lines might indicate the influence of host-specific factors. Unfortunately, the precise bank vole origin of the PUUV strain used is not known, but might be the Carpathian or Ural evolutionary lineage (Filipi et al., 2015). Therefore, we are not able here to speculate about a lineage specificity of the bank vole cell line infection model, keeping in mind also the necessity of a genome-based analysis instead of the mtDNA-based lineage definition. Future studies should evaluate bank vole-derived PUUV isolates of different clades for their preference for cell lines of specific bank vole lineages.

The reservoir host of CPXV is currently a matter of debate. In our experiments the CPXV strain of cow origin replicated and induced CPE in all common and bank vole cell lines tested. VACV, another zoonotic orthopox virus, also efficiently replicated in the used bank vole and common vole cell lines. This was not surprising, as these viruses are able to replicate efficiently in a variety of different cell lines. The recent isolation of novel common vole-derived CPXV strains and the availability of common and bank vole animal models may allow a future evaluation of host specificity of CPXV (Hoffmann et al., 2015; Franke et al., 2017a,b).

Vector-transmitted pathogens must be highly adapted to both reservoir and vector. Interestingly, BVK168 cells have the capacity to efficiently replicate all tick- and mosquito-borne viruses investigated here. TBEV, RVFV and SINV replicated, at least to a certain level, in different other cell lines. The lacking CPE or low and late CPE formation observed here for TBEV in common and bank vole cell lines might reflect the situation in the natural host. In addition to the BVK168 cell line, all other cell lines supported replication of SINV to the same level as the control setup with Vero 76 cells. In line with these findings, SINV has been intensively studied for its growth characteristics in a broad range of vertebrate and also invertebrate cells with barely a cell line

Table 5
Summary of cell lines and viruses tested.

Virus	Common vole							Bank vole											
	FMN				FMG				BVK168				MGLU				MGN		
	CPE	susceptibility	titration ref. cells	titration vole cells	CPE	susceptibility	titration ref. cells	titration vole cells	CPE	susceptibility	titration ref. cells	titration vole cells	CPE	susceptibility	titration ref. cells	titration vole cells	CPE	susceptibility	titration ref. cells	titration vole cells
zoonotic, rodent																				
PUUV	–	–	–	–	–	–	–	–	–	–	–	–	–	–	–	–	–	+	+ +	+ +
TULV	–	+	+	+	–	–	–	–	–	+	–	–	–	–	–	–	n.d.			
CPXV	+	+	+ +	+ +	+	+	+ +	+ +	+	+	+	+	+	+	+ +	+ +	n.d.			
VACV	+	+	+	+ +	+	+	+	+	+	+	+	+	+	+	+ +	+ +	n.d.			
EMCV 1	+	+	+	+ +	–	+	–	–	+	+	+ +	+ +	+	+	+	–	n.d.			
EMCV 2	–	–	–	–	–	–	–	–	+	+	+	+	–	–	–	–	n.d.			
zoonotic, rodent, with vector																				
TBEV	–	+	+ +	–	–	+	+	–	+	+	+ +	+ +	(+)	+	+ +	–	n.d.			
non-zoonotic, rodent																				
MNV	–	–	–	–	–	–	–	–	–	–	–	–	–	+	+	–	n.d.			
MHV-68	+	+	+ +	+ +	+	+	+ +	+ +	+	+	+ +	+ +	+	+	+ +	+ +	n.d.			
zoonotic, other, with vector																				
USUV	–	+	+		–	–	–	–	+	+	+	+ +	–	–	–	–	n.d.			
WNV	+	+	+ +	–	–	–	–	–	+	+	+ +	+ +	–	–	–	–	n.d.			
RVFV	+	+	+ +	+ +	+	+	+ +	–	+	+	+ +	+	+	+	+ +	+ +	n.d.			
SINV	+	+	+ +	+ +	–	–	–	–	+	+	+ +	+ +	+	+	+ +	+ +	n.d.			
non-zoonotic, other																				
FMDV	–	–	–	–	–	–	–	–	+	+	+	+	–	–	–	–	n.d.			
non-zoonotic, other, with vector																				
SBV	(+)	+	+	–	–	+	+	–	+	+	+ +	+ +	(+)	+	+	+ +	n.d.			

Abbreviations: ref., reference; CPE, cytopathic effect; –, none; (+), low/late CPE; +, moderate replication (30–70% of control infection); + + high replication (> 70% of control infection); n.d., not determined; PUUV, Puumala orthohantavirus; TULV, Tula orthohantavirus; CPXV, Cowpox virus; VACV, Vaccinia virus; EMCV, Encephalomyocarditis virus; TBEV, Tick-borne encephalitis virus; MNV, Murine norovirus; MHV-68, Murine gammaherpesvirus 68; USUV, Usutu virus; WNV, West Nile virus; RVFV, Rift Valley fever virus; SINV, Sindbis virus; FMDV, Foot-and-mouth disease virus; SBV, Schmallenberg virus.

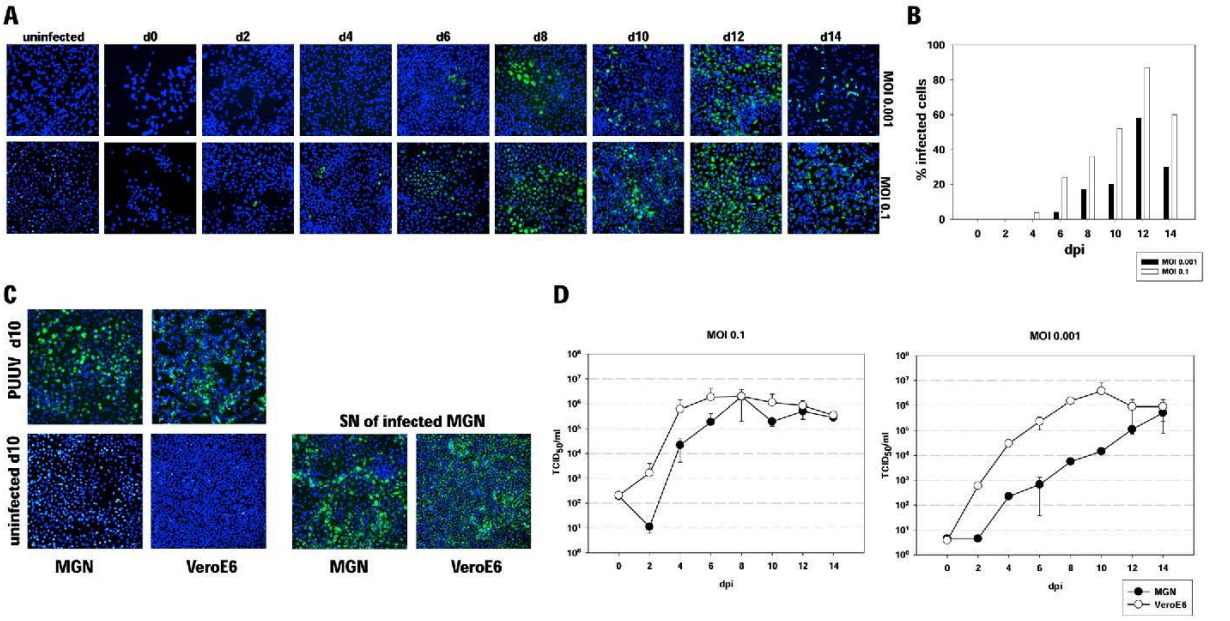

Fig. 5. Immunofluorescence analysis of Puumala orthohantavirus (PUUV) infected MGN cells (A), percentage of infection (B), reinfection of MGN and Vero E6 cells (C), and PUUV titers on MGN cells (D). (A) MGN cells were inoculated with PUUV strain Vranica/Hällnäs at MOI of 0.1 or 0.001 for 2 h, washed and incubated at 37 °C for up to 14 days or left untreated. At the indicated time points, cells were fixed and stained with nucleocapsid (*N*)-protein specific monoclonal antibody 5E11 and an Alexa fluor 488 labelled secondary anti-mouse antibody. Nuclei were stained with DAPI. Merge images are shown. (B) Percentage of infected cells from Fig. 5A. (C) Left panel: MGN and Vero E6 cells were incubated with PUUV strain Vranica/Hällnäs for 2 h, washed and kept at 37 °C for 10 days until supernatant was collected. Right panel: Vero E6 and MGN cells were incubated with supernatant of infected MGN cells. Infected cells were detected by immunostaining of hantaviral N protein. (D) PUUV titers on MGN cells in comparison to Vero E6 standard cell line at two different MOI. MGN (black dots) and Vero E6 (white dots) cells were infected at MOI 0.1 and 0.001 as described. Titration of supernatants of PUUV-infected MGN cells was done on Vero E6 cells using indirect immunofluorescence test as described. Titers were calculated by the Spearman/Kärber method and mean titers of three experiments are given with standard deviation.

which did not support its propagation (Hernandez et al., 2010). Remarkably, the common vole brain cell line FMG did not support SINV replication. RVFV caused CPE in all four vole cell lines investigated and 3 out of 4 vole cells showed efficient titer production of the virus. Astonishingly, RVFV can infect a wide range of insect vectors, wild and domesticated animals as well as humans and replicates in a broad variety of cell lines (McMillen and Hartman, 2018). The virus was also shown to efficiently infect and replicate in airway epithelial cells of cotton rats (*Sigmodon hispidus*), another cricetid species (Ehlen et al., 2016). Based on these results, further investigations are urgently needed to prove whether vole species may represent a potential intermediate host of RVFV. A comparison of the replication in the four vole cell lines may indicate a kidney tissue preference for WNV and USUV – these viruses did not replicate at all in brain and lung cells used.

EMCV 1 replicated in three cell lines and induced a prominent CPE, except in FMG cells. This finding is in line with the broad host range of EMCV 1 including voles and squirrels. Infected rodents may play a role in virus spread when they occur in proximity to farms with infected swine (Carocci and Bakkali-Kassimi, 2012). In addition, EMCV is a rapidly lytic virus that causes necrotic cell death.

Even SBV, a non-zoonotic pathogen with no evidence of a rodent-association (Mouchantat et al., 2015), replicated to a certain level in all four tested cell lines. Non-zoonotic agents FMDV and MNV demonstrated a very low level of replication. FMDV was found to replicate in the BVK168 cell line, while MNV showed some level of replication in MGLU cells. Kidney derived cell lines of mice are able to propagate FMDV in culture (Campbell, 1965) and the BHK-21[C13] (Macpherson and Stoker, 1962) cell line is the cell line of choice for the industrial production of FMDV vaccines (Doel, 2003). The low or absent replication of MNV in the novel vole cell lines might be explained by the specific tropism of this virus for cells of the hematopoietic lineage such as macrophages and dendritic cells (Wobus et al., 2004).

Our results show that MHV-68 was able to efficiently replicate in all four tested vole cell lines. This finding is unexpected as *DPOL* and *gB* genes of MHV-68 showed in a previous study a close phylogenetic similarity to those of wood mouse (*Apodemus sylvaticus*) and yellow necked mouse (*A. flavicollis*) associated rhadinoviruses, whereas a bank vole associated rhadinovirus formed a separate clade (Ehlers et al., 2007). Therefore, future studies in *Apodemus* derived cell lines and detailed *in vivo* studies are necessary to address this interesting finding.

5. Conclusion

Productive replication in the vole cell lines was observed for several viruses, for some without or delayed induction of CPE. Potent host cell lines for the propagation of PUUV and TULV were discovered that can be useful in revealing the yet unsolved virus-host interactions of these orthohantaviruses. These newly developed cell lines may represent a useful tool to study virus-cell interactions and to identify and characterize host cell factors involved in the replication of rodent associated viruses and thereby mediating host adaptation. Furthermore, *in vitro* studies in these cell lines may allow first conclusions on the potential reservoir host(s) which has to be proven in targeted host animal experiments. Future investigations would profit from using virus strains that were not or only in low frequency passaged in non-reservoir cell lines to exclude potential artefacts generated by long-term passage of viruses.

Declaration of Competing Interest

The authors declare that they have no known competing financial interests or personal relationships that could have appeared to

influence the work reported in this paper.

Acknowledgements

The authors would like to thank Ulrike M. Rosenfeld for trapping of the bank vole, Hans-Joachim Pelz and Jens Jacob for providing the common voles, and Pawel Koteja for providing bank voles of the Carpathian lineage. We also would like to thank Sven Sander and Cornelia Steffen for excellent technical assistance, Indre Kucinskaite-Kodze and Aurelija Zvirbliene for providing mAb 5E11 and the lab of Bernd Koellner for providing the anti-TULV-N antibody TULV1. Thanks to Susanne Röhrs for providing animals of the bank vole colony of the Carpathian lineage, Martin Beer and Martin Groschup for continuous support and additional funding, and Isabella Eckerle for critical reading of the manuscript. Florian Binder acknowledges intramural funding by the Friedrich-Loeffler-Institut.

Appendix A. Supplementary data

Supplementary material related to this article can be found, in the online version, at doi:https://doi.org/10.1016/j.jviromet.2019.113729.

References

Achazi, K., Ruzek, D., Donoso-Mantke, O., Schlegel, M., Ali, H.S., Wenk, M., et al., 2011. Rodents as sentinels for the prevalence of tick-borne encephalitis virus. Vector Borne Zoon. Dis. 11 (6), 641–647.

Alexandersen, S., Mowat, N., 2005. Foot-and-mouth disease: host range and pathogenesis. Curr. Top. Microbiol. Immunol. 288, 9–42.

Antoine, G., Scheiflinger, F., Dorner, F., Falkner, F.G., 1998. The complete genomic sequence of the modified vaccinia Ankara strain: comparison with other orthopoxviruses. Virology 244 (2), 365–396.

Becker, N., Jost, H., Ziegler, U., Eiden, M., Hoper, D., Emmerich, P., et al., 2012. Epizootic emergence of Usutu virus in wild and captive birds in Germany. PLoS One 7 (2), e32604.

Blaškovič, D., Stančeková, M., Svobodová, J., Mistríková, J., 1980. Isolation of five strains of herpesviruses from two species of free-living small rodents. Acta Virol. 24, 468.

Brito, B.P., Rodriguez, L.L., Hammond, J.M., Pinto, J., Perez, A.M., 2017. Review of the global distribution of foot-and-mouth disease virus from 2007 to 2014. Transbound. Emerg. Dis. 64 (2), 316–332.

Bryja, J., Konečný, A., 2003. Fast Sex Identification in Wild Mammals Using PCR Amplification of the Sry Gene. pp. 269–274.

Campbell, C.H., 1965. Relationship of donor age to *in-vivo* production of foot-and-mouth disease virus by mouse kidney cells. J. Exp. Med. 121, 69–83.

Carocci, M., Bakkali-Kassimi, L., 2012. The encephalomyocarditis virus. Virulence 3 (4), 351–367.

Castel, G., Chevenet, F., Razzauti, M., Murri, S., Marianneau, P., Cosson, J.F., et al., 2019. Phylogeography of Puumala orthohantavirus in Europe. Viruses 11 (8).

Doel, T.R., 2003. FMD vaccines. Virus Res. 91 (1), 81–99.

Drewes, S., Strakova, P., Drexler, J.F., Jacob, J., Ulrich, R.G., 2017a. Assessing the diversity of rodent-borne viruses: exploring of high-throughput sequencing and classical amplification/sequencing approaches. Adv. Virus Res. 99, 61–108.

Drewes, S., Ali, H.S., Saxenhofer, M., Rosenfeld, U.M., Binder, F., Cuypers, F., et al., 2017b. Host-associated absence of human Puumala virus infections in northern and Eastern Germany. Emerging Infect. Dis. 23 (1), 83–86.

Eckerle, I., Lenk, M., Ulrich, R.G., 2014. More novel hantaviruses and diversifying reservoir hosts–time for development of reservoir-derived cell culture models? Viruses 6 (3), 951–967.

Ehlen, L., Todtmann, J., Specht, S., Kallies, R., Papies, J., Muller, M.A., et al., 2016. Epithelial cell lines of the cotton rat (Sigmodon hispidus) are highly susceptible in vitro models to zoonotic Bunya-, Rhabdo-, and Flaviviruses. Virol. J. 13, 74.

Ehlers, B., Kuchler, J., Yasmum, N., Dural, G., Voigt, S., Schmidt-Chanasit, J., et al., 2007. Identification of novel rodent herpesviruses, including the first gammaherpesvirus of Mus musculus. J. Virol. 81 (15), 8091–8100.

Eiden, M., Ziegler, U., Keller, M., Müller, K., Granzow, H., Jöst, H., et al., 2014. Isolation of Sindbis virus from a hooded crow in Germany. Vector-Borne Zoon. Dis. 14 (3), 220–222.

Elliott, L.H., Ksiazek, T.G., Rollin, P.E., Spiropoulou, C.F., Morzunov, S., Monroe, M., et al., 1994. Isolation of the causative agent of hantavirus pulmonary syndrome. Am. J. Trop. Med. Hyg. 51 (1), 102–108.

Emeny, J.M., Morgan, M.J., 1978. Regulation of the interferon system: evidence that Vero cells have a genetic defect in interferon production. J. Gen. Virol. (43), 247–252.

Essbauer, S., Pfeffer, M., Meyer, H., 2010. Zoonotic poxviruses. Vet. Microbiol. 140 (3–4), 229–236.

Essbauer, S.S., Krautkrämer, E., Herzog, S., Pfeffer, M., 2011. A new permanent cell line derived from the bank vole (Myodes glareolus) as cell culture model for zoonotic viruses. Virol. J. 8, 339.

Filipi, K., Markova, S., Searle, J.B., Kotlik, P., 2015. Mitogenomic phylogenetics of the bank vole Clethrionomys glareolus, a model system for studying end-glacial colonization of Europe. Mol. Phylogenet. Evol. 82 (Pt A), 245–257.

Franke, A., Ulrich, R.G., Weber, S., Osterrieder, N., Keller, M., Hoffmann, D., et al., 2017a. Experimental cowpox virus (CPXV) infections of bank voles: exceptional clinical resistance and variable reservoir competence. Viruses 9 (12).

Franke, A., Pfaff, F., Jenckel, M., Hoffmann, B., Hoper, D., Antwerpen, M., et al., 2017b. Classification of cowpox viruses into several distinct clades and identification of a novel lineage. Viruses 9 (6).

Hernandez, R., Sinodis, C., Brown, D.T., 2010. Sindbis virus: propagation, quantification, and storage. Curr. Protoc. Microbiol. (16), 15H.1.1–15B.1.41. https://doi.org/10.1002/9780471729259.mc15b01s16.

Hoffmann, D., Franke, A., Jenckel, M., Tamosiunaite, A., Schluckebier, J., Granzow, H., et al., 2015. Out of the reservoir: phenotypic and genotypic characterization of a novel cowpox virus isolated from a common vole. J. Virol. 89 (21), 10959–10969.

Jaenson, T.G., Hjertqvist, M., Bergstrom, T., Lundkvist, A., 2012. Why is tick-borne encephalitis increasing? A review of the key factors causing the increasing incidence of human TBE in Sweden. Parasit. Vectors 5, 184.

Jameson, L.J., Logue, C.H., Atkinson, B., Baker, N., Galbraith, S.E., Carroll, M.W., et al., 2013. The continued emergence of hantaviruses: isolation of a Seoul virus implicated in human disease, United Kingdom, October 2012. Euro Surveill. 18 (1), 4–7.

Johnson, N., de Marco, M.F., Giovannini, A., Ippoliti, C., L. DM, Svartz, G., et al., 2018. Emerging mosquito-borne threats and the response from European and Eastern Mediterranean countries. Int. J. Environ. Res. Public Health 15 (2775).

Jones, K.E., Patel, N.G., Levy, M.A., Storeygard, A., Balk, D., Gittleman, J.L., et al., 2008. Global trends in emerging infectious diseases. Nature 451 (7181), 990–993.

Kärber, G., 1931. Beitrag zur kollektiven Behandlung pharmakologischer Reihenversuche. Arch. Exp. Pathol. Pharmakol. 162, 480–483.

Kitamura, T., Morita, C., Komatsu, T., Sugiyama, K., Arikawa, J., Shiga, S., et al., 1983. Isolation of virus causing hemorrhagic fever with renal syndrome (HFRS) through a cell culture system. Jpn. J. Med. Sci. Biol. 36 (1), 17–25.

Klingström, J., Heyman, P., Escutenaire, S., Sjolander, K.B., De Jaegere, F., Henttonen, H., et al., 2002. Rodent host specificity of European hantaviruses: evidence of Puumala virus interspecific spillover. J. Med. Virol. 68 (4), 581–588.

Kucinskaite-Kodze, I., Petraityte-Burneikiene, R., Zvirbliene, A., Hjelle, B., Medina, R.A., Gedvilaite, A., et al., 2011. Characterization of monoclonal antibodies against hantavirus nucleocapsid protein and their use for immunohistochemistry on rodent and human samples. Arch. Virol. 156 (3), 443–456.

Liebermann, H., Schulze, P., Liebermann, H., 1967. Euterpocken in Deutschland. Arch. Exp. Veterinärmed. 21, 1419–1433.

Lloyd-Smith, J.O., George, D., Pepin, K.M., Pitzer, V.E., Pulliam, J.R., Dobson, A.P., et al., 2009. Epidemic dynamics at the human-animal interface. Science 326 (5958), 1362–1367.

Macpherson, I., Stoker, M., 1962. Polyoma transformation of hamster cell clones–an investigation of genetic factors affecting cell competence. Virology 16, 147–151.

Mandl, C.W., Heinz, F.X., Stockl, E., Kunz, C., 1989. Genome sequence of tick-borne encephalitis virus (western subtype) and comparative analysis of nonstructural proteins with other flaviviruses. Virology 173 (1), 291–301.

McMillen, C.M., Hartman, A.L., 2018. Rift Valley fever in animals and humans: current perspectives. Antiviral Res. 156, 29–37.

Meerburg, B.G., Singleton, G.R., Kijlstra, A., 2009. Rodent-borne diseases and their risks for public health. Crit. Rev. Microbiol. 35 (3), 221–270.

Meyer, B.J., Schmaljohn, C.S., 2000. Persistent hantavirus infections: characteristics and mechanisms. Trends Microbiol. 8 (2), 61–67.

Mouchantat, S., Wernike, K., Lutz, W., Hoffmann, B., Ulrich, R.G., Borner, K., et al., 2015. A broad spectrum screening of Schmallenberg virus antibodies in wildlife animals in Germany. Vet. Res. 46, 99.

Mowat, G.N., Brooksby, J.B., Pay, T.W.F., 1962. Use of BHK 21 cells in the preparation of mouse attenuated live foot-and-mouth disease vaccines for the immunization of cattle. Nature 196, 655.

Oliveira, J.S., Figueiredo, P.O., Costa, G.B., Assis, F.L., Drumond, B.P., da Fonseca, F.G., et al., 2017. Vaccinia virus natural infections in Brazil: the good, the bad, and the ugly. Viruses 9 (11).

Papa, A., Nemirov, K., Henttonen, H., Niemimaa, J., Antoniadis, A., Vaheri, A., et al., 2001. Isolation of Dobrava virus from Apodemus flavicollis in Greece. J. Clin. Microbiol. 39 (6), 2291–2293.

Peres, M.G., Bacchiega, T.S., Appolinario, C.M., Vicente, A.F., Mioni, M.S.R., Ribeiro, B.L.D., et al., 2018. Vaccinia virus in Feces and Urine of Wild Rodents from Sao Paulo State, Brazil. Viruses 10 (2).

Plyusnin, A., Cheng, Y., Lehvaslaiho, H., Vaheri, A., 1996. Quasispecies in wild-type Tula hantavirus populations. J. Virol. 70 (12), 9060–9063.

Plyusnin, A., Vaheri, V., 1994. Tula virus: a newly detected hantavirus carried by European common voles. J. Virol. 68, 7833–7839.

Saxenhofer, M., Weber de Melo, V., Ulrich, R.G., Heckel, G., 2017. Revised time scales of RNA virus evolution based on spatial information. Proc. Biol. Sci. 284 (1860).

Saxenhofer, M., Schmidt, S., Ulrich, R.G., Heckel, G., 2019. Secondary contact between diverged host lineages entails ecological speciation in a European hantavirus. PLoS Biol. 17 (2), e3000142.

Schlegel, M., Ali, H.S., Stieger, N., Groschup, M.H., Wolf, R., Ulrich, R.G., 2012a. Molecular identification of small mammal species using novel cytochrome B gene-derived degenerated primers. Biochem. Genet. 50 (5–6), 440–447.

Schlegel, M., Kindler, E., Essbauer, S.S., Wolf, R., Thiel, J., Groschup, M.H., et al., 2012b. Tula virus infections in the Eurasian water vole in Central Europe. Vector Borne Zoonotic Dis. 12 (6), 503–513.

Schmidt, S., Saxenhofer, M., Drewes, S., Schlegel, M., Wanka, K.M., Frank, R., et al., 2016. High genetic structuring of Tula hantavirus. Arch. Virol. 161 (5), 1135–1149.

Schmidt-Chanasit, J., Essbauer, S., Petraityte, R., Yoshimatsu, K., Tackmann, K., Conraths, F.J., et al., 2010. Extensive host sharing of central European Tula virus. J. Virol. 84 (1), 459–474.
Schmitz, S., 2011. Der Experimentator: Zellkultur. Verlag Spektrum der Wissenschaft, Heidelberg.
Sola-Riera, C., Gupta, S., Ljunggren, H.G., Klingstrom, J., 2019. Orthohantaviruses belonging to three phylogroups all inhibit apoptosis in infected target cells. Sci. Rep. 9 (1), 834.
Stoltz, M., Sundstrom, K.B., Hidmark, A., Tolf, C., Vene, S., Ahlm, C., et al., 2011. A model system for in vitro studies of bank vole borne viruses. PLoS One 6 (12), e28992.
Suthar, M.S., Diamond, M.S., Gale Jr., M., 2013. West Nile virus infection and immunity. Nat. Rev. Microbiol. 11 (2), 115–128.
Temonen, M., Vapalahti, O., Holthofer, H., Brummer-Korvenkontio, M., Vaheri, A., Lankinen, H., 1993. Susceptibility of human cells to Puumala virus infection. J. Gen. Virol. 74 (Pt 3), 515–518.
Vaheri, A., Henttonen, H., Voutilainen, L., Mustonen, J., Sironen, T., Vapalahti, O., 2013. Hantavirus infections in Europe and their impact on public health. Rev. Med. Virol. 23 (1), 35–49.
Vapalahti, O., Lundkvist, A., Kukkonen, S.K., Cheng, Y., Gilljam, M., Kanerva, M., et al., 1996. Isolation and characterization of Tula virus, a distinct serotype in the genus Hantavirus, family Bunyaviridae. J. Gen. Virol. 77 (Pt 12), 3063–3067.
Vapalahti, O., Mustonen, J., Lundkvist, Å., Henttonen, H., Plyusnin, A., Vaheri, A., 2003. Hantavirus infections in Europe. Lancet Infect. Dis. 3 (10), 653–661.
Varela, M., Schnettler, E., Caporale, M., Murgia, C., Barry, G., McFarlane, M., et al., 2013. Schmallenberg virus pathogenesis, tropism and interaction with the innate immune system of the host. PLoS Pathog. 9 (1), e1003133.
Virgin, H.W., Latreille, P., Wamsley, P., Hallsworth, K., Weck, K.E., Dal Canto, A.J., et al., 1997. Complete sequence and genomic analysis of murine gammaherpesvirus 68. J. Virol. 71 (8), 5894–5904.
Vrbová, M., BelvončíkovÁ, P., Kovalová, A., Matúsková, R., Slovák, M., Kúdelová, M., 2016. Molecular detection of murine gammaherpesvirus 68 (MHV-68) in Haemaphysalis concinna ticks collected in Slovakia. Acta Virol. 60 (4), 426–428.
Wobus, C.E., Karst, S.M., Thackray, L.B., Chang, K.O., Sosnovtsev, S.V., Belliot, G., et al., 2004. Replication of Norovirus in cell culture reveals a tropism for dendritic cells and macrophages. PLoS Biol. 2 (12), e432.
Wodak, E., Richter, S., Bago, Z., Revilla-Fernandez, S., Weissenbock, H., Nowotny, N., et al., 2011. Detection and molecular analysis of West Nile virus infections in birds of prey in the eastern part of Austria in 2008 and 2009. Vet. Microbiol. 149 (3–4), 358–366.
Yanagihara, R., Svedmyr, A., Amyx, H.L., Lee, P., Goldgaber, D., Gajdusek, D.C., et al., 1984. Isolation and propagation of nephropathia epidemica virus in bank voles. Scand. J. Infect. Dis. 16 (3), 225–228.
Ziegler, U., Luhken, R., Keller, M., Cadar, D., van der Grinten, E., Michel, F., et al., 2018. West Nile virus epizootic in Germany, 2018. Antiviral Res. 162, 39–43.

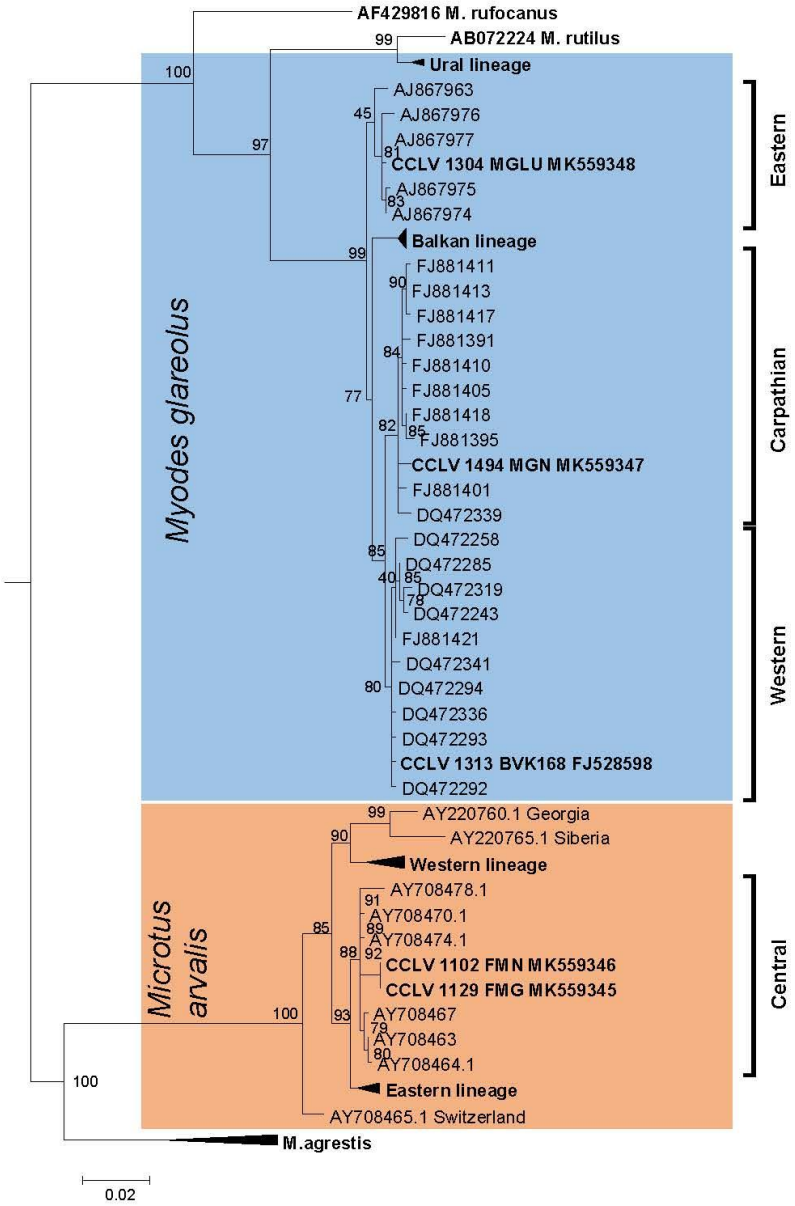

Supplementary Figure 1: Phylogenetic relationships of common vole and bank vole lineages. Sequences are categorized on the basis of mitochondrial cytochrome *b* gene sequences and shown as a maximum likelihood phylogenetic tree with posterior probabilities displayed for major nodes. Bank and common vole cell line sequences are shown in bold. Additional published sequences are included as references for bank vole and common vole evolutionary lineages, labeled with GenBank accession number and lineage labelling with brackets on the side. Phylogenetic analyses were performed with MEGA7 maximum likelihood tree calculation mode and *cytochrome b* sequences of 843-bp length. A mixed nucleotide substitution matrix was specified in 4 independent runs. Cytochrome *b* sequences of *Microtus agrestis*, *Myodes rutilus* and *Myodes rufocanus* voles were used as outgroups.

(IV) ISOLATION AND CHARACTERIZATION OF NEW PUUMALA ORTHOHANTAVIRUS STRAINS FROM GERMANY

Binder, F., Reiche, S., Roman-Sosa, G., Saathoff, M., Ryll, R., Kunec, D., Höper, D., Ulrich, R.G.

Virus Genes

Volume 56, Issue 4

Published online, April 2020

DOI:10.1007/s11262-020-01755-3.

Virus Genes
https://doi.org/10.1007/s11262-020-01755-3

ORIGINAL PAPER

Isolation and characterization of new *Puumala orthohantavirus* strains from Germany

Florian Binder[1] · Sven Reiche[2] · Gleyder Roman-Sosa[3,4] · Marion Saathoff[5] · René Ryll[1] · Jakob Trimpert[6] · Dusan Kunec[6] · Dirk Höper[3] · Rainer G. Ulrich[1,7]

Received: 20 November 2019 / Accepted: 3 April 2020

Abstract

Orthohantaviruses are re-emerging rodent-borne pathogens distributed all over the world. Here, we report the isolation of a *Puumala orthohantavirus* (PUUV) strain from bank voles caught in a highly endemic region around the city Osnabrück, north-west Germany. Coding and non-coding sequences of all three segments (S, M, and L) were determined from original lung tissue, after isolation and after additional passaging in VeroE6 cells and a bank vole-derived kidney cell line. Different single amino acid substitutions were observed in the RNA-dependent RNA polymerase (RdRP) of the two stable PUUV isolates. The PUUV strain from VeroE6 cells showed a lower titer when propagated on bank vole cells compared to VeroE6 cells. Additionally, glycoprotein precursor (GPC)-derived virus-like particles of a German PUUV sequence allowed the generation of monoclonal antibodies that allowed the reliable detection of the isolated PUUV strain in the immunofluorescence assay. In conclusion, this is the first isolation of a PUUV strain from Central Europe and the generation of glycoprotein-specific monoclonal antibodies for this PUUV isolate. The obtained virus isolate and GPC-specific antibodies are instrumental tools for future reservoir host studies.

Keywords *Puumala orthohantavirus* · Bank vole · Cell culture · Virus adaptation · Glycoprotein-specific antibodies

Introduction

Puumala orthohantavirus (PUUV) is the most important hantavirus in Europe [1]. It causes the majority of human hantavirus infections and hemorrhagic fever with renal syndrome (HFRS) cases [2]. In Central and Western Europe hantavirus outbreaks occur in two to five year intervals and are driven by massive increase of the bank vole (*Myodes glareolus*) population, the reservoir of this orthohantavirus species [3]. Human hantavirus disease is notifiable in Germany since 2001 and the majority of recorded cases is mainly due to PUUV infections in southern and western parts of Germany, whereas *Dobrava-Belgrade orthohantavirus* (DOBV) with the striped

Edited by Detlev H. Kruger.

Electronic supplementary material The online version of this article (https://doi.org/10.1007/s11262-020-01755-3) contains supplementary material, which is available to authorized users.

✉ Rainer G. Ulrich
rainer.ulrich@fli.de

[1] Institute of Novel and Emerging Infectious Diseases, Federal Research Institute for Animal Health, Friedrich-Loeffler-Institut, Greifswald - Insel Riems, Germany

[2] Department of Experimental Animal Facilities and Biorisk Management, Federal Research Institute for Animal Health, Friedrich-Loeffler-Institut, Greifswald - Insel Riems, Germany

[3] Institute of Diagnostic Virology, Federal Research Institute for Animal Health, Friedrich-Loeffler-Institut, Greifswald - Insel Riems, Germany

[4] Department of Diagnostic Medicine/Pathobiology, Kansas State University, Manhattan, KS, USA

[5] Specialist Pest Control, Veterinary Task Force, Lower Saxony State Office for Consumer Protection and Food Safety, Oldenburg, Germany

[6] Department of Veterinary Medicine, Institute of Virology, Freie Universität Berlin, Berlin, Germany

[7] German Center for Infection Research (DZIF), Partner Site Hamburg-Lübeck-Borstel-Insel Riems, Greifswald - Insel Riems, Germany

Published online: 23 April 2020

field mouse as reservoir causes infections in the northeastern part of Germany [3].

The characterization of the pathogenicity and identification of virulence markers are highly dependent on adequate PUUV isolates. Currently, the number of PUUV isolates is very limited and does not represent the real diversity of PUUV strains in Europe. In particular, no Central European PUUV isolate exists [4]. The majority of PUUV isolates, and hantaviruses in general, was obtained based on passaging in reservoir animals or VeroE6 cells and is highly adapted [5–7]. Previous investigations indicated that VeroE6 cell adaptation of PUUV Kazan strain results in the inability of the adapted strain to infect the bank vole reservoir [8]. The recent development of bank vole-derived primary or permanent cell lines may allow the isolation of reservoir-adapted PUUV strains [9–12].

Hantavirus proteins are usually detected in infected cells by monoclonal antibodies. Nucleocapsid (N) protein-specific monoclonal antibodies have been developed against a large range of hantaviruses [13–15]. In contrast, the number of glycoprotein precursor (GPC), as well as Gc- and Gn-specific monoclonal antibodies is rather low [16–18]. The majority of these antibodies were raised by infection of bank voles or immunization with recombinant N protein or heterologous virus-like particles (VLPs). The generation of envelope protein-specific monoclonal antibodies with reactivity to virus proteins in infected cells is highly dependent on structural constraints [19]. Autologous VLPs represent a useful tool to generate highly efficient immune responses against a variety of viruses and for the generation of monoclonal antibodies in particular [20]. PUUV strain Astrup [21] GPC-derived VLPs were generated in this study as previously described for Maporal orthohantavirus [22].

Lower Saxony, north-west Germany, and district Osnabrück in particular, is a well-known endemic region for PUUV infections [23, 24]. This endemic region was also again heavily affected by the hantavirus outbreak year 2019 [25]. Here, we aimed to isolate a Central European PUUV strain from bank voles in the district of Osnabrück using standard VeroE6 cells and the recently established Carpathian lineage bank vole-derived kidney cell line (MGN-2-R [10]). Complete genome determination by shot-gun and hybrid-capture-mediated high-throughput sequencing (HTS) was used to follow the potential adaptation of the PUUV isolates in VeroE6 and reservoir cell lines. Finally, the reactivity of the isolates was determined with novel monoclonal antibodies raised against PUUV GPC VLPs.

Materials and methods

Trapping and dissection

Bank voles were trapped in spring 2019 in the PUUV endemic region around Osnabrück following a standard snap trapping protocol [25, 26]. In the field, a small piece of lung was taken for virus isolation and RT-qPCR analysis. Thereafter, carcasses were frozen, transported to the laboratory and completely dissected according to standard protocols. Chest cavity lavage was collected by rinsing the chest cavity by 1 ml phosphate-buffered saline (PBS) and investigated for the presence of PUUV-reactive antibodies. The presence of hantavirus RNA was analyzed from lung tissue and were, in part, previously published in a surveillance study [25].

Cell lines

For virus isolation and further infection studies, VeroE6 and bank vole kidney (MGN-2-R; [10]) cells were used in parallel. Virus titration was done on VeroE6 cells only. MGN-2-R cells were grown in an equal mixture of Hams' F12 and Iscove's modified Dulbecco's medium (IMDM) + 10% fetal calf serum (FCS) and passaged two times per week at a 1:6 ratio. VeroE6 cells were passaged twice a week in minimal essential medium (MEM) + 10% fetal calf serum (FCS) and a split ratio of 1:4.

Virus isolation

For virus isolation, 1×10^5 MGN-2-R or VeroE6 cells were seeded in 12.5 cm^2 flasks one day before rodent sampling in the field. The cells were carried to trapping sites in an isolation box with heat packs (around 33 °C constant for 2 days with outside temperature of 5–10 °C). After collecting voles from traps, a small incision in the chest area was made and a piece of lung (pea-sized) was taken and transferred into 1 ml Dulbecco's Modified Eagle's Medium (DMEM) + 5% FCS + penicillin/streptomycin (PS) in a 5 ml safe lock tube. Lung tissue material was homogenized in the field by grinding it through a fine metal grid against the tube wall. The homogenized tissue material was sterile filtered (0.45 µm) directly onto the cells resulting in approximately 500 µl tissue/medium suspension per 12.5 cm^2 flask. After 1–2 h incubation in the isolation box, 4 ml DMEM + 5% FCS + PS was added. Upon arrival in the laboratory flasks were incubated in a cell culture incubator at 37 °C and 5% CO_2 for 10 days until first passage. In parallel, a pinhead-sized piece of lung was taken for RNA isolation in 1 ml Trizol (QIAGEN, Hilden, Germany).

After 10 days, trypsinized cells were resuspended in 2 ml DMEM + 5% FCS + PS. For PUUV RNA screening, 325 µl of each cell suspension was taken for RNA extraction and analyzed by RT-qPCR (see below). Fresh VeroE6 cells were resuspended in 2 ml DMEM + 5% FCS + PS and 200 µl were mixed 1:1 with 200 µl of the inoculated cell suspension in a new 12.5 cm^2 flask. Afterwards, 4 ml DMEM + 5% FCS + PS were added and cells were incubated for 10 days until next passage. In parallel, one uninfected

flask of VeroE6 or MGN-2-R cells was passaged as a control. This procedure was continued until RT-qPCR-positive samples were detected. After first screening, only the flasks of the RT-qPCR-positive samples were further passaged.

Hantavirus RNA detection

For detection of PUUV nucleic acid, RNA was extracted from homogenized lung tissue, or cell culture passages using QIAzol Lysis Reagent (QIAGEN, Hilden, Germany) followed by a novel PUUV S segment-specific RT-qPCR. For RT-qPCR, primers PUUV-NSs-s (5′-GWNATARCYCGY CATGARC-3′) and PUUV-NSs-as (5′-ARTGCTGACACT GTYTGTTG-3′) and the probe (5′-6-FAM-CRGTGGRRRT-GKACCCRGATGA-BHQ-1-3′) were used. The PCR was done according to the QuantiTect Probe One-Step RT-qPCR Mix (QIAGEN, Hilden Germany) protocol and contained 20 pmol/µl of each primer and 5 pmol/µl probe (Eurofins, Hamburg, Germany). The following cycler protocol was used: 30 min of reverse transcription at 50 °C; 15 min initial denaturation at 95 °C; 45 cycles of 10 sec at 95 °C, 25 sec at 50 °C and 25 sec at 72 °C. For quantification of the number of RNA copies/µl and sample, an in vitro transcribed RNA was used. The in vitro transcription of a plasmid coding for nucleotides 83–355 of the S segment of a PUUV strain from Baden-Wuerttemberg (Binder et al., unpublished) was done according to the protocol of the manufacturer (Riboprobe® in vitro Transcription System T7, Promega GmbH, Mannheim, Germany). The transcribed RNA was serially diluted from 10^{-2} to 10^{-11} ng/ml with 700 RNA copies/µl limit of detection (LOD). Initial tissue samples were screened for PUUV RNA and viral load as RNA copies/µl was determined in triplicates for organs of isolated positive animals. RNA from the cell culture adapted strains PUUV Sotkamo and TULV Moravia were used as positive and negative control for the RT-qPCR, respectively.

Library preparation, target enrichment, sequencing and analysis

For metagenomics, we extracted RNA from either a pinhead-sized piece of lung tissue or 250 µl cell culture supernatant using 750 µl QIAzol Lysis Reagent (QIAGEN, Hilden, Germany) in combination with RNeasy Mini Kit (QIAGEN, Hilden, Germany). For generation of complete genomes of cell culture supernatants, a previously published workflow was used [27]. Double-stranded, non-directional cDNA libraries from lung tissue for sequencing on the Illumina platform were prepared from total RNA using the NEBNext Ultra II RNA Library Prep Kit for Illumina (New England Biolabs, Ipswich, MA, USA). Per reaction, a total of 100 ng RNA was used as an input. RNA was fragmented for 8 min and final cDNA libraries were amplified by 8 cycles of PCR to complete adapter ligation and to generate enough material for target sequence enrichment. A custom-made myBaits target capture array (Arbor Biosciences, Ann Arbor, MI, USA), containing biotinylated RNA probes against all available PUUV sequences deposited in NCBI GenBank database (August, 2018), was employed to capture PUUV-containing sequences from total cellular cDNA sequencing libraries. The hybridization-based sequence enrichment (chemistry v3) was performed according to the manufacturer's instructions (Arbor Biosciences, Ann Arbor, MI, USA). The enriched cDNA sequencing libraries were amplified with 14 PCR cycles to produce enough DNA material for HTS on the Illumina platform. The enriched cDNA libraries were quantified with the NEBNext Library Quantification Kit (New England Biolabs, Ipswich, MA, USA), pooled in equimolar amounts, and sequenced with a 600 cycle MiSeq Reagent Kit v3 (Illumina, San Diego, CA, USA) using paired-end sequencing (2 × 300 cycles) on a MiSeq sequencer (Illumina, San Diego, CA, USA). The resulting reads were trimmed and assembled against the known complete genome of strain Astrup from the Osnabrück region [21] with Geneious R11.1.5 (https://www.geneious.com). For sequences lacking the 5′ and 3′ ends of the M segment, RNA ligation was done using T4 RNA Ligase (Thermo Fisher Scientific, Waltham, MA, USA) and subsequent in vitro transcription with a First Strand cDNA Synthesis Kit (Thermo Fisher Scientific, Waltham, MA, USA). Sequences were obtained by conventional dideoxy-chain termination sequencing after PCR with primers PUUV OS M2 fwd-5′ TGAGGGCAATTATTATGT AA 3′ and PUUV OS M2 rev 5′ CCAATTGTATGTGGG CATTCC 3′. The obtained sequences were deposited at GenBank, accession numbers MN639737–MN639763.

Phylogenetic analysis of PUUV sequences

Phylogenetic trees were reconstructed with four novel and 18 published concatenated S, M, and L coding sequences or 202 partial S segment sequences of 365 nucleotides length. Published sequences of other hantaviruses were obtained from GenBank. Analysis was performed by Bayesian algorithms via MrBayes v.3.2.6 (https://sourceforge.net/projects/mrbayes/files/mrbayes/) on the CIPRES online portal [28]. A mixed nucleotide substitution matrix was specified in 4 independent runs of 10^7 generations. Phylogenetic relations are shown as a maximum clade credibility phylogenetic tree with posterior probabilities for major nodes.

Virus infection and titration

For immunofluorescence assay (IFA), VeroE6 and MGN-2-R cells were inoculated with 500 µl PUUV Osnabrück/V29 or PUUV Osnabrück/M43 supernatant in DMEM + 5% FCS as described previously [10]. Infected cells were fixed 10 days

post infection with a 1:1 mixture of acetone and methanol for 20 min at − 20 °C. After fixation cells were dried, re-hydrated with phosphate-buffered saline (PBS) and incubated with nucleocapsid (N) protein-specific antibody 5E11 [13] diluted 1:1000 in PBS for 1 h at room temperature (RT). A secondary anti-mouse Alexa fluor 488 conjugated antibody (Abcam, Cambridge, UK) was used for detection of hantavirus proteins. Nuclei were stained with 4′,6-diamidino-2-phenylindole (DAPI, Thermo Fisher Scientific).

For titration studies of PUUV, MGN-2-R and VeroE6 cells were inoculated with 500 µl of the PUUV Osnabrück/V29 or PUUV Osnabrück/M43 virus isolate and passaged three times as described above. Supernatants of both cell lines were collected after passage three and frozen at − 80 °C. Subsequently, supernatants were serially diluted from 10^{-1} to 10^{-7} in DMEM containing 5% FCS in a 96-well plate with three replicates each. A volume of 100 µl of each dilution was added to 24 h old cell monolayers of VeroE6 cells in a 96-well plate. After incubation for 10 days, the virus titer was calculated using IFA for PUUV N protein detection as described above. Titers were calculated as 50% tissue culture infectious dose ($TCID_{50}$)/ml by the Spearman/Kärber method [29] and mean titers of three experiments are given. Titers after isolation (passage 3 of original lung tissue-derived sample) were used for comparison.

Generation of recombinant virus-like particles

For expression and generation of VLPs in HEK293 cells, a codon-optimized synthetic gene of the PUUV GPC of the strain Astrup [21] was purchased (GeneArt, Regensburg, Germany). The gene encoding the glycoproteins was PCR amplified using primer pair O GRS 101/O GRS 102 (aattaaGGTACCTCCAGAGGCGACACCCGGAACC and aattattAAGCTTTCAGGGCTTGTGTTCTTTGG) and the PCR product and the acceptor vector pHAN-1 (Roman-Sosa, unpublished) were digested with the restriction endonucleases KpnI and HindIII. The expression plasmid pHAN-2 was generated by standard molecular biology protocols. In this plasmid, the endogenous signal sequence of the PUUV Gn is substituted by the IgG-light chain signal sequence and a double strep-tag with a glycine/serine-rich linker between the tags. Then a permanently transfected HEK293 cell line was generated upon transfection of the cells and selection in the presence of geneticin at 0.5 mg/ml. The VLPs were affinity purified from the cell supernatants essentially as described [22].

Generation of monoclonal antibodies against PUUV GPC

Recombinant VLPs were used for five immunizations of four weeks apart of female BALB/c mice. Hybridoma cells producing monoclonal antibodies (mAbs) were generated by standard fusion procedure [30, 31] and screened using a 2 µg/ml stock solution of VLPs according to an in-house ELISA protocol [32] and buffers without Tween. Resulting mAbs were analyzed by IFA and Western blot test for their reactivity to PUUV Osnabrück/V29, PUUV Sotkamo, PUUV Vranica and TULV Moravia.

Immunofluorescence assay analysis of mAbs

VeroE6 cells were infected with PUUV Osnabrück/V29, PUUV Sotkamo, PUUV Vranica or TULV Moravia at multiplicity of infection (MOI) 0.1 in DMEM + 5% FCS. Infected cells were fixed 10 (PUUV Osnabrück/V29, Sotkamo) or 3 (PUUV Vranica, TULV Moravia) days post infection with a 1:1 mixture of acetone and methanol for 20 min at − 20 °C. After fixation cells were dried, re-hydrated with PBS and incubated with mAbs raised against GPC, 2E10 (diluted in PBS, 1:1), 5F12 (1:1), 3B12 (1:200), 5B8 (1:1), 5H1 (1:1), 4G10 (1:100), 1B12 (1:2), 1G9 (1:100), 8G4 (1:50), 1H7 (1:1), 2H11 (1:5), or N protein-specific antibody 5E11 (1:1000, [13]) for 1 h at RT. A secondary anti-mouse Alexa fluor 488 conjugated antibody (Abcam, Cambridge, UK) was used for detection of hantavirus proteins. Nuclei were stained with DAPI. After staining, slides were mounted on glass slides for imaging with Ibidi mounting medium (Ibidi, Gräfelfing, Germany).

Western blot analysis of mAbs

VeroE6 cells were infected with PUUV Osnabrück/V29, PUUV Sotkamo, PUUV Vranica or TULV Moravia at MOI 0.1 in DMEM + 5% FCS. Cells were harvested 10 (PUUV Osnabrück/V29, Sotkamo) or 3 (PUUV Vranica, TULV Moravia) days post infection in SDS sample buffer (62.5 mM TrisHCl pH 6.8, 2% SDS,10% glycerol, 6 M Urea, 0.01% bromophenol blue, 0.01% phenol red) and proteins were separated by SDS PAGE, blotted onto polyvinylidenfluorid (PVDF) membranes. After blocking, the membranes were cut into strips and incubated over night with the antibodies 2E10 (1:1), 5F12 (1:1), 3B12 (1:200), 5B8 (1:1), 5H1 (1:1), 4G10 (1:100), 1B12 (1:2), 1G9 (1:100), 8G4 (1:50), 1H7 (1:1), 2H11 (1:5) or N protein-specific antibody 5E11 (1:1000, [13], all diluted in PBS-Tween 0.05%) at 4 °C. A horseradish peroxidase (HRP) labeled secondary goat anti-mouse IgG antibody diluted 1:3000 in PBS-Tween 0.05% (Bio-Rad, Hercules, CA, USA) was used for detection of hantaviral proteins. A rabbit anti-β-tubulin antibody (Abcam, Cambridge, UK) was used as a loading control.

IgG ELISA analysis of chest cavity lavage of bank voles

Investigation of chest cavity lavage samples from bank voles was done by IgG ELISA using recombinant PUUV strain BaWa N protein, as described earlier [32]. The monoclonal antibody 5E11 was used as a positive control [13], chest cavity lavage of a IgG ELISA- and RT-PCR-negative bank vole was used as negative control. Chest cavity lavage samples with an optical density (OD) value below the lower cut-off value were considered as negative. Positive and doubtful samples were retested a second time. When the OD value of the ELISA was in a range between the lower and upper cut-off value defined according to our standard protocol [32], animals were considered doubtful. When the OD value was above the upper cut-off value, the samples were considered as positive.

Results

Isolation of PUUV from bank voles in the field

Rodent trapping at five sites from April 11th to 12th, 2019 in the Osnabrück region resulted in the collection of 57 bank voles [25]. Dissection on site and inoculation of VeroE6 and bank vole MGN-2-R cells with homogenized lung samples resulted after three blind passages in four potential isolates that were detected by a novel PUUV RT-qPCR (Table S1, Fig. 1). Two of the potential candidates showed only low levels of PUUV RNA and were not able to consistently infect further passages (M52, M62). Quantification by RT-qPCR analysis of different tissues from these four bank voles confirmed lung tissue for most of the samples as having the highest PUUV RNA load, although it was detected in almost all other tissues investigated (Fig. S1).

RT-PCR and IgG ELISA analysis of bank voles

RT-qPCR investigation of lung tissues of all 57 bank voles resulted in the detection of hantavirus RNA in 44 animals (Tables 1, S1, [25]). PUUV RNA-positive animals originated from all five trapping sites. Serological analysis of chest cavity lavages detected PUUV N protein reactive antibodies in 24 of 57 bank voles (Tables 1, S1). Five additional animals, positive for PUUV RNA, were found to be equivocal in our serological test. All 24 antibody-positive animals were also found to be PUUV RNA positive, indicating a high number of persistently infected voles. Fifteen additional bank voles were only positive for PUUV RNA, but not for anti-PUUV antibodies, indicating a high number of acutely infected animals in spring in this region (Table 1). Interestingly three of the four potential isolates originated from seronegative bank voles (Table S1).

Characterization of the PUUV isolates

Two isolates (Osnabrück V29 and Osnabrück M43) were obtained by passaging in VeroE6 or MGN-2-R cells, which reached titers of almost 10^3 $TCID_{50}$/ml (Fig. 2a and b, titer after isolation). Shot-gun and hybrid-capture-mediated HTS of both isolates resulted in the generation of complete genome sequences which are identical in sequence to the respective original strain in bank vole lung tissue except for one amino acid (aa) exchange each in the RNA-dependent

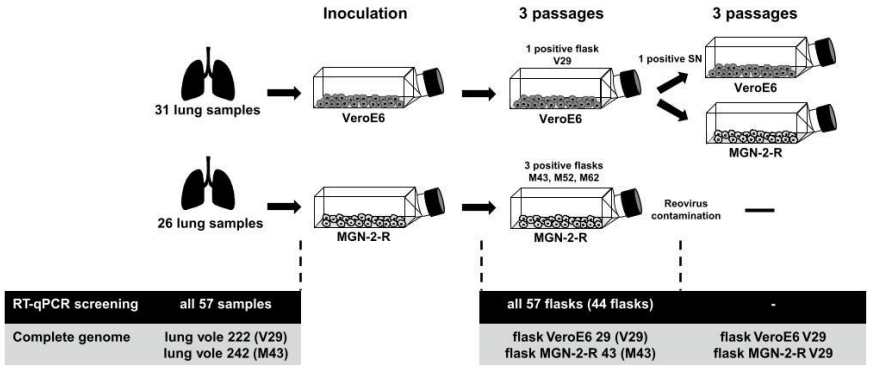

Fig. 1 Schematic representation of the workflow. Bank voles were collected in forests within the district Osnabrück and a small piece of lung was taken by an incision in the chest area directly in the field. Lung tissue was meshed by grinding against a metal grid in a reaction tube containing 1 ml DMEM + 5% FCS and sterile filtered directly onto the cells. Cells were passaged three times until PUUV RT-qPCR screening. Supernatant of PUUV-positive flasks was taken and used for infection and further passaging in VeroE6 and MGN-2-R cells. Sequencing of complete genomes was done for PUUV RT-qPCR-positive passages and the corresponding original bank vole lung tissue. Isolates M52 and M62 were lost upon virus stock generation, presumably due to low viral load

Table 1 Results of molecular and serological *Puumala orthohantavirus* testing of trapped bank voles

Trapping site	Total number of bank voles	RT-qPCR positive[a]/ total number investigated	IgG ELISA doubtful/ positive/total number investigated	RT-qPCR positive and IgG ELISA doubtful/ positive/total number investigated	Only RT-qPCR positive[b]/ total number investigated
Schledehausen Forest	18	16/18	3/9/18	3/9/18	4/18
Schledehausen Field	21	16/21	1/9/21	1/9/21	6/21
Ellerbeck	5	5/5	1/2/5	1/2/5	2/5
Astrup I	6	4/6	0/3/6	0/3/6	1/6
Astrup II	7	3/7	0/1/7	0/1/7	2/7
Total	57	44/57	5/24/57	5/24/57	15/57

RT-qPCR real-time reverse transcription-polymerase chain reaction targeting the *Puumala orthohantavirus* S segment

[a]Results of RT-qPCR-positive animals were partly already published in [25]

[b]RT-qPCR positive, but IgG ELISA negative

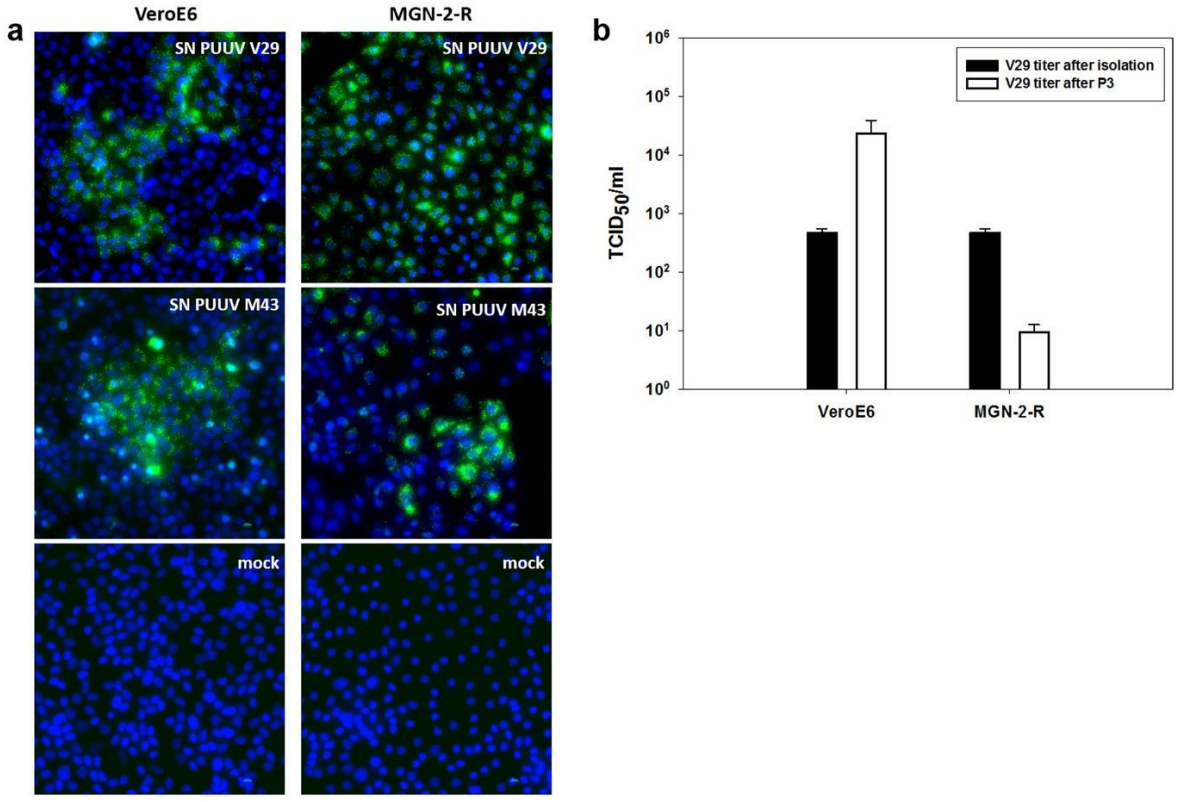

Fig. 2 Infection studies of PUUV isolates in VeroE6 and MGN-2-R cells. **a** Immunofluorescence analysis of VeroE6 and MGN-2-R cells inoculated with supernatants (SN) of PUUV Osnabrück/V29, isolated on VeroE6 cells, or PUUV Osnabrück/M43, isolated on MGN-2-R cells. PUUV-inoculated and mock-infected cells were fixed 10 days post infection and stained with nucleocapsid protein-specific antibody 5E11 and a secondary anti-mouse Alexa fluor 488 conjugated anti-body. Nuclei were stained with DAPI. **b** Determination of virus titers of PUUV Osnabrück/V29 isolate ($TCID_{50}$/ml) after three passages (P3) in VeroE6 and MGN-2-R cells (white columns) in comparison to titers directly after isolation in VeroE6 cells (black columns). Titers were obtained by immunofluorescence staining of 96-well plates 10 days post inoculation

RNA polymerase (RdRP) of strain M43 (I3749M) and V29 (D3963Y; Fig. 3).

The genome organization of the novel PUUV isolates indicated the typical sequence elements for PUUV: The small (S) segment encodes an N protein of 433 aa residues and a putative NSs protein of 90 aa in an + 1 overlapping reading frame, the medium (M) segment codes for the 1148 aa GPC and the large (L) segment for the RdRP of 2156 aa (see Fig. 3, GenBank accession numbers: MN639737–MN639748). Phylogenetic analysis of the concatenated S, M and L segment coding sequences grouped the novel isolates together with Astrup prototype strain in sister relationship to PUUV sequences from France (Fig. 4a). The phylogenetic analysis of a partial S segment sequence of the novel isolates and representative strains of all PUUV clades and subclades from Germany confirmed the close relationship of the new isolates to the Osnabrück hills subclade (Fig. 4b).

The PUUV Osnabrück M43 isolate was found to be contaminated by a bank vole reovirus; HTS derived sequences of the passaged reovirus (GenBank accession numbers: MN639755–MN639763) showed a strong similarity to a bank vole reovirus strain, but much lower similarity to a common vole reovirus [33]).

The non-reovirus contaminated isolate Osnabrück V29 from VeroE6 cells was found to have an insertion of 20 nucleotides in the 3′ non-coding region (NCR) when compared to the other isolate and the Astrup reference sequence (Fig. 3). However, this insertion was also found in the original lung sample and therefore no cell culture-specific adaptations were observed in the NCRs of both virus isolates (Fig. 3).

Passaging experiment for isolate V29 in vole and VeroE6 cells

V29 isolate was passaged in parallel again in VeroE6 cells and in MGN-2-R cells (Figs. 1 and 2). This passaging resulted in no further mutations (GenBank accession numbers: MN639749–MN639754). However, the virus isolate passaged in VeroE6 cells is accompanied by an increase in the virus titer to 10^4 $TCID_{50}$/ml (Fig. 2). In contrast, the passaging of the Osnabrück V29 strain in MGN-2-R cells resulted in a decreased virus titer. As no cytopathic effect was observed, virus detection for titration in both cell lines was done by immunofluorescence assay using an N protein-specific monoclonal antibody (Fig. 2a).

Development of monoclonal antibodies against the new PUUV isolate

Eleven monoclonal antibodies were produced in this study by immunization of mice with PUUV strain Astrup GPC-derived VLPs. Evaluation of the virus isolate Osnabrück V29 using these monoclonal antibodies resulted in typical immunofluorescence patterns in the cytoplasm (Fig. 5). Further analysis by Western blot test using a lysate of isolate Osnabrück V29 from VeroE6 cells suggested that the majority of anti-GPC antibodies are directed against conformational epitopes; however, some recognize linear epitopes in Gc or Gn (Table 2). Subsequent evaluation of the reactivity of these monoclonal antibodies with other PUUV strains and TULV strain Moravia indicated some level of cross-reactivity for some of them (Table 2).

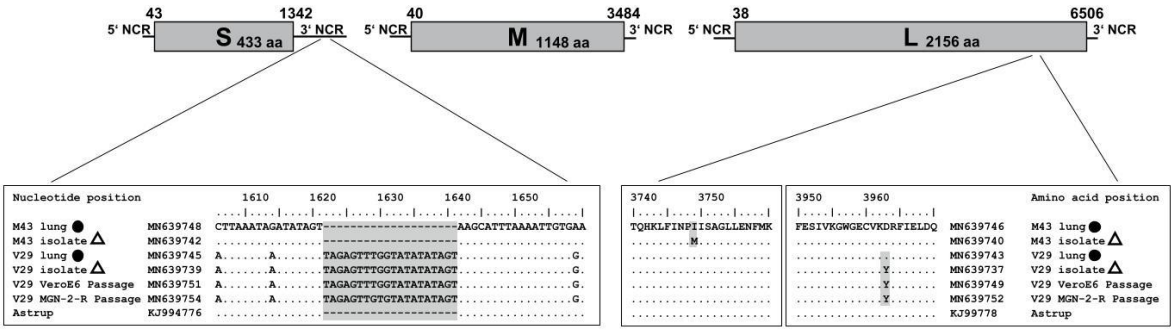

Fig. 3 Complete genome analysis of PUUV isolates. Complete PUUV genomes isolated from lung tissues and positive cell line passages were determined by HTS and dideoxy-chain termination sequencing in combination with RNA ligation to obtain complete NCRs. Nucleotide sequence insertion in the S segment NCR and amino acid exchanges in the L segment encoded RdRP are compared. Black dots indicate sequences derived from lung tissue and triangles indicate sequences obtained from cell culture passages. The complete genome of PUUV strain Astrup was used as a reference sequence ([21]; GenBank accession numbers: KJ994776-78). Coding regions of the three segments are indicated by numbers. NCR, non-coding region; M43, PUUV Osnabrück/MGN-2-R 43; V29, PUUV Osnabrück/VeroE6 29

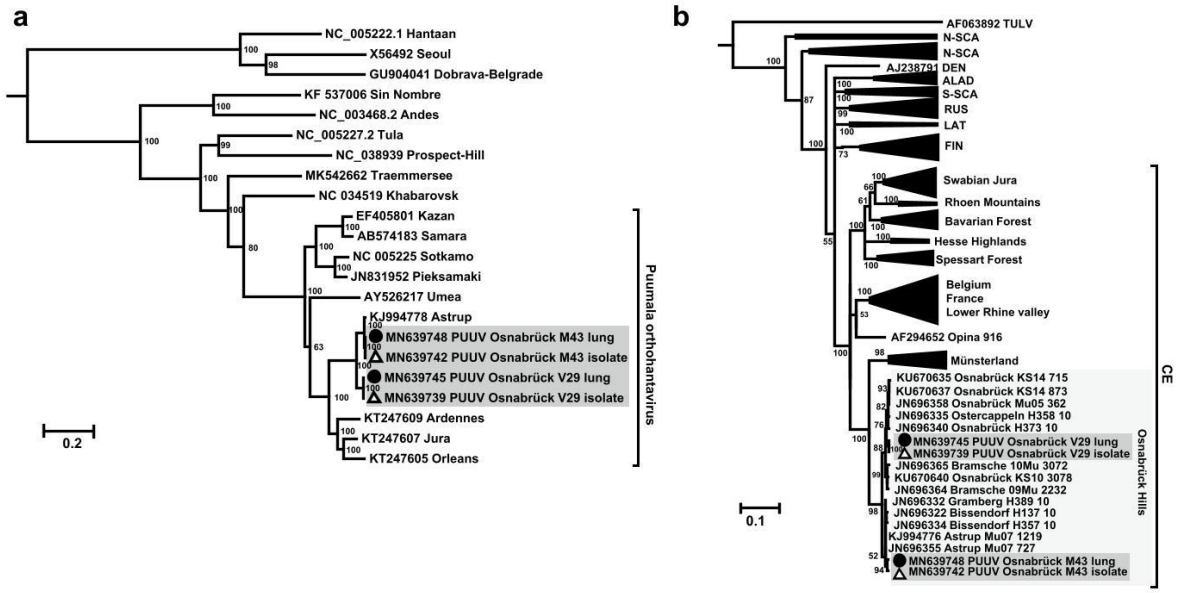

Fig. 4 Hantavirus phylogenetic trees. Hantavirus phylogenetic tree of concatenated S, M, and L coding sequences of 18 published and four novel complete genomes (**a**). Partial S segment coding sequences of 365 nucleotides length, reconstructed with four novel and 202 published partial sequences (**b**). New PUUV isolates (GenBank accession numbers: MN639737-MN639742) are indicated with triangles and sequences derived from their original lung tissue (GenBank accession numbers: MN639743-MN639748) are labeled with black dots. Published sequences of other hantaviruses are labeled with GenBank accession numbers. Novel sequences are highlighted in gray. Posterior probabilities for major nodes of the maximum clade credibility phylogenetic tree are displayed. Analysis was performed by Bayesian algorithms via MrBayes v.3.2.6 (https://sourceforge.net/projects/mrbayes/files/mrbayes/) on the CIPRES online portal [28]. A mixed nucleotide substitution matrix was specified in 4 independent runs of 10^7 generations. Scale bar indicates nucleotide substitutions per site. For clarity, previously characterized PUUV clades from other parts of Europe are shown in simplified form. CE, Central European; LAT, Latvian; ALAD, Alpe-Adrian; S-SCA, South Scandinavian; N-SCA, North Scandinavian; RUS, Russian; FIN, Finnish; DEN, Danish

Discussion

Here, we describe the first isolation of a Central European PUUV strain. This strain of the Central European lineage increases the available panel of PUUV isolates: Currently available isolates Sotkamo, Umea, Vranica, and Kazan, belong to the clades Finnish, North Scandinavian, most likely North Scandinavian, and Russian, respectively [34]. The PUUV-like Hokkaido virus strain Kitahiyama128 originates from Japan [12]. In our study, the isolation was based on an in-field dissection and inoculation of cells to prevent freeze/thaw cycles. The subsequent investigation of all 57 bank voles indicated that three of four isolates originated from anti-PUUV-seronegative voles. This finding illustrates that a serological test in the field might be misleading in selection of samples for successful virus isolation. Instead, an on-site molecular assay may enhance the chance for a successful virus isolation. Nevertheless, the approach used here still indicates the challenges of hantavirus isolation; only four isolates were obtained from a total of 15 acutely infected bank voles. In addition, the determination of the complete genome sequences of two isolates including the NCRs expands our knowledge on the sequence diversity of PUUV strains within the different regions of the genome. Moreover, the hybrid-capture-based enrichment of PUUV sequences allows a rapid determination of the complete genome and underlines the value of this workflow for hantavirus surveillance and molecular evolution studies [35]. A phylogenetic analysis of partial S segment nucleotide sequences confirmed the previously reported subclades of PUUV in Germany; the novel isolates belong to the subclade Osnabrück hills within the Central European clade. The position within the phylogenetic tree also confirms the local evolution pattern of PUUV reported before [23, 36].

The observed high level of RT-qPCR-positive bank voles (44/57; 77%) confirms the district of Osnabrück in spring 2019 as a hantavirus outbreak region [25]. The PUUV RNA detection rate was similarly high at all five trapping sites of bank voles. Although 2019 was identified as a hantavirus outbreak year in Germany, the distribution of notified human PUUV cases was not as homogeneous as in previous outbreak years [25].

The passage of the PUUV strains for isolation resulted in non-synonymous nucleotide exchanges in the L segment

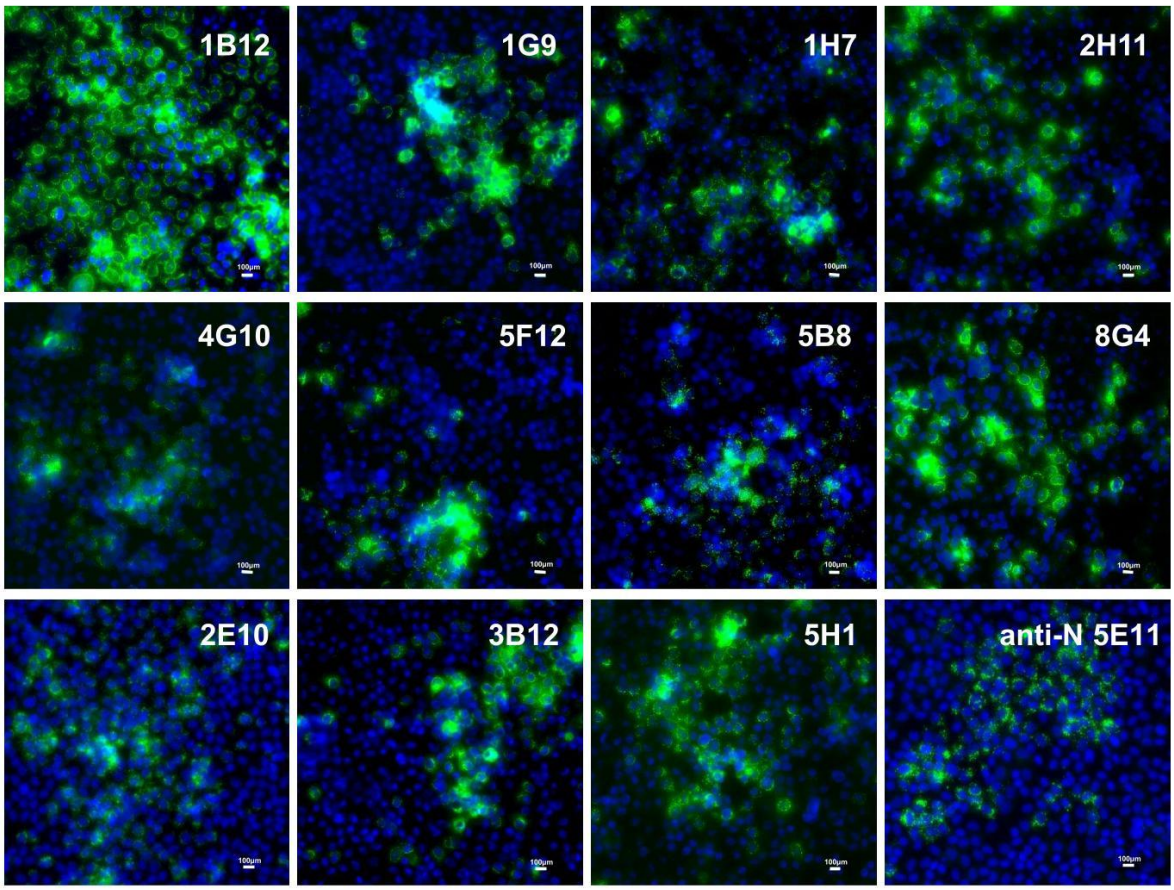

Fig. 5 Reactivity of novel PUUV GPC-specific monoclonal antibodies with hantavirus-infected VeroE6 cells in immunofluorescence assay (IFA). Antibodies were generated by immunization of BALB/c mice with GPC-derived virus-like particles of PUUV strain Astrup. After screening and subcloning, monoclonal antibodies were tested in IFA. VeroE6 cells were infected with PUUV Osnabrück V29 isolate on coverslips and fixed for IFA after 10 days. The monoclonal antibodies were administered for 1 h at RT. Detection of the specific antibody binding was done using an anti-mouse Alexa fluor 488 conjugated antibody. After staining, coverslips were mounted on glass slides for imaging

responsible for single amino acid exchanges in the RdRP (I3749M in M43 and D3963Y in V29). The substituted amino acid residues are each very similar in their properties and, presumably, might not influence protein function. A more divergent adaptation at position S2053F has previously been observed for PUUV strain Kazan [8, 37]. Although in this previous study nucleotide exchanges in the NCR of the S segment were observed [37], here we did not find relevant mutations in this region after passaging in cell culture. The V29 strain showed an insertion in the 3′ NCR, but this insert was also found in the original lung material used for isolation. Additionally, this sequence insert was found in another sequence from the same region (JN696358.1, [36]).

The isolate V29 was shown to replicate in VeroE6 and a bank vole kidney cell line. The low titer in the bank vole MGN-2-R cell line might be due to the evolutionary lineage origin of this cell line (Carpathian lineage); in Central Europe PUUV is harbored by the Western evolutionary lineage with spillover to the Carpathian lineage in regions with sympatric occurrence of both [24]. In line with the assumption of an association of a PUUV clade with an evolutionary bank vole lineage, the Vranica PUUV strain replicated in MGN-2-R cells, but not in bank vole kidney cells of another evolutionary lineage [9, 10]. Interestingly, replication of PUUV-like Hokkaido virus in cells of its host, the gray red-backed vole, was comparable to PUUV infection [12]. Future investigations in cell lines and animals of different bank vole lineages are required to confirm this conclusion directly.

The orthoreovirus contamination of one of the PUUV isolates illustrates that bank voles may harbor additional

Table 2 Reactivity of monoclonal antibodies with hantavirus-infected VeroE6 cells in immunofluorescence assay (IFA) and Western blot test (WB)

Antibody	PUUV V29 Osnabrück		PUUV Sotkamo		PUUV Vranica		TULV Moravia	
	IFA	WB	IFA	WB	IFA	WB	IFA	WB
1B12	++	−	−	−	−	−	−	−
5H1	++	−	−	−	−	−	−	−
2H11	++	−	−	−	−	−	−	−
1G9	++	−	(+)	−	+	−	−	−
5F12	++	−	+	−	+	−	−	−
3B12	++	−	+	−	++	−	++	−
8G4	++	−	+	−	++	−	+	−
4G10	++	−	+	−	(+)	−	++	−
1H7	++	+(Gn)	−	+	−	+	−	−
5B8	++	+(Gc)	+	+	+	−	+	−
2E10	(+)	+(Gc)	(+)	+	++	−	+	−

VeroE6 cells were inoculated with Puumala virus (PUUV) Osnabrück/V29, PUUV Sotkamo, PUUV Vranica or Tula virus (TULV) strain Moravia. Infected cells were fixed 10 (PUUV Osnabrück/V29, Sotkamo) or 3 (PUUV Vranica, TULV Moravia) days post infection for immunofluorescence assays or collected in sample buffer for Western blot analysis. After fixation or Western blot transfer, novel GPC-specific mAbs 2E10, 5F12, 3B12, 5B8, 5H1, 4G10, 1B12, 1G9, 8G4, 1H7, and 2H11 were administered. Gn- and Gc-reactive mAbs were assigned where possible according to molecular weight of the immunoreactive bands in Western blot analysis

− negative; (+) weak reactivity; + positive; ++ strongly positive

infectious agents that may influence the susceptibility to PUUV infections or their outcome. Of note, in bank voles several viruses have been detected, i.e., polyoma-, herpes- and hepaciviruses [38–41], but also bacterial agents and endoparasites [42–44]. Similarly, a hantavirus isolation approach was previously hampered by the coinfection by a striped field mouse adenovirus [45]. Future investigations are needed to evaluate potential influences of coinfections in bank voles.

It has been shown that hantavirus Gn and Gc form complex spike-shaped structures [46] that build conformational epitopes [17, 18]. Therefore, we selected an immunization procedure using PUUV-GPC-derived VLPs, as the organization of the glycoproteins resembles the one of the virion. A panel of eleven monoclonal antibodies was produced here and all of them were reactive with the new PUUV isolate in immunofluorescence assay. The staining pattern, which is reminiscent of the one of the secretory pathway organelles, i.e., the Golgi apparatus and the endoplasmic reticulum, suggests that the epitopes recognized by these antibodies are already accessible during the maturation process of the proteins. Interestingly, some of the monoclonal antibodies recognize linear epitopes as revealed by a Western blot assay. Although preliminary results suggest that the antibodies do not neutralize the virus when tested individually, synergistic effects with a protective effect cannot be ruled out yet as shown for anti-Ebola virus monoclonal antibodies [47]. Therefore, the novel antibodies represent a useful tool for further experimental, diagnostic, and therapeutic applications.

In conclusion, the PUUV isolate described here replicates in a bank vole cell line and its N and GPC proteins can be detected by specific monoclonal antibodies. Therefore, this isolate will be useful for further studies on the virulence markers of Central European PUUV, its reservoir host association and the route of pathogenicity in the bank vole model. The novel GPC-specific monoclonal antibodies will enable future studies on virus entry and important domains for exposed immunogenic regions.

Acknowledgements Open Access funding provided byProjekt DEAL. The authors would like to thank Sönke Röhrs for help with rodent trapping, Stephan Drewes for help with phylogenetic analysis and Sven Sander and Patrick Zitzow for excellent technical support with generation of monoclonal antibodies and sequencing of PUUV isolates. The authors thank Martin Beer, Klaus Osterrieder and Nicole Tischler for constant support and helpful discussions.

Author contributions RGU and FB designed the study and wrote the manuscript. FB did virus isolation, infection studies, sequence analysis, phylogenetic analysis, and testing of monoclonal antibodies. SR and FB generated and screened the monoclonal antibodies. GRS produced the VLPs for immunization. MS and FB performed rodent trapping. DH, JT, and DK did the complete genome sequencing of PUUV isolates. RR developed the PUUV-specific RT-qPCR assay. All authors gave significant ideas for the presented work and were involved in writing and proof reading of the manuscript.

Funding Florian Binder acknowledges intramural funding by the Friedrich-Loeffler-Institut. Additional funding was provided by the Bundesminsterium für Bildung und Forschung through the Research Network Zoonotic Infections (RoBoPub consortium, FKZ 01KI1721A, awarded to RGU; FKZ 01KI1721H, awarded to LAVES) for trapping and rodent screening, the RAPiD project within the Infect Control

2020 Consortium (FKZ 03ZZ0821A awarded to RGU) for development of novel real-time PCRs and the Bundesminsterium für Bildung und Forschung through the National Research Platform for Zoonosis (FKZ 01KI1730, awarded to DK).

Compliance with ethical standards

Conflict of interest The authors declare that they have no competing interests.

Ethical approval All animals were handled according to the applicable institutional, national and international guidelines for the care and use of animals. Bank vole trapping was conducted in line with the regular pest control of the LAVES Veterinary Task-Force in Lower Saxony, Germany (Department of Pest Control, Oldenburg) according to German federal law (§ 18, Gesetz zur Verhütung und Bekämpfung von Infektionskrankheiten beim Menschen). The immunization of mice was done in line with the general immunization program of the Friedrich-Loeffler-Institut (Landesamt für Landwirtschaft, Lebensmittelsicherheit und Fischerei, Mecklenburg-Vorpommern, permit: 28/17).

Informed consent This study did not include investigations on human participants.

References

1. Avsic-Zupanc T, Saksida A, Korva M (2015) Hantavirus infections. Clin Microbiol Infect. https://doi.org/10.1111/1469-0691.12291
2. Krüger DH, Figueiredo LT, Song JW, Klempa B (2015) Hantaviruses-globally emerging pathogens. J Clin Virol 64:128–136. https://doi.org/10.1016/j.jcv.2014.08.033
3. Faber M, Krüger DH, Auste B, Stark K, Hofmann J (2019) Weiss S (2019) Molecular and epidemiological characteristics of human Puumala and Dobrava-Belgrade hantavirus infections, Germany, 2001 to 2017. Euro Surveillance. https://doi.org/10.2807/1560-7917.Es.2019.24.32.1800675
4. Reip A, Haring B, Sibold C, Stohwasser R, Bautz EK, Darai G, Meisel H, Kruger DH (1995) Coding strategy of the S and M genomic segments of a hantavirus representing a new subtype of the Puumala serotype. Adv Virol 140(11):2011–2026. https://doi.org/10.1007/bf01322689
5. Elliott LH, Ksiazek TG, Rollin PE, Spiropoulou CF, Morzunov S, Monroe M, Goldsmith CS, Humphrey CD, Zaki SR, Krebs JW et al (1994) Isolation of the causative agent of hantavirus pulmonary syndrome. Am J Trop Med Hygiene 51(1):102–108
6. Yanagihara R, Goldgaber D, Lee PW, Amyx HL, Gajdusek DC, Gibbs CJ Jr, Svedmyr A (1984) Propagation of nephropathia epidemica virus in cell culture. Lancet (London, England) 1(8384):1013
7. Lundkvist A, Mehl R, Wiger D, Vaheri A, Hörling J, Sjolander KB, Plyusnin A (1998) Isolation and characterization of Puumala hantavirus from Norway: evidence for a distinct phylogenetic sublineage. J Gen Virol 79:2603–2614
8. Lundkvist A, Cheng Y, Sjölander KB, Niklasson B, Vaheri A, Plyusnin A (1997) Cell culture adaptation of Puumala hantavirus changes the infectivity for its natural reservoir, *Clethrionomys glareolus*, and leads to accumulation of mutants with altered genomic RNA S segment. J Virol 71(12):9515–9523
9. Essbauer SS, Krautkrämer E, Herzog S, Pfeffer M (2011) A new permanent cell line derived from the bank vole (*Myodes glareolus*) as cell culture model for zoonotic viruses. Virol J 8:339. https://doi.org/10.1186/1743-422X-8-339
10. Binder F, Lenk M, Weber S, Stoek F, Dill V, Reiche S, Riebe R, Wernike K, Hoffmann D, Ziegler U, Adler H, Essbauer S, Ulrich RG (2019) Common vole (*Microtus arvalis*) and bank vole (*Myodes glareolus*) derived permanent cell lines differ in their susceptibility and replication kinetics of animal and zoonotic viruses. J Virol Methods. https://doi.org/10.1016/j.jviromet.2019.113729
11. Eckerle I, Lenk M, Ulrich RG (2014) More novel hantaviruses and diversifying reservoir hosts-time for development of reservoir-derived cell culture models? Viruses 6(3):951–967. https://doi.org/10.3390/v6030951
12. Sanada T, Seto T, Ozaki Y, Saasa N, Yoshimatsu K, Arikawa J, Yoshii K, Kariwa H (2012) Isolation of Hokkaido virus, genus Hantavirus, using a newly established cell line derived from the kidney of the grey red-backed vole (*Myodes rufocanus bedfordiae*). J Gen Virol 93(Pt 10):2237–2246. https://doi.org/10.1099/vir.0.045377-0
13. Kucinskaite-Kodze I, Petraityte-Burneikiene R, Zvirbliene A, Hjelle B, Medina RA, Gedvilaite A, Razanskiene A, Schmidt-Chanasit J, Mertens M, Padula P, Sasnauskas K, Ulrich RG (2011) Characterization of monoclonal antibodies against hantavirus nucleocapsid protein and their use for immunohistochemistry on rodent and human samples. Adv Virol 156(3):443–456. https://doi.org/10.1007/s00705-010-0879-6
14. Lundkvist A, Horling J, Bjorsten S, Niklasson B (1995) Sensitive detection of hantaviruses by biotin-streptavidin enhanced immunoassays based on bank vole monoclonal antibodies. J Virol Methods 52(1–2):75–86. https://doi.org/10.1016/0166-0934(94)00143-5
15. Schlegel M, Tegshduuren E, Yoshimatsu K, Petraityte R, Sasnauskas K, Hammerschmidt B, Friedrich R, Mertens M, Groschup MH, Arai S, Endo R, Shimizu K, Koma T, Yasuda S, Ishihara C, Ulrich RG, Arikawa J, Kollner B (2012) Novel serological tools for detection of Thottapalayam virus, a Soricomorpha-borne hantavirus. Adv Virol 157(11):2179–2187. https://doi.org/10.1007/s00705-012-1405-9
16. Lundkvist A, Niklasson B (1992) Bank vole monoclonal antibodies against Puumala virus envelope glycoproteins: identification of epitopes involved in neutralization. Adv Virol 126(1–4):93–105
17. Zvirbliene A, Kucinskaite-Kodze I, Razanskiene A, Petraityte-Burneikiene R, Klempa B, Ulrich RG, Gedvilaite A (2014) The use of chimeric virus-like particles harbouring a segment of hantavirus Gc glycoprotein to generate a broadly-reactive hantavirus-specific monoclonal antibody. Viruses 6(2):640–660. https://doi.org/10.3390/v6020640
18. Koch J, Liang M, Queitsch I, Kraus AA, Bautz EK (2003) Human recombinant neutralizing antibodies against hantaan virus G2 protein. Virology 308(1):64–73. https://doi.org/10.1016/s0042-6822(02)00094-6
19. Cifuentes-Munoz N, Salazar-Quiroz N, Tischler ND (2014) Hantavirus Gn and Gc envelope glycoproteins: key structural units for

virus cell entry and virus assembly. Viruses 6(4):1801–1822. https://doi.org/10.3390/v6041801

20. Diederich S, Gedvilaite A, Zvirbliene A, Kazaks A, Sasnauskas K, Johnson N, Ulrich RG (2015) Virus-like particles: a versatile tool for basic and applied research on emerging and reemerging viruses. Viral nanotechnologies. CRC Press, Boca Raton, pp 137–160
21. Ali HS, Drewes S, Weber de Melo V, Schlegel M, Freise J, Groschup MH, Heckel G, Ulrich RG (2015) Complete genome of a Puumala virus strain from Central Europe. Virus Genes 50(2):292–298. https://doi.org/10.1007/s11262-014-1157-6
22. Jangra RK, Herbert AS, Li R, Jae LT, Kleinfelter LM, Slough MM, Barker SL, Guardado-Calvo P, Roman-Sosa G, Dieterle ME, Kuehne AI, Muena NA, Wirchnianski AS, Nyakatura EK, Fels JM, Ng M, Mittler E, Pan J, Bharrhan S, Wec AZ, Lai JR, Sidhu SS, Tischler ND, Rey FA, Moffat J, Brummelkamp TR, Wang Z, Dye JM, Chandran K (2018) Protocadherin-1 is essential for cell entry by New World hantaviruses. Nature 563(7732):559–563. https://doi.org/10.1038/s41586-018-0702-1
23. Weber de Melo V, Sheikh Ali H, Freise J, Kuhnert D, Essbauer S, Mertens M, Wanka KM, Drewes S, Ulrich RG, Heckel G (2015) Spatiotemporal dynamics of Puumala hantavirus associated with its rodent host *Myodes glareolus*. Evol Appl 8(6):545–559. https://doi.org/10.1111/eva.12263
24. Drewes S, Ali HS, Saxenhofer M, Rosenfeld UM, Binder F, Cuypers F, Schlegel M, Rohrs S, Heckel G, Ulrich RG (2017) Host-associated absence of human Puumala virus infections in Northern and Eastern Germany. Emerg Infect Dis 23(1):83–86. https://doi.org/10.3201/eid2301.160224
25. Binder F, Drewes S, Imholt C, Saathoff M, Alexandra Below D, Bendl E, Conraths FJ, Tenhaken P, Mylius M, Brockmann S, Oehme R, Freise J, Jacob J, Ulrich RG (2019) Heterogeneous *Puumala orthohantavirus* situation in endemic regions in Germany in summer 2019. Transbound Emerg Dis. https://doi.org/10.1111/tbed.13408
26. Drewes S, Schmidt S, Jacob J, Imholt C, Ulrich RG (2016) APHAEA/EWDA Species card: voles and mouses. https://www.aphaea.org/cards/species
27. Wylezich C, Papa A, Beer M, Hoper D (2018) A versatile sample processing workflow for metagenomic pathogen detection. Sci Rep 8(1):13108. https://doi.org/10.1038/s41598-018-31496-1
28. Miller MA, Schwartz T, Pickett BE, He S, Klem EB, Scheuermann RH, Passarotti M, Kaufman S, O'Leary MA (2015) A RESTful API for access to phylogenetic tools via the CIPRES Science Gateway. Evol Bioinform Online 11:43–48. https://doi.org/10.4137/EBO.S21501
29. Kärber G (1931) Beitrag zur kollektiven Behandlung pharmakologischer Reihenversuche. Arch Exp Pathol Pharm 162:480–483
30. Bussmann BM, Reiche S, Jacob LH, Braun JM, Jassoy C (2006) Antigenic and cellular localisation analysis of the severe acute respiratory syndrome coronavirus nucleocapsid protein using monoclonal antibodies. Virus Res 122(1–2):119–126. https://doi.org/10.1016/j.virusres.2006.07.005
31. Fischer K, Diederich S, Smith G, Reiche S, Pinho Dos Reis V, Stroh E, Groschup MH, Weingartl HM, Balkema-Buschmann A (2018) Indirect ELISA based on Hendra and Nipah virus proteins for the detection of henipavirus specific antibodies in pigs. PLoS ONE 13(4):e0194385. https://doi.org/10.1371/journal.pone.0194385
32. Mertens M, Kindler E, Emmerich P, Esser J, Wagner-Wiening C, Wolfel R, Petraityte-Burneikiene R, Schmidt-Chanasit J, Zvirbliene A, Groschup MH, Dobler G, Pfeffer M, Heckel G, Ulrich RG, Essbauer SS (2011) Phylogenetic analysis of Puumala virus subtype Bavaria, characterization and diagnostic use of its recombinant nucleocapsid protein. Virus Genes 43(2):177–191. https://doi.org/10.1007/s11262-011-0620-x
33. Feher E, Kemenesi G, Oldal M, Kurucz K, Kugler R, Farkas SL, Marton S, Horvath G, Banyai K, Jakab F (2017) Isolation and complete genome characterization of novel reassortant orthoreovirus from common vole (*Microtus arvalis*). Virus Genes 53(2):307–311. https://doi.org/10.1007/s11262-016-1411-1
34. Castel G, Chevenet F, Razzauti M, Murri S, Marianneau P, Cosson JF, Tordo N, Plyusnin A (2019) Phylogeography of *Puumala orthohantavirus* in Europe. Viruses. https://doi.org/10.3390/v11080679
35. Saxenhofer M, Schmidt S, Ulrich RG, Heckel G (2019) Secondary contact between diverged host lineages entails ecological speciation in a European hantavirus. PLoS Biol 17(2):e3000142. https://doi.org/10.1371/journal.pbio.3000142
36. Ettinger J, Hofmann J, Enders M, Tewald F, Oehme RM, Rosenfeld UM, Ali HS, Schlegel M, Essbauer S, Osterberg A, Jacob J, Reil D, Klempa B, Ulrich RG (2012) Multiple synchronous outbreaks of Puumala virus, Germany, 2010. Emerg Infect Dis 18(9):1461–1464. https://doi.org/10.3201/eid1809.111447
37. Nemirov K, Lundkvist A, Vaheri A, Plyusnin A (2003) Adaptation of Puumala Hantavirus to cell culture is associated with point mutations in the coding region of the L segment and in the noncoding regions of the S segment. J Virol 77(16):8793–8800. https://doi.org/10.1128/jvi.77.16.8793-8800.2003
38. Drexler JF, Corman VM, Muller MA, Lukashev AN, Gmyl A, Coutard B, Adam A, Ritz D, Leijten LM, van Riel D, Kallies R, Klose SM, Gloza-Rausch F, Binger T, Annan A, Adu-Sarkodie Y, Oppong S, Bourgarel M, Rupp D, Hoffmann B, Schlegel M, Kummerer BM, Kruger DH, Schmidt-Chanasit J, Setien AA, Cottontail VM, Hemachudha T, Wacharapluesadee S, Osterrieder K, Bartenschlager R, Matthee S, Beer M, Kuiken T, Reusken C, Leroy EM, Ulrich RG, Drosten C (2013) Evidence for novel hepaciviruses in rodents. PLoS Pathog 9(6):e1003438. https://doi.org/10.1371/journal.ppat.1003438
39. Nainys J, Timinskas A, Schneider J, Ulrich RG, Gedvilaite A (2015) Identification of Two Novel Members of the Tentative Genus Wukipolyomavirus in Wild Rodents. PLoS ONE 10(10):e0140916. https://doi.org/10.1371/journal.pone.0140916
40. Ehlers B, Kuchler J, Yasmum N, Dural G, Voigt S, Schmidt-Chanasit J, Jakel T, Matuschka FR, Richter D, Essbauer S, Hughes DJ, Summers C, Bennett M, Stewart JP, Ulrich RG (2007) Identification of novel rodent herpesviruses, including the first gammaherpesvirus of *Mus musculus*. J Virol 81(15):8091–8100. https://doi.org/10.1128/JVI.00255-07
41. Jeske K, Weber S, Pfaff F, Imholt C, Jacob J, Beer M, Ulrich RG, Hoffmann D (2019) Molecular Detection and Characterization of the First Cowpox Virus Isolate Derived from a Bank Vole. Viruses 11 (11). doi:10.3390/v11111075
42. Fischer S, Mayer-Scholl A, Imholt C, Spierling NG, Heuser E, Schmidt S, Reil D, Rosenfeld UM, Jacob J, Nockler K, Ulrich RG (2018) *Leptospira* genomospecies and sequence type prevalence in small mammal populations in Germany. Vector Borne Zoonotic Dis (Larchmont, NY) 18(4):188–199. https://doi.org/10.1089/vbz.2017.2140
43. Fischer S, Spierling NG, Heuser E, Kling C, Schmidt S, Rosenfeld UM, Reil D, Imholt C, Jacob J, Ulrich RG, Essbauer S (2018) High prevalence of *Rickettsia helvetica* in wild small mammal populations in Germany. Ticks and tick-borne diseases 9(3):500–505. https://doi.org/10.1016/j.ttbdis.2018.01.009
44. Riebold D, Russow K, Schlegel M, Wollny T, Thiel J, Freise J, Huppop O, Eccard JA, Plenge-Bonig A, Loebermann M, Ulrich RG, Klammt S, Mettenleiter TC, Reisinger EC (2020) Occurrence of gastrointestinal parasites in small mammals

from Germany. Vector Borne Zoonotic Dis (Larchmont, NY) 20(2):125–133. https://doi.org/10.1089/vbz.2019.2457
45. Klempa B, Kruger DH, Auste B, Stanko M, Krawczyk A, Nickel KF, Uberla K, Stang A (2009) A novel cardiotropic murine adenovirus representing a distinct species of mastadenoviruses. J Virol 83(11):5749–5759. https://doi.org/10.1128/jvi.02281-08
46. Bignon EA, Albornoz A, Guardado-Calvo P, Rey FA, Tischler ND (2019) Molecular organization and dynamics of the fusion protein Gc at the hantavirus surface. eLife. https://doi.org/10.7554/eLife.46028
47. Howell KA, Brannan JM, Bryan C, McNeal A, Davidson E, Turner HL, Vu H, Shulenin S, He S, Kuehne A, Herbert AS, Qiu X, Doranz BJ, Holtsberg FW, Ward AB, Dye JM, Aman MJ (2017) Cooperativity enables non-neutralizing antibodies to neutralize ebolavirus. Cell Rep 19(2):413–424. https://doi.org/10.1016/j.celrep.2017.03.049

Supplementary Material

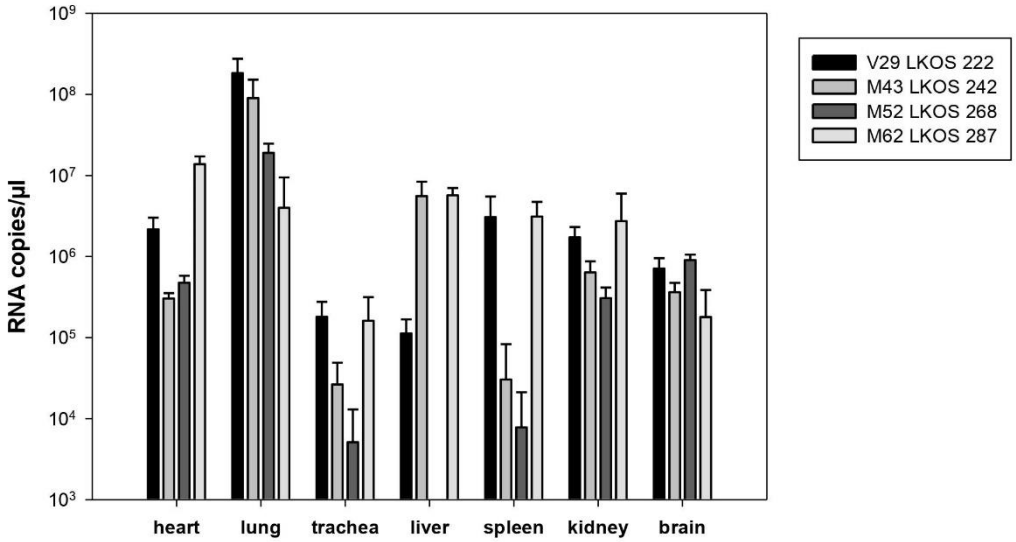

Supplementary Figure S1: Viral RNA load analysis of bank vole tissue. For Puumala virus (PUUV) nucleic acid detection, RNA was extracted from homogenized heart, lung, trachea, liver, spleen, kidney, and brain tissue using QIAzol Lysis Reagent followed by specific quantitative real-time RT-PCR. For quantification of the number of RNA copies/µl and sample, the PUUV S segment sequence of nucleotides 83-355 was *in vitro* transcribed from a plasmid. The transcribed RNA was serially diluted from 10^{-2} to 10^{-11} ng/ml with 700 RNA copies/µl limit of detection (LOD). Viral load as RNA copies/µl was determined in triplicates for organs of the four isolation positive animals.

Supplementary Table S1: Results of the investigations of all bank voles trapped for PUUV isolation (isolates are indicated in bold face).

Cell culture number	Trapping number LKOS	Trapping date	Trapping site	RT-qPCR	lung sample Ct-value	Results of IgG ELISA*	First RT-qPCR positive passage	Cells used for isolation
V1	164	11.04.2019	Schledehausen Forest	positive	20.05	negative		VeroE6
V2	165	11.04.2019	Schledehausen Forest	positive	19.69	doubtful		VeroE6
V3	166	11.04.2019	Schledehausen Forest	positive	25.51	negative		VeroE6
V4	167	11.04.2019	Schledehausen Forest	positive	21.28	positive		VeroE6
V5	168	11.04.2019	Schledehausen Forest	positive	20.07	positive		VeroE6
V6	169	11.04.2019	Schledehausen Forest	positive	22.77	positive		VeroE6
V7	170	11.04.2019	Schledehausen Forest	positive	20.95	positive		VeroE6
V8	171	11.04.2019	Schledehausen Forest	negative	-	negative		VeroE6
V9	172	11.04.2019	Schledehausen Forest	positive	21.21	positive		VeroE6
V10	173	11.04.2019	Schledehausen Forest	positive	19.71	positive		VeroE6
V11	174	11.04.2019	Schledehausen Forest	positive	18.55	doubtful		VeroE6
V12	175	11.04.2019	Schledehausen Forest	positive	18.00	boubtful		VeroE6
V13	190	11.04.2019	Schledehausen Field	positive	22.24	negative		VeroE6
V14	191	11.04.2019	Schledehausen Field	negative	-	negative		VeroE6
V15	192	11.04.2019	Schledehausen Field	negative	-	negative		VeroE6
V16	193	11.04.2019	Schledehausen Field	positive	21.56	negative		VeroE6
V17	194	11.04.2019	Schledehausen Field	negative	-	negative		VeroE6
V18	195	11.04.2019	Schledehausen Field	positive	24.32	positive		VeroE6
V19	196	11.04.2019	Schledehausen Field	negative	-	negative		VeroE6
V20	206	11.04.2019	Ellerbeck	positive	26.77	negative		VeroE6
V21	207	11.04.2019	Ellerbeck	positive	22.53	positive		VeroE6
V22	211	11.04.2019	Astrup I	negative	-	negative		VeroE6
V23	212	11.04.2019	Astrup I	negative	-	negative		VeroE6
V24	213	11.04.2019	Astrup I	positive	23.20	negative		VeroE6
V25	214	11.04.2019	Astrup I	positive	22.41	positive		VeroE6
V26	215	11.04.2019	Astrup I	positive	18.92	positive		VeroE6
V27	220	11.04.2019	Astrup II	positive	16.94	negative		VeroE6
V28	221	11.04.2019	Astrup II	positive	21.97	positive		VeroE6
V29	**222**	**11.04.2019**	**Astrup II**	**positive**	**17.22**	**negative**	**2**	**VeroE6**
V30	223	11.04.2019	Astrup II	negative	-	negative		VeroE6
V31	224	11.04.2019	Astrup II	negative	-	negative		VeroE6
M41	240	12.04.2019	Schledehausen Forest	negative	-	negative		MGN-2-R
M42	241	12.04.2019	Schledehausen Forest	positive	22.20	positive		MGN-2-R
M43	**242**	**12.04.2019**	**Schledehausen Forest**	**positive**	**22.76**	**negative**	**3**	**MGN-2-R**
M44	243	12.04.2019	Schledehausen Forest	positive	17.85	positive		MGN-2-R
M45	244	12.04.2019	Schledehausen Forest	positive	19.10	negative		MGN-2-R
M46	245	12.04.2019	Schledehausen Forest	positive	18.77	positive		MGN-2-R
M47	263	12.04.2019	Schledehausen Field	positive	17.03	doubtful		MGN-2-R
M48	264	12.04.2019	Schledehausen Field	positive	16.74	positive		MGN-2-R
M49	265	12.04.2019	Schledehausen Field	negative	-	negative		MGN-2-R
M50	266	12.04.2019	Schledehausen Field	positive	18.98	positive		MGN-2-R
M51	267	12.04.2019	Schledehausen Field	positive	22.49	negative		MGN-2-R
M52	**268**	**12.04.2019**	**Schledehausen Field**	**positive**	**23.52**	**positive**	**3***	**MGN-2-R**
M53	269	12.04.2019	Schledehausen Field	positive	18.31	negative		MGN-2-R
M54	270	12.04.2019	Schledehausen Field	positive	23.04	positive		MGN-2-R
M55	271	12.04.2019	Schledehausen Field	positive	19.29	positive		MGN-2-R
M56	272	12.04.2019	Schledehausen Field	positive	20.09	negative		MGN-2-R
M57	273	12.04.2019	Schledehausen Field	positive	18.99	positive		MGN-2-R
M58	274	12.04.2019	Schledehausen Field	positive	26.58	negative		MGN-2-R
M59	275	12.04.2019	Schledehausen Field	positive	19.35	positive		MGN-2-R
M60	276	12.04.2019	Schledehausen Field	positive	20.43	positive		MGN-2-R
M61	286	12.04.2019	Ellerbeck	positive	18.81	doubtful		MGN-2-R
M62	**287**	**12.04.2019**	**Ellerbeck**	**positive**	**19.21**	**negative**	**3***	**MGN-2-R**
M63	288	12.04.2019	Ellerbeck	positive	19.72	positive		MGN-2-R
M64	290	12.04.2019	Astrup I	positive	27.58	positive		MGN-2-R
M65	299	12.04.2019	Astrup II	negative	-	negative		MGN-2-R
M66	300	12.04.2019	Astrup II	negative	-	negative		MGN-2-R

Ct, cycle threshold; LKOS, district Osnabrück.

*negative, optical density (OD) < lower cut-off value; positive, OD > upper cut-off value; doubtful: lower cut-off value < OD < upper cut-off value

* PUUV isolates were lost during generation of virus stocks after third passage.

(V) INHIBITION OF THE INTERFERON I INDUCTION BY NON-STRUCTURAL PROTEIN NSs OF PUUMALA AND OTHER VOLE ASSOCIATED ORTHOHANTAVIRUSES: PLASTICITY OF THE PROTEIN AND ROLE OF THE N-TERMINAL REGION

Binder, F., Gallo, G., Bendl, E., Eckerle, I., Ermonval, M., Luttermann, C., Ulrich, R.G.

Archives of Virology

Submitted June 30th 2020

Inhibition of the interferon I induction by non-structural protein NSs of Puumala and other vole associated orthohantaviruses: Plasticity of the protein and role of its N-terminal region

Florian Binder[1], Giulia Gallo[2], Elias Bendl[1,5], Isabella Eckerle[3], Myriam Ermonval[2], Christine Luttermann[4], Rainer G. Ulrich[1*]

[1] Friedrich-Loeffler-Institut, Federal Research Institute for Animal Health, Institute of Novel and Emerging Infectious Diseases, Greifswald - Insel Riems, Germany

[2] Institut Pasteur, Department of Virology, Antiviral Strategies, Paris, France

[3] University of Bonn, Medical Centre, Bonn, Germany; Present address: Geneva Centre for Emerging Viral Diseases, Division of Infectious Diseases, University Hospital of Geneva, Geneva, Switzerland

[4] Friedrich-Loeffler-Institut, Federal Research Institute for Animal Health, Institute of Immunology, Greifswald - Insel Riems, Germany

[5] Current address: University Hospital Freiburg, Institute of Virology, Freiburg, Germany

*Correspondence: rainer.ulrich@fli.de

Abstract

Puumala orthohantavirus (PUUV), transmitted by the bank vole (*Clethrionomys glareolus*), and other vole-borne hantaviruses, contain in their small (S) genome segment two overlapping open reading frames, coding for the nucleocapsid and a non-structural (NSs) protein, a putative type I interferon (IFN-I) antagonist. To investigate the role of NSs of PUUV and other orthohantaviruses, recombinant NSs constructs were investigated for their expression pattern and human IFN-I inhibitory activity. The NSs proteins of PUUV and related orthohantaviruses showed strong inhibition of IFN-I induction, whereas Sin Nombre and Andes orthohantavirus NSs exhibited a lower effect. We identified protein products originating from three methionine initiation codons in the NSs ORF of PUUV during transfection and infection. Translation initiation at these start codons influenced the inhibitory activity of the NSs products, with the wild type (wt) expressing two proteins at the first and second methionine showing the highest inhibition. Analyses of *in vitro* generated variants and naturally occurring PUUV NSs proteins indicated that amino acid variation in the NSs protein is well tolerated, suggesting its phenotypic plasticity, and the importance of its 23 N-terminal amino acids for its inhibitory activity. Infection studies on human, bank vole, and VeroE6 cells did not show differences in the replication capacity between PUUV Sotkamo wt and a truncated NSs (NSs21Stop) strain, showing that the lack of full length NSs is compensated by its N-terminal peptide. Our results contribute to the understanding of virus-host interactions and highlight the importance of future innate immunity studies in reservoir hosts.

Keywords

Orthohantavirus, non-structural protein, type I IFN, reporter assay, bank vole, bunyavirus

Introduction

Rodent-borne orthohantaviruses belong to the family *Hantaviridae* in the order *Bunyavirales* and are distributed all over the world. Infections with pathogenic orthohantaviruses can cause hemorrhagic fever with renal syndrome (HFRS) or hantavirus cardiopulmonary syndrome (HCPS) in humans [1]. In Europe, Puumala orthohantavirus (PUUV) is responsible for most HFRS cases. The bank vole (*Clethrionomys glareolus*, syn. *Myodes glareolus*), which is widely distributed in Europe and parts of Asia, acts as reservoir host of this virus [2]. The small (S) segment of most bunyaviruses encodes, besides the nucleocapsid (N) protein, a non-structural (NSs) protein in an overlapping or antisense open reading frame (ORF) [3]. The NSs ORF of orthohantaviruses is exclusively present in those associated to the Cricetidae rodents family (voles, lemmings, and New World rats/mice) and not in the genome of hantaviruses with other hosts (Figure 1a; [4]). Orthohantavirus NSs protein is expressed from a +1 overlapping ORF in the N protein mRNA via a leaky scanning mechanism, initiated by the first AUG codon following the N protein start codon [5]. PUUV and Tula orthohantavirus (TULV) NSs proteins were suggested to be functional and act as a weak type I interferon (IFN-I) inhibitor in immortalized monkey CV-1 (COS-7) cells [6]; however, detailed information on the particular interference with the signaling cascade leading to IFN-β promoter activation is not available. For TULV and Andes orthohantavirus (ANDV), NSs proteins were reported to accumulate, early during infection, in the cytoplasm and in the perinuclear area where they could interact with factors of the innate immune system [5,7]. Arthropod-borne bunyaviruses like Rift Valley fever phlebovirus (RVFV) and Bunyamwera orthobunyavirus (BUNV) express well-studied NSs proteins as main virulence factors, inhibiting transcription and protein synthesis in host cells [8,9]. For BUNV, La Crosse orthobunyavirus (LACV), RVFV and Toscana phlebovirus (TOSV), the NSs proteins inhibit the IFN-I system by blocking RNA polymerase II transcription or by degradation of dsRNA-dependent protein kinase (PKR) [8,10-14].

Interactions of the host immune system with invading viruses are of outstanding importance for susceptibility, transmission, and outcome of viral infections in host organisms. Viruses invading a host are detected at the host-pathogen interface by the innate immune system early during infection [15,16]. Pattern recognition receptors (PRRs) interact with conserved structural motifs, called pathogen-associated molecular patterns (PAMPs), displayed by infectious agents. PRRs activate factors of the innate immune response such as IFN-I and pro-inflammatory cytokines which impair virus replication and induce long-term immune responses. IFN-I expression is tightly controlled by latent transcription factors, which are activated upon recognition of intruding viruses by cytoplasmic PRRs that sense viral double-stranded RNA such as retinoic acid inducible gene I (RIG-I) or melanoma differentiation antigen 5 (MDA-5). The activating part of RIG-I, the caspase recruitment domain (CARD), initiates signaling through tumor necrosis factor (TNF) receptor associated factor 3 (TRAF3), TRAF-family member-associated NFκB activator binding kinase 1 (TBK-1) and IκB-Kinase ε (IKKε), leading to phosphorylation of transcription factors such as interferon regulatory factor-3 (IRF-3) and subsequent IFN-β synthesis [15]. The synthesized IFN-I induces a crucial host defense mechanism by activating immune cells or effector proteins like myxovirus resistance (Mx) protein [17].

Here we aimed to assess the expression pattern of wild-type and modified hantaviral NSs proteins after transfection and infection. Additionally, we investigated the RIG-I signaling cascade for activation of the IFN-β promoter for different wild-type orthohantavirus-derived NSs proteins and PUUV NSs proteins from wild bank voles of different geographic origin, and investigated the influence of introduced mutations on the expression pattern and activity of PUUV NSs variants. Finally, we investigated the role of NSs for viral growth in human and bank vole cells using cell culture-derived wild-type (wt) and mutant PUUV strain with a stop codon at position 21 (PUUV NSs21Stop). This mutant virus was isolated by plaque purification but had not been characterized before on its replication capacities in IFN-I competent cells [18].

Materials and Methods

SimPlot analysis

NSs sequences of 78 PUUV strains from all PUUV clades obtained from GenBank NCBI (accession numbers: AB010730, AB010731, AB297665, AB433843, AB433845, AB675453, AB675463, AF063892, AF294652, AF367071, AF442613, AJ223369, AJ223371, AJ223374, AJ223375, AJ223380, AJ238790, AJ238791, AJ277030, AJ277031, AJ277033, AJ314598, AJ314599, AJ888751, AM695638, AY526219, AY954722, DQ016432, EU439968, FN377821, GQ339474, GQ339476, GQ339477, GQ339478, GQ339479, GQ339480, GQ339481, GQ339482, GQ339483, GQ339484, GQ339485, GQ339486, GQ339487, GU808824, GU808825, JN657228, JN657229, JN657230, JN657231, JN696358, JN696372, JN696373, JN696374, JN696375, JN831943, JQ319162, JQ319163, JQ319168, JQ319170, JQ319171, KJ994776, KT247592, KT247593, KT247595, KT247596, KT247597, L08804, M32750, U14137, U22423, Z21497, Z30702, Z30704, Z30705, Z46942, Z48586, Z69991, Z84204) were compared on nucleotide and amino acid level with the NSs sequence of the PUUV Sotkamo wt strain (NC_005224.1). For SimPlot analysis with a window size of 9 and a step size of 3 for nucleotide sequence analysis or window size of 3 and step size of 1 for amino acid sequence analysis, scripts were written in R [19].

Viruses and cells

VeroE6 and bank vole renal epithelial cells (MyglaSWRec.B, western evolutionary lineage [20]) were grown in Dulbecco's modified Eagle medium (DMEM) containing 10% fetal calf serum (FCS). Human A549 cells were cultivated in Ham´s F12 medium with 10% FCS in 5% CO_2 at 37°C. Baby Hamster Kidney (BHK-21) and Human Embryonal Kidney (HEK 293-T) cells were grown in modified Eagle´s medium supplemented with 10% FCS. PUUV wt strain Sotkamo or a cell culture-derived PUUV Sotkamo variant (PUUV NSs21Stop) with a stop

codon mutation at position W21 in the NSs ORF [18] were used for infection studies at a multiplicity of infection (MOI) of 0.5.

Generation of polyclonal anti-NSs serum

For generation of a rabbit polyclonal antiserum the NSs-ORF nucleotide sequence of PUUV strain Sotkamo was genetically fused between a 5'-6x his tag-coding sequence and the coding sequence for the bacterial lumazine-synthase (LS) at the 3' end, a protein previously described as efficient carrier for generation of highly-titered antisera [21]. The 6xHis-NSs-LS complex was expressed in *Escherichia coli* and purified via Ni-NTA agarose (Thermo Fisher). Two rabbits were immunized and boostered 2 times every 4 weeks until sera were collected 3 months after initial immunization.

Plasmids

RNA was extracted from PUUV strain Sotkamo wt infected cell culture or lung tissue of PUUV infected bank voles from Baden-Wuerttemberg (BW), south-west Germany, North Rhine-Westphalia (NW) and Osnabrück (OS) region, Lower Saxony, both in north-west Germany, using QIAzol Lysis Reagent (Qiagen). Afterwards the NSs-ORF of wt PUUV Sotkamo (HE801633.1) and the field strains from BW, NW and OS region (for details, see Supplementary Tables 1 and 2) were amplified via conventional RT-PCR (Superscript III RT-PCR Kit, Thermo Fisher) with the primers 40f (5'-CTGGAATGAGTGACTTAAC-3') and 393r (5'-CTCCAATTGTATACCAATCT-3') and then cloned into a pCR2.1-TOPO plasmid using a TOPO TA cloning kit (Thermo Fisher). Restriction sites (underlined) were added to the NSs-ORF by PCR using the primers NSs BamHI fwd (5' CAGGAGGATATAAGGATCCATGAACAGCAACTTA 3') and NSs EcoRI rev (5' CCTCTATGTCAATGGGAATTCCATCAAGG 3'). The N-ORF was amplified using the same PUUV Sotkamo RNA preparation, but using primers Sot N BamHI fwd (5'

GATCCTGGATCCATGAGTGACTTGACAG-3') and Sot N EcoRI rev (5' GTCATATGAATTCTATCTTTAGTGGTTCCTG-3'). After restriction digest of the RT-PCR products, the NSs-ORFs were inserted into pcDNA3 (Invitrogen) containing the coding sequence for a C-terminal hemagglutinin (HA)-tag at the 3' end. NSs-ORFs of TULV (AF164093.1), ANDV (NC_003466.1), Sin Nombre orthohantavirus (SNV, KF537003.1), Prospect Hill orthohantavirus (PHV, M34011.1), and Khabarovsk orthohantavirus (KHAV, NC_034527.1) were obtained as synthetic genes (Eurofins Genomics) and inserted into pcDNA3-HA in the same way as described above.

For reporter assays the following plasmids were used: p125-FFluc containing the human IFN-β promoter and firefly luciferase coding sequence; pcDNA3-RIG I, for activation of the human IFN-β signaling pathway; pRluc coding the renilla luciferase under control of a human cytomegalovirus (HCMV) immediate early (IE) promoter for monitoring the transfection efficiency; pcDNA3 as a vector control and Rabies virus (RABV) phospho (P)-protein encoding positive control plasmid pCR3-P [22].

Mutagenesis

Plasmids coding for PUUV wt NSs protein were further modified using quick change site directed mutagenesis using Phusion high fidelity polymerase (Thermo Fisher). Stop codons were introduced at codon positions 2 and 14 in the NSs ORF. To evaluate the functionality of alternative putative translation initiation codons, the methionine codons 1, 14, 24 were substituted each alone or in combination (1+14, 14+24, 1+14+24, Figure 1a). Residues or regions of interest in the PUUV OS strain KS19/16 NSs plasmid were substituted by alanine codons for evaluation of the plasticity of the NSs protein at codon positions 2-4 (NNN2-4$(A)_3$), 11 (S11A), 16-19 (RRQW16-19$(A)_4$), 21-23 (WTQ21-23$(A)_3$), 25-28 (TLTR25-28$(A)_4$), 31 (C31A), 38 (C38A), 49 (S49A), and 56 (C56A). Primer sequences are available upon request.

Luciferase assays

For transfection of HEK 293-T cells in 6-well plates, a plasmid DNA mix of 0.5µg p125-FFluc, 0.005µg pRluc, 0.5µg pcDNA3-huRIG-I, and 1µg pcDNA3-HA plasmid containing one of the NSs coding sequences was generated in 300µl Opti-MEM. The resulting plasmid DNA mix and 4µl Lipofectamine 2000 transfection reagent (Thermo Fisher) in 300µl Opti-MEM were mixed, incubated for 20min at RT and applied to the cells. After 3h the transfection mix was substituted by 1ml MEM + 10% FCS. Eighteen hours later cell extracts were prepared and luciferase activities were measured using the Dual-Luciferase Reporter Assay System (Promega) according to manufacturer's instructions. Luciferase activities were measured from technical triplicate samples with a TriStar² LB 942 Modular Multimode Microplate Reader (Berthold). Alternatively cells were harvested in 400µl 2x SDS-PAGE sample buffer (0.5M Tris pH 6.8, 25% glycerin, 10% SDS and 0.5% bromophenol blue) and subjected to Western blot analysis using an anti-HA rabbit monoclonal antibody (ab20084, Abcam) and a horse radish peroxidase (HRP) coupled anti-rabbit IgG as secondary antibody (Bio-Rad).

Immunofluorescence analysis

VeroE6 cells were transfected with 2µg of the PUUV NSs protein derivatives encoding pcDNA3-HA plasmid DNAs using Lipofectamine 3000 (Thermo Fisher). For transfection, $2x10^5$ cells were seeded simultaneously with transfection mix in a 6-well plate. 48h after transfection, cells were fixed with 4% paraformaldehyde and stained for immunofluorescence analysis using an anti-HA specific mouse monoclonal antibody (HA-probe antibody (F-7): sc-7392, Santa Cruz Biotechnologies) and an Alexa fluor 488 labelled anti-mouse secondary antibody (Abcam). Nuclei were stained with 4′,6-Diamidin-2-phenylindol (DAPI). For confocal microscopy cells were seeded on glass cover slips which were mounted with Ibidi mounting medium (Ibidi).

Infection experiments

For Western blot analysis, VeroE6, A549, and MyglaSWRec.B cells were inoculated in a 6-well plate with either PUUV wt or the NSs21Stop strain at MOI 0.5 for 1h at 37°C in 0.3ml medium containing 5% FCS. After adsorption, 1ml DMEM with 5% FCS was added and cells were incubated at 37°C for up to 8 days. Cells were harvested at several time points, lysed in 2x SDS-PAGE sample buffer and subjected to Western blot analysis with N-protein specific mouse monoclonal antibody A1C5 (1:500, Promega). A polyclonal rabbit anti-NSs serum (1:50 in PBS-Tween 0.05%) was used for detection of the NSs protein in VeroE6 cells. Primary antibodies were incubated over night at 4°C under constant rotation. HRP-labelled goat anti-mouse/anti-rabbit IgG (Bio-Rad) diluted 1:3000 in PBS-Tween 0.05% were used as secondary antibodies for final detection with a ChemiDoc imaging system (Bio-Rad) using development times of 30 min (NSs) or 10 sec (N).

For virus growth kinetics $5x10^5$ cells were seeded in a $25cm^2$ flask the day before inoculation. Cells were incubated with PUUV Sotkamo or its NSs21Stop variant at MOI 0.1 for 1h at 37°C. Thereafter, 6.5ml medium was added and cells were kept at 37°C. Supernatant was collected at days 2, 5, and 7 post inoculation (p.i). For titration, supernatants of the three cell lines were serially diluted from 10^{-1} to 10^{-7} in DMEM containing 5% FCS in a 96-well plate with three replicates each and processed as described recently [23]. Titers of supernatants of the three cell lines were depicted as the 50% tissue culture infectious dose ($TCID_{50}$)/ml.

Results

Expression analysis of hantaviral wild-type NSs-ORFs and inhibition of the IFN-β promoter-signaling pathway in human HEK 293-T cells

The S segment of vole-associated orthohantaviruses encodes a conserved N-overlapping NSs ORF with three conserved in-frame AUG codons (M1, M14 and M24, shown in yellow in Figure 1a and b). However, only two of these initiation codons are present in PHV NSs ORF

(M1 and M24) and in the shorter NSs ORFs of SNV and ANDV (M14 and M24), having their first initiating codon at position M14 (PUUV reference). Of note, the sequence of KHAV NSs is longer with the first AUG located five codons ahead of M1 (PUUV reference). In contrast, hantaviruses specific for another rodent family (Muridae), or other non-rodent mammals (orders Chiroptera and Eulipotyphla), do not exhibit the coding capacity for an NSs protein due to lacking translation start codons and to multiple stop codons (Figure 1a).

Transfection of HEK 293-T cells with expression plasmids encoding C-terminally HA-tagged NSs proteins from PUUV, TULV, PHV, SNV, ANDV, and KHAV resulted in the detection of one to three protein products (Figure 2a). All bands in the Western blot assay were detected *via* the C-terminal HA tag that allows the detection of protein variants that originate from one of the AUG codons in the 5´-NSs coding sequence (Figure 1a, Supplementary Table 1, panel I). NSs proteins of PUUV and PHV gave two distinct bands. The upper band with a molecular mass around 12kDa derived from the first 5´ start codon (M1) and the lower band with a predicted molecular mass around 10.5kDa for PUUV and 9kDa for PHV derived from the next downstream AUG codons (M14 and M24, respectively; Figure 2a and 1a). KHAV and TULV constructs express three proteins probably due to translation initiation at each of the three AUG codons within the first 24 codons of their NSs-encoding sequence (Figure 2a and 1a). As expected, the upper band of KHAV migrated slower than the ones of the other viruses due to a longer full-length NSs (expected molecular mass 12.4kDa, see Supplementary Table 1). Remarkably, for PUUV a NSs protein corresponding to translation initiation at codon M24 is not expressed or detectable in contrast to the NSs expression pattern for KHAV and TULV. The predicted and observed full-length NSs proteins of SNV and ANDV, with an expected molecular mass around 9kDa, are shorter than the ones of vole-associated hantaviruses investigated here (Figure 1a; Supplementary Table 1, panel I); at least ANDV NSs protein translation seems to be initiated not only at a start codon corresponding to M14 of vole-borne hantavirus NSs, but a second start codon corresponding to M24 is also used in its sequence (Figure 2a and 1a). Of note, TULV NSs protein is more

prominently expressed or more stable than the other NSs proteins, with NSs of PUUV, SNV and ANDV being the weekly expressed proteins.

To investigate the influence of orthohantaviral NSs proteins on the IFN-β promoter driven induction of IFN-I we used a dual luciferase reporter assay with RABV-P protein as positive control for inhibition of IFN-I induction. When HEK 293-T cells were transfected with the luciferase reporter constructs and the RIG-I activator plasmid, almost all of the co-transfected orthohantaviral NSs-encoding plasmids led to an efficient reduction of the IFN-β promoter activation (Figure 2b). NSs proteins of PUUV, TULV and PHV strongly inhibited the IFN pathway with respectively 30%, 18% and 20% of the IFN-β promoter activity left as compared to 100% activation observed without a viral NSs protein (vector control). PUUV, TULV and PHV NSs proteins are therefore potent inhibitors of this pathway. KHAV NSs protein reduced the activity to about 40%, whereas NSs proteins of SNV and ANDV reduced it to 80% of the IFN-β promoter activity induced by RIG-I (Figure 2b).

Bank vole PUUV field strain-derived NSs proteins from two endemic regions in Germany exhibit a prominent protein expression and interferon antagonist activity

The conservation of the PUUV NSs ORF concerning its position within the S segment and the length of 90 amino acid codons is contrasted by the high amino acid sequence divergence of PUUV strains from different endemic regions in Germany (Figure 3a). Therefore, we aimed to evaluate the potential consequences of naturally occurring amino acid substitutions within the putative NSs proteins of PUUV strains from bank voles collected in 2007, 2010, 2012, and 2014 at seven trapping sites in BW, south-west Germany and one site in NW, north-west Germany (Supplementary Table 2). Sequences from the seven different trapping sites in BW had only few amino acid substitutions (Figure 3a, numbers 2-6 and 11-16). In contrast, the sequences from NW showed an amino acid sequence divergence of 16.8-24.5% to the BW sequences (Figure 3a, 7-10). Expression of the two major NSs variants with translation initiation at M1 and M14 was shown for all constructs

(Figure 3b). As expected, the NSs proteins from PUUV strains in NW showed an increased molecular weight, compared to the PUUV sequences from BW (Figure 3b, NW: lanes 7-10, BW: lanes 2-6 and 11-16; Supplementary Table 1, panel II). All NSs proteins from the different trapping regions showed inhibition of RIG-I-induced IFN-I promoter activation similar to the levels observed for PUUV Sotkamo wt NSs (Figure 3b, lanes 2-16). There was no obvious correlation of a specific amino acid exchange and increased or reduced IFN-I inhibition observed.

N-terminally truncated NSs variants of PUUV show reduced inhibitory effects

For further characterization of the PUUV NSs protein and the importance of the leaky scanning in generating NSs variants, eight mutants of the PUUV Sotkamo wt NSs sequence were generated by introduction of stop codons or by alanine codon substitution of methionine codons as well as combinations of these mutations (Figure 4a, Supplementary Table 1, panel III). Mutants were analyzed for their expression patterns by Western blot assay and for their inhibitory function in a RIG-I activated IFN-β luciferase reporter assay in HEK 293-T cells. Expression of the HA tagged protein variants was in addition confirmed after transfection of VeroE6 cells by immunofluorescence assay (Supplementary Figure 1). When a stop codon was introduced at codon position 2 (NSs2Stop; Figure 4a), no protein could be detected and the inhibitory effect of the PUUV NSs was strongly abrogated (Figure 4c, lane 3 and Supplementary Figure 1). This indicated, that the NSs protein, and not the RNA, was responsible for the inhibitory effects on the IFN-I induction as the mRNA should be transcribed in the same way for both constructs (NSs wt and NSs2Stop). The NSs14Stop variant expressed a protein of around 8.9kDa translated from the third start codon at position 24. This shortened NSs protein also showed almost no inhibitory activity in the reporter assay (Figure 4c, lane 4). Thus, the first 23 amino acids of the PUUV NSs protein appeared to be important for the inhibitory function on IFN-I induction. Similarly to what was seen by Western blot analysis, a weak signal of immunofluorescence staining was obtained with the

NSs14Stop-derived protein as compared to the wt NSs protein (Supplementary Figure 1). A reduced immunofluorescence and Western blot signal was also observed for the M1A M14A double mutant lacking the first two start codons and therefore expressing the same NSs protein variant of 8.9kDa starting at codon 24 like mutant NSs14Stop (Figure 4c, lane 8, Supplementary Figure 1). The double mutant M1AM14A showed almost no inhibition of the IFN-β promoter activity (Figure 4c, lane 8), like it is the case for the NSs14Stop construct (lane 4).

Substitution of the first methionine start codon by alanine codon (M1A) in the NSs sequence of PUUV, resulted in the expression of only one protein variant corresponding to the shorter NSs of the two distinct bands found with wt NSs (Figure 4c, lane 5). This pattern is most likely due to translation initiation at the M14 AUG codon. This comes along with a highly reduced inhibitory effect on the IFN-β promoter induction (Figure 4c) confirming the importance of the N-terminal region of NSs protein for its function in blocking IFN-I signaling. When the second putative start codon (M14A) was substituted, the full-length NSs was expressed together with a smaller band (8.9kDa) of weaker intensity (Figure 4c, lane 6), also observed for the NSs14Stop mutant (Figure 4c, lane 4), but not with the wt NSs (Figure 4c, lane 2). This smaller NSs variant probably arises from a translation initiation at codon M24. Only a slight inhibition of IFN-I promoter induction was observed with this mutant M14A protein as compared to the wt NSs protein. Alanine codon substitution of the third AUG (M24A) resulted in detection of the full-length NSs band together with the 10.3kDa band representing the same expression pattern as the wt NSs ORF (Figure 4c, compare lane 7 with lane 2). This mutation resulted in high inhibition comparable to the wt NSs as expected from the expression pattern. However, NSs proteins with combinations of these alanine/start codon substitutions had no inhibitory effect in the luciferase reporter assay (Figure 4c, lanes 9-10). The double mutant M14A M24A, although expressing the expected single band of full-length PUUV NSs protein, induced only a background reduction of the IFN-β promoter activity. Therefore, these two substitutions within the first 24 amino acids had a severe impact on the inhibitory function of NSs. In the case of the triple mutant M1A M14A M24A, no

protein could be detected (Figure 4b, lane 10) and, as expected, only background influence on IFN-I signaling could be observed. The N protein was for comparison also expressed in HEK 293-T cells and showed upregulation of the IFN-I response pathway (Figure 4c, lane 11).

Mutational analysis of NSs proteins from PUUV field strains from the region Osnabrück confirmed the phenotypic plasticity of the NSs protein

For identification of important amino acid residues or motifs in PUUV NSs protein responsible for its IFN-I inhibitory function, we substituted amino acid residues in conserved regions (Figure 4b) within NSs protein of PUUV OS strain KS19/16 by alanine. This field strain NSs sequence (Figure 4d, lane 2) as well as another field strain PUUV OS KS17/1084 (Figure 4d, lane 12) showed similar IFN-I inhibition levels as the laboratory-adapted PUUV Sotkamo wt-derived NSs sequence (Figure 4d, lane 2 and Figure 2b). We targeted serine S11A and S49A, as they constitute potential phosphorylation sites, cysteine residues C31A, C38A, C56A for the formation of disulfide bonds or catalytic functions and larger hydrophobic regions of interest RRQW16-19$(A)_4$ and TLTR25-28$(A)_4$ by site directed mutagenesis (Figure 4b). All alanine replacement variants showed a clear inhibition of the IFN-β promoter activity. Only N-terminal amino acid exchanges NNN2-4$(A)_3$ (Figure 4d, lane 3) and WTQ21-23$(A)_3$ (lane 6) showed a slightly reduced IFN-I inhibition capacity in comparison to the parental KS19/16 wt NSs protein (Figure 4d, lane 2). The Western blot analysis showed that all NSs-HA constructs were well expressed in the transfected HEK 293-T cells and they produced double bands about one kDa apart from each other (Figure 4d), corresponding to the two bands seen with the wt NSs protein of PUUV Sotkamo strain thought to initiate at M1 and M14 start codons (Supplementary Table 1, panel IV). However, the amount of NSs-HA tagged proteins appeared to be different for all variants. The NSs proteins of wt KS19/16 and variants S11A and S49A were expressed at higher levels, whereas TLTR25-28$(A)_4$, C38A and NNN2-4$(A)_3$ NSs proteins were less prominent (Figure 4d, lanes 3,7 and 9). There was

no obvious correlation between the amount of NSs proteins present in the assay and the level of their inhibitory effect on IFN-I promoter induction. Thus, an influence on NSs inhibitory function can be observed for the tested mutants but no essential residue or motif could be determined, indicating a high phenotypic plasticity of the NSs protein.

Replication of PUUV in different cell lines is not affected by NSs protein variants

First, we analyzed NSs expression of PUUV Sotkamo in *in vitro* infected cells using a rabbit anti-PUUV NSs serum. The PUUV NSs protein could be detected from day 2 to day 8 p.i. in VeroE6 cells infected at MOI 0.1 (Figure 5a, left panel). Interestingly, two bands could be detected by Western blot analysis suggesting that the first two AUG codons (Figure 1a and 5a, left panel) in the NSs ORF are used as alternative starting points for leaky scanning translation of the NSs protein. When we used the PUUV Sotkamo NSs variant virus (PUUV NSs21Stop) [18] no specific protein was detected using the anti-NSs serum (Figure 5a, right panel).

To evaluate the influence of the NSs protein on viral replication during infection, we infected three different cell lines with wt PUUV Sotkamo and the PUUV Sotkamo strain with a truncated NSs (NSs21Stop). VeroE6 cells (African green monkey kidney cells), an IFN-I deficient reference cell line, human A549 cells and bank vole renal epithelial cells (MyglaSWRec.B) were simultaneously infected at MOI 0.5 and assessed for their expression of N protein and titer production as evidence of PUUV replication. In all three cell lines no obvious differences were seen by Western blot analysis in the level of N expression between the two virus isolates. However, VeroE6 and MyglaSWRec.B cells showed high expression levels of PUUV N on days 5 and 7 p.i., whereas in A549 cells a significantly lower amount was observed for both viruses at all time points (Figure 5b). A similar observation was made for the virus titers obtained from the supernatants of all three cell lines (Figure 5c). The amount of virus in the supernatant increased from day 2 to day 7 in VeroE6 and MyglaSWRec.B cells from 10^3 to 10^5 $TCID_{50}$/ml without differences for the wt and the mutant

PUUV strain. A549 cells showed only weak increase in viral titers, which is in line with the observations from Western blot analysis (Figure 5b and c). The similar level of replication of both PUUV strains in all three cell lines shows that the truncated NSs might have a similar activity as the full-length NSs in the viral context. The reduced replication of both strains in A549 cells might be explained by a general reduced growth in the IFN-I competent cells compared to reservoir-derived MyglaSWRec.B cells and IFN-I defective VeroE6 cells. The high replication rate in bank vole cells might be related to reservoir host-related factors supporting virus replication.

Discussion

Our transfection studies indicated the synthesis of different NSs protein variants of various cricetid-borne orthohantaviruses that can be explained by translation initiation at multiple start codons, M1, M14 or M24 by a leaky scanning mechanism. This mechanism of NSs translation initiation was shown for ANDV on RNA level, however without detection of different NSs protein variants [5]. This finding obtained from expression plasmid based transfection studies was confirmed to occur as well during infection with PUUV strain Sotkamo as two NSs protein bands were detected by a newly generated anti-NSs serum in the lysates of PUUV wt infected cells. Mutational analysis of the potential start codons in the transfection system gave additional proof for the use of different NSs initiation codons. Alanine substitution at the first start codon resulted in only one NSs variant starting at position M14 whereas the wt showed two proteins starting at M1 and M14. Therefore, in these two cases (wt and M1A) no translation initiation by leaky scanning occurred at the third start codon (M24). However, initiation at codon 24 was observed for the NSs variants M14A, M1A M14A and NSs14Stop probably because of the deletion of the AUG at position 14 which is located in a favorable Kozak sequence context, so that translational scanning probably continues to the next AUG at position 24.

The lacking activity of the full-length NSs protein alone (construct M14A M24A) raises the question whether two (or three) NSs protein variants are needed for a fine-tuned downregulation of IFN-I production mediated by their interaction (NSs amino acid residues 1-90 and 14-90) or an alternative influence of smaller NSs ORF products. This conclusion is supported by the observation that mutants where two of the three AUG codons are mutated did not show any inhibitory function in our luciferase system. The almost complete loss of IFN-I inhibitory function, when NSs protein translation of any NSs protein product seems to be blocked, by a stop codon at position two, indicates that the protein itself is causing the inhibitory effects on IFN-I induction as the encoding mRNAs of all constructs are almost the same, except for the few introduced single nucleotide exchanges. The block of translation through insertion of a stop codon directly downstream of the first start codon is obviously leading to prevention of scanning beyond this site to the next start codon or the amount of protein expressed is too low to be detected.

Both, performing Western blot and IFN-promoter driven luciferase reporter analyses showed that NSs ORFs from 17 bank vole field strains from three endemic regions in Germany behave similar to the NSs ORF from the cell culture-adapted PUUV wt strain. Additional amino acid exchanges introduced into the PUUV NSs protein of a bank vole field strain did not interfere strongly with protein function. Furthermore, the substitution of potentially functional amino acid residues, such as cysteine or serine, did not have a clear effect on the inhibitory function of the NSs protein. Only the exchange of three or four amino acid residues in a row showed slightly reduced NSs activity for a few mutants. This result as well as the functional activity of the different wt NSs proteins suggest a high phenotypic plasticity of the NSs protein tolerating the exchange of amino acid residues.

PUUV and TULV NSs proteins have already been shown to be expressed also during infection and to inhibit NF-κB and IRF 3 responsive promoters after poly(I:C) stimulation [6]. A recent study also showed that ANDV NSs protein antagonizes the IFN-I response by inhibiting IFN-I signaling downstream of RIG-I and MDA-5 but upstream of TBK-1 [24]. We

expressed hantaviral NSs ORFs from PUUV, TULV, PHV, KHAV, SNV, and ANDV and they all inhibited IFN-I induction to a certain extent. Otarola et al. showed antagonistic effects on IFN-I induction of ANDV NSs that reduced IFN-I signaling to about 50%, whereas in our expression system, ANDV NSs was only weakly expressed and still allowed around 80% IFN-I promoter activity [24]. This can be explained by the use of different expression constructs, as we used a C-terminal HA tag and not an N-terminally tagged NSs protein, which could be more stable. The different transfection setups in general can also cause these differences in inhibition potency. However, in our experiments comparison to other NSs constructs, all with C-terminal HA-tag, still showed a higher potency of IFN-I inhibition by NSs proteins of PUUV, TULV, PHV and KHAV in comparison to ANDV (and related SNV). The expression patterns of the NSs proteins of the different virus strains used here were in line with the multiple internal start codons for each viral NSs, suggesting a selection pressure for the conservation of multiple start codons within the NSs ORF of various orthohantaviruses.

The N-terminal region of NSs protein appeared to have a prominent effect on the IFN-β promoter activity. The smallest (10kDa) variant of PUUV NSs, expressed by the M1A M14A double mutant or the NSs14Stop construct, has no effect on IFN-I induction. This points to a role of the first 23 amino acids of NSs in the inhibition of IFN-I induction. Similarly, for NSs of BUNV N-terminally truncated variants were still able to interact with Med8, a factor involved in regulating the activity of cellular RNA polymerase II, but failed to degrade cellular RNA polymerase II and thereby block IFN transcription [25]. In line with these findings PUUV NSs protein missing the N-terminus did not efficiently block IFN-I promoter induction. This reinforces our finding concerning the importance of the first 23 amino acids of the PUUV NSs protein for its IFN-antagonism. In line with these findings from transfection experiments, the NSs21Stop variant of PUUV strain Sotkamo replicates in different cell lines to the same extent as the wt counterpart of this PUUV strain. Most likely, the N-terminal 20 amino acid residues of PUUV NSs protein are sufficient for inhibition of IFN-I induction in human cells. However, since we cannot detect this short peptide or the NSs protein variant initiating at

codon M24 in cells after PUUV infection with the truncated NSs21Stop virus, we cannot exclude that other viral proteins partly contribute to this process in the viral context.

In conclusion, the NSs ORF of cricetid-borne hantaviruses is expressed as different variants via leaky scanning and the expressed NSs proteins inhibit the IFN-I promoter activity. The NSs protein of PUUV demonstrated a high phenotypic plasticity as shown by activity of natural NSs proteins of highly divergent amino acid sequence and *in vitro* modified NSs variants. The N-terminal part seems to be important for the function of PUUV NSs protein. The manipulation of the potential translation initiation sites has a much stronger influence on NSs activity. The assumption that different NSs ORF products could interact for precise function remains speculative and needs to be further investigated. Future investigations should confirm the results with other pathogenic and low or non-pathogenic hantaviruses, identify essential targets for NSs function and prove the potential interaction of different NSs translation products. A virus-reservoir cell system would be of substantial interest to understand the influence of hantaviruses on the immune system of their reservoir hosts.

Declarations

Funding

The investigations were supported in part by the Bundesministerium für Bildung und Forschung within the Research Network Zoonotic Infectious Diseases (RoBoPub consortium, FKZ 01KI1721A granted to RGU). Florian Binder acknowledges intramural funding from the Friedrich-Loeffler-Institut within project HR-0012. The collection of bank voles at sites Weissach and Billerbeck have been performed in a previous study [26] that was commissioned and funded by the Federal Environment Agency (UBA) within the Environment Research Plan of the German Federal Ministry for the Environment, Nature Conservation and Nuclear Safety (BMU) (grant number 3709 41 401 and grant number 3713 48 401).

Conflicts of Interest

Not applicable.

Author Contributions

Conceptualization, Florian Binder, Myriam Ermonval, Christine Luttermann and Rainer G. Ulrich; Funding acquisition, Christine Luttermann and Rainer G. Ulrich; Investigation, Florian Binder, Giulia Gallo, Elias Bendl; Methodology, Florian Binder, Isabella Eckerle and Christine Luttermann; Project administration, Christine Luttermann and Rainer G. Ulrich; Resources, Isabella Eckerle; Supervision, Myriam Ermonval; Validation, Florian Binder, Giulia Gallo and Elias Bendl; Visualization, Florian Binder; Writing – original draft, Florian Binder, Christine Luttermann and Rainer G. Ulrich; Writing – review & editing, Florian Binder, Giulia Gallo, Isabella Eckerle, Myriam Ermonval, Christine Luttermann and Rainer G. Ulrich.

Acknowledgments

The plasmids p125-FFluc, pcDNA3-huRIG I, and pRluc were kindly provided by Karl-Klaus Conzelmann (Gene Center - Max von Pettenkofer-Institute of Virology, Ludwig-Maximilians-University Munich). Andreas Rang (Institute for Virology, Charité, Berlin) is kindly acknowledged for providing the PUUV strains. The authors acknowledge Andrea Aebischer, Sven Reiche and Bärbel Hammerschmidt for their help with generating recombinant NSs proteins and rabbit anti-NSs serum. Many thanks to Kristin Trippler, Gabriele Stooß and Sven Sander for excellent technical support and René Ryll for calculations of SimPlots in figure 1.

Captions

Figure 1: Sequence comparison of putative hantavirus NSs proteins and the coding regions (**a**), and SimPlot analysis of NSs nucleotide and amino acid sequences of 78 PUUV strains from all clades compared to the PUUV Sotkamo wt strain (**b**). (**a**) Sequence alignment of the putative NSs protein encoded by different hantavirus S segments associated to Cricetidae, and for comparison the corresponding region of hantaviruses in Muridae, Chiroptera, and Eulipotyphla hosts. Conserved methionine (start) codons are shown in yellow, most divergent protein regions are highlighted in grey and stop codons are indicated by a dot (●). The accession numbers are indicated on the left of the NSs sequences of the different species (and strains) of orthohantaviruses used for the analysis and which are as follow: PUUV = Puumala virus (strain Sotkamo), TULV = Tula virus (strain g20-s), PHV = Prospect Hill virus, TRAV = Traemmersee virus, KHAV = Khabarovsk virus (strain Fuyuan), SNV = Sin Nombre virus (strain 77734), ANDV = Andes virus (strain Chile-9717869), DOBV = Dobrava-Belgrade virus (genotype Dobrava 3970/87), HTNV = Hantaan virus (strain CUMC-B11), SEOV = Seoul virus (strain SEOV/NL/Rn2147/2016), BRNV = Brno virus (strain 7/2012/CZE), ASIV = Asikkala virus (strain Asikkala), BRGV = Bruges virus (strain DE/Wandlitz/TE/2013/1) , SWSV = Seewis virus (strain EWS25). Of note, the shown region in non-cricetid associated hantaviruses did not contain a start codon and contain multiple stop codons within the region corresponding to the NSs ORF in cricetid-borne hantaviruses. (**b**) SimPlot analysis of NSs nucleotide and amino acid sequences of 78 PUUV sequences from all clades obtained from GenBank with PUUV Sotkamo wt strain (NC_005224.1) as query. For SimPlot analysis with a window size of 9 nucleotides (nt)/3 amino acids (aa) and a step size of 3 nt/1 aa, scripts were written in R [24]. The three putative start (methionine) codons of PUUV NSs are depicted in yellow at the corresponding peak of the highest sequence conservation and most divergent amino acid regions are shown in grey.

Figure 2: Western blot analysis of expression of the different HA-tagged NSs proteins of hantaviruses in transfected HEK 293-T cells (**a**) and corresponding results of RIG-I activated interferon-β promoter assay (**b**). (**a**) The different NSs proteins were detected with an anti-HA antibody reacting with their C-terminal HA-tag and the protein loading in the cell lysates was controlled using an anti-actin antibody (1:1000). (**b**) HEK 293-T cells were transfected with a plasmid DNA mix of 0.5µg p125-FFluc, 0.005µg pRluc, 0.5µg pcDNA3-huRIG I and 1µg pcDNA3-HA plasmid containing one of the different viral NSs coding sequences. Calculation of % values was done with luciferase luminescence values in reference to the vector control (Firefly (FF)/Renilla (RI) value; vector control=100% activation; vector control without activation=basal level). RABV-P = Rabies virus phosphoprotein, PUUV = Puumala orthohantavirus, TULV = Tula orthohantavirus, PHV = Prospect Hill orthohantavirus, SNV = Sin Nombre orthohantavirus, ANDV = Andes orthohantavirus, KHAV = Khabarovsk orthohantavirus.

Figure 3: Amino acid sequence comparison of putative NSs proteins of PUUV strains from Baden-Wuerttemberg (BW) and North Rhine-Westphalia (NW) (**a**), their influence on interferon-β promoter activity and protein expression after RIG-I activation (**b**). (**a**) Amino acid sequences of PUUV NSs constructs shown with HA tag (see also Supplementary Table 2); (●), stop codon. (**b**) Western blot analysis of the expression of the different PUUV NSs constructs and their effect on inhibition of the human IFN-β promoter activity. NSs derivatives are expressed from 1µg of plasmids transfected into HEK 293-T cells and the effect of different NSs constructs was measured in the luciferase reporter assay after IFN-β promoter activation by RIG-I. Inhibition of the human IFN-β promoter activity induced by RIG-I was measured in HEK 293-T cells 18 h post transfection with the plasmid DNA mix for the dual luciferase reporter assay and 1µg pcDNA3-HA plasmid containing the viral NSs variants. Expression of NSs proteins in cell lysates of the transfected cells was tested in Western blot assay using an anti-HA rabbit monoclonal antibody and an anti-rabbit HRP coupled

secondary antibody. An anti-actin antibody was used as a loading control. Rabies virus phosphoprotein (RABV-P) was used as a positive control of inhibition.

Figure 4: Influence of mutations in the Puumala orthohantavirus (PUUV) NSs ORF on interferon-β promoter activity and protein expression after RIG-I activation. (**a**) Amino acid sequences of PUUV Sotkamo NSs constructs shown with HA tag. Conserved putative start (methionine) codons are highlighted in yellow. Detected protein variants are shown in grey from the first potential start codon in the different constructs with stop codon (●) or alanine substitution of the different methionine residues M1, M14, M24. (**b**) Amino acid exchanges introduced at particular putative functional residues in NSs of PUUV OS strain KS19/16 such as cysteine, serine and hydrophobic regions, highlighted respectively in blue, red and green. (**c**) Western blot analysis of the expression of the different PUUV NSs constructs from (a) and their effect on inhibition of the human IFN-β promoter activity. NSs derivatives are expressed from 1µg of plasmids transfected into HEK 293-T cells and the effect of alternative start codon usage of NSs constructs was measured in the luciferase reporter assay after RIG-I-mediated IFN-β activation by the same plasmid mix as in Figure 2b. (**d**) Influence of alanine codon mutagenesis in NSs protein was studied for PUUV Osnabrück (PUUV OS) strain KS19/16 (see panel b). Inhibition of the RIG-I-induced human IFN-β promoter activity was measured in HEK 293-T cells 18 h post transfection with the plasmid DNA mix for the dual luciferase reporter assay and 1µg pcDNA3-HA plasmid containing one of the viral NSs coding sequences. Expression of NSs proteins in cell lysates of the transfected cells was tested in Western blot assay using an anti-HA rabbit monoclonal antibody and an anti-rabbit HRP coupled secondary antibody. An anti-actin antibody was used as a loading control. Rabies virus phosphoprotein (RABV-P) was used as a positive control of inhibition and is shown in the last lane in (c) and (d).

Figure 5: Expression of PUUV Sotkamo NSs protein after infection of VeroE6 cells (**a**) and replication of PUUV Sotkamo wt and NSs21Stop strains in VeroE6, A549 and MyglaSWRec.B cells analysed by Western blot assay (**b**) and virus titration (**c**). Cells were infected at MOI 0.5 and harvested at the indicated time points. For Western blot analysis of NSs protein, a polyclonal rabbit anti-NSs serum (1:50 in PBS-Tween 0.05%) was incubated overnight at 4°C. N-protein was detected using the specific mouse monoclonal antibody A1C5 (1:500, Promega). Titers of supernatants of the three cell lines are depicted as the 50% tissue culture infectious dose ($TCID_{50}$)/ml determined by titration on VeroE6 cells by indirect immunofluorescence assay for PUUV N protein. Calculation was done by the Spearman/Kärber method and mean titers of 3 replicates each are given.

References

1. Meyer BJ, Schmaljohn CS (2000) Persistent hantavirus infections: characteristics and mechanisms. Trends in microbiology 8 (2):61-67

2. Vaheri A, Henttonen H, Voutilainen L, Mustonen J, Sironen T, Vapalahti O (2013) Hantavirus infections in Europe and their impact on public health. Reviews in medical virology 23 (1):35-49. doi:10.1002/rmv.1722

3. Hedil M, Kormelink R (2016) Viral RNA Silencing Suppression: The Enigma of Bunyavirus NSs Proteins. Viruses 8 (7). doi:10.3390/v8070208

4. Plyusnin A (2002) Genetics of hantaviruses: implications to taxonomy. Archives of virology 147 (4):665-682

5. Vera-Otarola J, Solis L, Soto-Rifo R, Ricci EP, Pino K, Tischler ND, Ohlmann T, Darlix JL, Lopez-Lastra M (2012) The Andes hantavirus NSs protein is expressed from the viral small mRNA by a leaky scanning mechanism. Journal of virology 86 (4):2176-2187. doi:10.1128/JVI.06223-11

6. Jääskelainen KM, Kaukinen P, Minskaya ES, Plyusnina A, Vapalahti O, Elliott RM, Weber F, Vaheri A, Plyusnin A (2007) Tula and Puumala hantavirus NSs ORFs are functional and

the products inhibit activation of the interferon-beta promoter. Journal of medical virology 79 (10):1527-1536. doi:10.1002/jmv.20948

7. Virtanen JO, Jääskelainen KM, Djupsjobacka J, Vaheri A, Plyusnin A (2010) Tula hantavirus NSs protein accumulates in the perinuclear area in infected and transfected cells. Archives of virology 155 (1):117-121. doi:10.1007/s00705-009-0546-y

8. Billecocq A, Spiegel M, Vialat P, Kohl A, Weber F, Bouloy M, Haller O (2004) NSs protein of Rift Valley fever virus blocks interferon production by inhibiting host gene transcription. Journal of virology 78 (18):9798-9806. doi:10.1128/jvi.78.18.9798-9806.2004

9. Schoen A, Weber F (2015) Orthobunyaviruses and innate immunity induction: alieNSs vs. PredatoRRs. European journal of cell biology 94 (7-9):384-390. doi:10.1016/j.ejcb.2015.06.001

10. Habjan M, Pichlmair A, Elliott RM, Overby AK, Glatter T, Gstaiger M, Superti-Furga G, Unger H, Weber F (2009) NSs protein of Rift Valley fever virus induces the specific degradation of the double-stranded RNA-dependent protein kinase. Journal of virology 83 (9):4365-4375. doi:10.1128/jvi.02148-08

11. Hollidge BS, Weiss SR, Soldan SS (2011) The role of interferon antagonist, non-structural proteins in the pathogenesis and emergence of arboviruses. Viruses 3 (6):629-658. doi:10.3390/v3060629

12. Kalveram B, Ikegami T (2013) Toscana virus NSs protein promotes degradation of double-stranded RNA-dependent protein kinase. Journal of virology 87 (7):3710-3718. doi:10.1128/jvi.02506-12

13. Thomas D, Blakqori G, Wagner V, Banholzer M, Kessler N, Elliott RM, Haller O, Weber F (2004) Inhibition of RNA polymerase II phosphorylation by a viral interferon antagonist. The Journal of biological chemistry 279 (30):31471-31477. doi:10.1074/jbc.M400938200

14. Weber F, Bridgen A, Fazakerley JK, Streitenfeld H, Kessler N, Randall RE, Elliott RM (2002) Bunyamwera bunyavirus nonstructural protein NSs counteracts the induction of alpha/beta interferon. Journal of virology 76 (16):7949-7955. doi:10.1128/jvi.76.16.7949-7955.2002

15. Kell AM, Gale M, Jr. (2015) RIG-I in RNA virus recognition. Virology 479-480:110-121. doi:10.1016/j.virol.2015.02.017

16. Basler CF, Garcia-Sastre A (2002) Viruses and the type I interferon antiviral system: induction and evasion. International reviews of immunology 21 (4-5):305-337. doi:10.1080/08830180213277

17. Haller O, Staeheli P, Schwemmle M, Kochs G (2015) Mx GTPases: dynamin-like antiviral machines of innate immunity. Trends in microbiology 23 (3):154-163. doi:10.1016/j.tim.2014.12.003

18. Rang A, Heider H, Ulrich R, Krüger DH (2006) A novel method for cloning of non-cytolytic viruses. Journal of virological methods 135 (1):26-31. doi:10.1016/j.jviromet.2006.01.014

19. R Core team (2015) R: A Language and Environment for Statistical Computing. R Foundation for Statistical Computing.

20. Strandin T, Smura T, Ahola P, Aaltonen K, Sironen T, Hepojoki J, Eckerle I, Ulrich RG, Vapalahti O, Kipar A, Forbes KM (2020) Orthohantavirus Isolated in Reservoir Host Cells Displays Minimal Genetic Changes and Retains Wild-Type Infection Properties. Viruses 12 (4). doi:10.3390/v12040457

21. Brune KD, Leneghan DB, Brian IJ, Ishizuka AS, Bachmann MF, Draper SJ, Biswas S, Howarth M (2016) Plug-and-Display: decoration of Virus-Like Particles via isopeptide bonds for modular immunization. Scientific reports 6:19234. doi:10.1038/srep19234

22. Brzózka K, Finke S, Conzelmann KK (2005) Identification of the rabies virus alpha/beta interferon antagonist: phosphoprotein P interferes with phosphorylation of interferon regulatory factor 3. Journal of virology 79 (12):7673-7681. doi:10.1128/JVI.79.12.7673-7681.2005

23. Binder F, Lenk M, Weber S, Stoek F, Dill V, Reiche S, Riebe R, Wernike K, Hoffmann D, Ziegler U, Adler H, Essbauer S, Ulrich RG (2019) Common vole (*Microtus arvalis*) and bank vole (*Myodes glareolus*) derived permanent cell lines differ in their susceptibility and replication kinetics of animal and zoonotic viruses. Journal of virological methods:113729. doi:10.1016/j.jviromet.2019.113729

24. Otarola JV, Solis L, Lowy F, Olguin V, Angulo J, Pino K, Tischler ND, Otth C, Padula P, Lopez-Lastra M (2020) The Andes orthohantavirus NSs protein antagonizes the type I interferon response by inhibiting MAVS signaling. Journal of virology. doi:10.1128/JVI.00454-20

25. van Knippenberg I, Carlton-Smith C, Elliott RM (2010) The N-terminus of Bunyamwera orthobunyavirus NSs protein is essential for interferon antagonism. The Journal of general virology 91 (Pt 8):2002-2006. doi:10.1099/vir.0.021774-0

26. Binder F, Ryll R, Drewes S, Jagdmann S, Reil D, Hiltbrunner M, Rosenfeld UM, Imholt C, Jacob D, Heckel G, Ulrich RG. Spatial and temporal evolutionary patterns in Puumala Orthohantavirus (PUUV) S segment. Pathogens (accepted).

Figure

Figure 1

Click here to access/download;Figure;Binder_hantavirus NSs_function_Figures_endfinal.pptx

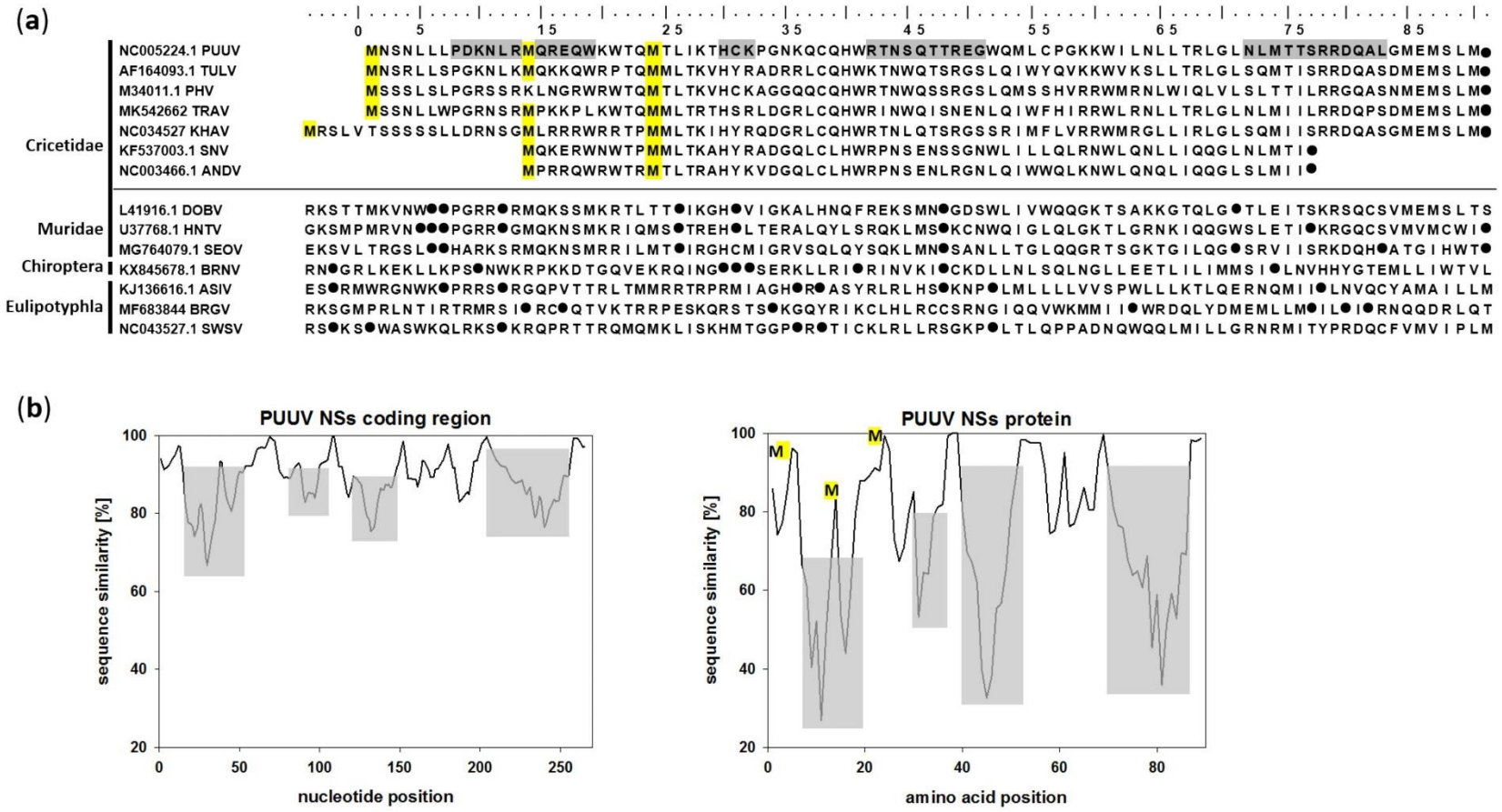

Figure 2

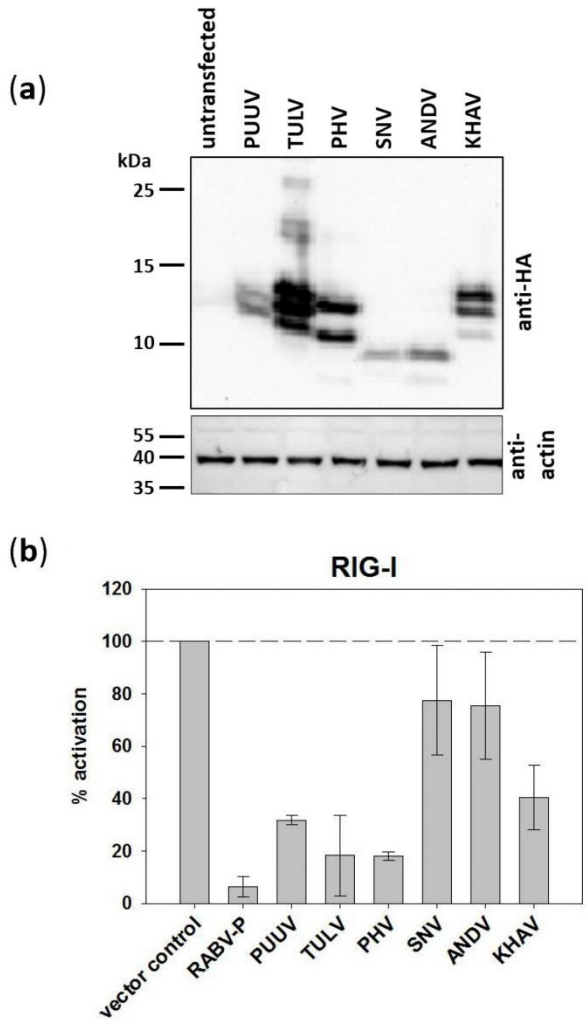
(a)
untransfected
PUUV
TULV
PHV
SNV
ANDV
KHAV
kDa
25
15
10
anti-HA
55
40
35
anti-actin
(b)
RIG-I
% activation
120
100
80
60
40
20
0
Vector control
RABV-P
PUUV
TULV
PHV
SNV
ANDV
KHAV

Figure 3

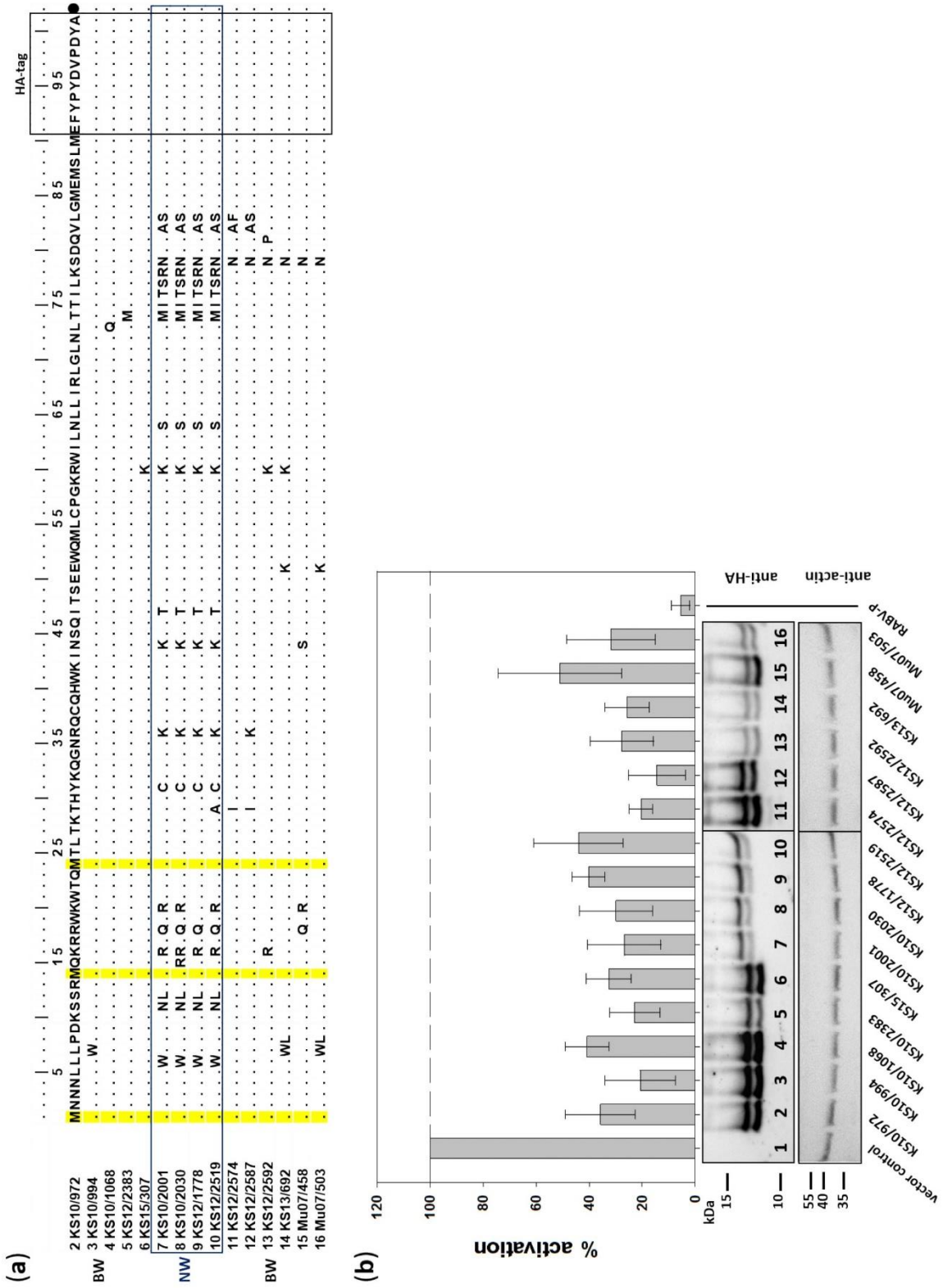
(a)
HA-tag
2 KS10/972
3 KS10/994
BW
4 KS10/1068
5 KS12/2383
6 KS15/307
7 KS10/2001
NW
8 KS10/2030
9 KS12/1778
10 KS12/2519
11 KS12/2574
12 KS12/2587
BW
13 KS12/2592
14 KS13/692
15 Mu07/458
16 Mu07/503
(b)
% activation
kDa
anti-HA
anti-actin
vector control
KS10/972
KS10/994
KS10/1068
KS10/2383
KS15/307
KS10/2001
KS10/2030
KS12/1778
KS12/2519
KS12/2574
KS12/2587
KS12/2592
KS13/692
Mu07/458
Mu07/503
RABV-P

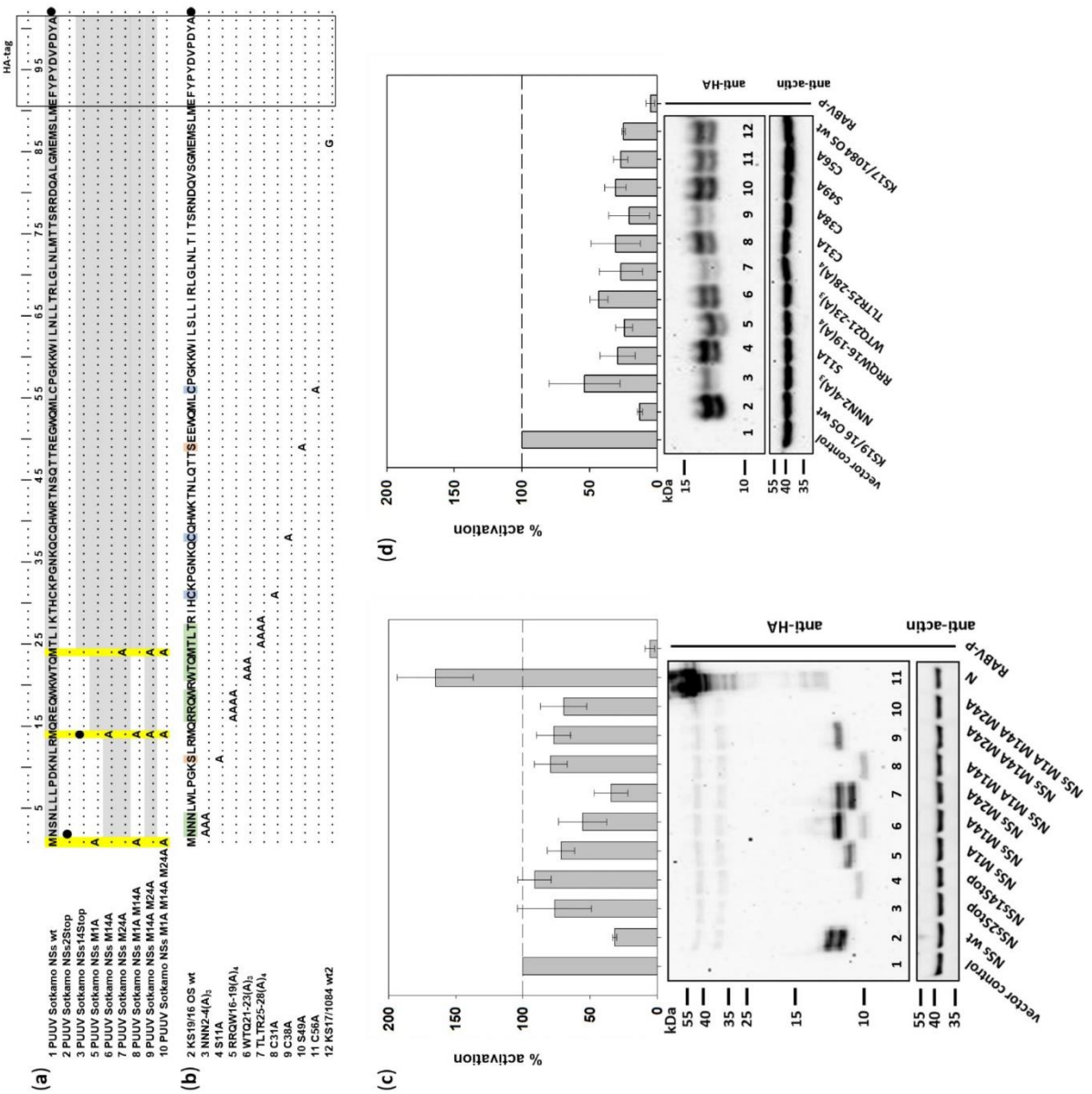
(a)
HA-tag
1 PUUV Sotkamo NSs wt
2 PUUV Sotkamo NSs2Stop
3 PUUV Sotkamo NSs14Stop
5 PUUV Sotkamo NSs M1A
6 PUUV Sotkamo NSs M14A
7 PUUV Sotkamo NSs M24A
8 PUUV Sotkamo NSs M1A M14A
9 PUUV Sotkamo NSs M14A M24A
10 PUUV Sotkamo NSs M1A M14A M24A
(b)
2 KS19/16 OS wt
3 NNN2-4(A)3
4 S11A
5 RRQW16-19(A)4
6 WTQ21-23(A)3
7 TLTR25-28(A)4
8 C31A
9 C38A
10 S49A
11 C56A
12 KS17/1084 wt2
(c)
% activation
kDa
anti-HA
anti-actin
vector control
NSs wt
NSs2Stop
NSs14Stop
NSs M1A
NSs M14A
NSs M24A
NSs M1A M14A
NSs M14A M24A
NSs M1A M14A M24A
N
RABV-P
(d)
% activation
kDa
anti-HA
anti-actin
vector control
KS19/16 OS wt
NNN2-4(A)3
S11A
RRQW16-19(A)4
WTQ21-23(A)3
TLTR25-28(A)4
C31A
C38A
S49A
C56A
KS17/1084 OS wt
RABV-P

Figure 4

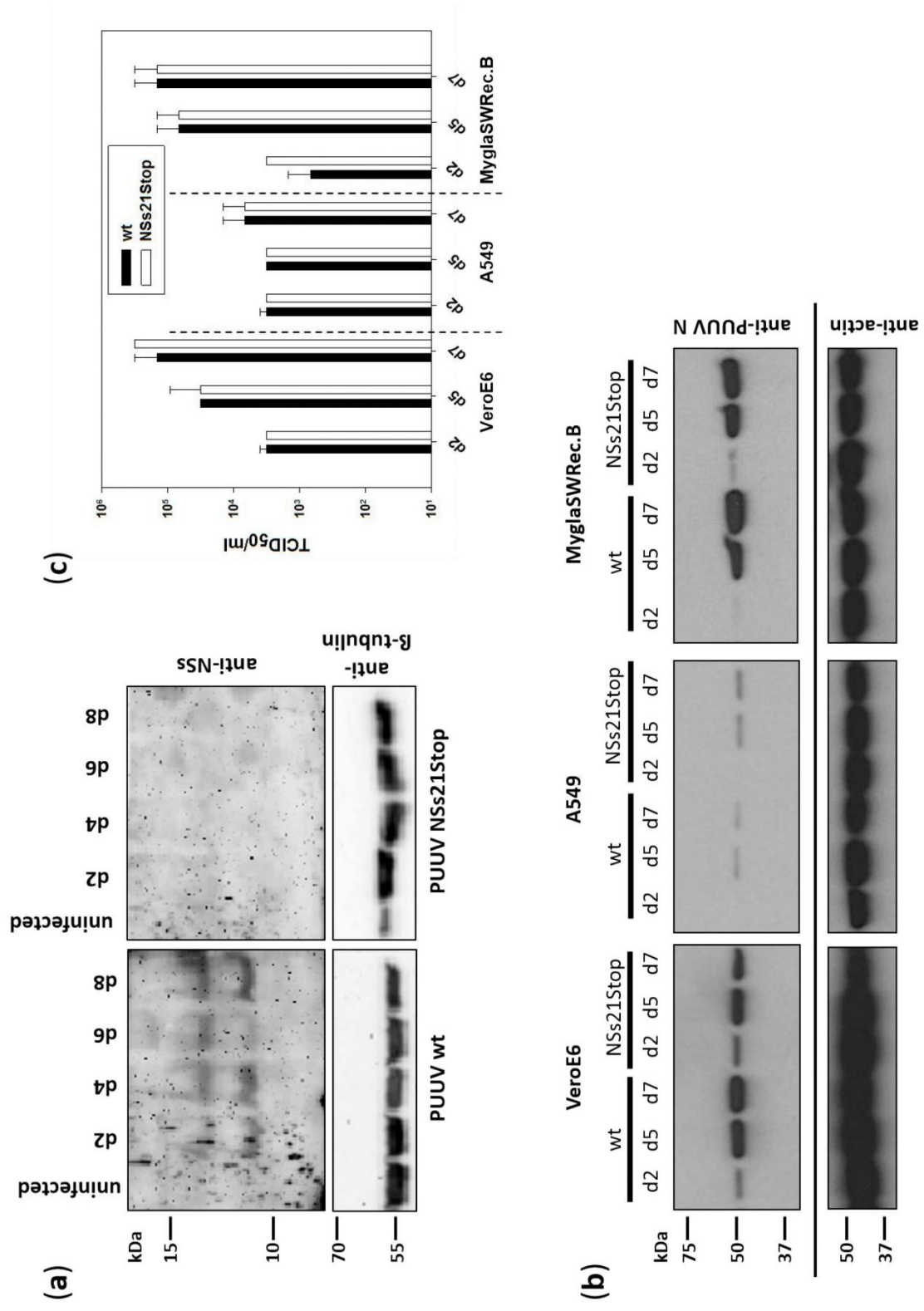
(a)
kDa
15
10
70
55
uninfected
d2
d4
d6
d8
PUUV wt
PUUV NSs21Stop
anti-NSs
anti-β-tubulin
(b)
VeroE6
A549
MyglaSWRec.B
wt
NSs21Stop
d2
d5
d7
kDa
75
50
37
anti-PUUV N
anti-actin
(c)
TCID50/ml
wt
NSs21Stop
VeroE6
A549
MyglaSWRec.B

Figure 5

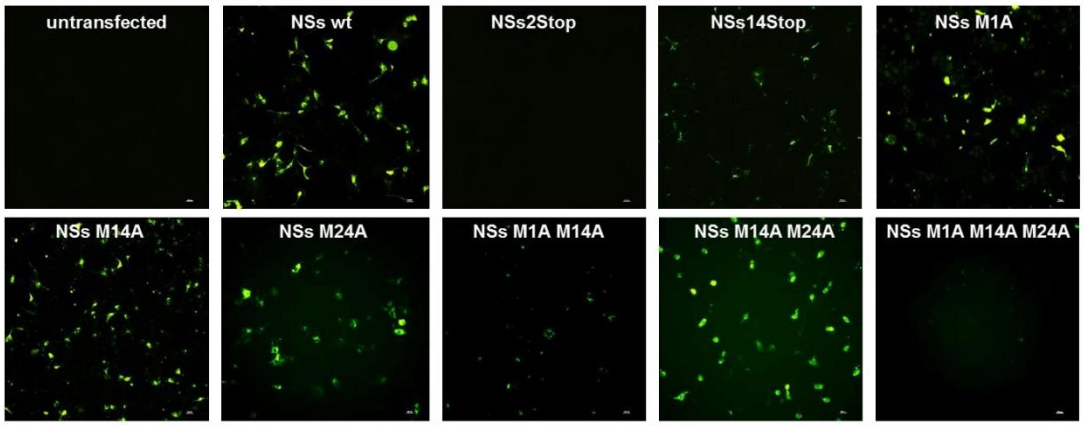

Supplementary Figure 1: Immunofluorescence analysis of PUUV Sotkamo NSs expression constructs. VeroE6 cells were transfected with 2µg plasmid DNA encoding the respective HA-tagged PUUV NSs protein. Cells were seeded simultaneously with transfection mix in a 6-well plate. 48 h after transfection, cells were stained for immunofluorescence analysis using an anti-HA specific monoclonal antibody and an Alexa fluor 488 labelled secondary antibody (green fluorescence).

Supplementary Table 1: Summary of NSs fusion protein expression patterns and their inhibitory activity on human interferon type I (IFN-I) promoter.

	Protein variant	Predicted molecular mass (kDa)	Observed IFN-I promoter inhibition
I	PUUV Sotkamo NSs wt	11.8 and 10.3	++
	TULV NSs	12, 10.5 and 9.8	++
	PHV NSs	11.6 and 8.9	++
	KHAV NSs	12.4, 10.5 and 9.1	+
	SNV NSs	8.7 and 7.3	(+)
	ANDV NSs	8.9 and 7.5	(+)
II	PUUV KS10/972 BW	11.8 and 10.3	++
	PUUV KS10/994 BW	11.8 and 10.3	++
	PUUV KS10/1068 BW	11.8 and 10.3	++
	PUUV KS12/2383 BW	11.8 and 10.3	++
	PUUV KS15/307 BW	11.8 and 10.3	++
	PUUV KS10/2001 NW	12.5 and 10.8	++
	PUUV KS10/2030 NW	12.5 and 10.8	++
	PUUV KS12/1778 NW	12.5 and 10.8	++
	PUUV KS12/2519 NW	12.5 and 10.8	++
	PUUV KS12/2574 BW	11.8 and 10.3	++
	PUUV KS12/2587 BW	11.8 and 10.3	++
	PUUV KS12/2592 BW	11.8 and 10.3	++
	PUUV KS13/692 BW	11.8 and 10.3	++
	PUUV Mu07/458 BW	11.8 and 10.3	++
	PUUV Mu07/503 BW	11.8 and 10.3	++
III	PUUV Sotkamo NSs2Stop	-	-
	PUUV Sotkamo NSs14Stop	8.9	-
	PUUV Sotkamo NSs M1A	10.3	+
	PUUV Sotkamo NSs M14A	11.8 and 8.9	+
	PUUV Sotkamo NSs M24A	11.8 and 10.3	++
	PUUV Sotkamo NSs M1A M14A	8.9	-
	PUUV Sotkamo NSs M14A M24A	11.8	-
	PUUV Sotkamo NSs M1A M14A M24A	-	-
IV	PUUV NSs KS19/16 (OS)	11.8 and 10.3	++
	PUUV NSs KS17/1084 (OS)	11.8 and 10.3	++
	PUUV KS19/16 NNN2-4(A)3	11.8 and 10.3	+
	PUUV KS19/16 S11A	11.8 and 10.3	++
	PUUV KS19/16 RRQW16-19(A)4	11.8 and 10.3	++
	PUUV KS19/16 WTQ21-23(A)3	11.8 and 10.3	+
	PUUV KS19/16 TLTR25-28(A)4	11.8 and 10.3	++
	PUUV KS19/16 C31A	11.8 and 10.3	++
	PUUV KS19/16 C38A	11.8 and 10.3	++
	PUUV KS19/16 S49A	11.8 and 10.3	++
	PUUV KS19/16 C56A	11.8 and 10.3	++
	PUUV Sotkamo N	48	-

The predicted molecular mass was calculated from the amino acid sequence using the 'Compute pI/Mw' tool of the Swiss Institute of Bioinformatics Resource Portal ExPASy (https://web.expasy.org/compute_pi/); BW = Baden-Wuerttemberg, IFN = interferon, kDa = kilo dalton, NW, North Rhine-Westphalia, OS = Osnabrück.

Supplementary Table 2: Bank vole-derived PUUV NSs sequences used for functional studies on IFN-I promoter inhibition.

NSs Sequence	Origin	Year	Accession number	Reference
KS19/16	Osnabrück, LS, North-west Germany	2018	MN906316	this study
KS17/1084	Osnabrück, LS, North-west Germany	2017	MN906315	this study
KS10/972	Weissach, BW, South-west Germany	2010	MT453485	Binder et al., accepted
KS10/994	Weissach, BW, South-west Germany	2010	MT453491	Binder et al., accepted
KS10/1068	Weissach, BW, South-west Germany	2010	MT453516	Binder et al., accepted
KS12/2383	Weissach, BW, South-west Germany	2012	MT453655	Binder et al., accepted
KS15/307	Weissach, BW, South-west Germany	2014	MT453675	Binder et al., accepted
KS10/2001	Billerbeck, NW, North-west Germany	2010	MT453553	Binder et al., accepted
KS10/2030	Billerbeck, NW, North-west Germany	2010	MT453559	Binder et al., accepted
KS12/1778	Billerbeck, NW, North-west Germany	2012	MT453649	Binder et al., accepted
KS12/2519	Billerbeck, NW, North-west Germany	2012	MT453666	Binder et al., accepted
KS12/2574	Steinheim, BW, South-west Germany	2012	MT453680	Binder et al., accepted
KS12/2587	Stuttgart, BW, South-west Germany	2012	MT453682	Binder et al., accepted
KS12/2592	Moessingen-Belsen, BW, South-west Germany	2012	MT453683	Binder et al., accepted
KS13/692	Crailsheim, BW, South-west Germany	2012	MT453692	Binder et al., accepted
Mu07/458	Zussdorf-Wilhelmsdorf, BW, South-west Germany	2007	MT453698	Binder et al., accepted
Mu07/503	Michelbach, BW, South-west Germany	2007	MT453705	Binder et al., accepted

LS, Lower Saxony, BW, Baden-Wuerttemberg; NW, North Rhine-Westphalia

References

Binder F, Ryll R, Drewes S, Jagdmann S, Reil D, Hiltbrunner M, Rosenfeld UM, Imholt C, Jacob D, Heckel G, Ulrich RG (accepted) Spatial and temporal evolutionary patterns in Puumala Orthohantavirus (PUUV) S segment. Pathogens

OWN CONTRIBUTIONS TO PUBLICATIONS

Publication I

Binder, F., Drewes, S., Imholt, C., Saathoff, M., Below, A.D., Bendl, E., Conraths, F.J., Tenhaken, P., Mylius, M., Brockmann, S., Oehme, R., Freise, J., Jacob, J., Ulrich, R.G., 2019. "Heterogeneous Puumala orthohantavirus situation in endemic regions in Germany in summer 2019". Transboundary and Emerging Diseases 67(2), 502-509. DOI:10.1111/tbed.13408.

Florian Binder*:	Rodent trapping, dissection of animals, molecular and serological analysis, data evaluation, writing of the manuscript
Stephan Drewes*:	Dissection of animals, molecular and serological analysis, data evaluation, writing of the manuscript
Christian Imholt:	Rodent trapping, providing tree mast data, data evaluation, proofreading of the manuscript
Marion Saathoff:	Rodent trapping
Alexandra D. Below:	Rodent trapping
Elias Bendl:	Dissection of animals, molecular and serological analysis
Franz J. Conraths:	Publication ideas, proofreading of the manuscript
Peter Tenhaken:	Data evaluation, proofreading of the manuscript
Maren Mylius:	Data evaluation, proofreading of the manuscript
Stefan Brockmann:	Rodent trapping, data evaluation, proofreading of the manuscript
Rainer Oehme:	Rodent trapping, data evaluation, proofreading of the manuscript
Jona Freise:	Rodent trapping management
Jens Jacob:	Design of study, rodent trapping, providing tree mast data, data evaluation, writing of the manuscript
Rainer G. Ulrich:	Design of study, data evaluation, writing of the manuscript

*authors contributed equally to this publication

Publication II

Binder, F., Ryll, R., Drewes, S., Jagdmann, S., Reil,D., Hiltbrunner, M., Rosenfeld, U.M., Imholt, C., Jacob, J., Heckel, G., Ulrich, R.G. "Spatial and temporal evolutionary patterns in Puumala Orthohantavirus (PUUV) S segment". Pathogens 9(7), 548, DOI: 10.3390/pathogens9070548.

Florian Binder:	Molecular and serological analysis, data evaluation, phylogenetic analysis, writing of the manuscript
René Ryll:	Data evaluation, phylogenetic analysis, proofreading of the manuscript
Stephan Drewes:	Molecular and serological analysis, proofreading of the manuscript
Sandra Jagdmann:	Molecular and serological analysis, proofreading of the manuscript
Daniela Reil:	Organization of rodent trapping, proofreading of the manuscript
Melanie Hiltbrunner:	Phylogenetic analysis (isolation-by-distance analysis)
Ulrike M. Rosenfeld:	Organization of rodent trapping
Christian Imholt:	Organization of rodent trapping, data evaluation, proofreading of the manuscript
Jens Jacob:	Organization of rodent trapping, data evaluation, proofreading of the manuscript
Gerald Heckel:	Phylogenetic analysis, proofreading of the manuscript
Rainer G. Ulrich:	Design of study, data evaluation, writing of the manuscript

Publication III

Binder, F., Lenk, M., Weber, S., Stoek, F., Dill, V., Reiche, S., Riebe, R., Wernike, K., Hoffmann, D., Ziegler, U., Adler, H., Essbauer, S., Ulrich, R.G., 2019. "Common vole (*Microtus arvalis*) and bank vole (*Myodes glareolus*) derived permanent cell lines differ in their susceptibility and replication kinetics of animal and zoonotic viruses". Journal of Virological Methods 274, 113729. DOI:10.1016/j.jviromet.2019.113729.

Florian Binder:	Design of study, cell line experiments with EMCV 1 and EMCV 2, MNV, SINV, USUV, SBV, VACV, MHV-68, RVFV, TULV and PUUV, phylogenetic analysis, data evaluation, writing of the manuscript
Matthias Lenk:	Generation of cell lines, proofreading of manuscript
Saskia Weber:	Cell line experiments with CPXV, data evaluation, proofreading of manuscript
Franziska Stoek:	Cell line experiments with RVFV, proofreading of manuscript
Veronika Dill:	Cell line experiments with FMDV, proofreading of manuscript
Sven Reiche:	Contribution of reagents/materials/analysis tools, data evaluation, proofreading of manuscript
Roland Riebe:	Generation of cell lines
Kerstin Wernike:	Contribution of SBV material, proofreading of manuscript
Donata Hoffmann:	Cell line experiments with CPXV, proofreading of manuscript
Ute Ziegler:	Cell line experiments with TBEV and WNV, proofreading of manuscript
Heiko Adler:	Contribution of MHV-68 material, proofreading of manuscript
Sandra Essbauer:	Contribution of PUUV material and BVK168 cell line, proofreading of manuscript
Rainer G. Ulrich:	Design of study, writing of the manuscript

Publication IV

Binder, F., Reiche, S., Roman-Sosa, G., Saathoff, M., Ryll, R., Trimpert, J., Kunec, D., Höper, D., Ulrich, R.G., (2020). "Isolation and characterization of new Puumala orthohantavirus strains from Germany". Virus Genes, 56(4), 448-460, DOI:10.1007/s11262-020-01755-3.

Florian Binder:	Design of study, rodent trapping, in-field isolation, all virus/cell line experiments, testing of monoclonal antibodies, establishment of PUUV qRT-PCR, phylogenetic analysis, data evaluation, writing of the manuscript
Sven Reiche:	Generation of monoclonal antibodies, proofreading of manuscript
Gleyder Roman-Sosa:	Generation of virus-like particles, proofreading of manuscript
Marion Saathoff:	Rodent trapping
René Ryll:	Establishment of PUUV qRT-PCR, proofreading of manuscript
Jakob Trimpert:	High throughput sequencing, data evaluation, proofreading of manuscript
Dusan Kunec:	High throughput sequencing, data evaluation, proofreading of manuscript
Dirk Höper:	High throughput sequencing, data evaluation
Rainer G. Ulrich:	Study design, data evaluation, writing of the manuscript

Publication V

Binder, F., Gallo, G., Bendl, E., Eckerle, I., Ermonval, M., Luttermann, C., Ulrich, R.G. “Inhibition of the interferon I induction by non-structural protein NSs of Puumala and other vole associated orthohantaviruses: Plasticity of the protein and role of the N-terminal region”. Archives of Virology (submitted).

Florian Binder:	Study design, cloning, molecular-biological experiments, establishment of bank vole assay, virus replication experiments, phylogenetic analysis, data evaluation, writing of manuscript
Giulia Gallo:	Virus replication experiments, data evaluation, proofreading of manuscript
Elias Bendl:	Cloning, molecular-biological experiments, data evaluation
Isabella Eckerle:	Development of bank vole cell line, proofreading of manuscript
Myriam Ermonval:	Virus replication experiments, data evaluation, proofreading of manuscript
Christine Luttermann:	Study design, molecular-biological experiments, data evaluation, writing of manuscript
Rainer G. Ulrich:	Study design, data evaluation, writing of manuscript

The information above is confirmed by signature: _____

Doctorate

Signature of scientific supervisor: _____

Prof. Dr. Rainer G. Ulrich

3. RESULTS AND DISCUSSION

3.1 PUUV SITUATION IN GERMANY

The screening efforts carried out in this work contribute to a more detailed knowledge about hantavirus and rodent reservoir cycles. They provide additional knowledge to the current state of hantavirus mapping and cyclic disease occurrence in Germany. We found that observations in rodent trapping and hantavirus prevalence during a monitoring period of 5 years (2010 – 2014) in the south and west of Germany and in spring 2019 in Osnabrück are in line with the reports of human cases during that time (Faber et al., 2019; Robert-Koch-Institut, 2020). All PUUV samples from Baden-Wuerttemberg (BW), North Rhine-Westphalia (NW), and Osnabrück belonged to the central European lineage of PUUV and were derived from bank voles in regions where the western evolutionary bank vole lineage occurs (**Publication I and II**, Drewes et al., 2017a).

Public health departments in regions with high PUUV incidence (e.g. BW, Münsterland, Bavarian Forest) need to be aware of environmental factors increasing the probability of a hantavirus infection. In contrast to previous data, vole abundance and human PUUV incidence 2019 and beech and oak mast in 2018 varied strongly between regions (**Publication I,** Table 1). A typical outbreak situation in spring 2019 was only observed in Stuttgart and Osnabrück, but not in the other regions. Only in these regions, values where high enough to reach or exceed the mean of the last outbreak years (**Publication I**, Table 1, Figure 3). This variation of human PUUV cases in endemic regions, especially in western Germany may be due to regional differences in forest structure (Voutilainen et al., 2012). The region in North Rhine-Westphalia exhibits the highest degree of landscape fragmentation in Germany (Walz et al., 2011), a more continuous forest cover in the south could increase human PUUV incidence. This may be a reason for the high PUUV RNA detection rate 2019 at the southern trapping plots Stuttgart and Goeppingen, that generally followed the high beech mast intensity observed at these plots (**Publication I,** Table 1). Despite the effect of beech mast on bank vole population dynamics, it is possible that other factors such as local interaction in the food web or diseases have caused a heterogeneous abundance of bank voles and thereby the regional and local differences of human PUUV incidence. Temporal trends of cumulative human PUUV incidence are mainly consistent and seem to be a promising feature for the development of district scale prediction of human infection risk early in the year (**Publication I,** Figure 3). Alternatively, a combination of bank vole abundance and PUUV prevalence or beech mast information might be used in an early warning model (Reil et al., 2018). However, existing prediction models are not precise enough, due to the lack of detailed parameters or the availability only on district scale (Reil et al., 2018). The human PUUV incidence 2020 is very low (Figure 3b), which is mainly caused by an expected breakdown of bank vole populations. Finally, physicians should consider hantavirus disease as differential diagnosis, especially in risk groups that are

prone to contract pathogens that cause diseases with similar symptoms such as leptospirosis (Nau et al., 2019).

Interestingly, a high percentage of voles was found to be seropositive for anti-PUUV antibodies but negative for PUUV RNA (**Publication II**). This finding is in contrast to the general assumption of a persistent PUUV infection in bank voles. However, in young animals several infection experiments and field reports in rodents support the transmission of maternal antibodies (Dohmae and Nishimune, 1998; Bernshtein et al., 1999; Borucki et al., 2000; Kallio et al., 2006b). These maternal antibodies can protect young rodents until maturity, as demonstrated in rats (Dohmae et al., 1993) or bank voles (Kallio et al., 2006b). As adults, rodents are again susceptible to hantavirus infection (Dohmae and Nishimune, 1998). As many voles in the study, both in BW and NW (**Publication II**) were already mature, they might also have cleared the virus through yet unknown mechanisms. Another explanation might be a low viral load at the time point of capture, due to oscillation or general decline of viral load at higher age of adult animals (Voutilainen et al., 2015).

3.2 SEQUENCE EVOLUTION OF PUUV

In **Publication 2**, the fluctuation of PUUV prevalence in local bank vole populations during outbreak and non-outbreak years and the differences of sequence conservation and variability in S segment regions were investigated. In our trapping sites in BW and NW we found, that the temporal variation of PUUV sequences indicated a continuous presence of certain sequence types, whereas other minor sequence types seemed to emerge and get extinct (**Publication II**). Similar patterns were observed also in previous studies (Weber de Melo et al., 2015). The persistence of sequence types over time and the emergence of novel sequence types might be explained by bottleneck event-driven genetic drift or selection processes in the bank vole population that shape the genetic diversity of PUUV. In general, the PUUV NSs-ORF was found to be conserved – it was detected in all 226 of 226 infected bank voles investigated and in a spillover infected field vole at the same position within the S segment and with the identical length. However, the general conservation of the NSs ORF is in contrast to the high amino acid sequence variability that raises questions about its functional consequences (see below). Additionally, sequencing of PUUV S segment did not reveal any stop codon mutations within the NSs ORF similar to that observed in the cell culture adapted Sotkamo strain (**Publication II**, Rang et al., 2006). This indicates, that putative loss of function-mutations occur preferably in specific selection pressure free environments as cell cultures, in the case of NSs, IFN-deficient VeroE6 cells. Finally, these results increase our sequence knowledge for future identification of the geographical origin of human infections in high endemic regions of NW and BW.

Future investigations will have to prove if PUUV strains with lower virulence may increase the over winter survival of bank voles.

3.3 RESERVOIR-DERIVED CELL CULTURES

Due to improved high-throughput sequencing methods and novel approaches in virus ecology, today there are numerous newly identified viruses in a variety of mammalian reservoir host species, in the orders Rodentia and Chiroptera in particular, but also in many other different animal taxa (Han et al., 2015a; Han et al., 2015b; Drewes et al., 2017b; Shi et al., 2018). The importance of such research is impressively demonstrated by the actual Severe Acute Respiratory Syndrome Coronavirus 2 (SARS-CoV-2) pandemic 2019/20, where a new corona virus was transmitted from wildlife to humans (Brook et al., 2020; Hui et al., 2020). In contrast to viruses with a broad host range, the strict association of hantaviruses to a single rodent reservoir host makes these viruses interesting for studies on cellular interaction but also evolutionary processes of virus and rodent host *in vitro*. Yet, available cell culture models for hantaviruses are often outdated and display a heterologous virus-host relationship that is only of limited value (Table 3). Well established cell lines (VeroE6, Huh7) are easy to culture and many reagents and assays are available but they often have deregulations of important cellular pathways or do not reflect complex questions of the reservoir host situation. On the other hand, reservoir-derived cells need to be thoroughly characterized but their value for scientific questions remains out of question.

Natural reservoir host species that are available as laboratory animals or in breeding colonies (such as Norway rats (*R. norvegicus*), deer mice (*P. maniculatus*), bank voles, common voles (*M. arvalis*), cotton rats (*S. hispidus*) are of special interest: cell lines derived from these animals can be compared to the *in vivo* infection in an animal model with the associated virus, e.g. cowpox virus (CPXV) (Jeske et al., 2019b; Weber et al., 2020). In **Publication III**, a variety of rodent-associated, suspected to be rodent associated and non-rodent-derived viruses were tested in bank vole and common vole cells that can be compared to *in vivo* studies from existing colonies of these animals.

The novel cell lines FMN (common vole) and MGN (bank vole) support productive replication of TULV and PUUV, respectively (**Publication III**). The fact that TULV replication was only detected in common vole cells after very long incubation times, could indicate a long lasting natural host-like infection. Bank vole cells were not susceptible to TULV (**Publication III**) and experimental inoculation of bank voles with TULV could be shown, but only few animals seroconverted and antibody titers remained low (Klingström et al., 2002). Therefore, FMN cell line might be suitable as a cell culture model system for TULV investigations. The novel bank vole cell line MGN of the Carpathian lineage was reliably infected and replicated PUUV strain Vranica/Hällnäs of the Northern Scandinavian (N-SCA) clade (**Publication III**). This N-SCA PUUV clade and

the Carpathian bank vole lineage also occur sympatrically in nature. For PUUV, the assignment of a certain virus clade to a specific evolutionary lineage of the bank vole was documented (Drewes et al., 2017a). However, more bank vole-derived PUUV isolates and cell lines of different lineages are necessary to clarify this question in cell culture in every possible combination.

Table 3: Cell lines available for hantavirus research.

Cell line	Tissue	Type	Origin	Replication of Hantavirus	Reference
VeroE6	kidney, epithelial	permanent	African green monkey	PUUV, HTNV, SEOV, TULV, SNV, ANDV, DOBV	(Lundkvist et al., 1997; Jin et al., 2002)
COS-7	kidney, fibroblastoid	permanent	African green monkey	HTNV, PUUV	(Pensiero et al., 1992; Jääskelainen et al., 2007)
Huh7	liver, epithelial	permanent	human	PUUV, PHV	(Handke et al., 2010)
HUVEC	umbilical cord, endothelial	permanent	human	PUUV, HTNV, NYV, PHV, TULV	(Gavrilovskaya et al., 1999; Alff et al., 2006; Klingström et al., 2006b)
A549	alveolar, epithelial	permanent	human	PUUV, PHV	(Handke et al., 2010), this work
A-253	submaxillary gland	permanent	human	PUUV	(Temonen et al., 1993)
A-704	kidney	permanent	human	PUUV	(Temonen et al., 1993)
WI-38	lung	permanent	human	PUUV	(Temonen et al., 1993)
Detroit 562	pharynx carcinoma	permanent	human	PUUV	(Temonen et al., 1993)
Hep G2	liver	permanent	human	PUUV	(Temonen et al., 1993)
HSVEC	saphenous vein, endothelial	primary	human	HTNV	(Pensiero et al., 1992)
DCs	PBMCs	primary	human	HTNV	(Raftery et al., 2002)
VEF	embryonic, fibroblastoid	primary	bank vole	PUUV	(Stoltz et al., 2011)
MRK101	kidney	permanent	grey red-backed vole	HOKV, PUUV	(Sanada et al., 2012)
BVK168	kidney, epithelial	permanent	bank vole	PUUV	(Essbauer et al., 2011), this work
FMN-R	kidney, epithelial	permanent	common vole	TULV	publication III
MGN-2-R	kidney, epithelial	permanent	bank vole	PUUV	publication III and IV
MyglaREC.B	kidney, epithelial	permanent	bank vole	PUUV, TULV	publication V, (Strandin et al., 2020)

white, human permanent cell lines; grey, primary cell models; dark grey, reservoir host-derived permanent cell lines. DCs, dendritic cells; VEF, vole embryonic fibroblasts; HSVEC, human saphoneous vein endothelial cells; PBMC, peripheral blood mononuclear cells..

A special requirement applies to vector-borne viruses, such as Rift Valley fever virus, West Nile virus, Usutu virus, Sindbis virus, and Tick-borne encephalitis virus (TBEV). They need to have the capacity to infect and replicate in at least the vector and the reservoir, if not multiple dead-end hosts. The lack of detection of cytopathic effect, which is commonly observed for these viruses, might reflect the situation in the natural host in some constellations of virus and vole cell line tested (**Publication III**). As an example,

for TBEV sophisticated animal models are available and bank voles are already used to experimentally assess infection in a reservoir context (Michelitsch et al., 2019a; Michelitsch et al., 2019b).

Reservoir-derived cell lines are not only a suitable tool for the study of evolutionary virus-host combinations, but they can also be used for deciphering cross-species transmission (**Publication III**). This feature is at the moment more important than ever. Successful examples are the demonstration of efficient replication of Middle East Respiratory Syndrome Coronavirus (MERS-CoV) replication in bats and ungulates (Eckerle et al., 2014a), St. Louis encephalitis virus and various bunya-, alpha-, and flaviviruses but also influenza viruses in bats (Dlugolenski et al., 2013; Kopp et al., 2013; Mourya et al., 2013; Raj et al., 2013). A main part of virus-host interaction takes place at the cell surface and includes receptor attachment and binding, but also release and budding from the host cell membrane. Nipah virus and Ebola virus glycoproteins are only two examples for different functional phenotypes in bat reservoir cells compared to human cells (Kuhl et al., 2011; Hoffmann et al., 2019; Takadate et al., 2020). For the two hantaviruses ANDV and SNV, the human asthma-associated gene PCDH1 was identified as an essential determinant of entry and infection in human pulmonary endothelial cells. The surface glycoproteins of ANDV and SNV directly recognize the outermost extracellular repeat domain of PCDH1 for entry (Jangra et al., 2018). Targeting PCDH1 in vole cells was not done, but could reveal differences in viral cell entry and give implications to reduce infection by hantaviruses also in humans. Similar to the different interaction of glycoproteins in human and reservoir cells, these hosts may simply have different entry receptors for hantaviruses than humans. Comparative analysis of β3 integrins in bank vole and Vero cells showed 100-fold reduction in β3 integrin transcription levels in bank vole cells and no expression of the protein on the cell surface. Simultaneously, bank vole cells were still susceptible to PUUV infection, therefore indicating a different entry requirement in reservoir derived cells (Müller et al., 2019). These findings make glycoprotein interactions with both cell lines a highly interesting research target and the developed antibodies against PUUV Gn and Gc can be used for such experiments (**Publication IV**). Such investigations are highly valuable and indicate, that a main application of reservoir-derived cell lines is the investigation of virus-host interactions in standardized infection experiments.

Another important point of action of virus host interaction are the intracellular viral defense mechanisms, for which many viruses have developed evasion strategies. Using reservoir systems, species specific IFN can be characterized and immune mechanisms can be investigated not only for hantaviruses but other vole associated viruses, and, as previously shown, for paramyxoviruses (Virtue et al., 2011). An additional tool for investigating interferon mechanisms in bank voles is the recent development and functional characterization of a recombinant bank vole IFN-γ, a central mediator of host's innate and adaptive immune responses (Torelli et al., 2018). This highlights the importance of laboratory systems to address immunological questions in bank voles. How bank vole immunity can contribute to virus pathogenesis and

transmission within humans remains unclear. For bats, this issue was addressed by virus infectivity assays on bat cell lines expressing induced and constitutive immune phenotypes. These studies supported robust antiviral defenses in bat cells. These bat specific elevated immune responses control virus-induced cellular morbidity, which can contribute to rapidly-propagating persistent infections. When transmitted to other hosts, these viruses likely cause enhanced virulence (Brook et al., 2020).

To study these regulators in the reservoir host are now an interesting option and the developed cell lines represent a valuable tool for identification of host factors. In the field of bat-borne viruses, reservoir-derived cell lines have already served as a valuable *in vitro* tool for functional studies but also virus isolation (Eckerle et al., 2014b).

3.4 ISOLATION OF HANTAVIRUSES

Hantavirus isolation from rodents has been challenging due to low replication during the persistent phase, unsuitable cell culture models and many more reasons. However, cell culture remains the main method for investigation and isolation of a virus. It enables its thorough phenotypical characterization. Cell lines such as Vero cells, derived from the kidney of an African green monkey, are widely used for virus isolation and especially the subclone VeroE6 provides an excellent environment for RNA viruses to replicate, due to an impaired IFN-I response (Emeny and Morgan, 1978; Chew et al., 2009). However, many viruses remain uncultured and here, cell lines derived from reservoir hosts could provide a huge benefit. As shown in **Publication IV**, we were able to isolate PUUV on VeroE6 and bank vole (MGN-2-R) cells. In vole cells, initially cell cultures of three samples were positive for PUUV but during passaging, these isolates where either contaminated with a bank vole reovirus or lost due to low titers. Even though isolation on vole cells in our first approach was only partly successful, these results indicate, that virus growth on reservoir cell lines can be beneficial, not only for hantaviruses (**Publications III and IV**). There are other examples that reservoir-derived cells can be beneficial over conventional cell lines to isolate reservoir-borne viruses, e.g. Cedar virus in bat cells (Marsh et al., 2012) or the first isolation of a PUUV in Japan (HOKV) in vole cells (Sanada et al., 2012).

One problem in hantavirus research is, that most isolates have been obtained a long time ago and were propagated over years on Vero E6 cells. Therefore, they might have accumulated adaptations to these cell lines and do not completely represent all characteristics of the viruses found in the field. For PUUV, mutations associated with cell culture adaptation were found preferentially in the non-coding region of the S-segment at positions 26 and 1577, and one serine versus phenylalanine substitution at position 2053 of the PUUV L protein (Nemirov et al., 2003), which is in line with our observations (**Publication IV**). Another example that supports this consideration is that this PUUV strain was partly attenuated and lost

its ability to infect the natural reservoir animal after passaging due to mutations in the S segment (Lundkvist et al., 1997). Here, a wild-type variant that was passaged in bank voles was well adapted for replication in the reservoir host but not in cell culture, while the strains passaged on VeroE6 cells replicated with high efficiency in cell culture but did not reproducibly infect bank voles (Lundkvist et al., 1997). Unfortunately this *in vivo* experiment could not be performed with the isolated strains in the time frame of this work, but such experiments were almost simultaneously reported from another group (Strandin et al., 2020). The isolation, genetic, and phenotypic characterization of a novel Puumala orthohantavirus from Finland in bank vole cells resulted in cell culture infection that evaded antiviral responses, persisted cell passaging, and similarly had minor viral genome alterations (Strandin et al., 2020, **Publication IV**). Experimental infections of bank voles with the new isolate from Finland resembled natural infections in terms of viral load and host cell distribution. When compared to an attenuated VeroE6-adapted Puumala Kazan strain, the novel isolate demonstrated delayed virus-specific responses in bank voles (Strandin et al., 2020).

Similar to what was found in **Publication IV**, Sundström et al. investigated hantavirus strain evolution during multiple cell culture passages. PUUV strains were isolated after passaging in cell culture which differed from the corresponding parental strain not only in plaque size, but also their ability to replicate in interferon-defective versus interferon-competent cell lines and the potential to induce innate immune responses (Sundström et al., 2011). The insertion of a stop codon within the coding sequence of the NSs ORF was not observed during our initial passaging, however, long term passaging in VeroE6 cells without innate immune response-driven selection pressure might lead to such mutations. The emergence of such stop codons in the virus genome, during passaging in the IFN-deficient VeroE6 cell line, were already observed for TULV isolate Moravia (Jääskelainen et al., 2008) and, as described above, for the PUUV prototype strain Sotkamo (Rang et al., 2006). In contrast, the vole reservoir-derived PUUV and TULV sequences from field studies as well as S segment sequences of other vole-borne hantaviruses were found to contain a conserved intact NSs ORF (**Publication II and IV**, Jääskelainen et al., 2007; Jeske et al., 2019a).

The virus isolation was started in the field with lung samples from 57 bank voles. Three of four obtained isolates originated from anti-PUUV-seronegative voles (**Publication IV**) illustrating that a serological test in the field might be misleading in selection of samples for successful virus isolation. Instead, an on-site molecular assay may enhance the chance for a successful hantavirus isolation.

3.5 HANTAVIRUS NSs PROTEIN AND ITS ROLE IN INTERFERON ANTAGONISM

In **Publication V** the role of hantaviral NSs proteins was investigated in human cells. Analysis of expression patterns of the NSs ORF of six cricetide-borne hantaviruses confirmed a leaky scanning-mediated expression of NSs proteins with a C-terminal HA-tag. This finding obtained from expression plasmid-based transfection studies was confirmed to occur as well during PUUV infection. All tested NSs proteins showed inhibition of a RIG-I induced IFN-I signaling cascade. Deletion of the first initiation codon of the PUUV NSs ORF was accompanied with a loss of IFN-I promoter inhibition in the human cell transfection system and expression of the remaining downstream protein products indicating a prominent role in IFN-I inhibition of the N-terminal part of the NSs protein (**Publication V**). Similar results were previously observed for Bunyamwera orthobunyavirus (BUNV) NSs protein. N-terminally truncated variants of BUNV NSs protein failed to degrade RNA polymerase II and thereby block IFN transcription. In line with these findings PUUV NSs protein missing the N-terminus seems not to be sufficient to block IFN-I induction. However, since we were not able to detect this short peptide or a smaller NSs variant with expression initiating at codon M24 in cells infected with the PUUV variant with the truncated NSs21stop (**Publication V**, Figure 5), we cannot exclude that other viral proteins might play a role in this mechanism in the viral context.

In addition to what was done in **Publication V**, we analyzed IKKε and TBK-1 in HEK 293-T cells, two kinases further downstream within the signaling cascade of RIG-I. Preliminary experiments showed a similar pattern of IKKε inhibition with NSs proteins of PUUV, TULV, PHV, and KHAV reducing the activity to 40-50% (Figure 5a, unpublished data). SNV and ANDV NSs proteins showed reduced inhibition compared to other NSs proteins even though the proteins were clearly expressed in HEK 293-T cells (**Publication V**). Interestingly, when the interaction partner of IKKε, TBK-1, was used in the reporter assay, the inhibition of IFN-β promotor activation was not observed for PUUV, KHAV, SNV, and ANDV NSs proteins (Figure 5b, unpublished data). PHV NSs protein showed minimal inhibition and TULV NSs protein could still block the pathway to 60%. This might indicate a different targeting within the human signaling pathway for the NSs proteins of TULV and PHV compared to PUUV, ANDV, SNV, and KHAV at the TBK-1-IKKε interaction or an expression level dependent effect. To examine if the NSs protein is involved in inhibition of different pathways of the IFN-I-mediated responses, the potential inhibitory effect of the six NSs proteins on the important IFN-I induced JAK/STAT pathway was evaluated. Transfections with the plasmid coding the firefly luciferase under control of an interferon sensitive responsive element (ISRE) promoter showed no influence on its activation by IFN-I by any of the NSs proteins (Figure 5c, unpublished data).

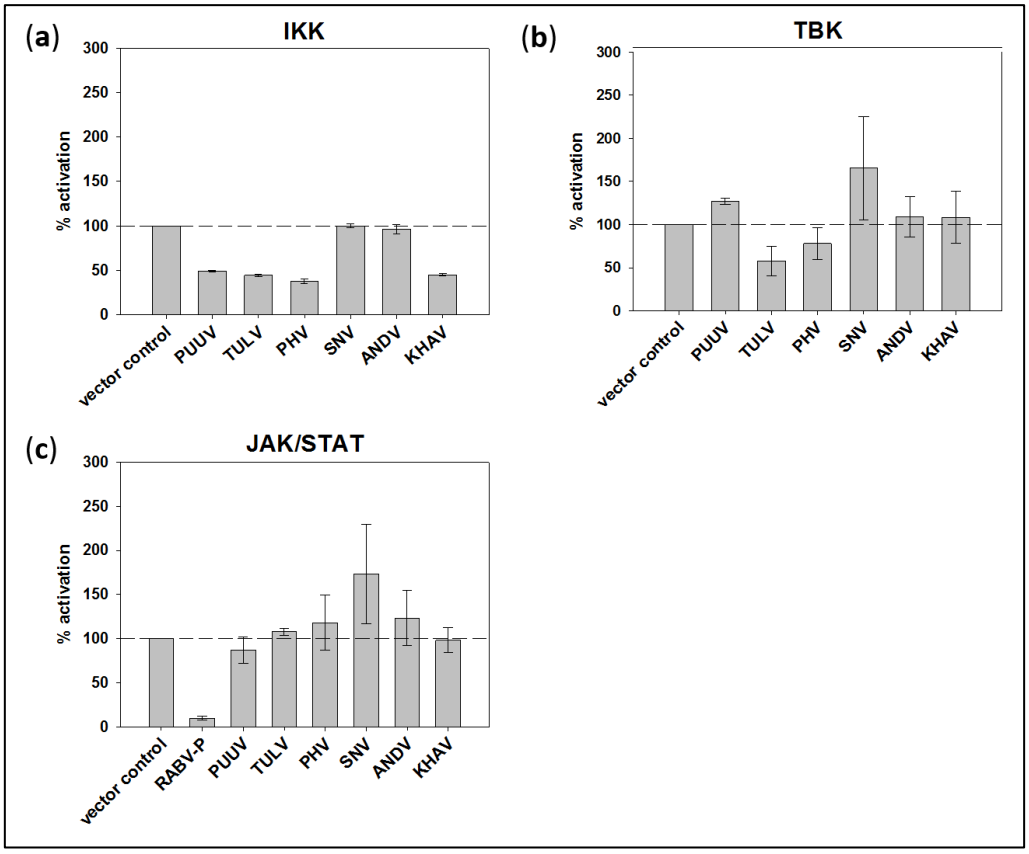

Figure 5: Interferon-β promoter and ISRE reporter assay of different hantaviral NSs ORFs in human HEK 293-T cells. *(a) RIG-I activated IFN-β promoter pathway, (b) IKK activated IFN-β promoter pathway, (c) TBK-1 activated IFN-β promoter pathway, and the JAK/STAT pathway (d). HEK 293 T-cells were transfected with a plasmid DNA mix of 0.5µg p125-FFluc, 0.005µg pRluc, 0.5µg pcDNA3-huRIG I, pcDNA3-huIKKε, or pcDNA3-huTBK-1 and 1µg pcDNA3 plasmid containing the viral NSs coding sequence and analyzed after 18 h with a Dual-Luciferase Reporter Assay System (Promega). RABV-P = Rabies virus phosphoprotein, PUUV = Puumala orthohantavirus, TULV = Tula orthohantavirus, PHV = Prospect Hill orthohantavirus, SNV = Sin Nombre orthohantavirus, ANDV = Andes orthohantavirus, KHAV = Khabarovsk orthohantavirus.*

The results suggest an interference of NSs at the interface of the TBK-1 – IKKε complex. This is supported by a simultaneous study, showing that ANDV NSs protein antagonizes the IFN-I response by inhibiting IFN-I signaling downstream of RIG-I and MDA-5 but upstream of TBK-1 (Otarola et al., 2020). A previous report on the NSs protein of Heartland bandavirus (HRTV), a phenuivirus, showed that HRTV NSs protein inhibits TBK-1 phosphorylation (Rezelj et al., 2017). Another phenuivirus, severe fever with thrombocytopenia syndrome virus (SFTSV), forms cytosolic inclusion bodies containing these signaling host factors (STAT proteins and RIG-I signaling) and thereby preventing their interaction in the IFN-I pathway (Chaudhary et al., 2015; Ning et al., 2015; Rezelj et al., 2017; Hong et al., 2019). We did not determine the exact interaction of the hantaviral NSs proteins. In addition to the signaling pathway for IFN-ß induction, we tested all hantaviral NSs for their influence on the JAK/STAT pathway, a cellular response to cytokines and growth factors (Harrison, 2012). None of the NSs proteins had an impact on its activation indicating a

specific influence on the production of cytokines rather than their downstream mechanisms (Figure 5c, unpublished data).

The NSs proteins of the peribunyaviruses, BUNV and La Crosse orthobunyavirus (LACV), or phleboviruses RVFV and Toscana virus (TOSV), inhibit the IFN-I system by blocking RNA polymerase II transcription or degradation of dsRNA-dependent protein kinase (PKR) (Weber et al., 2002; Billecocq et al., 2004; Thomas et al., 2004; Habjan et al., 2009; Hollidge et al., 2011; Kalveram and Ikegami, 2013). Interestingly, TOSV NSs protein interferes with the production of IFN through targeted activation of IRF-3. This occurs through a RIG-I dependent signaling pathway where interaction between the NSs protein and RIG-I leads to a proteasome-mediated degradation of RIG-I (Gori-Savellini et al., 2013). Thus, the NSs proteins of the different peribunyaviruses, phenuiviruses and hantaviruses (Table 1) all show inhibitory function on interferon signaling but by different mechanisms and target pathways. Different targets for future studies could be IKKε and its suppressor (SIKE), NF-kappa-B essential modulator (NEMO) as a regulatory subunit for IKK complexes or the formation of cytosolic structures as observed for SFTSV (Onoguchi et al., 2011).

It seems unlikely though, that hantavirus persistence and infectivity in humans are regulated exclusively by immune-modulating mechanisms. As already mentioned, during the acute phase of hantavirus infection, a strong CD8 T-cell response is observed. However, no obvious damage of infected endothelial cells has been observed in humans and reservoir, suggesting that hantaviruses, including PUUV, might protect infected cells from being killed by CTLs (Lindgren et al., 2011). Remarkably, activated human natural killer (NK) cells readily killed uninfected cells but infected cells were protected from degradation. Simultaneously, interference of the hantavirus N protein with granzyme B and caspase 3 enzymatic activities was observed (Gupta et al., 2013; Solá-Riera et al., 2019). This suggests that hantaviruses protect infected cells from being killed by CTLs through inhibition of NK cell mediated apoptosis. All together, understanding hantavirus disease pathology is still a challenge and remains to be not completely uncovered.

4. OUTLOOK

The heterogeneous distribution of PUUV in Germany and Europe in general, and the re-occurring outbreak years of the related disease makes it obvious that further surveillance of PUUV and its reservoir is necessary. Future studies will have to evaluate, if the borders of PUUV distribution in Germany will expand to the north/east. The running field study-based monitoring of PUUV strains in bank voles should be accompanied by *in vitro* studies in reservoir cell lines and by animal experiments in different bank vole lineages. This combination of field and laboratory studies will have to prove if new sequence variants will occur that can have impact on host fitness and immune response. Reservoir host sequence analysis can give further insights into host-virus adaptation. Targets, such as integrins or PRRs, and a high sample size should be used for host gene analysis in line with transcriptome analysis of infected and non-infected control animals. Identification of important virus and reservoir gene regions or amino acid exchanges within the encoded proteins involved in host-virus interaction have to be identified for a better understanding of how a persistent infection is established in reservoir hosts without disease manifestation.

Important for such analysis is the availability of PUUV isolates. A first step to generate more PUUV isolates was done in this work by the first isolation of a German strain and providing new cell lines for isolation and infection experiments. However, isolated virus must also be used in animal experiments to understand immune-modulatory mechanisms. Until now, most PUUV isolates are highly adapted to a single cell line. An important factor is that these new isolates should not be highly passaged for infection experiments. Another highly valuable achievement is the generation of new antibodies against the glycoproteins (Gn and Gc). Future studies will have to yield their protective potential and binding capacities. This is important for development of highly specific antibodies for diagnostic and research applications, for identification of therapeutical monoclonal antibodies and development of prophylactic vaccines against hantavirus disease.

Concerning the NSs protein, molecular evolution and expression investigations, as well as a more detailed analysis of inhibition mechanisms and screening of potential cellular interaction partners are needed. Its involvement in other (immune) mechanisms has to be clarified and immunofluorescence analysis, *in situ* hybridization, or correlative light-electron microscopy might give more knowledge about the association of NSs with specific organelles or replication sites and its role IFN inhibition.

The established vole cell lines can be used in future cross-species infection studies of PUUV of a certain clade and the associated bank vole lineage occurring in the same region. This can give insights in the specific adaptation and entry mechanisms of PUUV to its host, that evolved during a long lasting co-evolution scenario. Another highly valuable goal in the future would be the establishment of a vole (or

other hantavirus host) cell line for reporter assays and entry studies. This would give the opportunity to investigate viral proteins, such as NSs protein, RdRP or the glycoproteins, individually for each virus in its specific reservoir host cell. These investigations may compensate the current lack of a reverse genetics system for hantaviruses; otherwise, the novel tools might enhance just the chance to develop a reverse genetics system.

5. SUMMARY

Orthohantaviruses are rodent-borne pathogens distributed all over the world, which do not cause visible disease in their reservoir host. Puumala orthohantavirus (PUUV) causes most human hantavirus disease cases in Europe and is transmitted by the bank vole (*Clethrionomys glareolus*). Hantaviruses have a tri-segmented genome consisting of the large (L) segment, coding for the RNA-dependent RNA polymerase (RdRP), the medium (M) segment, encoding the glycoproteins, and the small (S) segment. The S-segment contains two major overlapping open reading frames (ORF) coding for the nucleocapsid (N) protein and a non-structural (NSs) protein, a putative type I interferon (IFN-I) antagonist. To date, pathogenesis and reservoir host adaptation of hantaviruses are poorly understood due to missing adequate cell culture and animal models.

In contrast to previous studies, in this work, data from spring and summer 2019 indicated a high vole abundance, a high PUUV prevalence in voles and high human incidence for some endemic regions in Germany, but elsewhere values were low to moderate. Regional and local human health institutions need to be aware about the heterogeneous distribution of human PUUV infection risk.

For a better understanding of virus-host associations, two novel cell lines from bank voles and common voles each were generated and their susceptibility and replication capacities for a variety of zoonotic and non-zoonotic viruses were analyzed. The PUUV strain Vranica/Hällnäs showed efficient replication in a new bank vole kidney cell line, but not in four other cell lines of bank and common voles. Vice versa, Tula orthohantavirus (TULV) replicated in the kidney cell line of common voles, but was hampered in its replication in other cell lines. Several viruses, such as Cowpox virus, Vaccinia virus, Rift Valley fever virus, and Encephalomyocarditis virus 1 replicated in all four cell lines. West Nile virus, Usutu virus, Sindbis virus and Tick-borne encephalitis virus replicated only in a part of the cell lines. These results indicate a tissue or species specific tropism for many of the tested viruses and the potential value of vole cell lines to address such questions in detail.

Using one of these new cell lines, the first German PUUV strains were isolated from bank voles caught in the highly endemic region around Osnabrück. Complete genomes were determined by target-enrichment-mediated high-throughput sequencing from original lung tissue, after isolation and after additional passaging in VeroE6 cells and a bank vole-derived kidney cell line. Different single amino acid substitutions were observed in the RdRP of the two stable PUUV isolates. The PUUV strain isolated on VeroE6 cells showed a lower titer when propagated on bank vole cells compared to VeroE6 cells. Additionally, glycoprotein precursor (GPC)-derived virus-like particles of a German PUUV strain from the same region allowed the generation of monoclonal antibodies that reacted with the isolated PUUV strains.

To investigate the role of PUUV and other vole-borne hantavirus NSs proteins, the evolution of the NSs and N encoding sequences was investigated by a field study in bank voles and the NSs sequences were characterized *in vitro* for their inhibitory effect on the human interferon-β promoter. Analysis of blood and lung samples of 851 bank voles trapped during 2010-2014 in Baden-Wuerttemberg and North Rhine-Westphalia resulted in detection of 27.8% PUUV-specific antibody positive bank voles, whereas in 22.3% PUUV-specific RNA was detected. In the hantavirus outbreak years 2010 and 2012 PUUV prevalence in bank voles was higher compared to 2011, 2013 and 2014. Sequences of the S segment of all positive bank voles showed amino acid and nucleotide sequence types of the NSs-ORF with temporal and/or local variation, whereas the N-ORF was highly conserved. One sequence type persisted over the whole observation period in both regions. The NSs coding sequence was highly divergent among regional bank vole populations in the outbreak year 2012.

Transfection experiments resulted in the detection of different products of the NSs-ORF of PUUV, TULV, Prospect Hill and Khabarovsk orthohantaviruses, due to translation initiation at different methionine codons along the coding sequence. Using luciferase reporter assays, the NSs proteins of PUUV, TULV, Prospect Hill and Khabarovsk orthohantaviruses showed inhibition of IFN-I induction of up to 70%, whereas Sin Nombre and Andes orthohantavirus NSs proteins showed a reduced effect compared to the other NSs proteins. The first 20 amino acids of the N-terminal region of PUUV NSs were found to be crucial for IFN-I promoter inhibition.

In conclusion, the newly established cell lines, antibodies, reporter assays and PUUV isolates are highly valuable tools for future hantavirus research. The activity of PUUV NSs protein in human cells contributes to our understanding of virus-host interactions and highlights the importance of corresponding future reservoir host studies. Hantavirus surveillance studies showed the necessity for timely information of the potential human PUUV infection risk to public health institutions in endemic areas to initiate appropriate actions.

6. ZUSAMMENFASSUNG

Orthohantaviren sind Nagetier-assoziierte Viren, die weltweit verbreitet sind und in ihrem Reservoirwirt keine symptomatische Erkrankung hervorrufen. Puumala-Orthohantavirus (PUUV) verursacht in Europa die meisten Hantavirus-Erkrankungen und wird von der Rötelmaus (*Clethrionomys glareolus*) übertragen. Das Genom von Hantaviren ist in drei Segmente gegliedert: das große (L) Segment (kodiert die RNA-abhängige RNA Polymerase (RdRP)), das mittlere (M) Segment (kodiert die Glykoproteine), und das kleine (S) Segment. Das S Segment enthält zwei überlappende offene Leserahmen (ORF). Diese exprimieren ein Nukleokapsidprotein (N) und ein Nicht-Struktur (NSs) Protein, einen potentiellen Typ I-Interferon (IFN-I)-Antagonisten. Bis heute ist über die Pathogenese und Anpassung von Hantaviren an ihren Wirt nur wenig bekannt, was auch daran liegt, dass es keine adäquaten Zellkultur- oder Tiermodelle gibt.

Im Gegensatz zu den genannten früheren Daten zeigten die Untersuchungen von Rötelmäusen aus dem Frühling und Sommer 2019 in dieser Arbeit eine hohe Abundanz an Rötelmäusen und PUUV Prävalenz in Rötelmäusen, sowie eine hohe humane Inzidenz in manchen Endemiegebieten Deutschlands, wohingegen diese Werte in anderen Endemieregionen niedrig waren. Regionale und lokale Gesundheitsämter müssen über das heterogen verteilte Gesundheitsrisiko für die Bevölkerung informiert werden.

Zum besseren Verständnis von Virus-Wirt-Interaktionen wurden in dieser Arbeit neue Zelllinien von Rötel- und Feldmäusen etabliert und auf ihre Suszeptibilität und Replikationsfähigkeit für verschiedene zoonotische und nicht-zoonotische Viren getestet. Der PUUV-Stamm Vranica/Hällnäs replizierte sehr effektiv in nur einer der neuen Rötelmauszelllinien der Niere, aber nicht in den anderen vier untersuchten Rötelmaus- und Feldmauszelllinien. Tula-Orthohantavirus (TULV) hingegen replizierte in Nierenzellen der Feldmaus, aber war in den anderen Zelllinien von Rötel- und Feldmaus stark eingeschränkt. Einige Viren, darunter Kuhpockenvirus, Vaccinia-Virus, Rifttal Fieber-Virus und Enzephalomyokarditis-Virus 1, zeigten in allen Zelllinien eine effektive Replikation, wohingegen sich West Nil-Virus, Usutu-Virus, Sindbis-Virus und Frühsommer-Meningoenzephalitis-Virus nur in einem Teil der Zelllinien vermehren ließen. Diese Ergebnisse lassen einen Spezies- und Gewebe-spezifischen Tropismus für viele der untersuchten Viren vermuten und zeigen, die Bedeutung der Wühlmaus-Zelllinien für zukünftige detaillierte Untersuchungen zu diesen Fragen.

Mit Hilfe einer der neuen Rötelmauszelllinien, konnten die ersten deutschen PUUV-Isolate aus Rötelmäusen isoliert werden, die in der Hochendemieregion um Osnabrück gefangen worden sind. Mit Hilfe einer Target-Enrichment-vermittelten High-Throughput-Sequencing-Technologie wurden PUUV-Komplettgenome für das zugrundeliegende Originalmaterial der Lunge, nach der Isolation und nach Passagieren in VeroE6-Zellen und Rötelmaus-Nierenzellen bestimmt und miteinander verglichen. Hier

wurden einzelne Aminosäureaustausche in der RdRP nach Anzucht bei beiden stabilen Isolaten beobachtet. Ein Isolat aus VeroE6-Zellen, zeigte nach weiteren Passagen auf Rötelmauszellen einen niedrigeren Titer als nach Passage auf VeroE6-Zellen. Außerdem wurden mit Hilfe von virusähnlichen Partikeln, basierend auf der Sequenz für den Glykoprotein-Vorläufer (GPC) eines deutschen PUUV-Stammes aus der gleichen Region, monoklonale Antikörper hergestellt, die mit den neuen Isolaten reagierten.

Zur Analyse des NSs-Proteins von PUUV und anderen Hantaviren wurde zunächst im Rahmen einer Feldstudie die Evolution von NSs- und N-kodierenden Sequenzen des PUUV aus Rötelmäusen untersucht und die NSs-Sequenzen durch in vitro-Studien auf ihren inhibitorischen Einfluss auf den IFN-β Promoter untersucht. Die Analyse von Blut- und Lungenproben von 851 in Baden-Württemberg und Nordrhein-Westfalen in den Jahren 2010-2014 gefangenen Rötelmäusen, zeigte 27.8% positive Rötelmäuse für PUUV-spezifische Antikörper und 22.3% positive Tiere für PUUV-RNA. In den Hantavirus-Ausbruchsjahren 2010 und 2012 war die PUUV-Prävalenz in Rötelmäusen höher als 2011, 2013 und 2014. S-Segment-Sequenzen von allen positiven Tieren zeigten Aminosäure- und DNA-Sequenztypen des NSs-offenen Leserahmens (ORF), die zeitlich und örtlich variierten, wohingegen der N-ORF hoch konserviert war. Ein Sequenztyp pro Fangort dominierte über die gesamte Beobachtungsperiode. Der NSs-ORF unterschied sich stark zwischen PUUV-Stämmen in den regionalen Rötelmauspopulationen im Ausbruchsjahr 2012.

Mittels molekularbiologischer Analysen rekombinanter NSs-Proteine, wurden Expressionsprodukte von drei internen Initiationskodons im NSs identifiziert. Mittels Luziferase-Reporter-Assay wurde die Inhibition von IFN-I durch NSs-Proteine verschiedener Hantaviren bestimmt. PUUV, TULV, Prospect Hill- und Khabarovsk-Orthohantavirus NSs inhibierten die IFN-I-Induktion um bis zu 70%. Sin Nombre- und Andes-Orthohantavirus-NSs Proteine zeigten dagegen einen geringeren Effekt im Vergleich zu den anderen NSs Proteinen. Die 20 N-terminalen Aminosäuren des PUUV-NSs-Proteins stellten sich als besonders wichtig für die Hemmung des IFN-I-Promoters heraus.

Zusammenfassend sind die hier neu eingeführten Zelllinien, Antikörper, Reporter-Assays und PUUV-Isolate wertvolle neue Werkzeuge für die zukünftige Hantavirusforschung. Der Nachweis der Aktivität des NSs-Proteins von PUUV in humanen Zellen trägt zum Verständnis der Virus-Wirt-Interaktionen im Fehlwirt Mensch bei und unterstreicht die Notwendigkeit zukünftiger Studien in einem Rötelmaussystem. Die Surveillancestudien zeigten die Notwendigkeit der zeitnahen Weitergabe von Informationen zum potentiellen Infektionsrisiko der Bevölkerung in Endemiegebieten zur Einleitung geeigneter Gegenmaßnahmen.

7. LITERATURE

Albornoz, A., Hoffmann, A.B., Lozach, P.Y., and Tischler, N.D. (2016). Early Bunyavirus-Host Cell Interactions. Viruses *8*.

Alff, P.J., Gavrilovskaya, I.N., Gorbunova, E., Endriss, K., Chong, Y., Geimonen, E., Sen, N., Reich, N.C., and Mackow, E.R. (2006). The pathogenic NY-1 hantavirus G1 cytoplasmic tail inhibits RIG-I- and TBK-1-directed interferon responses. Journal of virology *80*, 9676-9686.

Avšič-Županc, T., Saksida, A., and Korva, M. (2019). Hantavirus infections. Clinical microbiology and infection *21s*, e6-e16.

Bagamian, K.H., Douglass, R.J., Alvarado, A., Kuenzi, A.J., Amman, B.R., Waller, L.A., and Mills, J.N. (2012). Population density and seasonality effects on Sin Nombre virus transmission in North American deermice (*Peromyscus maniculatus*) in outdoor enclosures. PloS one *7*, e37254.

Bernshtein, A.D., Apekina, N.S., Mikhailova, T.V., Myasnikov, Y.A., Khlyap, L.A., Korotkov, Y.S., and Gavrilovskaya, I.N. (1999). Dynamics of Puumala hantavirus infection in naturally infected bank voles (*Clethrinomys glareolus*). Archives of virology *144*, 2415-2428.

Billecocq, A., Spiegel, M., Vialat, P., Kohl, A., Weber, F., Bouloy, M., and Haller, O. (2004). NSs protein of Rift Valley fever virus blocks interferon production by inhibiting host gene transcription. Journal of virology *78*, 9798-9806.

Björkström, N.K., Lindgren, T., Stoltz, M., Fauriat, C., Braun, M., Evander, M., Michaëlsson, J., Malmberg, K.-J., Klingström, J., Ahlm, C., and Ljunggren, H.-G. (2011). Rapid expansion and long-term persistence of elevated NK cell numbers in humans infected with hantavirus. The Journal of experimental medicine *208*, 13-21.

Borucki, M.K., Boone, J.D., Rowe, J.E., Bohlman, M.C., Kuhn, E.A., DeBaca, R., and St Jeor, S.C. (2000). Role of maternal antibody in natural infection of *Peromyscus maniculatus* with Sin Nombre virus. Journal of virology *74*, 2426-2429.

Botten, J., Mirowsky, K., Kusewitt, D., Bharadwaj, M., Yee, J., Ricci, R., Feddersen, R.M., and Hjelle, B. (2000). Experimental infection model for Sin Nombre hantavirus in the deer mouse (*Peromyscus maniculatus*). Proceedings of the National Academy of Sciences of the United States of America *97*, 10578-10583.

Botten, J., Mirowsky, K., Kusewitt, D., Ye, C., Gottlieb, K., Prescott, J., and Hjelle, B. (2003). Persistent Sin Nombre virus infection in the deer mouse (*Peromyscus maniculatus*) model: sites of replication and strand-specific expression. Journal of virology *77*, 1540-1550.

Brook, C.E., Boots, M., Chandran, K., Dobson, A.P., Drosten, C., Graham, A.L., Grenfell, B.T., Muller, M.A., Ng, M., Wang, L.F., and van Leeuwen, A. (2020). Accelerated viral dynamics in bat cell lines, with implications for zoonotic emergence. eLife *9*.

Chaudhary, V., Zhang, S., Yuen, K.S., Li, C., Lui, P.Y., Fung, S.Y., Wang, P.H., Chan, C.P., Li, D., Kok, K.H., Liang, M., and Jin, D.Y. (2015). Suppression of type I and type III IFN signalling by NSs protein of severe fever with thrombocytopenia syndrome virus through inhibition of STAT1 phosphorylation and activation. The Journal of general virology *96*, 3204-3211.

Chew, T., Noyce, R., Collins, S.E., Hancock, M.H., and Mossman, K.L. (2009). Characterization of the interferon regulatory factor 3-mediated antiviral response in a cell line deficient for IFN production. Molecular immunology *46*, 393-399.

Childs, J.E., Glass, G.E., Korch, G.W., and LeDuc, J.W. (1989). Effects of hantaviral infection on survival, growth and fertility in wild rat (*Rattus norvegicus*) populations of Baltimore, Maryland. Journal of wildlife diseases *25*, 469-476.

Choi, Y., Kwon, Y.C., Kim, S.I., Park, J.M., Lee, K.H., and Ahn, B.Y. (2008). A hantavirus causing hemorrhagic fever with renal syndrome requires gC1qR/p32 for efficient cell binding and infection. Virology *381*, 178-183.

Cifuentes-Munoz, N., Salazar-Quiroz, N., and Tischler, N.D. (2014). Hantavirus Gn and Gc envelope glycoproteins: key structural units for virus cell entry and virus assembly. Viruses *6*, 1801-1822.

Cimica, V., Dalrymple, N.A., Roth, E., Nasonov, A., and Mackow, E.R. (2014). An innate immunity-regulating virulence determinant is uniquely encoded by the Andes virus nucleocapsid protein. mBio *5*.

Dlugolenski, D., Jones, L., Tompkins, S.M., Crameri, G., Wang, L.F., and Tripp, R.A. (2013). Bat cells from *Pteropus alecto* are susceptible to influenza A virus infection and reassortment. Influenza and other respiratory viruses *7*, 900-903.

Dohmae, K., Koshimizu, U., and Nishimune, Y. (1993). *In utero* and mammary transfer of hantavirus antibody from dams to infant rats. Laboratory animal science *43*, 557-561.

Dohmae, K., and Nishimune, Y. (1998). Maternal transfer of hantavirus antibodies in rats. Laboratory animal science *48*, 395-397.

Drewes, S., Ali, H.S., Saxenhofer, M., Rosenfeld, U.M., Binder, F., Cuypers, F., Schlegel, M., Rohrs, S., Heckel, G., and Ulrich, R.G. (2017a). Host-Associated Absence of Human Puumala Virus Infections in Northern and Eastern Germany. Emerging infectious diseases *23*, 83-86.

Drewes, S., Strakova, P., Drexler, J.F., Jacob, J., and Ulrich, R.G. (2017b). Assessing the Diversity of Rodent-Borne Viruses: Exploring of High-Throughput Sequencing and Classical Amplification/Sequencing Approaches. Advances in virus research *99*, 61-108.

Eckerle, I., Corman, V.M., Müller, M.A., Lenk, M., Ulrich, R.G., and Drosten, C. (2014a). Replicative Capacity of MERS Coronavirus in Livestock Cell Lines. Emerging infectious diseases *20*, 276-279.

Eckerle, I., Lenk, M., and Ulrich, R.G. (2014b). More novel hantaviruses and diversifying reservoir hosts-time for development of reservoir-derived cell culture models? Viruses *6*, 951-967.

Emeny, J.M., and Morgan, M.J. (1978). Regulation of the Interferon System: Evidence that Vero Cells have a Genetic Defect in Interferon Production. J gen Virol, 247-252.

Essbauer, S.S., Krautkrämer, E., Herzog, S., and Pfeffer, M. (2011). A new permanent cell line derived from the bank vole (*Myodes glareolus*) as cell culture model for zoonotic viruses. Virology journal *8*, 339.

Faber, M., Krüger, D.H., Auste, B., Stark, K., Hofmann, J., and Weiss, S. (2019). Molecular and epidemiological characteristics of human Puumala and Dobrava-Belgrade hantavirus infections, Germany, 2001 to 2017. Euro surveillance *24*.

French, G.R., Foulke, R.S., Brand, O.A., Eddy, G.A., Lee, H.W., and Lee, P.W. (1981). Korean hemorrhagic fever: propagation of the etiologic agent in a cell line of human origin. Science (New York, NY) *211*, 1046-1048.

Frese, M., Kochs, G., Feldmann, H., Hertkorn, C., and Haller, O. (1996). Inhibition of bunyaviruses, phleboviruses, and hantaviruses by human MxA protein. Journal of virology *70*, 915-923.

García, M., Iglesias, A., Landoni, V.I., Bellomo, C., Bruno, A., Córdoba, M.T., Balboa, L., Fernández, G.C., Sasiain, M.d.C., Martínez, V.P., and Schierloh, P. (2017). Massive plasmablast response elicited in the acute phase of hantavirus pulmonary syndrome. Immunology *151*, 122-135.

Garcin, D., Lezzi, M., Dobbs, M., Elliott, R.M., Schmaljohn, C., Kang, C.Y., and Kolakofsky, D. (1995). The 5' ends of Hantaan virus (Bunyaviridae) RNAs suggest a prime-and-realign mechanism for the initiation of RNA synthesis. Journal of virology *69*, 5754-5762.

Gavrilovskaya, I.N., Brown, E.J., Ginsberg, M.H., and Mackow, E.R. (1999). Cellular entry of hantaviruses which cause hemorrhagic fever with renal syndrome is mediated by beta3 integrins. Journal of virology *73*, 3951-3959.

Geimonen, E., Neff, S., Raymond, T., Kocer, S.S., Gavrilovskaya, I.N., and Mackow, E.R. (2002). Pathogenic and nonpathogenic hantaviruses differentially regulate endothelial cell responses. Proceedings of the National Academy of Sciences of the United States of America *99*, 13837-13842.

Gori-Savellini, G., Valentini, M., and Cusi, M.G. (2013). Toscana virus NSs protein inhibits the induction of type I interferon by interacting with RIG-I. Journal of virology *87*, 6660-6667.

Gu, S.H., Markowski, J., Kang, H.J., Hejduk, J., Sikorska, B., Liberski, P.P., and Yanagihara, R. (2013). Boginia virus, a newfound hantavirus harbored by the Eurasian water shrew (*Neomys fodiens*) in Poland. Virology journal *10*, 160.

Gupta, S., Braun, M., Tischler, N.D., Stoltz, M., Sundström, K.B., Björkström, N.K., Ljunggren, H.G., and Klingström, J. (2013). Hantavirus-infection confers resistance to cytotoxic lymphocyte-mediated apoptosis. PLoS pathogens *9*, e1003272.

Habjan, M., Andersson, I., Klingström, J., Schümann, M., Martin, A., Zimmermann, P., Wagner, V., Pichlmair, A., Schneider, U., Mühlberger, E., Mirazimi, A., and Weber, F. (2008). Processing of genome 5' termini as a strategy of negative-strand RNA viruses to avoid RIG-I-dependent interferon induction. PloS one *3*, e2032.

Habjan, M., Pichlmair, A., Elliott, R.M., Overby, A.K., Glatter, T., Gstaiger, M., Superti-Furga, G., Unger, H., and Weber, F. (2009). NSs protein of Rift Valley fever virus induces the specific degradation of the double-stranded RNA-dependent protein kinase. Journal of virology *83*, 4365-4375.

Haller, O., Kochs, G., and Weber, F. (2007). Interferon, Mx, and viral countermeasures. Cytokine & growth factor reviews *18*, 425-433.

Han, B.A., Schmidt, J.P., Bowden, S.E., and Drake, J.M. (2015a). Rodent reservoirs of future zoonotic diseases. Proceedings of the National Academy of Sciences of the United States of America *112*, 7039-7044.

Han, H.J., Wen, H.L., Zhou, C.M., Chen, F.F., Luo, L.M., Liu, J.W., and Yu, X.J. (2015b). Bats as reservoirs of severe emerging infectious diseases. Virus research *205*, 1-6.

Handke, W., Oelschlegel, R., Franke, R., Wiedemann, L., Krüger, D.H., and Rang, A. (2010). Generation and characterization of genetic reassortants between Puumala and Prospect Hill hantavirus in vitro. The Journal of general virology *91*, 2351-2359.

Hannah, M.F., Bajic, V.B., and Klein, S.L. (2008). Sex differences in the recognition of and innate antiviral responses to Seoul virus in Norway rats. Brain, behavior, and immunity *22*, 503-516.

Harrison, D.A. (2012). The Jak/STAT pathway. Cold Spring Harb Perspect Biol *4*.

Hedil, M., and Kormelink, R. (2016). Viral RNA Silencing Suppression: The Enigma of Bunyavirus NSs Proteins. Viruses *8*.

Hepojoki, J., Strandin, T., Lankinen, H., and Vaheri, A. (2012). Hantavirus structure--molecular interactions behind the scene. The Journal of general virology *93*, 1631-1644.

Hepojoki, J., Strandin, T., Vaheri, A., and Lankinen, H. (2009). Interactions and Oligomerization of Hantavirus Glycoproteins. Journal of virology *84*, 227-242.

Hepojoki, J., Strandin, T., Wang, H., Vapalahti, O., Vaheri, A., and Lankinen, H. (2010). Cytoplasmic tails of hantavirus glycoproteins interact with the nucleocapsid protein. The Journal of general virology *91*, 2341-2350.

Hepojoki, J., Vaheri, A., and Strandin, T. (2014). The fundamental role of endothelial cells in hantavirus pathogenesis. Front Microbiol *5*, 727.

Heyman, P., Ceianu, S., Christova, I., Tordo, N., and Vaheri, A. (2011). A five-year perspective on the situation of haemorrhagic fever with renal syndrome and status of the hantavirus reservoirs in Europe, 2005–2010. Eurosurveillance *16*.

Heyman, P., Plyusnina, A., Berny, P., Cochez, C., Artois, M., Zizi, M., Pirnay, J.P., and Plyusnin, A. (2004). Seoul hantavirus in Europe: first demonstration of the virus genome in wild *Rattus norvegicus* captured in France. Eur J Clin Microbiol Infect Dis *23*, 711-717.

Hoffmann, M., Nehlmeier, I., Brinkmann, C., Krähling, V., Behner, L., Moldenhauer, A.S., Krüger, N., Nehls, J., Schindler, M., Hoenen, T., Maisner, A., Becker, S., and Pöhlmann, S. (2019). Tetherin Inhibits Nipah Virus but Not Ebola Virus Replication in Fruit Bat Cells. Journal of virology *93*.

Hollidge, B.S., Weiss, S.R., and Soldan, S.S. (2011). The role of interferon antagonist, non-structural proteins in the pathogenesis and emergence of arboviruses. Viruses *3*, 629-658.

Holmes, E.C., and Zhang, Y.Z. (2015). The evolution and emergence of hantaviruses. Current opinion in virology *10*, 27-33.

Hong, Y., Bai, M., Qi, X., Li, C., Liang, M., Li, D., Cardona, C.J., and Xing, Z. (2019). Suppression of the IFN-alpha and -beta Induction through Sequestering IRF7 into Viral Inclusion Bodies by Nonstructural Protein NSs in Severe Fever with Thrombocytopenia Syndrome Bunyavirus Infection. Journal of immunology (Baltimore, Md : 1950) *202*, 841-856.

Hui, D.S., E, I.A., Madani, T.A., Ntoumi, F., Kock, R., Dar, O., Ippolito, G., McHugh, T.D., Memish, Z.A., Drosten, C., Zumla, A., and Petersen, E. (2020). The continuing 2019-nCoV epidemic threat of novel coronaviruses to global health - The latest 2019 novel coronavirus outbreak in Wuhan, China. International journal of infectious diseases *91*, 264-266.

Huiskonen, J.T., Hepojoki, J., Laurinmäki, P., Vaheri, A., Lankinen, H., Butcher, S.J., and Grünewald, K. (2010). Electron cryotomography of Tula hantavirus suggests a unique assembly paradigm for enveloped viruses. Journal of virology *84*, 4889-4897.

Hussein, I.T., Haseeb, A., Haque, A., and Mir, M.A. (2011). Recent advances in hantavirus molecular biology and disease. Advances in applied microbiology *74*, 35-75.

ICTV (2020). International Committee on Taxonomy of Viruses. https://talk.ictvonline.org/taxonomy/, *30-06-2020*.

Jääskelainen, K.M., Kaukinen, P., Minskaya, E.S., Plyusnina, A., Vapalahti, O., Elliott, R.M., Weber, F., Vaheri, A., and Plyusnin, A. (2007). Tula and Puumala hantavirus NSs ORFs are functional and the products inhibit activation of the interferon-beta promoter. Journal of medical virology *79*, 1527-1536.

Jääskelainen, K.M., Plyusnina, A., Lundkvist, A., Vaheri, A., and Plyusnin, A. (2008). Tula hantavirus isolate with the full-length ORF for nonstructural protein NSs survives for more consequent passages in interferon-competent cells than the isolate having truncated NSs ORF. Virology journal *5*, 3.

Jacob, J., Manson, P., Barfknecht, R., and Fredricks, T. (2014). Common vole (*Microtus arvalis*) ecology and management: implications for risk assessment of plant protection products. Pest management science *70*, 869-878.

Jangra, R.K., Herbert, A.S., Li, R., Jae, L.T., Kleinfelter, L.M., Slough, M.M., Barker, S.L., Guardado-Calvo, P., Roman-Sosa, G., Dieterle, M.E., Kuehne, A.I., Muena, N.A., Wirchnianski, A.S., Nyakatura, E.K., Fels, J.M., Ng, M., Mittler, E., Pan, J., Bharrhan, S., Wec, A.Z., Lai, J.R., Sidhu, S.S., Tischler, N.D., Rey, F.A., Moffat, J., Brummelkamp, T.R., Wang, Z., Dye, J.M., and Chandran, K. (2018). Protocadherin-1 is essential for cell entry by New World hantaviruses. Nature *563*, 559-563.

Jayaraman, B., Smith, A.M., Fernandes, J.D., and Frankel, A.D. (2016). Oligomeric viral proteins: small in size, large in presence. Critical reviews in biochemistry and molecular biology *51*, 379-394.

Jeske, K., Hiltbrunner, M., Drewes, S., Ryll, R., Wenk, M., Špakova, A., Petraitytė-Burneikienė, R., Heckel, G., and Ulrich, R.G. (2019a). Field vole-associated Traemmersee hantavirus from Germany represents a novel hantavirus species. Virus genes *55*, 848-853.

Jeske, K., Weber, S., Pfaff, F., Imholt, C., Jacob, J., Beer, M., Ulrich, R.G., and Hoffmann, D. (2019b). Molecular Detection and Characterization of the First Cowpox Virus Isolate Derived from a Bank Vole. Viruses *11*.

Jiang, H., Zheng, X., Wang, L., Du, H., Wang, P., and Bai, X. (2017). Hantavirus infection: a global zoonotic challenge. Virologica Sinica *32*, 32-43.

Jin, M., Park, J., Lee, S., Park, B., Shin, J., Song, K.J., Ahn, T.I., Hwang, S.Y., Ahn, B.Y., and Ahn, K. (2002). Hantaan virus enters cells by clathrin-dependent receptor-mediated endocytosis. Virology *294*, 60-69.

Kallio, E.R., Begon, M., Henttonen, H., Koskela, E., Mappes, T., Vaheri, A., and Vapalahti, O. (2009). Cyclic hantavirus epidemics in humans--predicted by rodent host dynamics. Epidemics *1*, 101-107.

Kallio, E.R., Klingström, J., Gustafsson, E., Manni, T., Vaheri, A., Henttonen, H., Vapalahti, O., and Lundkvist, A. (2006a). Prolonged survival of Puumala hantavirus outside the host: evidence for indirect transmission via the environment. The Journal of general virology *87*, 2127-2134.

Kallio, E.R., Poikonen, A., Vaheri, A., Vapalahti, O., Henttonen, H., Koskela, E., and Mappes, T. (2006b). Maternal antibodies postpone hantavirus infection and enhance individual breeding success. Proceedings Biological sciences *273*, 2771-2776.

Kallio, E.R., Voutilainen, L., Vapalahti, O., Vaheri, A., Henttonen, H., Koskela, E., and Mappes, T. (2007). Endemic hantavirus infection impairs the winter survival of its rodent host. Ecology *88*, 1911-1916.

Kalveram, B., and Ikegami, T. (2013). Toscana virus NSs protein promotes degradation of double-stranded RNA-dependent protein kinase. Journal of virology *87*, 3710-3718.

Kanerva, M., Melen, K., Vaheri, A., and Julkunen, I. (1996). Inhibition of Puumala and Tula hantaviruses in Vero cells by MxA protein. Virology *224*, 55-62.

Kang, H.J., Bennett, S.N., Sumibcay, L., Arai, S., Hope, A.G., Mocz, G., Song, J.W., Cook, J.A., and Yanagihara, R. (2009). Evolutionary insights from a genetically divergent hantavirus harbored by the European common mole (*Talpa europaea*). PloS one *4*, e6149.

Kariwa, H., Kimura, M., Yoshizumi, S., Arikawa, J., Yoshimatsu, K., Takashima, I., and Hashimoto, N. (1996). Modes of Seoul virus infections: persistency in newborn rats and transiency in adult rats. Archives of virology *141*, 2327-2338.

Kaukinen, P., Vaheri, A., and Plyusnin, A. (2005). Hantavirus nucleocapsid protein: a multifunctional molecule with both housekeeping and ambassadorial duties. Archives of virology *150*, 1693-1713.

Kell, A.M., and Gale, M., Jr. (2015). RIG-I in RNA virus recognition. Virology *479-480*, 110-121.

Klein, S.L., Bird, B.H., and Glass, G.E. (2001). Sex differences in immune responses and viral shedding following Seoul virus infection in Norway rats. The American journal of tropical medicine and hygiene *65*, 57-63.

Klempa, B., Avsic-Zupanc, T., Clement, J., Dzagurova, T.K., Henttonen, H., Heyman, P., Jakab, F., Kruger, D.H., Maes, P., Papa, A., Tkachenko, E.A., Ulrich, R.G., Vapalahti, O., and Vaheri, A. (2013). Complex evolution and epidemiology of Dobrava-Belgrade hantavirus: definition of genotypes and their characteristics. Archives of virology *158*, 521-529.

Klingström, J., Akerström, S., Hardestam, J., Stoltz, M., Simon, M., Falk, K.I., Mirazimi, A., Rottenberg, M., and Lundkvist, A. (2006a). Nitric oxide and peroxynitrite have different antiviral effects against hantavirus replication and free mature virions. European journal of immunology *36*, 2649-2657.

Klingström, J., Hardestam, J., Stoltz, M., Zuber, B., Lundkvist, A., Linder, S., and Ahlm, C. (2006b). Loss of cell membrane integrity in Puumala hantavirus-infected patients correlates with levels of epithelial cell apoptosis and perforin. Journal of virology *80*, 8279-8282.

Klingström, J., Heyman, P., Escutenaire, S., Sjolander, K.B., De Jaegere, F., Henttonen, H., and Lundkvist, A. (2002). Rodent host specificity of European hantaviruses: evidence of Puumala virus interspecific spillover. Journal of medical virology *68*, 581-588.

Klingström, J., Smed-Sörensen, A., Maleki, K.T., Solà-Riera, C., Ahlm, C., Björkström, N.K., and Ljunggren, H.G. (2019). Innate and adaptive immune responses against human Puumala virus infection: immunopathogenesis and suggestions for novel treatment strategies for severe hantavirus-associated syndromes. Journal of Internal Medicine *285*, 510-523.

Kopp, A., Gillespie, T.R., Hobelsberger, D., Estrada, A., Harper, J.M., Miller, R.A., Eckerle, I., Müller, M.A., Podsiadlowski, L., Leendertz, F.H., Drosten, C., and Junglen, S. (2013). Provenance and geographic spread of St. Louis encephalitis virus. mBio *4*, e00322-00313.

Kraus, A.A., Raftery, M.J., Giese, T., Ulrich, R., Zawatzky, R., Hippenstiel, S., Suttorp, N., Kruger, D.H., and Schonrich, G. (2004). Differential antiviral response of endothelial cells after infection with pathogenic and nonpathogenic hantaviruses. Journal of virology *78*, 6143-6150.

Krautkrämer, E., and Zeier, M. (2008). Hantavirus causing hemorrhagic fever with renal syndrome enters from the apical surface and requires decay-accelerating factor (DAF/CD55). Journal of virology *82*, 4257-4264.

Krautkrämer, E., Zeier, M., and Plyusnin, A. (2013). Hantavirus infection: an emerging infectious disease causing acute renal failure. Kidney international *83*, 23-27.

Kruger, D.H., Figueiredo, L.T., Song, J.W., and Klempa, B. (2015). Hantaviruses--globally emerging pathogens. Journal of clinical virology *64*, 128-136.

Kühl, A., Hoffmann, M., Müller, M.A., Munster, V.J., Gnirss, K., Kiene, M., Tsegaye, T.S., Behrens, G., Herrler, G., Feldmann, H., Drosten, C., and Pöhlmann, S. (2011). Comparative analysis of Ebola virus glycoprotein interactions with human and bat cells. The Journal of infectious diseases *204 Suppl 3*, S840-849.

Laenen, L., Vergote, V., Kafetzopoulou, L.E., Wawina, T.B., Vassou, D., Cook, J.A., Hugot, J.P., Deboutte, W., Kang, H.J., Witkowski, P.T., Koppen-Rung, P., Kruger, D.H., Lickova, M., Stang, A., Strieskova, L., Szemes, T., Markowski, J., Hejduk, J., Kafetzopoulos, D., Van Ranst, M., Yanagihara, R., Klempa, B., and Maes, P. (2018). A Novel Hantavirus of the European Mole, Bruges Virus, Is Involved in Frequent Nova Virus Coinfections. Genome Biol Evol *10*, 45-55.

Latus, J., Schwab, M., Tacconelli, E., Pieper, F.M., Wegener, D., Dippon, J., Müller, S., Zakim, D., Segerer, S., Kitterer, D., Priwitzer, M., Mezger, B., Walter-Frank, B., Corea, A., Wiedenmann, A., Brockmann, S., Pohlmann, C., Alscher, M.D., and Braun, N. (2015). Clinical course and long-term outcome of hantavirus-associated nephropathia epidemica, Germany. Emerging infectious diseases *21*, 76-83.

Lee, H.W., Baek, L.J., and Johnson, K.M. (1982). Isolation of Hantaan virus, the etiologic agent of Korean hemorrhagic fever, from wild urban rats. The Journal of infectious diseases *146*, 638-644.

Lee, H.W., Lee, P.W., Baek, L.J., Song, C.K., and Seong, I.W. (1981). Intraspecific transmission of Hantaan virus, etiologic agent of Korean hemorrhagic fever, in the rodent *Apodemus agrarius*. The American journal of tropical medicine and hygiene *30*, 1106-1112.

Lee, H.W., Lee, P.W., and Johnson, K.M. (1978). Isolation of the etiologic agent of Korean Hemorrhagic fever. The Journal of infectious diseases *137*, 298-308.

Lee, M., Lee, J.S., and Kim, B.K. (1983). Disseminated intravascular coagulation in Korean hemorrhagic fever. Bibliotheca haematologica, 181-199.

Levine, J.R., Prescott, J., Brown, K.S., Best, S.M., Ebihara, H., and Feldmann, H. (2010). Antagonism of type I interferon responses by New World hantaviruses. Journal of virology *84*, 11790-11801.

Linderholm, M., Bjermer, L., Juto, P., Roos, G., Sandström, T., Settergren, B., and Tärnvik, A. (1993). Local host response in the lower respiratory tract in nephropathia epidemica. Scandinavian journal of infectious diseases *25*, 639-646.

Lindgren, T., Ahlm, C., Mohamed, N., Evander, M., Ljunggren, H.G., and Björkström, N.K. (2011). Longitudinal Analysis of the Human T Cell Response during Acute Hantavirus Infection. Journal of virology *85*, 10252-10260.

Lozach, P.Y., Mancini, R., Bitto, D., Meier, R., Oestereich, L., Overby, A.K., Pettersson, R.F., and Helenius, A. (2010). Entry of bunyaviruses into mammalian cells. Cell Host Microbe *7*, 488-499.

Luis, A.D., Douglass, R.J., Mills, J.N., and Bjornstad, O.N. (2010). The effect of seasonality, density and climate on the population dynamics of Montana deer mice, important reservoir hosts for Sin Nombre hantavirus. The Journal of animal ecology *79*, 462-470.

Lundkvist, A., Cheng, Y., Sjölander, K.B., Niklasson, B., Vaheri, A., and Plyusnin, A. (1997). Cell Culture Adaptation of Puumala Hantavirus Changes the Infectivity for Its Natural Reservoir, *Clethrionomys glareolus*, and Leads to Accumulation of Mutants with Altered Genomic RNA S Segment. Journal of virology *Vol. 71*, p. 9515–9523.

Lyubsky, S., Gavrilovskaya, I., Luft, B., and Mackow, E. (1996). Histopathology of Peromyscus leucopus naturally infected with pathogenic NY-1 hantaviruses: pathologic markers of HPS viral infection in mice. Laboratory investigation; a journal of technical methods and pathology *74*, 627-633.

Mackow, E.R., and Gavrilovskaya, I.N. (2001). Cellular receptors and hantavirus pathogenesis. Current topics in microbiology and immunology *256*, 91-115.

Manigold, T., and Vial, P. (2014). Human hantavirus infections: epidemiology, clinical features, pathogenesis and immunology. Swiss medical weekly *144*, w13937.

Marsh, G.A., de Jong, C., Barr, J.A., Tachedjian, M., Smith, C., Middleton, D., Yu, M., Todd, S., Foord, A.J., Haring, V., Payne, J., Robinson, R., Broz, I., Crameri, G., Field, H.E., and Wang, L.F. (2012). Cedar virus: a novel Henipavirus isolated from Australian bats. PLoS pathogens *8*, e1002836.

Matthys, V., Gorbunova, E.E., Gavrilovskaya, I.N., Pepini, T., and Mackow, E.R. (2011). The C-terminal 42 residues of the Tula virus Gn protein regulate interferon induction. Journal of virology *85*, 4752-4760.

Michelitsch, A., Tews, B.A., Klaus, C., Bestehorn-Willmann, M., Dobler, G., Beer, M., and Wernike, K. (2019a). *In Vivo* Characterization of Tick-Borne Encephalitis Virus in Bank Voles (*Myodes glareolus*). Viruses *11*.

Michelitsch, A., Wernike, K., Klaus, C., Dobler, G., and Beer, M. (2019b). Exploring the Reservoir Hosts of Tick-Borne Encephalitis Virus. Viruses *11*.

Mir, M.A., Duran, W.A., Hjelle, B.L., Ye, C., and Panganiban, A.T. (2008). Storage of cellular 5' mRNA caps in P bodies for viral cap-snatching. Proceedings of the National Academy of Sciences of the United States of America *105*, 19294-19299.

Mourya, D.T., Lakra, R.J., Yadav, P.D., Tyagi, P., Raut, C.G., Shete, A.M., and Singh, D.K. (2013). Establishment of cell line from embryonic tissue of *Pipistrellus ceylonicus* bat species from India & its susceptibility to different viruses. The Indian journal of medical research *138*, 224-231.

Müller, A., Baumann, A., Essbauer, S., Radosa, L., Krüger, D.H., Witkowski, P.T., Zeier, M., and Krautkrämer, E. (2019). Analysis of the integrin beta3 receptor for pathogenic orthohantaviruses in rodent host species. Virus research *267*, 36-40.

Murphy, K., Travers, P., and Walport, M. (2008). Janeway´s Immunobiology. Garland Science *7th edition*.

Nau, L.H., Emirhar, D., Obiegala, A., Mylius, M., Runge, M., Jacob, J., Bier, N., Nöckler, K., Imholt, C., Below, D., Princk, C., Dreesman, J., Ulrich, R.G., Pfeffer, M., and Mayer-Scholl, A. (2019). Leptospirosis in Germany: current knowledge on pathogen species, reservoir hosts, and disease in humans and animals. Bundesgesundheitsblatt, Gesundheitsforschung, Gesundheitsschutz *62*, 1510-1521.

Nemirov, K., Lundkvist, A., Vaheri, A., and Plyusnin, A. (2003). Adaptation of Puumala Hantavirus to Cell Culture Is Associated with Point Mutations in the Coding Region of the L Segment and in the Noncoding Regions of the S Segment. Journal of virology *77*, 8793-8800.

Netski, D., Thran, B.H., and St Jeor, S.C. (1999). Sin Nombre virus pathogenesis in Peromyscus maniculatus. Journal of virology *73*, 585-591.

Nichol, S.T., Spiropoulou, C.F., Morzunov, S., Rollin, P.E., Ksiazek, T.G., Feldmann, H., Sanchez, A., Childs, J., Zaki, S., and Peters, C.J. (1993). Genetic identification of a hantavirus associated with an outbreak of acute respiratory illness. Science (New York, NY) *262*, 914-917.

Niklasson, B., and Le Duc, J. (1984). Isolation of the nephropathia epidemica agent in Sweden. Lancet (London, England) *1*, 1012-1013.

Ning, Y.J., Feng, K., Min, Y.Q., Cao, W.C., Wang, M., Deng, F., Hu, Z., and Wang, H. (2015). Disruption of type I interferon signaling by the nonstructural protein of severe fever with thrombocytopenia syndrome virus via the hijacking of STAT2 and STAT1 into inclusion bodies. Journal of virology *89*, 4227-4236.

Oelschlegel, R., Krüger, D.H., and Rang, A. (2007). MxA-independent inhibition of Hantaan virus replication induced by type I and type II interferon in vitro. Virus research *127*, 100-105.

Onoguchi, K., Takahasi, K., Yoneyama, M., and Fujita, T. (2011). Type I interferon production by viruses. In Viruses and Interferon: Current Research, K. Mossman, ed. (Caister Academic Press), pp. 19-30.

Otarola, J.V., Solis, L., Lowy, F., Olguin, V., Angulo, J., Pino, K., Tischler, N.D., Otth, C., Padula, P., and Lopez-Lastra, M. (2020). The Andes orthohantavirus NSs protein antagonizes the type I interferon response by inhibiting MAVS signaling. Journal of virology.

Padula, Edelstein A, Miguel SD, López NM, Rossi CM, and RD, R. (1998). Hantavirus pulmonary syndrome outbreak in Argentina: molecular evidence for person-toperson transmission of Andes virus. Virology *241*, 323–330.

Pensiero, M.N., Sharefkin, J.B., Dieffenbach, C.W., and Hay, J. (1992). Hantaan virus infection of human endothelial cells. Journal of virology *66*, 5929-5936.

Plyusnin, A., Vapalahti, O., Lankinen, H., Lehväslaiho, H., Apekina, N., Myasnikov, Y., Kallio-Kokko, H., Henttonen, H., Lundkvist, A., Brummer-Korvenkontio, M., Gavrilovskaia, I.N., and Vaheri, A. (1994). Tula Virus: a Newly Detected Hantavirus Carried by European Common Voles. Journal of virology *68*, p. 7833-7839.

Radosa, L., Schlegel, M., Gebauer, P., Ansorge, H., Heroldova, M., Jánová, E., Stanko, M., Mosansky, L., Fricova, J., Pejcoch, M., Suchomel, J., Purchart, L., Groschup, M.H., Krüger, D.H., Ulrich, R.G., and Klempa, B. (2013). Detection of shrew-borne hantavirus in Eurasian pygmy shrew (*Sorex minutus*) in Central Europe. Infection, genetics and evolution *19*, 403-410.

Raftery, M.J., Kraus, A.A., Ulrich, R., Krüger, D.H., and Schönrich, G. (2002). Hantavirus infection of dendritic cells. Journal of virology *76*, 10724-10733.

Raj, V.S., Mou, H., Smits, S.L., Dekkers, D.H., Muller, M.A., Dijkman, R., Muth, D., Demmers, J.A., Zaki, A., Fouchier, R.A., Thiel, V., Drosten, C., Rottier, P.J., Osterhaus, A.D., Bosch, B.J., and Haagmans, B.L. (2013). Dipeptidyl peptidase 4 is a functional receptor for the emerging human coronavirus-EMC. Nature *495*, 251-254.

Ramanathan, H.N., Chung, D.H., Plane, S.J., Sztul, E., Chu, Y.K., Guttieri, M.C., McDowell, M., Ali, G., and Jonsson, C.B. (2007). Dynein-dependent transport of the Hantaan virus nucleocapsid protein to the endoplasmic reticulum-Golgi intermediate compartment. Journal of virology *81*, 8634-8647.

Ramanathan, H.N., and Jonsson, C.B. (2008). New and Old World hantaviruses differentially utilize host cytoskeletal components during their life cycles. Virology *374*, 138-150.

Randall, R.E., and Goodbourn, S. (2008). Interferons and viruses: an interplay between induction, signalling, antiviral responses and virus countermeasures. The Journal of general virology *89*, 1-47.

Rang, A. (2010). Modulation of innate immune responses by hantaviruses. Critical reviews in immunology *30*, 515-527.

Rang, A., Heider, H., Ulrich, R., and Krüger, D.H. (2006). A novel method for cloning of non-cytolytic viruses. Journal of virological methods *135*, 26-31.

Reguera, J., Weber, F., and Cusack, S. (2010). Bunyaviridae RNA polymerases (L-protein) have an N-terminal, influenza-like endonuclease domain, essential for viral cap-dependent transcription. PLoS pathogens *6*, e1001101.

Reil, D., Binder, F., Freise, J., Imholt, C., Beyrer, K., Jacob, J., H. Krüger, D., Hofmann, J., Dreesman, J., and Ulrich, R.G. (2018). Hantaviren in Deutschland: Aktuelle Erkenntnisse zu Erreger, Reservoir, Verbreitung und Prognosemodellen. Berliner und Münchener tierarztliche Wochenschrift. ePub.

Reil, D., Imholt, C., Eccard, J.A., and Jacob, J. (2015). Beech Fructification and Bank Vole Population Dynamics - Combined Analyses of Promoters of Human Puumala Virus Infections in Germany. PloS one *10*, e0134124.

Reil, D., Rosenfeld, U.M., Imholt, C., Schmidt, S., Ulrich, R.G., Eccard, J.A., and Jacob, J. (2017). Puumala hantavirus infections in bank vole populations: host and virus dynamics in Central Europe. BMC ecology *17*, 9.

Reuter, M., and Krüger, D.H. (2017). The nucleocapsid protein of hantaviruses: much more than a genome-wrapping protein. Virus genes *54*, 5-16.

Rezelj, V.V., Li, P., Chaudhary, V., Elliott, R.M., Jin, D.Y., and Brennan, B. (2017). Differential Antagonism of Human Innate Immune Responses by Tick-Borne Phlebovirus Nonstructural Proteins. mSphere *2*.

Robert-Koch-Institut (2020). Hantavirus Infektionen.
https://www.rki.de/DE/Content/InfAZ/H/Hantavirus/Hantavirus.html, *04-15-2020*.

Ronnberg, T., Jääskelainen, K., Blot, G., Parviainen, V., Vaheri, A., Renkonen, R., Bouloy, M., and Plyusnin, A. (2012). Searching for cellular partners of hantaviral nonstructural protein NSs: Y2H screening of mouse cDNA library and analysis of cellular interactome. PloS one *7*, e34307.

Rowe, R.K., Suszko, J.W., and Pekosz, A. (2008). Roles for the recycling endosome, Rab8, and Rab11 in hantavirus release from epithelial cells. Virology *382*, 239-249.

Sanada, T., Seto, T., Ozaki, Y., Saasa, N., Yoshimatsu, K., Arikawa, J., Yoshii, K., and Kariwa, H. (2012). Isolation of Hokkaido virus, genus Hantavirus, using a newly established cell line derived from the kidney of the grey red-backed vole (*Myodes rufocanus bedfordiae*). The Journal of general virology *93*, 2237-2246.

Schlegel, M., Radosa, L., Rosenfeld, U.M., Schmidt, S., Triebenbacher, C., Lohr, P.W., Fuchs, D., Heroldova, M., Janova, E., Stanko, M., Mosansky, L., Fricova, J., Pejcoch, M., Suchomel, J., Purchart, L., Groschup, M.H., Kruger, D.H., Klempa, B., and Ulrich, R.G. (2012). Broad geographical distribution and high genetic diversity of shrew-borne Seewis hantavirus in Central Europe. Virus genes *45*, 48-55.

Schmaljohn, C.S., Hasty, S.E., Dalrymple, J.M., LeDuc, J.W., Lee, H.W., von Bonsdorff, C.H., Brummer-Korvenkontio, M., Vaheri, A., Tsai, T.F., Regnery, H.L., and et al. (1985). Antigenic and genetic properties of viruses linked to hemorrhagic fever with renal syndrome. Science (New York, NY) *227*, 1041-1044.

Schmidt, S., Saxenhofer, M., Drewes, S., Schlegel, M., Wanka, K.M., Frank, R., Klimpel, S., von Blanckenhagen, F., Maaz, D., Herden, C., Freise, J., Wolf, R., Stubbe, M., Borkenhagen, P., Ansorge, H., Eccard, J.A., Lang, J., Jourdain, E., Jacob, J., Marianneau, P., Heckel, G., and Ulrich, R.G. (2016). High genetic structuring of Tula hantavirus. Archives of virology *161*, 1135-1149.

Scholz, S., Baharom, F., Rankin, G., Maleki, K.T., Gupta, S., Vangeti, S., Pourazar, J., Discacciati, A., Höijer, J., Bottai, M., Björkström, N.K., Rasmuson, J., Evander, M., Blomberg, A., Ljunggren, H.G., Klingström, J., Ahlm, C., and Smed-Sörensen, A. (2017). Human hantavirus infection elicits pronounced redistribution of mononuclear phagocytes in peripheral blood and airways. PLoS pathogens *13*, e1006462.

Schönrich, G., Rang, A., Lutteke, N., Raftery, M.J., Charbonnel, N., and Ulrich, R.G. (2008). Hantavirus-induced immunity in rodent reservoirs and humans. Immunological reviews *225*, 163-189.

Schultze, D., Lundkvist, A., Blauenstein, U., and Heyman, P. (2002). Tula virus infection associated with fever and exanthema after a wild rodent bite. European Journal of Clinical Microbiology and Infectious Diseases *21*, 304-306.

Shi, M., Lin, X.-D., Chen, X., Tian, J.-H., Chen, L.-J., Li, K., Wang, W., Eden, J.-S., Shen, J.-J., Liu, L., Holmes, E.C., and Zhang, Y.-Z. (2018). The evolutionary history of vertebrate RNA viruses. Nature *556*, 197-202.

Simons, M.J., Gorbunova, E.E., and Mackow, E.R. (2019). Unique Interferon Pathway Regulation by the Andes Virus Nucleocapsid Protein Is Conferred by Phosphorylation of Serine 386. Journal of virology *93(10)*, e00338-00319.

Solá-Riera, C., Gupta, S., Ljunggren, H.G., and Klingström, J. (2019). Orthohantaviruses belonging to three phylogroups all inhibit apoptosis in infected target cells. Scientific reports *9*, 834.

Spiropoulou, C.F. (2011). Molecular Biology of Hantavirus Infection. In Bunyaviridae Molecular and Cellular Biology A. Plyusnin, and R.M. Elliott, eds. (Caister Academic Press), pp. 41-60.

Spiropoulou, C.F., Albarino, C.G., Ksiazek, T.G., and Rollin, P.E. (2007). Andes and Prospect Hill hantaviruses differ in early induction of interferon although both can downregulate interferon signaling. Journal of virology *81*, 2769-2776.

Stoltz, M., and Klingström, J. (2010). Alpha/beta interferon (IFN-alpha/beta)-independent induction of IFN-lambda1 (interleukin-29) in response to Hantaan virus infection. Journal of virology *84*, 9140-9148.

Stoltz, M., Sundström, K.B., Hidmark, A., Tolf, C., Vene, S., Ahlm, C., Lindberg, A.M., Lundkvist, A., and Klingström, J. (2011). A model system for *in vitro* studies of bank vole borne viruses. PloS one *6*, e28992.

Strakova, P., Dufkova, L., Sirmarova, J., Salat, J., Bartonicka, T., Klempa, B., Pfaff, F., Hoper, D., Hoffmann, B., Ulrich, R.G., and Ruzek, D. (2017). Novel hantavirus identified in European bat species *Nyctalus noctula*. Infection, genetics and evolution *48*, 127-130.

Strandin, T., Hepojoki, J., Wang, H., Vaheri, A., and Lankinen, H. (2011). The cytoplasmic tail of hantavirus Gn glycoprotein interacts with RNA. Virology *418*, 12-20.

Strandin, T., Smura, T., Ahola, P., Aaltonen, K., Sironen, T., Hepojoki, J., Eckerle, I., Ulrich, R.G., Vapalahti, O., Kipar, A., and Forbes, K.M. (2020). Orthohantavirus Isolated in Reservoir Host Cells Displays Minimal Genetic Changes and Retains Wild-Type Infection Properties. Viruses *12*.

Sundström, K.B., Stoltz, M., Lagerqvist, N., Lundkvist, A., Nemirov, K., and Klingström, J. (2011). Characterization of two substrains of Puumala virus that show phenotypes that are different from each other and from the original strain. Journal of virology *85*, 1747-1756.

Takadate, Y., Kondoh, T., Igarashi, M., Maruyama, J., Manzoor, R., Ogawa, H., Kajihara, M., Furuyama, W., Sato, M., Miyamoto, H., Yoshida, R., Hill, T.E., Freiberg, A.N., Feldmann, H., Marzi, A., and Takada, A. (2020). Niemann-Pick C1 Heterogeneity of Bat Cells Controls Filovirus Tropism. Cell reports *30*, 308-319.e305.

Takeuchi, O., and Akira, S. (2007). Recognition of viruses by innate immunity. Immunological reviews *220*, 214-224.

Temonen, M., Vapalahti, O., Holthofer, H., Brummer-Korvenkontio, M., Vaheri, A., and Lankinen, H. (1993). Susceptibility of human cells to Puumala virus infection. The Journal of general virology *74 (Pt 3)*, 515-518.

Terasaki, K., Murakami, S., Lokugamage, K.G., and Makino, S. (2011). Mechanism of tripartite RNA genome packaging in Rift Valley fever virus. Proceedings of the National Academy of Sciences of the United States of America *108*, 804-809.

Thomas, D., Blakqori, G., Wagner, V., Banholzer, M., Kessler, N., Elliott, R.M., Haller, O., and Weber, F. (2004). Inhibition of RNA polymerase II phosphorylation by a viral interferon antagonist. The Journal of biological chemistry *279*, 31471-31477.

Torelli, F., Zander, S., Ellerbrok, H., Kochs, G., Ulrich, R.G., Klotz, C., and Seeber, F. (2018). Recombinant IFN-gamma from the bank vole *Myodes glareolus*: a novel tool for research on rodent reservoirs of zoonotic pathogens. Scientific reports *8*, 2797.

Vaheri, A., Henttonen, H., Voutilainen, L., Mustonen, J., Sironen, T., and Vapalahti, O. (2013a). Hantavirus infections in Europe and their impact on public health. Reviews in medical virology *23*, 35-49.

Vaheri, A., Strandin, T., Hepojoki, J., Sironen, T., Henttonen, H., Mäkelä, S., and Mustonen, J. (2013b). Uncovering the mysteries of hantavirus infections. Nature Reviews Microbiology *11*, 539-550.

Villarreal, L.P., Defilippis, V.R., and Gottlieb, K.A. (2000). Acute and persistent viral life strategies and their relationship to emerging diseases. Virology *272*, 1-6.

Virtanen, J.O., Jääskelainen, K.M., Djupsjobacka, J., Vaheri, A., and Plyusnin, A. (2010). Tula hantavirus NSs protein accumulates in the perinuclear area in infected and transfected cells. Archives of virology *155*, 117-121.

Virtue, E.R., Marsh, G.A., Baker, M.L., and Wang, L.F. (2011). Interferon production and signaling pathways are antagonized during henipavirus infection of fruit bat cell lines. PloS one *6*, e22488.

Voutilainen, L., Savola, S., Kallio, E.R., Laakkonen, J., Vaheri, A., Vapalahti, O., and Henttonen, H. (2012). Environmental change and disease dynamics: effects of intensive forest management on Puumala hantavirus infection in boreal bank vole populations. PloS one *7*, e39452.

Voutilainen, L., Sironen, T., Tonteri, E., Bäck, A.T., Razzauti, M., Karlsson, M., Wahlström, M., Niemimaa, J., Henttonen, H., and Lundkvist, A. (2015). Life-long shedding of Puumala hantavirus in wild bank voles (*Myodes glareolus*). The Journal of general virology *96*, 1238-1247.

Walz, U., Krüger, T., and Schumacher, U. (2011). Landschaftszerschneidung und Waldfragmentierung: Neue Indikatoren des IÖR-Monitors. In Flächennutzungsmonitoring III, G.a.S. Meinel, Ulrich, ed. (Rhombos-Verlag), pp. 163-170.

Wang, H., Alminaite, A., Vaheri, A., and Plyusnin, A. (2010). Interaction between hantaviral nucleocapsid protein and the cytoplasmic tail of surface glycoprotein Gn. Virus research *151*, 205-212.

Weber de Melo, V., Sheikh Ali, H., Freise, J., Kuhnert, D., Essbauer, S., Mertens, M., Wanka, K.M., Drewes, S., Ulrich, R.G., and Heckel, G. (2015). Spatiotemporal dynamics of Puumala hantavirus associated with its rodent host, *Myodes glareolus*. Evolutionary applications *8*, 545-559.

Weber, F., Bridgen, A., Fazakerley, J.K., Streitenfeld, H., Kessler, N., Randall, R.E., and Elliott, R.M. (2002). Bunyamwera bunyavirus nonstructural protein NSs counteracts the induction of alpha/beta interferon. Journal of virology *76*, 7949-7955.

Weber, S., Jeske, K., Ulrich, R.G., Imholt, C., Jacob, J., Beer, M., and Hoffmann, D. (2020). In Vivo Characterization of a Bank Vole-Derived Cowpox Virus Isolate in Natural Hosts and the Rat Model. Viruses *12*.

Yanagihara, R., Amyx, H.L., and D.C., G. (1985). Experimental infection with Puumala virus, the etiologic agent of nephropathia epidemica, in bank voles (*Clethrionomys glareolus*). Journal of virology *55(1)*, 34–38.

Yanagihara, R., Goldgaber, D., Lee, P.W., Amyx, H.L., Gajdusek, D.C., Gibbs, C.J., Jr., and Svedmyr, A. (1984). Propagation of nephropathia epidemica virus in cell culture. Lancet (London, England) *1*, 1013.

Zheng, W., and Tao, Y.J. (2013). Structure and assembly of the influenza A virus ribonucleoprotein complex. FEBS letters *587*, 1206-1214.

8. APPENDIX

8.1 PUBLICATIONS AND CONFERENCE PARTICIPATIONS

8.1.1 List of Publications

Binder, F., Gallo, G., Bendl, E., Eckerle, I., Ermonval, M., Luttermann, C., Ulrich, R.G. "Inhibition of the interferon I induction by non-structural protein NSs of Puumala and other vole associated orthohantaviruses: Plasticity of the protein and role of the N-terminal region". Archives of Virology (submitted).

Binder, F., Ryll, R., Drewes, S., Jagdmann, S., Reil,D., Hiltbrunner, M., Rosenfeld, U.M., Imholt, C., Jacob, J., Heckel, G., Ulrich, R.G. "Spatial and temporal evolutionary patterns in Puumala orthohantavirus (PUUV) S segment". Pathogens 9(7), 548, DOI: 10.3390/pathogens9070548.

Binder, F., Reiche, S., Roman-Sosa, G., Saathoff, M., Ryll, R., Kunec, D., Höper, D., Ulrich, R.G., 2020. „Isolation and characterization of new Puumala orthohantavirus strains from Germany". Virus Genes 56(4), 448-460, DOI:10.1007/s11262-020-01755-3.

Binder, F., Drewes, S., Imholt, C., Saathoff, M., Below, A.D., Bendl, E., Conraths, F.J., Tenhaken, P., Mylius, M., Brockmann, S., Oehme, R., Freise, J., Jacob, J., Ulrich, R.G., 2019. "Heterogeneous Puumala orthohantavirus situation in endemic regions in Germany in summer 2019", Transboundary and emerging diseases 67(2), 502-509. DOI:10.1111/tbed.13408.

Binder, F., Lenk, M., Weber, S., Stoek, F., Dill, V., Reiche, S., Riebe, R., Wernike, K., Hoffmann, D., Ziegler, U., Adler, H., Essbauer, S., Ulrich, R.G., 2019. "Common vole (*Microtus arvalis*) and bank vole (*Myodes glareolus*) derived permanent cell lines differ in their susceptibility and replication kinetics of animal and zoonotic viruses", Journal of Virological Methods 274, 113729. DOI:10.1016/j.jviromet.2019.113729.

Reil, D., Binder, F., Freise, J., Imholt, C., Beyrer, K., Jacob, J., Krüger, D.H., Hofmann, J., Dreesman, J., Ulrich, R.G., 2018. "Hantaviren in Deutschland: Aktuelle Erkenntnisse zu Erreger, Reservoir, Verbreitung und Prognosemodellen / Hantaviruses in Germany: current knowledge on pathogens, reservoirs, distribution and forecast models", Berliner Münchner Tierärztliche Wochenschrift, [online first - open access: https://vetline.de/index.cfm?cxml:id=2806&q=hanta viren +in+deuts chlan d], DOI:10.2376/0005-9366-18003.

Drewes, S., Ali, H.S., Saxenhofer, M., Rosenfeld, U.M., Binder, F., Cuypers, F., Schlegel, M., Röhrs, S., Heckel, G., Ulrich, R.G., 2017. "Host-Associated Absence of Human Puumala Virus Infections in Northern and Eastern Germany", Emerging Infectious Diseases 23(1), 83–86. DOI:http://dx.doi.org/10.3201/eid2301.160224.

8.1.2 Conference participations

Zoonoses 2019 – International Symposium on Zoonoses Research, 16-18 October 2019, Berlin, Germany

11th International Conference on Hantaviruses, 1-4 September 2019, Leuven, Belgium

Symposium “Emerging infections: Increasing preparedness by networking”, 27 November 2018, Berlin, Germany

6th Workshop of the Network “Rodent-borne pathogens (NaÜPaNet)”, 27-30 November 2018, Berlin, Germany

7th FLI internal Symposium for Young Scientists, 24-26 September 2018, Greifswald, Germany

Sino-German Summer School on Structural Biology in Infection, 26-31 August 2018, Lübeck-Hamburg, Germany

2nd International Symposium on RNA virus persistence: Mechanisms and consequences, 23-25 August 2018, Freiburg, Germany

28th Annual Meeting of the Society for Virology, 14-17 March 2018, Würzburg, Germany

National Symposium on Zoonosis Research 2017, 12-13 October 2017, Berlin, Germany

91st Annual Meeting German Society of Mammalogy, 18-20 September 2017, Greifswald, Germany

Junior Scientist Zoonoses Meeting 2017, 7-9 June 2017, Langen, Germany

1st International Workshop on Bank Vole Research, 11-12 May 2017, University of Sciences Lublin, Poland

27th Annual Meeting of the Society for Virology, 22-25 March 2017, Marburg, Germany

Workshop “One Past Health”, 15-17 February 2017, Max-Planck Institute for Evolutionary Biology, Plön, Germany

5th Workshop of the Network “Rodent-borne pathogens (NaÜPaNet)”, 28-30 November 2016, Gießen, Germany

National Symposium on Zoonosis Research 2016, 13-14 October 2016, Berlin, Germany

8.1.3 Oral presentations

Binder, F., Saathoff, M., Freise, J., Ulrich, R.G., 18.10.2019. “Isolation and characterization of Puumala orthohantavirus from Germany”, Zoonoses 2019 – International Symposium on Zoonoses Research, 16-18 October 2019, Berlin, Germany.

Binder, F., 19.09.2019. “Progress Report VI - Reservoir population-driven emergence and persistence of Puumala orthohantavirus: Host specificity of PUUV NSs and generation of monoclonal antibodies against PUUV GPC“, Progress Report FLI, Greifswald - Insel Riems, Germany.

Binder, F., Gallo, G., Ryll, R., Imholt, C., Ermonval, M., Luttermann, C., Ulrich, R.G., 03.09.2019. “Puumala virus S-segment sequence evolution in the bank vole and functional analysis of NSs protein”, 11th International Conference on Hantaviruses, 1-4 September 2019, Leuven, Belgium.

Gallo, G., Binder, F., Baychelier, F., Eckerle, I., Ulrich, R.G., Tordo, N., Ermonval, M. “In vitro study on interactions of pathogenic and non-pathogenic orthohantaviruses with cellular factors of human host and rodent reservoir”, 11th International Conference on Hantaviruses, 1-4 September 2019, Leuven, Belgium.

Binder, F., 03.06.2019. “Characterization of Puumala orthohantavirus - host interactions: the NSs open reading frame and its functional relevance”, Hausseminar FLI, Greifswald - Insel Riems, Germany.

Binder, F., 18.04.2019. “Progress Report V - Reservoir population-driven emergence and persistence of Puumala orthohantavirus: Virus isolation and infection studies “, Progress Report FLI, Greifswald - Insel Riems, Germany.

Binder, F., 03.03.2019. “Reservoir population-driven emergence and persistence of Puumala hantavirus: sequence evolution and functional relevance”, Guest talk Institute Pasteur, Paris, France.

Binder, F., 29.11.2018. “Sequence diversity of PUUV NSs protein and functional relevance“, 6th Workshop of the Network “Rodent-borne pathogens (NaÜPaNet)”, 28-30 November 2018, Berlin, Germany.

Binder, F., 15.11.2018. “Progress Report IV - Reservoir population-driven emergence and persistence of Puumala hantavirus: sequence evolution and functional relevance“, Progress Report FLI, Greifswald - Insel Riems, Germany.

Binder, F., Lenk, M., Ulrich, R.G., 25.09.2018. Lightning Talk: “Replication kinetics of Puumala orthohantavirus strain Vranica/Hällnäs in a permanent bank vole cell line”, 7th FLI internal Symposium for Young Scientists, 24-26 September 2018, Greifswald, Germany.

Binder, F., 28.08.2018. “Reservoir population-driven emergence and persistence of Puumala orthohantavirus: sequence evolution and functional relevance”, Sino-German Summer School on Structural Biology in Infection, 26-31 August 2018, Lübeck-Hamburg, Germany.

Binder, F., 01.02.2018. “Progress Report III - Reservoir population-driven emergence and persistence of Puumala hantavirus: sequence evolution and functional relevance“, Progress Report FLI, Greifswald - Insel Riems, Germany.

Binder, F., 07.09.2017. “Progress Report II - Reservoir population-driven emergence and persistence of Puumala hantavirus: sequence evolution and functional relevance“, Progress Report FLI, Greifswald - Insel Riems, Germany.

Binder, F., 17.07.2017. “Vorstellung Promotionsvorhaben: Reservoir population-driven emergence and persistence of Puumala hantavirus: sequence evolution and functional relevance”, Hausseminar FLI, Greifswald - Insel Riems, Germany.

Drewes, S., Ali, H.S., Rosenfeld, U.M., Binder, F., Cuypers, F., Schlegel, M., Röhrs, S., Sadowska, E.T., Mikowska, M., Koteja, P., Heckel, G., Ulrich, R.G., 15.02.2017. “Does host evolution limit the distribution of Central European Puumala virus?”, 1st International Workshop on Bank Vole Research, 11-12 May 2017, University of Sciences Lublin, Poland.

Drewes, S., Ali, H.S., Rosenfeld, U.M., Binder, F., Cuypers, F., Weber de Melo, V., Heckel, G., Ulrich, R.G., 15.02.2017. “Does host evolution limit the distribution of Central European Puumala virus?”, Workshop “One Past Health”, 15-17 February 2017, Max-Planck Institute for Evolutionary Biology, Plön, Germany.

Binder, F., 02.02.2017. “Progress Report I - Reservoir population-driven emergence and persistence of Puumala hantavirus: sequence evolution and functional relevance“, Progress Report FLI, Greifswald - Insel Riems, Germany.

Binder, F., Jagdmann, S., Rosenfeld, U.M., Ryll, R., Reil, D., Imholt, C., Jacob, J., Ulrich, R.G., 29.11.2016. “Puumalavirus-prevalence and S-segment-sequence evolution in the bank vole“, 5th Workshop of the Network “Rodent-borne pathogens (NaÜPaNet)”, 28-30 November 2016, Gießen, Germany.

8.1.4 Poster presentations

Drewes, S., Ryll, R., Röhrs, S., Schlohsarczyk, E., Fischer, S., Fritzsche, W., Binder, F., Heckel, G., Ulrich, R.G., 01.09.2019. “Molecular detection of Puumala orthohantavirus: struggling with high nucleotide sequence variability”, 11th International Conference on Hantaviruses, 1-4 September 2019, Leuven, Belgium.

Binder, F., Lenk, M., Ulrich, R.G., 25.09.2018. “Replication kinetics of Puumala orthohantavirus strain Vranica/Hällnäs in a permanent bank vole cell line”, 7th FLI internal Symposium for Young Scientists, 24-26 September 2018, Greifswald, Germany.

Binder, F., Lenk, M., Ulrich, R.G., 23.08.2018. “Puumala orthohantavirus replicates efficiently in a kidney cell line of its host *Myodes glareolus*”, 2nd International Symposium on RNA virus persistence: Mechanisms and consequences, 23-25 August 2018, Freiburg, Germany.

Drewes, S., Röhrs, S., Schlohsarczyk, E., Fischer, S., Fritzsche, W., Binder, F., Heckel, G., Ulrich, R.G., 17.06.2018. “Molecular detection of Puumala orthohantavirus: struggling with high nucleotide sequence variability”, 17th Negative Strand RNA Virus meeting, 17-22 June 2018, Verona, Italy.

Binder, F., Ziegler, U., Stoek, F., Riebe, R., Essbauer, S., Lenk, M., Reiche, S., Ulrich, R.G., 14.03.2018. “Replicative capacity of emerging viruses in bank vole and common vole cell lines”, 28th Annual Meeting of the Society for Virology, 14-17 March 2018, Würzburg, Germany.

Binder, F., Ziegler, U., Hoffmann, D., Riebe, R., Essbauer, S., Lenk, M., Reiche, S., Ulrich, R.G., 12.10.2017. “Zoonotic virus infections in cell lines from bank voles and common voles”, National Symposium on Zoonosis Research 2017, 12-13 October 2017, Berlin, Germany.

Binder, F., Jagdmann, S., Rosenfeld, U.M., Ryll, R., Reil, D., Imholt, C., Heckel, G., Jacob, J., Ulrich, R.G., 18.09.2017. “Is sequence evolution of Puumala virus NSs protein related to bank vole population

dynamics?", 91st Annual Meeting German Society of Mammalogy, 18-20 September 2017, Greifswald, Germany.

Binder, F., Ziegler, U., Hoffmann, D., Dill, V., Riebe, R., Krautkrämer, E., Essbauer, S., Lenk, M., Reiche, S., Ulrich, R.G., 07.06.2017. "New rodent derived cell lines as a model for zoonotic virus infection", Junior Scientist Zoonoses Meeting 2017, 7-9 June 2017, Langen, Germany.

Binder, F., Jagdmann, S., Rosenfeld, U.M., Ryll, R., Reil, D., Imholt, C., Heckel, G., Jacob, J., Ulrich, R.G., 22.03.2017. "Puumala virus prevalence and S-segment sequence evolution in the bank vole (*Myodes glareolus*)", 27th Annual Meeting of the Society for Virology, 22-25 March 2017, Marburg, Germany.

8.1.5 Supervisions

Student Practical Course Virology, Bachelor, Universität Greifswald 2018 and 2019

Supervision of several internships

Supervision of apprentices

Master Thesis, Elias Bendl: Sequence Evolution of the Puumala Orthohantavirus NSs and the Effect of Amino Acid Substitutions on the Induction of Type-I Interferons

8.2 EIGENSTÄNDIGKEITSERKLÄRUNG

Hiermit erkläre ich, dass diese Arbeit bisher von mir weder an der Mathematisch-Naturwissenschaftlichen Fakultät der Universität Greifswald noch einer anderen wissenschaftlichen Einrichtung zum Zwecke der Promotion eingereicht wurde.

Ferner erkläre ich, dass ich diese Arbeit selbstständig verfasst und keine anderen als die darin angegebenen Hilfsmittel und Hilfen benutzt und keine Textabschnitte eines Dritten ohne Kennzeichnung übernommen habe.

_____

Unterschrift des Promovenden

8.3 DANKSAGUNG

Zuerst danke ich meiner Familie für die ununterbrochene Unterstützung während des Studiums, der Doktorarbeit und allem was mich auf dem Weg begleitet hat.

Bei meinem Doktorvater Rainer G. Ulrich bedanke ich mich für die Betreuung und die Unterstützung für meine Arbeit. Ich durfte immer frei meinen Interessen nachgehen und habe viele Perspektiven und tolle Kollegen kennenlernen dürfen. Ebenso möchte ich mich für die unzähligen Diskussions- & Arbeitsstunden bedanken, die in die Fertigstellung dieser Arbeit eingeflossen sind. Aber ich möchte mich auch für den gegenseitigen Respekt, die privaten Gespräche und den motivierenden Zuspruch für meine zukünftige Laufbahn bedanken.

Benjamin, René, Franziska, Ansgar, Arian, Friederike, Cora, Elias und Marie möchte ich für ihre Freundschaft danken, die tollen Mittagspausen, den Spaß im Labor und die gemeinsame Leidenszeit, was die Zeit am FLI unvergesslich macht.

Ein besonderer Dank gilt Tine, dass ich in meinem „zweiten“ Labor so toll aufgenommen und unterstützt wurde. Es hat riesig Spaß gemacht mit dir zu arbeiten und zu quatschen.

Stephan & Stefan, Sven & Sven, Andrea, Gregor, Dörte, Birke, Elisa, Kathrin, Maysaa, Maria, Tini, Gabi, Juliane und Yu danke ich für die tolle Zusammenarbeit, die Diskussionen und das kollegiale Miteinander. Patrick Wysocki möchte ich herzlich für das Bereitstellen von Karten danken!

Ich möchte mich auch bei allen Mitarbeitern des INNT für die tolle Zusammenarbeit bedanken und bei allen anderen FLIlern, die immer einen Antikörper, ein Enzym oder einen guten Rat parat hatten.

Bei Myriam und Giulia möchte ich mich besonders für ihre Gastfreundschaft während meines Aufenthalts in Paris bedanken, für ihre konstruktive Kritik, das Teilen unserer Ergebnisse und die wunderbaren Teepausen.

Auch bei allen anderen Kooperationspartnern möchte ich mich herzlich bedanken. Beim Friedrich-Loeffler-Institut bedanke ich mich für die Finanzierung des Projektes.

Den Virusjägern und Ballzauberern vom FLI möchte ich für die abwechslungsreiche Zeit danken.

Für die Zeit in Greifswald, Ablenkung und tolle Freundschaften danke ich dem Greifsbloc, sowie Nick, Laura, Tom und allen anderen.

Mein besonderer Dank gilt Sophia!

_____

Datum, Unterschrift